

Alma Mater Studiorum – Università di Bologna

DOTTORATO DI RICERCA IN

CHIMICA

Ciclo XXIX

Settore Concorsuale di afferenza: 03/C1

Settore Scientifico disciplinare: CHIM06

FIVE-MEMBERED NITROGEN HETEROCYCLE DERIVATIVES AS CORE
STRUCTURES FOR THE SYNTHESIS OF BIOACTIVE COMPOUNDS
CLASSES.

Presentata da:

Lucia Ferrazzano

Coordinatore Dottorato

Relatore

Prof. Aldo Roda

Dott.ssa Alessandra Tolomelli

Esame finale anno 2017

*“...il laboratorio è sorgente di gioia,
ed emana un fascino intenso,
che è quello della giovinezza,
dell'avvenire indeterminato e gravido di potenze,
e cioè della libertà.”*

Il sistema periodico, P. Levi, 1975.

A Sofia e Dario

Contents

1	The chemistry of heterocycles and their biological applications	1
1.1	Introduction	1
1.2	Heterocycles as isosteres in bioactive compounds and peptidomimetics	2
1.3	Aim of the thesis	6
2	Alkylidene derivatives as building blocks	11
2.1	Introduction	11
2.2	Results and discussions	13
2.2.1	Synthetic protocols base or Lewis acid founded	13
2.2.2	Microwaves-assisted synthetic protocols	16
2.3	Conclusions	26
2.4	Experimental procedures	26
2.4.1	General methods	26
2.4.2	Synthesis and characterization	27
2.5	Notes and references	37

3	Reactivity of alkylidene or arylidene derivatives for the synthesis of isoxazolidinones, isoxazolines and dehydro-β-prolines	39
3.1	Introduction	39
3.1.1	C-C bond formation in MCRs.	40
3.1.2	C-N bond formation for the synthesis of isoxazolidinones, isoxazolines and isoxazolidines.	44
3.1.3	C-N bond and subsequent C-C bond formation for the synthesis of 3,4-dehydro- β -proline.	49
3.2	Results and discussions	53
3.2.1	Conjugated addition of indole on alkylidene malonate and acetoacetate	53
3.2.2	1,4-addition of N,O-bis(trimethylsilyl)hydroxylamine for the synthesis of isoxazolidinones and isoxazolines	59
3.2.3	Lucho reduction and S _N 2' addition for the synthesis of 3,4-dehydro- β -prolines	63
3.3	Conclusions	66
3.4	Experimental procedures	69
3.4.1	General methods	69
3.4.2	Synthesis and characterization	70
3.5	Notes and references	94
4	Applications of isoxazolidin-5-ones and dehydro-β-prolines in the synthesis of Linezolid-like antibiotics and evaluation of the complex balance with MAO-inhibitory properties.	95
4.1	Introduction	95
4.1.1	Antibiotic resistance	96
4.1.2	Oxazolidinones: at the edge of antibiotic activity and anti-depressive role.	98
4.2	Results and discussions	103

4.2.1	Molecular design and synthesis	104
4.2.2	Evaluation of antibiotic activity and MAO inhibition	107
4.2.3	SAR studies	108
4.2.4	Docking experiments	109
4.3	Conclusions	115
4.4	Experimental procedures	116
4.4.1	General methods	116
4.4.2	Synthesis and characterization	118
4.5	Notes and references	126
5	Applications of dehydro-β-prolines and isoxazolines in the synthesis of integrin ligands as recognition and delivery systems in ligand-receptor interplay	127
5.1	Introduction	127
5.1.1	Integrins and their ligands: peptidomimetic-chemistry, new frontier of chemotherapy	129
5.2	Results and discussions	135
5.2.1	Design and synthesis of ligands	135
5.2.2	Biological evaluation	142
5.3	Conclusions	152
5.4	Experimental procedures	154
5.4.1	General methods	154
5.4.2	Synthesis and characterization	155
5.4.3	Cell culture	168
5.4.4	Cell Adhesion assay	169
5.4.5	Western blotting	171
5.4.6	Compounds (<i>R</i>)-98a and (<i>R</i>)-98b antagonize VCAM-1-induced ERK1/2 phosphorylation	173
5.4.7	Confocal laser scanning microscopy	174

5.5	Notes and references	174
6	Synthesis of red-shifted fluorescent self-assembled nanoparticles as diagnostic tools	175
6.1	Introduction	175
6.1.1	Nanoparticles based on fluorene oligomers	178
6.2	Results and discussions	182
6.2.1	Molecular design and synthesis	182
6.2.2	Formation and characterization of self-assembled nanoparticles	185
6.3	Conclusions	193
6.4	Experimental procedures	194
6.4.1	Synthesis and characterization	194
6.4.2	Preparation of nanoparticles	197
6.4.3	Optical Characterization	197
6.4.4	Dynamic Light Scattering	198
6.5	Notes and references	198
	Appendix	199
	Bibliography	203
	Acknowledgement	227

Chapter1

The chemistry of heterocycles and their biological applications

1.1 Introduction

The chemistry of heterocycles represents a modern interesting division of organic chemistry that collects cyclic compounds having at least two different elements, as defined by IUPAC, commonly identified as carbon and nitrogen, oxygen or sulphur.[1] For this reason, it's possible to divide ring systems on the basis of the heteroatom and, in each group, on the basis of the dimension of the resulting structure defined by the other atoms too;[2] moreover, they can be divided in aromatic or aliphatic heterocycles, which properties are influenced by the presence of strains attached to the ring and which are considered analogues of amines, esters, ethers, amides etc. These features are responsible for the different physiochemical properties of the heterocycles and of the compounds that contain themselves. In fact, heterocyclic cores can have various applications in several fields of chemistry, but in particular in medicinal chemistry to synthesize compounds with anti-bacterial, anti-inflammatory, anti-cancer and anti-fungal properties. The usefulness of

these systems is linked to the possibility to modulate the properties of a drug by the introduction of these motifs. Heterocycles can be considered bioisosteric replacements of parts of a drug, so they can guarantee the keeping of lipophilicity, hydrophilicity, polarity or reactivity of a drug or modulate its properties, altering or influencing the mechanism of action of the pharmaceutical agent.[3][4]

1.2 Heterocycles as isosteres in bioactive compounds and peptidomimetics

The potential of peptides and proteins as therapeutics is well known, as their limited stability to proteolysis and their inability to cross cell membranes. So, the general approach to overcome these limitations is the introduction of modifications on the peptide/protein to keep unchanged or improve the biochemical properties associated to an efficient drug action.[5] These results can be obtained changing the backbone structure of the peptide or incorporating peptide bond isosteres. In general, **peptidomimetics** are molecules in which the pharmacophore, the fundamental element responsible for the biological efficacy of the compound, is represented by a structure that mimics a peptide or a protein in their 3-dimensional disposition and in their biological behaviour. This class of molecules allows to overcome some problems associated to peptidic compounds, like low biodisponibility and low stability towards proteolysis, and in some cases to improve efficacy and receptor affinity and selectivity. So, peptidomimetics have great relevance in drug discovery programs.[6] Generally, the attempt is to substitute as much part of the peptide as possible with non-peptidic elements in order to enhance the lipophilicity and so the biodisponibility of the molecules. Then, the substitution of amide bond is required to improved the resistance to proteolysis and to make the compound metabolically stable.

Finally, conformational modifications in order to improve the flexibility and to guarantee a better interaction with the proper binding sites are evaluated.[7] It's possible to distinguish four different types of peptidomimetics: the *type I* mimetics are peptides backbone mimetics (so strictly defined peptidomimetics), that match peptide backbone atom-for-atom keeping some fundamental functionalities required for the interaction with the proper binding site; the *type II* mimetics are small molecules that act as functional mimetics, with good affinity toward the peptide receptor; the *type III* mimetics are novel structures which possess functional groups acting as topographical mimetics; the *type IV* mimetics are GRAB-peptidomimetics (GroupReplacementAssisted-Binding) that keep functional properties like type I mimetics, but they can bind receptor forms not accessible with the last mentioned.[8] A widely used technique in the design and synthesis of peptidomimetics is the replacement of amide-bond, the most suitable for proteolytic degradation, with amide-bond analogues or isosteres, which allows to understand the protease enzyme activity when the structure of the isoster mimics the transition state of the hydrolytic degradation.[9] The employment of bioisosteres is one of the most rational approach used in medicinal chemistry to modify a lead compound to generate other molecules with better biological properties. One of the first examples was reported in 1919 by Langmuir who compared the physiochemical properties of some atoms and molecules, like N_2 and CO_2 , founding them similar. With this study, he found 21 groups of isosteres, defined as group of atoms or compounds with the same number and arrangement of electrons.[10][11] This work represent the basis of the modern concept of *bioisosterism*. The first definition proposed by Friedman was founded on the ability of a group of atoms or molecules to repropose the biological behaviour of a well-defined compound. The concept was extended by Burger, including all those compounds with near-equal molecular shape, volume and

electronic disposition to those of the target compounds, acting as agonist or antagonist.[12][13] Bioisosteres can be divided in two classes: *classical* and *non-classical* isosteres. The first class includes monovalent/divalent/trivalent atoms, tetrasubstituted atoms and ring equivalents; the second class can be divided in ring vs noncyclic systems and exchangeable groups and includes systems which can have a number of atoms, steric and electronic properties different from the molecules that they should substitute.[14] We focused our attention in particular on non classical bioisosteres since they are widely used in the design and synthesis of drugs and bioactive compounds. Infact, one of the most lable functionalities is the ester, since esterases are ubiquitous in the organism and they can easily hydrolyze it. The substitution of an ester with an heterocycle is a solution to enhance the stability toward hydrolysis of these molecules. It was discovered the ability of the heterocycles to create efficient hydrogen bonds with the receptor binding site: for this reason, it is of common practice the use of Brönsted proton basicity scale as alternative to hydrogen bond capacity of heterocycles, in order to classify them. In the Figure 1.1 hydrogen bonding capacity (pK_{BHx}) and Brönsted basicity (pK_{HB}) are reported for some 5-membered heterocycles.

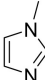
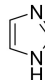
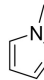
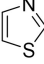
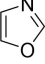
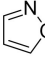
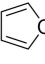
							
pK_{BHx}	2.72	2.42	1.84	1.37	1.30	0.81	-0.40
pK_{BH+}	7.12	6.95	2.06	2.52	0.80	1.30	

Figure 1.1: Hydrogen bonding (pK_{BHx}) and Brönsted basicity (pK_{HB}) of 5-membered heterocycles.

Another element that should be considered is the strenght of the C-H bonds of these systems. Infact, depending on their distance from the heteroatoms, these bonds can form hydrogen bonds strong enough to induce conformational and particular binding behaviour in the drug

candidate.[15] Lipophilicity is an important parameter that can influence the efficacy of a drug. In general, $\text{ClogP} < 5$ is considered fundamental to guarantee low lipophilicity and so good metabolic stability. Heterocyclic scaffolds can low ClogP if compared with the respective all-carbon counterpart. However, this aspect can be not always considered an advantage, if cell membrane penetration is reduced. Aqueous solubility is another property that can be modified by the introduction of heterocycles, more able of their corresponding all-carbon analogues to create hydrogen bonds. But between the heterocycles, it's possible to detect differences: for example, the isoxazole is more water-soluble than thiophene, due to the possibility to form hydrogen bonds with nitrogen and oxygen.[16] Heterocycles can be applied as cyclic or noncyclic bioisosteres in the synthesis of peptidomimetics. They can be used to recognize the different subtypes of receptor, since particular conformations of a peptide can show specificity only for one of them. For this reason, heterocyclic-based constrained peptidomimetics and mimetics of peptide secondary structures can be employed to study the conformation able to link specific receptor subtype. An example is the use of heterocycles to substitute non cyclic peptides in order to induce specific torsion angles and study the effects of conformational restrictions on biological activity. As esters, amide bonds are often substituted with bioisosteric analogues in the synthesis of peptides or drugs. In this case, cyclic vs noncyclic bioisosteres can be used: 1,2,4-oxadiazoles, 1,3,4-oxadiazoles and 1,2,4-triazoles are good bioisosteres of esters and amides (Figure 1.2). To these, 2-isoxazoline and imidazoline can be added, with specific applications in medicinal chemistry.[17][18][19]

The correlation of physicochemical parameters with the biological activity of a molecule is important to understand the little modifications introduced by bioisosteric heterocycles. They are used to optimize the efficacy and selectivity of a drug by means of pharmacokinetic e toxicolog-

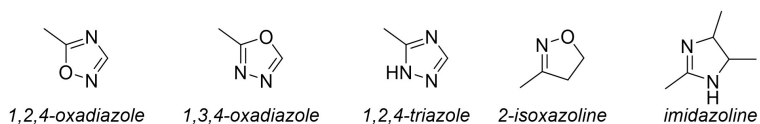


Figure 1.2: Heterocycles isosteres of amide bond.

ical properties. Even if the introduction of heterocycles in a compound can affect negatively the parameters of a drug, their careful manipulation can reach the good compromise between improvement and toxicity.

1.3 Aim of the thesis

As declared in the previous section, the relevance of heterocycles in medicinal chemistry and the inclusion of them in more complex structures represents a central matter. For this reason, the research towards new cyclic isosteres of functional groups and the optimization of their synthesis have been one of the basis of this work. In particular, the attention was paid to three different heterocycles: isoxazolines, isoxazolidinones and 3,4-dehydro- β -prolines (Figure 1.3).



Figure 1.3: Structure of the synthesized heterocycles.

The synthetic protocols developed for them are based on the electrophilic properties of alkylidene acetoacetates, malonates, acetoacetamide esters and malonamides that show great versatile reactivity. The preparation of these intermediates will be presented in Chapter 2 and it will be

focused on the development of two different protocols: the first one is the Knöevenagel condensation, a well-known reaction, performed at room temperature; the second one is a microwaves-assisted protocol, particularly interesting considering the growing application of these technology in organic synthesis. For this last topic, two examples of application will be reported: a microwave-assisted protocol for the Yonemitsu-type trimolecular condensation and the microwave-assisted one-pot two-steps synthesis of alkylidene acetoacetamide esters for the preparation of β -dehydropeptides. The reactivity of alkylidene derivatives will be studied in Chapter 3. The reactivity towards indoles, amines and diprotected-hydroxylamines will be discussed, since 1,4-Michael addition of C- and N-nucleophiles on α, β -unsaturated electrophiles is the ground for the synthesis of isoxazolines and isoxazolidinones, differently substituted. Then, the Luche-reduction of these unsaturated intermediates will be presented and the consequent enzymatic resolution for the enantioselective preparation of 3,4-dehydro- β -prolines. Connected to the theme of the relevance of bioisosteres in medicinal chemistry, applications of the synthesized heterocycles in molecules with biological target will be presented in Chapters 4 and 5. Since isoxazolidinones and 3,4-dehydro- β -prolines can be considered bioisosteres of oxazolidinones, the pharmacophore of a big family of drugs with antibiotic activity, we worked on the synthesis of a small library of antibiotic compounds based on the two synthesized heterocycles (Chapter 4) (Figure 1.4).

The structure of the compounds in the library reminds to the structure of Linezolid, an oxazolidinonic antibiotic active against gram-positive bacterial strains resistant to other antibiotic treatments, like those with Methicillin and Vancomycin. The oxazolidinones are pharmacophores of another important class of drugs too: the inhibitors of MonoAmino Oxidase (MAO), enzymes responsible for metabolism of monoamine neurotransmitters. For this reason, the library has been tested in its an-

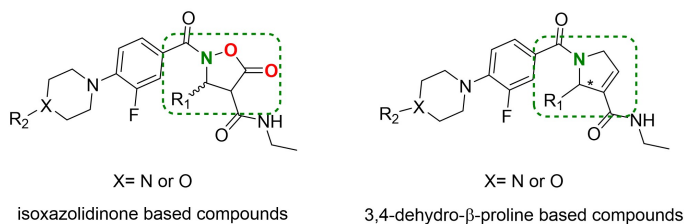


Figure 1.4: Structure of antibiotic compounds based on isoxazolidinone and 3,4-dehydro- β -proline.

antibiotic activity on specific bacterial strains and in its MAO-inhibitor activity on two isoforms of human monoamino oxidase. Considering their good activity towards MAO-A and B, docking experiments will be presented to understand their behaviour. The 3,4-dehydro- β -prolines and the isoxazolines are the focus of the second topic presented in Chapter 5: the synthesis on peptidomimetic integrin ligands. Going back to the importance of peptidomimetic chemistry in the subsection of medicinal chemistry, we studied the role of vascular cell adhesion molecule 1 (VCAM-1), in the regulation of cell membrane activity governed by $\alpha_4\beta_1$ integrins during inflammatory disease, and the role of fibronectin (FN) and RGD-peptides, in the regulation of $\alpha_v\beta_3$ and $\alpha_5\beta_1$ integrin activity. The 3,4-dehydro- β -proline was employed as heterocyclic bioisosteric scaffold for the synthesis of peptidomimetic analogues of the natural ligands of $\alpha_4\beta_1$ integrins: two different pattern of functionalizations of the heterocyclic core produced two classes of $\alpha_4\beta_1$ ligands, whose biological activity was evaluated. The isoxazolines were employed in the synthesis of $\alpha_5\beta_1$ and $\alpha_v\beta_3$ integrin peptidomimetic ligands as systems for drug or fluorescent molecules delivery (Figure 1.5). The structure of these ligands keeps some fundamental features required to be active on these proteins: good water solubility, flexibility, small dimension and amidic and acidic functionalities properly oriented and distanced. The designed ligands have a alkyne as substituent of the heterocycle, opening

the way to the "Click chemistry", widely used in the design of bioactive compounds: this allowed us to create a library of molecules by changing the side chain attached to the triazole ring obtained by this cycloaddition. The library was then tested on integrins to evaluate its eventual biological efficacy.

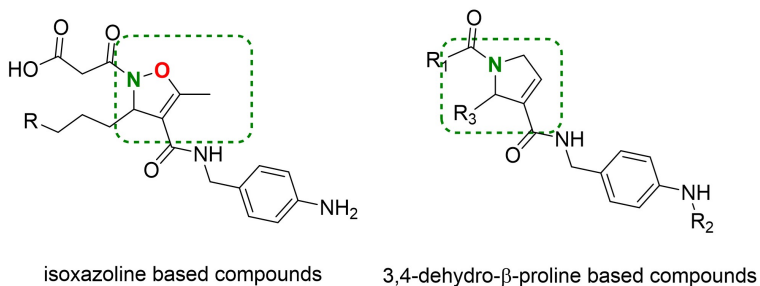


Figure 1.5: Structure of integrin ligands based on isoxazoline and 3,4-dehydro-β-proline.

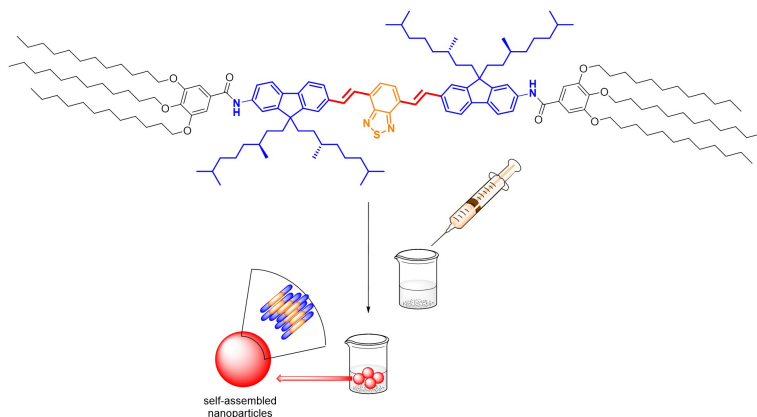


Figure 1.6: Structure of fluorene-based π -conjugated oligomer for the synthesis of red-shifted self-assembled nanoparticles

In a parallel way, the attention was paid on systems that can be deliv-

ered by the integrin ligands so synthesized. So, during the period spent in Prof. Brunsveld's laboratory in the Technische Universiteit of Eindhoven, the work presented in Chapter 6 has been developed: the synthesis of red-shifted self-assembled nanoparticles as tools for bioimaging (Figure 1.6). The emerging class of fluorescent π -conjugated oligomer based nanoparticles was studied as interesting probes for sensing and cellular in vivo imaging. In order to overcome the problem of autofluorescence usually observed during the in vivo tests with fluorescent agents, in this chapter the synthesis of nanoparticles based of fluorene π -conjugated oligomer and the preparation of nanoparticles starting from them will be discussed. The characterization and the comparison with not red-shifted analogues will be described too.

Chapter2

Alkylidene derivatives as building blocks

2.1 Introduction

In order to perform studies on the reactivity of alkylidene derivatives for the synthesis of more complex structures, it's important to develop solid, versatile, efficient and easy-to-do protocols for their synthesis. Knoevenagel condensation is the most widely employed reaction for the synthesis of these derivatives starting from an **aldehyde** and a **methylene-active compound**, in presence of a base or a Lewis-acid as **catalyst**. The first example was reported in 1894 by Knoevenagel and it involves formaldehyde and diethyl malonate or ethyl benzyloxyacetate in presence of ethylamine, to obtain in a reversible way (in a sort of extension of the aldol reaction) a functionalized olefin.[20] [21] The efficiency of the reaction depends on several factors: not only on the relative reactivity of reagents but also on the solvent and the base employed and on the chosen methodologies to remove the water produced during the reaction. The particular usefulness of dicarbonyl compounds in this reaction depends on the presence of a second carbonyl moieties that acts as electron-withdrawing group enhancing the nucleophilicity of the methy-

lene group: for this reason compounds in which the carbonyl is combined with nitro, cyano, sulfonyl or carbonyl moieties are mainly employed as nucleophilic counterpart of the reaction. Examples are malonic acid, malonic esters, malonic amides, Meldrum's acid, acetoacetates and acetoacetamides. At the same time, the electrophilic carbonyl compound is often an aldehyde, in particular 2-hydroxybenzaldehyde, benzaldehyde, isobutyraldehyde and salicylaldehyde. The reaction is generally catalyzed by strong bases, like NaOH, KOH and sodium ethoxide, or weak bases, such as tetrabutylammonium hydroxide, morpholinium acetate, piperidine, pyridine and amino acids; these bases can be immobilized on solid-state support too.[22] In addition, the reaction can be modified to be performed in ionic liquids or under microwave assistance.[23][24][25] There are two proposed mechanisms for this reaction: the first proposed on the basis of the results carried out by Knöevenagel in 1898; the second developed few years later by Hann and Lapworth. The first derives from two trials performed by Knöevenagel: an aldehyde, ethyl acetoacetate and an amine (primary or secondary), on one hand, and an alkylidene-bis-amine and ethyl acetoacetate, on the other. He found for both the cases the same product, alkylidene-ethyl acetoacetate, with two equivalents of diamine as coproduct in the second case. So he postulated that the second reaction can well describe the mechanism of a base (amine) catalyzed-condensation: the amine form a Schiff base with the aldehyde which is the real electrophile that undergoes the nucleophilic attack of methylene active compound. Related to the second part of the reaction, that is to say the activation of the nucleophile, the hypothesis regards the role of the amine catalyst (pyridine in the first trials performed by Hann and Lapworth in 1904): they assumed that the base allows the formation of a carbanion (or enol) resonance-stabilized intermediate from the methylene active compound, that added the aldehyde giving an hydroxyl-containing adduct. The hydroxyl-intermediate in them both the cases

undergoes β -elimination to give the final olefin. The stereochemical definition of the product depends in great part on the steric hindrance of the substituents during the condensation.[26]

2.2 Results and discussions

2.2.1 Synthetic protocols base or Lewis acid founded

After the first example reported by Knöevenagel and Hann-Lapworth, changes were made using pyridine as solvent and piperidine as catalyst, which became known as *Döebner Modifications*. According to this hypothesis, the two previously described mechanisms can be considered concerted (Figure 2.1): the pyridine represents the base responsible for the formation of the methylene-active intermediate that acts as nucleophilic species, in the same way in which Hann and Lapworth described their mechanism; the piperidine allows the formation of the Schiff base starting from the aldehyde, as proposed by Knöevenagel.[27] A lot of

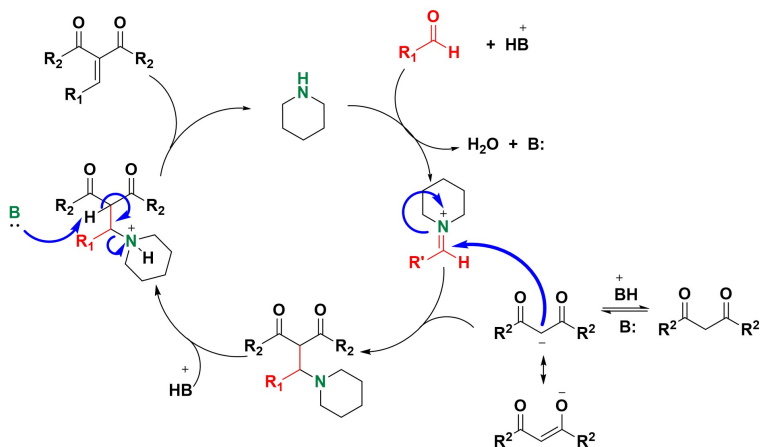


Figure 2.1: Mechanism of Knoevenagel condensation according to the Doebner's modifications.

works regarding the attempt to improve the protocols for this reaction have been reported, especially to make it less energy intensive and more green, rapid and safe. In fact, the use of pyridine should be avoided for many reasons, above all because it is a cancerogenic substance, hazardous for the environment and the operators and difficult to be handled in big scales.[28] Traditionally the reaction is performed in pyridine as solvent and piperidine as catalyst: this choice is particularly relevant when the reaction involves substrates that can be in situ decarboxylated, like malonic acid. For this purpose, we recently reported examples of Knoevenagel condensation catalyzed by proline for the synthesis of alkylidene and arylidene malonates.[29] In this case, the chirality of the catalyst was not relevant for the aim of the project, but allowed the development of a very mild condition-based protocol that involves dimethylmalonate, several alkylic or arylc aldehydes and 10% of proline in DMSO at room temperature, obtaining without the use of a dehydrating agent the alkylidene or arylidene malonate with yields upper 70%. Other examples in which the pyridine is substituted by a mixture of TEA/piperidine are reported in literature, particularly useful for the synthesis of arylidene and alkylidene malonate in high boiling point solvents and with the assistance of microwaves to reduce the reaction time.[30] As described before, the Knoevenagel condensation can be performed with the use of Lewis acid as catalyst too. $Ti(Cl)_4$ and its analogues are often used for this application even if there are few examples in literature regarding its employment as catalyst in the abovementioned condensation. In 1970's Lehnert and in 1980's Reetz described $Ti(IV)$ -catalyzed Knoevenagel reactions for the synthesis of alkylidene or arylidene malonate,[31] [32] ethyl acetoacetate, ethyl nitroacetate[33], triethyl phosphonoacetate [34] and ethyl (diethoxyphosphoryl)acetate [35]. Examples were proposed later with the substitution of pyridine with triethyl amine.[36][37]

In a first approach, we developed a protocol for a solvent-free condensation to prepare **alkylidene methyl malonylamides** [38] and **alkylidene tert-butyl acetoacetate**. The reaction was performed with excess of aldehyde in presence of 15 mol% of piperidine: this choice was possible since the excess of aldehyde acts a solvent of the reaction and it is easily removable by flash chromatography or by evaporation as consequence of their low boiling point. In this case, there is no need of dehydrating agents to obtain the desired olefin, as 1/4 mixture of *Z/E* isomers. The limit of this reaction is in the long reaction times, from 12h to 3 days. (Figure 2.2) The unsatisfactory yield observed for alkylidene

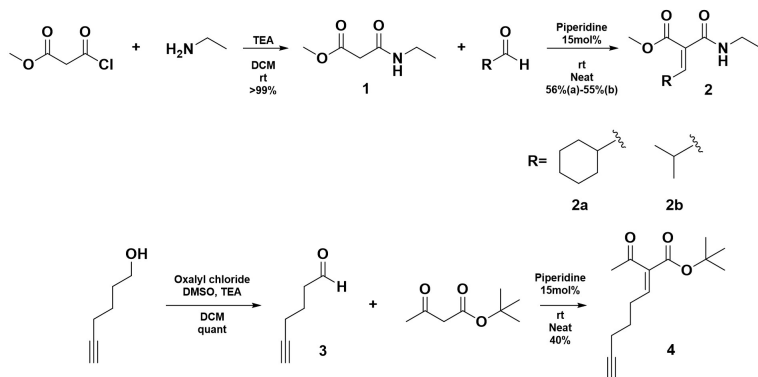


Figure 2.2: Synthesis of alkylidene malonamide and acetoacetate at room temperature.

acetoacetate **4** (calculated on two steps, since the aldehyde is synthesized by Swern oxidation of the corresponding 5-hexyn-1-ol) was attributed to side chain reaction of the alkyne moiety, due to its acidity. For this reason, we proceeded with a second approach on the model reported by Cruciani et al.[39] The Knöevenagel condensation was performed after protection of the alkyne moiety of the starting alcohol with TMS group, by the employment of TMS-Cl and *n*-BuLi as base. The quantitative conversion to give the intermediate **5** allowed to achieve the oxidation

product **6** in the same condition reported for intermediate **3**. As consequence of the presence of TMS-base sensitive group, the condensation was optimized using a mixture of TiCl_4 and pyridine, in THF, obtaining the desired product with yield of 83% (Figure 2.3). The assumed

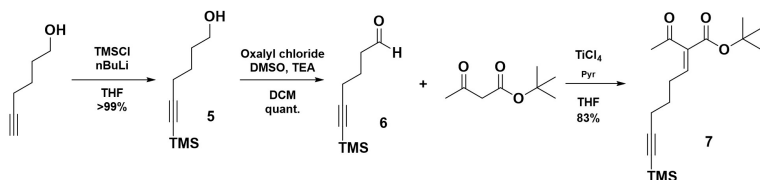


Figure 2.3: Synthesis of alkylidene tert-butyl acetoacetate $Ti(IV)$ -catalyzed.

mechanism postulates the formation of a 1:1 complex between tert-butyl acetoacetate and TiCl_4 , where the $\text{Ti}(IV)$ acts as a bidentate coordinating metal. Deprotonation of the acid proton gives the tetrachlorotitanium enolate that reacts with the aldehyde, whose carbonyl moiety replace one of the carbonyl functions of the acetoacetate in the coordination with the metal. There are two possible pathway according to which carbonyl group (ester or ketone) is replaced by the aldehyde, but the mechanism is the same for them both. The intramolecular aldol reaction allows the formation of a six-membered metallacycle with two stereogenic centers; then the dehydration occurs by deprotonation of the last acid proton by pyridine (Figure 2.4).[40]

2.2.2 Microwaves-assisted synthetic protocols

Microwave assisted organic synthesis (MAOS) is a growing area of research that gives the chance to significantly reduce reaction times from hours to minutes, enhancing in some cases the reactivity of systems that in conventional heating conditions are less reactive. In recent years, a lot of examples of microwave-assisted reaction have been reported starting

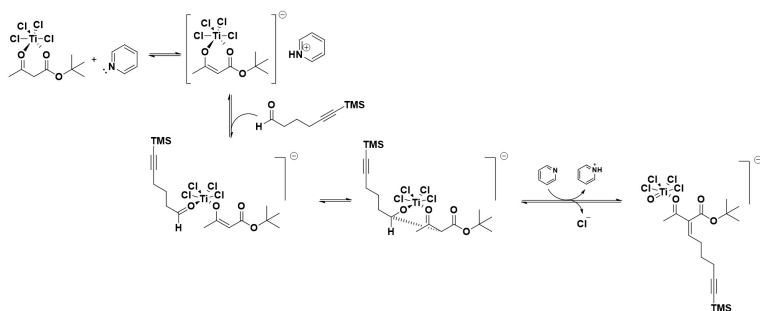


Figure 2.4: Mechanism of Ti(IV)-catalyzed condensation.

from cycloaddition and solvent-free reactions, going to heterocyclic and medicinal chemistry, but important effects can be observed in particular in the preparation of isotopically labelled drugs [41] and in catalyzed reactions where the short reaction times reduce the tendency of the catalyst to decomposition, increasing its efficiency.[42] The results can be explained by the existence of the so-called "microwave effect". This effect is a combination of several contributes like thermal and non-thermal effects, overheating, hot spots and selective heating.[43] The microwave-assisted technology is based on the "microwave dielectric heating" effects of a chosen material: it means that different materials (reagent or solvent) have different ability to absorb microwave energy that will be converted in heat. This is what we call *thermal effect*. Irradiation by microwaves gives allineation of dipoles or ions present in the sample according to the applied electric field. Since it oscillates, the dipoles and ions try to realign themselves with the alternating field: during this process there is loss of energy in the form of heat. This means that the amount of heating developed depends on the ability of the components of the sample to follow the oscillations of the field; if the dipoles don't have enough time to realign with the electric field no heating is produced. For this reason, the microwave-induced heating happens in homogeneous

way in all the sample, while the conductive heating starts from the surface and diffuses itself in heterogeneous way to the rest of the volume. In fact, the conventional heating occurs through external sources like oil bath: the heat has to penetrate through the vessel in the solution, with a great loss of units of temperature between the vessel itself and the volume inside it. So, the conductive heating process is slower and more inefficient if compared to the microwave-assisted one. The last produces internal heating and, as consequence of the material commonly used for the reaction equipment, the gradient of temperature is inverted if compared to the previous described.[44] This effect can be used to explain the higher yields and the enhanced efficacy of some microwave-assisted reactions. Due to the theory behind this technology, it is clear that polar substances are easily heated while apolar ones are not affected by the radiation, so they are not heated. Selective heating of solvents, reagents and catalyst can be observed. In particular, the polar nature of the catalysts brings to the definition of different temperatures for the catalyst and the bulk solution, which implicates that some catalyzed reactions are more efficient under microwave-assistance.[43]

Taking into account all these considerations, we proceeded setting the conditions to perform the Knöevenagel reaction previously mentioned (i.e. catalysis by 15 mol% of piperidine) under the assistance of microwaves for the synthesis of various alkylidene malonates, malonamides, acetoacetates and acetoacetamides. As regard alkylidene malonates and acetoacetates, we started with the optimization of the reaction of dimethylmalonate or tert-butyl acetoacetate with isobutanal: the reaction occurs with equimolar amount of the two reactants in presence of 15 mol% of piperidine under microwave-irradiation at 250 Watt for 7 min, obtaining the isobutylidene tert-butyl acetoacetate **8b** or isobutylidene dimethyl malonate **8a** with yield of 90% after flash chromatography (Figure 2.5) [45]. The same reaction was previously reported in literature with the

catalysis of proline (10mol%) at room temperature in DMSO for 16 h with yield of 72% [29] or with great excess of aldehyde (10 equivalents) under irradiation by microwave at 500 Watt for 7,5 min with yield of 87%. [46]

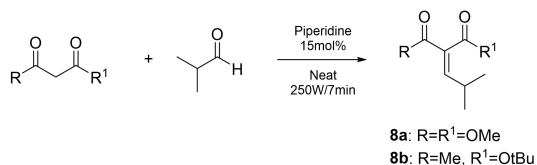


Figure 2.5: Synthesis of alkylidene malonate and acetoacetate under microwave assistance.

The same reaction was then extended in a small library of compounds obtained changing aldehyde and acetoacetate (Figure 2.6), in order to obtain the substrates for a Yonemitsu-type trimolecular condensation that will be described in the next chapters.

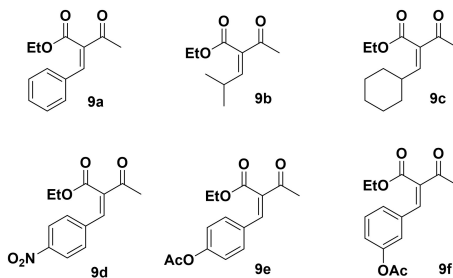


Figure 2.6: Alkylidene acetoacetate obtained through microwave assisted Knoevenagel condensation.

Further studies were made to optimize a microwave assisted protocol for the synthesis of alkylidene malonamides and acetoacetamides. We recently reported the synthesis of unsaturated malonamides as scaffolds for the synthesis of several heterocycles.[47] Starting from these results we proceeded with the synthesis of α,β -unsaturated acetoacetamides,

through the employment of Knövenagel condensation between β -ketoamides and aldehydes.[48] They have been synthesized by a one-pot two-step protocol based on the preparation of amino-acid-derived- β -keto amides **10** through microwave irradiation: the first step is the acetoacetylation of aminoacids, followed by Knövenagel condensation (Figure 2.7). The

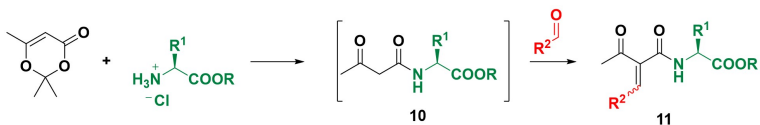


Figure 2.7: One-pot two-steps synthesis of α,β -unsaturated acetoacetamides.

optimization was initially performed on each step. The synthesis of β -ketoamides is carried out by opening of 2,2,6-trimethyl-4*H*-1,3-dioxin-4-one (DAA) [49] since simple acetoacetylating agents may afford the concurrent condensation of the amine on the ketone, leading to β -enamino derivatives. There are two mechanisms proposed for this reaction: the unimolecular formation of acetylketene concomitant to release of acetone (Figure 2.8, Path A) or a bimolecular pathways with nucleophilic attack of amine on dioxinone and elimination of acetone (Figure 2.8, Path B).

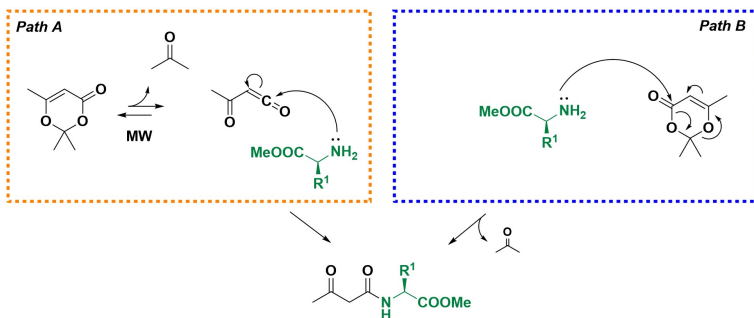


Figure 2.8: Possible mechanisms for the reaction of dioxinone with amino esters.

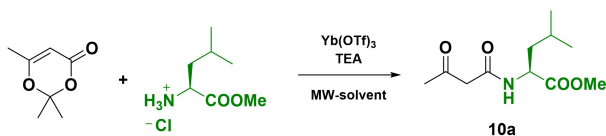


Figure 2.9: Model reaction between dioxinone and leucine methyl ester.

The first mechanism have been confirmed by kinetic and spectroscopic studies, which underline that the decomposition of dioxinone is a reversible process [50]. We chose as standard reaction that between leucine methyl ester and DAA (Figure 2.9). Some results are reported in Table 2.1.

Table 2.1: Optimization of dioxinone ring opening reaction.

Entry	Solvent	MW power	Time (min)	Catalyst (mol%)	Yield (%) ^[a]
1	toluene	250 W	5	10	—
2	1,4-dioxane	250 W	5	10	—
3	tol1, 4-dioxane	250 W	5	10	—
4	chlorobenzene	250 W	5	10	57
5	DMF	250 W	5	10	70
6	tolDMF(3:1)	250 W	5	10	24
7	tolDMF(2:1)	250 W	5	10	44
8	tolDMF(1:1)	250 W	5	10	> 95
9	solvent free	250 W	5	10	0
10	tolDMF(1:1)	250 W	5	0	72
11	tolDMF(1:1)	250 W	10	0	> 95
12	tolDMF(1:1)	80 W	45	10	67
13	tolDMF(1:1)	100 W	20	10	> 95
14	tolDMF(1:1)	300 W	5	10	77

[a] When the conversion was uncomplete, signals due to the dioxinone protons were observed in the ¹H NMR spectrum of the crude reaction mixture.

In the first screening, the solvent had to be selected, since the amino

acids are solid compounds. This matter represents a great improvement over the already reported methods, in which commonly liquid amines are used. Initially, the reaction was performed in presence of $\text{Yb}(\text{OTf})_3$, as catalyst, by MW irradiation at 250 Watt for 5 min. As reported in Table 2.1 (entry 1-3), the reaction doesn't work in toluene, dioxane or mixture of them, as consequence of their low ability to convert electromagnetic energy into heat. When chlorobenzene is used (entry 4), the product is isolated in 57% yield. If DMF is used as solvent (entry 5), the yield is 70% but the removal of the solvent is quite difficult. For this reason, 3:1 and 2:1 mixtures of toluene and DMF have been tried (entry 6 and 7) with encouraging results. So, with a 1:1 mixture of the same solvents (entry 8) the conversion is complete. The reaction in which the dioxinone is used as solvent (entry 9) doesn't occur. Moreover, we observed that when the conversion is not complete dioxinone is always present in the mixture: this information confirms that the decomposition to give acetylketene is a reversible process [50]. Further investigation showed that the presence of catalyst was not necessary even if without it the reaction time had to be doubled to obtain complete conversion (entry 10 and 11). Different setting conditions of the microwave oven showed that lowering the power longer time is required (entry 12 and 13), while stronger irradiation gave an increase in the formation of by-products (entry 14). The optimal conditions were then applied to different amino ester (Figure 2.10): the results are reported in Table 2.2.

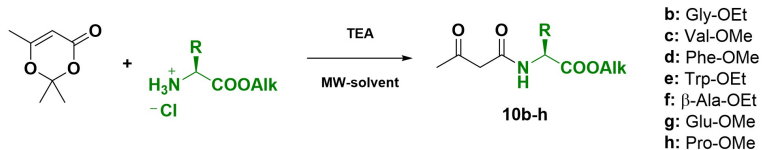


Figure 2.10: Reaction of dioxinone and amino ester under the optimized conditions.

Table 2.2: Reaction of dioxinone with amino esters.

Entry	Reagent	MW power	Time (min)	Catalyst (mol%)	Yield (%) ^[a]
1	Gly-OEt	250 W	5	10	> 95
2	Gly-OEt	250 W	5	0	41
3	Gly-OEt	250 W	10	0	> 95
4	Val-OMe	250 W	5	10	83
5	Val-OMe	250 W	5	0	72
6	Val-OMe	250 W	10	0	> 95
7	Phe-OMe	250 W	10	0	> 95
8	Trp-OEt	250 W	10	0	> 95
9	β -Ala-OEt	250 W	15	0	> 95
10	Glu-OMe	250 W	10	0	86
11	Pro-OMe	250 W	15	0	86

[a] When the conversion was uncomplete, signals due to the dioxinone protons were observed in the ¹H NMR spectrum of the crude reaction mixture.

Different trials were done with and without catalyst using amino esters of phenylalanine, glycine, valine and tryptophan. As reported in Table 2.2, when glycine ethyl ester was used, the reaction gives complete conversion in presence of catalyst (entry 1) while to obtain the same result without catalyst the irradiation time has to be increased to 10 min (entry 2 and 3). The same trend was observed using valine (entry 4-6): without the catalyst, yield of 72% was reached after 5 min of irradiation (entry 5), but elonging the reaction time to 10 min complete conversion was obtained (entry 6). As regards tryptophan ethyl ester (entry 8) and phenylalanine methyl ester (entry 7) good results comparable with those previously shown for the same conditions were detected. Considering the possibility to avoid the employment of catalyst by using longer irradiation times, we extended the study using β -alanine methyl ester (entry 9), methyl glutamate (entry 10) and proline methyl ester (entry 11). By

modulation of the reaction times for each amino ester, good results have been reported for them too by using the same conditions. Starting from these results, we proceeded with the optimization of the second step, the Knöevenagel condensation, in a microwave assisted one-pot two-steps protocol (Figure 2.11). As previously described, the procedure was first optimized for leucine methyl ester and then extended to other amino esters and aldehydes as reported in Table 2.3.

Table 2.3: Optimization of one-pot two-steps sequence with leucine methyl ester.

Entry	Reagent	Aldehyde (equiv.) ^[b]	Base (mol%)	Product	Yield (%)	ZE ratio
1	Leu-OMe	iPrCHO (3)	0	11a	9	9:1
2	Leu-OMe	iPrCHO (6)	0	11a	84	9:1
3	Leu-OMe	iPrCHO (12)	0	11a	90	9:1
4 ^[a]	Leu-OMe	iPrCHO (6)	10	11a	92	9:1
5	Leu-OMe	C ₆ H ₁₁ CHO (1.5)	0	12a	95	9:1
6	Leu-OMe	PhCHO (1.5)	0	13a	95	95 : 5

[a] The second step was stopped after 30 min.

[b] When conversion was incomplete, signals due to acetoacetamide intermediate were observed in the ¹H NMR spectrum of the crude reaction mixture.

The best results have been obtained by irradiation in the second step for 45 min, while longer times gave increasing of by-products without enhancement of yield. When volatile aldehydes have been used, great excess of them was required (entry 1-3), while as regards high boiling point aldehydes the amount decreased to 1.5 equivalents (entry 5 and

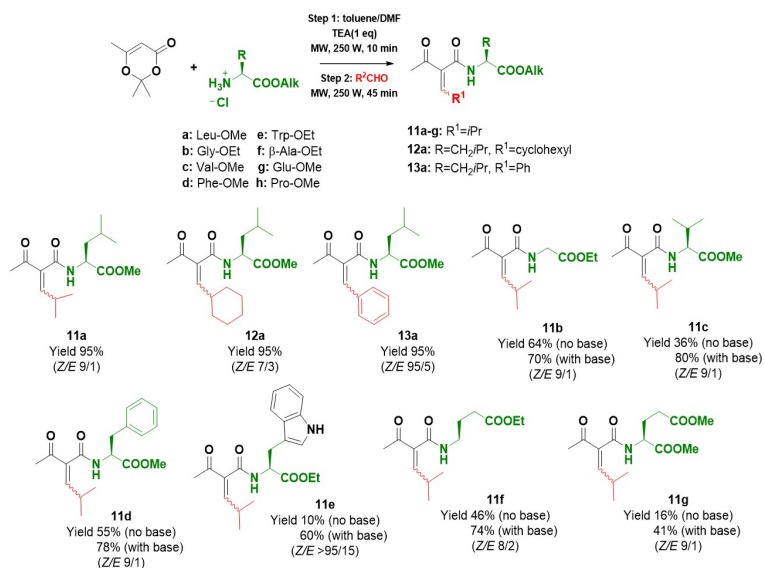


Figure 2.11: One-pot two-steps reaction for the synthesis of alkylidene-amides.

6). By addition of piperidine as catalyst in the Knoevenagel condensation (entry 4), reduction in time of reaction and increasing overall yield were possible. When this protocol was extended to proline methyl ester, none Knoevenagel product can be detected as consequence of the reduced reactivity of the methylene group of a tertiary amide and of the higher rigidity of the molecule [51]. The *Z/E* ratios were always in favor of *Z* isomer as consequence of the steric hindrance linked to the aldehyde and the side-chain of the amino ester [46]. This protocol shows how it is possible to realize the same reaction in bigger scales: in fact, the reaction with isobutyraldehyde and leucine methyl ester gave quantitative yield by elongation of the reaction time to 60 min. Moreover, trials to demonstrate that the conventional heating is unsuccessful were performed, since they require long reaction times and bring to formation of several

by-product.

2.3 Conclusions

By developing efficient protocols for the synthesis of alkylidene or arylidene malonamides, acetoacetamides, acetoacetate and malonate it was possible to obtain small libraries of compounds employed as starting materials for the synthesis of more complex structures. Performing the Knoevenagel condensation with the catalysis of piperidine or $\text{Ti}(\text{Cl})_4$, it is possible to synthesize with good yield but commonly long reaction times different kinds of alkylidene acetoacetates, malonamides and malonates. The introduction of microwave technology allowed improvements on the previous mentioned conditions: the MW-induced heating gives a reduction of the reaction times and an enhancement of the yield due to a bigger reactivity of the polar intermediate of the catalyzed and not catalyzed reactions. In particular, microwave have been used in a one-pot two-step protocol for the preparation of amino-acid derived unsaturated acetoacetamides, decreasing the amount of catalyst needed both for the dioxinone ring opening (concerning the synthesis of N-amino ester acetoacetamide) and for the Knoevenagel reaction.

2.4 Experimental procedures

2.4.1 General methods

All chemicals were purchased from commercial suppliers and were used without further purification. Microwave-assisted reaction were carried out in Milestone Mycosynth apparatus, with a dual magnetron system with a pyramid-shaped diffuser, 1000 W maximum power output, and temperature monitor and control by optical fiber up to a vessel tem-

perature of 250 °C. Flash chromatography was carried out on silica gel (230-400 mesh). Dowex®50WX2-200(H) ion exchange resin was used for purification of free amino acids or free amines. NMR spectra were recorded with a Varian Mercury Plus 400 or Varian Gemini 200 instruments. Chemical shifts are reported as δ values (ppm), and were calibrated using the residual solvent peaks of: CDCl_3 , set a $\delta = 7.27$ ppm (^1H NMR) or $\delta = 77.0$ ppm (^{13}C NMR); CD_3OD , set at $\delta = 3.31$ ppm (^1H NMR) and $\delta = 49.0$ ppm (^{13}C NMR); D_2O , set at $\delta = 4.79$ ppm (^1H NMR); CD_3CN , set at $\delta = 1.93$ ppm (^1H NMR) and $\delta = 117.7$ ppm (^{13}C NMR); $(\text{CD}_3)_2\text{CO}$, set at $\delta = 2.04$ ppm (^1H NMR) and $\delta = 29.8$ ppm (^{13}C NMR). Coupling constants are given in Hz. LC-MS analysis was carried out with an HP1100 liquid chromatograph coupled to an electrospray ionization mass spectrometer (LC-ESI-MS), using a Phenomenex Gemini C18 - 3μ - 110 \AA column, $\text{H}_2\text{O}/\text{CH}_3\text{CN}$ as neutral solvent or $\text{H}_2\text{O}/\text{CH}_3\text{CN}$ with 0.2% formic acid as acid solvent at 25 °C (positive-ion mode, $m/z = 100$ -500, fragmentor 70 V). Another set of experiments has been performed on an HP1100 liquid chromatograph coupled with an electrospray ionization-ion trap mass spectrometer MSD1100 using a Phenomenex Zorbax C18 - 3.5μ - 80 \AA column, $\text{H}_2\text{O}/\text{CH}_3\text{CN}$ with 0.08% trifluoroacetic acid as acid solvent (positive scan 100-500 m/z , fragmentor 70 eV).

2.4.2 Synthesis and characterization

Synthesis of N-ethyl methyl malonyl amide (1). In a 2-necked round-bottom flask, equipped to perform reaction under N_2 , ethylamine (1.2 eq) and TEA (2 eq) were added in dry DCM (1M). Methyl malonyl chloride (1 eq) was added dropwise at 0°C and the mixture stirred at room temperature overnight. The reaction was quenched with water and the product extracted with DCM. The product was used without further

purifications (Y% > 99%). ^1H NMR (400 MHz, CDCl_3) δ 7.02 (bs, 1H), 3.73 (s, 3H), 3.44-3.27 (m, 2H), 3.29 (s, 2H), 1.14 (dt, $^3\text{J}=7.2$ Hz, $^4\text{J}=1.6$ Hz, 3H). ^{13}C NMR (400 MHz, CDCl_3) δ 168.2, 166.4, 51.1, 36.5, 33.7, 14.9. LC-ESI-MS: 1.5 min, $[M + H]^+=146$, $[M + Na]^+=178$, $[2M + Na]^+=313$.

General procedure for the synthesis of alkylidene derivatives under basic catalysis at room temperature: (2a,b) and (4). Methylene active compound (1 eq), piperidine (0.15 eq) and aldehyde (1.7 eq) were stirred at room temperature for 12h/3days. The crude was poured in water and extracted with EtOAc. Purification by flash chromatography (silica gel, 9:1=Cy:EtOAc) allowed to isolate the product as a mixture of two isomers (Z/E).

Compound (2a): Y%=56%, Z/E=1/4. E-isomer: ^1H NMR (400 MHz, CDCl_3) δ 6.91 (d, $^3\text{J}=10.4$ Hz, 1H), 6.93 (bs, 1H), 3.74 (s, 3H), 3.41-3.30 (m, 2H), 3.75 (m, 1H), 1.73-1.64 (m, 5H), 1.37-1.07 (m, 5H), 1.17 (t, $^3\text{J}=7.2$ Hz, 3H); ^{13}C NMR (400 MHz, CDCl_3) δ 164.3, 163.7, 155.3, 125.6, 51.3, 38.0, 33.7, 31.3, 25.2, 24.7, 14.0; LC-ESI-MS: 8.9 min, $[M + H]^+=240$, $[M + Na]^+=262$, $[2M + Na]^+=501$. Z-isomer: ^1H NMR (400 MHz, CDCl_3) δ 6.80 (d, $^3\text{J}=10.4$ Hz, 1H), 6.93 (bs, 1H), 3.74 (s, 3H), 3.41-3.30 (m, 2H), 3.75 (m, 1H), 1.73-1.64 (m, 5H), 1.37-1.07 (m, 5H), 1.17 (t, $^3\text{J}=7.2$ Hz, 3H); ^{13}C NMR (400 MHz, CDCl_3) δ 166.7, 164.1, 155.3, 126.8, 51.5, 38.0, 33.7, 31.3, 25.2, 24.7, 14.0; LC-ESI-MS: 6.6 min, $[M + H]^+=240$, $[M + Na]^+=262$, $[2M + Na]^+=501$.

Compound (2b): Y%=55%, Z/E=1/4. E-isomer: ^1H NMR (400 MHz, CDCl_3) δ 6.90 (d, $^3\text{J}=10.4$ Hz, 1H), 6.88 (bs, 1H), 3.76 (s, 3H), 3.40-3.34 (m, 2H), 3.26 (m, 1H), 1.18 (t, $^3\text{J}=7.2$ Hz, 3H), 1.06 (d, $^3\text{J}=6.8$ Hz, 6H). ^{13}C NMR (400 MHz, CDCl_3) δ 166.5, 162.1, 160.3, 124.5, 51.2, 43.5, 29.1, 21.8, 14.9; LC-ESI-MS: 8.8 min $[M + H]^+=200$, $[M + K]^+=238$, $[2M + Na]^+=421$. Z-isomer: ^1H NMR (400 MHz, CDCl_3) δ 6.88 (bs, 1H), 6.79 (d, $^3\text{J}=10.4$ Hz, 1H), 3.76 (s, 3H), 3.40-3.34 (m, 2H), 3.26 (m,

1H), 1.18 (t, $^3J=7.2$ Hz, 3H), 1.06 (d, $^3J=6.8$ Hz, 6H); ^{13}C NMR (400 MHz, CDCl_3) δ 167.7, 163.3, 160.3, 125.0, 51.3, 43.3, 28.9, 21.8, 14.9; LC-ESI-MS: 8.0 min $[M+H]^+=200$, $[M+K]^+=238$, $[2M+Na]^+=421$.

Compound (4): Y%=40%, Z/E=1/4. ^1H NMR (400 MHz, CDCl_3) δ 6.77 (t, J = 8.0 Hz, 1H, E isomer), 6.74 (t, J = 7.6 Hz, 1H, Z isomer), 2.42 (dt, J= 7.6, 7.2 Hz, 2H), 2.29 (s, 3H), 2.23 (dt, J= 2.4, 6.8 Hz, 2H), 1.96 (t, J= 2.4 Hz, 1H), 1.72 (m, 2H), 1.53 (s, 9H); ^{13}C NMR (400 MHz, CDCl_3) δ 194.8, 165.5, 145.1, 138.6, 83.2, 82.1, 69.2, 28.6, 28.0, 27.0, 26.8, 18.0; LC-ESI-MS 9.1 min, $[M + Na]^+=259$, $[M + K]^+=275$, $[2M + Na]^+=495$.

Protection of 5-hexyn-1-ol with TMS-group (5). To a solution of 5-hexyn-1-ol (1 eq) in THF (0.5 M), n-butyllithium (1.5 M in hexane; 2 eq) was added. After 30 min of stirring at -78°C , the reaction was stirred at 0°C for 2 h. At -78°C trimethylsilyl chloride (2.1 eq) was added and the mixture heated to reflux for 12 h and then warmed at room temperature. It was treated with 10% HCl and stirred over 30 min. The reaction was extracted with ethyl ether, washed with brine, dried with sodium sulphate and evaporated under reduced pressure. The crude was used without further purification (Y% > 99%). ^1H NMR (400 MHz, CDCl_3) δ 3.63 (t, J= 6.0 Hz, 2H), 2.26 (t, J= 6.6 Hz, 2H), 1.65, (m, 4H), 0.14 (s, 9H); ^{13}C NMR (400 MHz, CDCl_3) δ 107.0, 84.7, 62.3, 31.7, 24.7, 19.5.

General procedure for the Swern oxidation: (3) and (6). In glasses equipped to perform reaction under inert atmosphere, keeping the temperature at -78°C , a solution of dimethyl sulfoxide (2.3 eq) in DCM (4M) was added to a solution of oxalyl chloride (1.2 eq) in DCM (0.52M), and the mixture was stirred for 5 min. The alcohol (1 eq) in DCM (0.9M) was added dropwise in 5 min and the solution was stirred for 15 min. TEA dry (5 eq) was added dropwise and the mixture was stirred for 10 min at room temperature. The mixture was extracted with ethyl ether and washed with water. The organic layer was evaporated and washed again

with NH_4Cl sat. It was then dried over sodium sulphate and evaporated under reduced pressure to give the product as a yellow oil, used without further purifications.

Compound (3): $\text{Y}\%> 99\%$, $^1\text{H NMR}$ (400 MHz, CDCl_3) δ 9.79 (t, $\text{J}= 1.3$ Hz, 1H), 2.59 (dt, $\text{J}= 1.3, 7.2$ Hz, 2H), 2.26 (dt, $\text{J}= 2.6, 7.2$ Hz, 2H), 1.96 (t, $\text{J}= 2.6$ Hz, 1H), 1.84 (m, 2H); $^{13}\text{C NMR}$ (400 MHz, CDCl_3) δ 200.1, 82.2, 68.6, 45.2, 20.0, 16.7.

Compound (6): $\text{Y}\%=93\%$, $^1\text{H NMR}$ (400 MHz, CDCl_3) δ 9.80 (s, 1H), 2.57 (t, $\text{J}= 6.7$ Hz, 2H), 2.28 (t, $\text{J}= 6.7$ Hz, 2H), 1.85 (m, 2H), 0.12 (s, 9H); $^{13}\text{C NMR}$ (400 MHz, CDCl_3) δ 201.8, 105.8, 85.7, 42.6, 20.9, 19.2, 0.0.

Procedure for the synthesis of alkylidene derivatives by TiCl_4 catalysis: (7). A 1 M solution of TiCl_4 in DCM (2 eq) was added dropwise to THF (0.55M) at 0°C and the mixture was stirred for few minutes. Then tert-butyl acetoacetate (1 eq) in THF (2.3M) and (6) (11 eq) in THF (2.3M) were added at 0°C ; the mixture was stirred for 75 min. A solution of pyridine (4 eq) in THF (5.7M) was then added dropwise in 90 min and the mixture stirred overnight. The solution was diluted with Et_2O and washed with water and brine. The organic layer was dried over Na_2SO_4 and then evaporated. The crude product was purified by flash chromatography (silica gel, 98/2 cyclohexane/ EtOAc) to obtain the product as a 1/4 mixture of Z/E isomers. $\text{Y}\%=83\%$, $^1\text{H NMR}$ (400 MHz, CDCl_3) δ 6.75 (t, $\text{J}= 8.0$ Hz, 1H, E isomer), 6.73 (t, $\text{J}= 7.6$ Hz, 1H, Z isomer), 2.39 (dt, $\text{J}= 7.6, 7.6$ Hz, 2H), 2.28 (s, 3H), 2.24 (m, 2H), 1.68 (m, 2H), 1.53 (s, 9H), 0.12 (s, 9H); $^{13}\text{C NMR}$ (400 MHz, CDCl_3) δ 201.0 (E), 194.8 (Z), 165.5 (Z), 163.3 (E), 145.8 (E), 145.4 (Z), 138.4 (Z), 137.9 (E), 105.9 (Z+E), 85.2 (Z+E), 82.1 (Z), 81.7 (E), 28.7 (Z+E), 28.0 (Z), 27.9 (E), 27.8 (E), 27.4 (E), 27.2 (Z), 26.8 (Z), 19.5 (Z), 19.3 (E), 0.0 (Z+E); LC-ESI-MS: 12.5 min, m/z: $[\text{M} + \text{Na}]^+=331$, $[\text{M} + \text{K}]^+=347$, $[2\text{M} + \text{Na}]^+=639$.

General procedure for the synthesis of alkylidene and arylidene

malonate or acetoacetate under microwave assistance: (8a,b) and (9a,f). Dimethyl malonate, ethyl acetoacetate or tert-butyl acetoacetate (1 eq), aldehyde (1 eq) and piperidine (0.15 equiv) were stirred in the microwave reactor and irradiated at 250 W for 7 min. The mixture was diluted with EtOAc, washed with water, dried on sodium sulphate and evaporated under reduced pressure. The crude was purified by flash chromatography (98/2=cyclohexane:AcOEt, in gradient) and the two Z/E isomers separated. The yield and Z/E ratio depends on the substrate.

Compound (8a): Y%=80%, E/Z > 95%, ^1H NMR (400 MHz, CDCl_3) δ 6.85 (d, J= 10.8 Hz, 1H), 3.80 (s, 3H), 3.76 (s, 3H), 2.60-2.73 (m, 1H), 1.08 (d, J= 6.6 Hz, 6H).

Compound (8b): Y% > 99%, Z/E=4/1. Z isomer: ^1H NMR (200 MHz, CDCl_3) δ 6.53 (d, 1H, J= 10.4 Hz), 2.65 (m, 1H), 2.30 (s, 3H), 1.55 (s, 9H), 1.09 (d, 6H, J= 6.45 Hz); LC-ESI-MS 9.5 min, m/z: $[M+H]^+=235$. E isomer: ^1H NMR (200 MHz, CDCl_3) δ 6.58 (d, 1H, J= 10.6 Hz), 2.60 (m, 1H), 2.34 (s, 3H), 1.51 (s, 9H), 1.45 (d, 6H, J= 6.6 Hz); LC-ESI-MS 10.2 min, m/z: $[M+H]^+=235$.

Compound (9a): Y%=95%, Z/E=3/1, Z isomer: ^1H NMR (200 MHz, CDCl_3) δ 7.58 (s, 1H), 7.28-7.48 (m, 5H), 4.34 (q, J = 7.2 Hz, 2H), 2.43 (s, 3H), 1.28 (t, J = 7.2 Hz); ^{13}C NMR (200 MHz, CDCl_3) δ 194.6, 167.7, 141.2, 134.6, 132.9, 130.7, 129.5, 128.8, 61.5, 26.5, 13.8. E isomer: ^1H NMR (200 MHz, CDCl_3) δ 7.68 (s, 1H), 7.34-7.39 (m, 5H), 4.30 (q, J = 7.2 Hz, 2H), 2.36 (s, 3H), 1.34 (t, J = 7.2 Hz); ^{13}C NMR (200 MHz, CDCl_3) δ 203.3, 164.3, 140.4, 134.0, 132.8, 130.3, 129.6, 128.8, 61.5, 31.1, 14.1. Anal. Calcd. For $\text{C}_{13}\text{H}_{14}\text{O}_3$: C, 71.54; H, 6.47. Found: C, 71.59; H, 6.48.

Compound (9b): Y%=87%, Z/E=2.3/1, Z isomer: ^1H NMR (200 MHz, CDCl_3) δ 6.60 (d, 1H, J= 10.6 Hz), 4.29 (q, 2H, J= 7.4 Hz), 2.65 (m, 1H), 2.30 (s, 3H), 1.31 (t, 3H, J= 7.4 Hz), 1.07 (d, 6H, J= 6.6 Hz); ^{13}C NMR (200 MHz, CDCl_3) δ 195.4, 166.6, 154.0, 134.9, 61.2, 29.6, 26.8, 21.9

(2), 14.1; GC-MS: 11.74 min, m/z: 184(2), 138(100), 123(60), 110(15), 96(57), 81(24), 67(32), 55(26). E isomer: ^1H NMR (200 MHz, CDCl_3) δ 6.69 (d, 1H, J= 10.6 Hz), 4.24 (q, 2H, J= 7.4 Hz), 2.62 (m, 1H), 2.37 (s, 3H), 1.30 (t, 3H, J= 7.4 Hz), 1.02 (d, 6H, J= 6.6 Hz); ^{13}C NMR (200 MHz, CDCl_3) δ 197.9, 166.5, 154.0, 134.8, 61.1, 29.4, 26.5, 21.8, 21.6, 13.9; GC-MS: 11.45 min, m/z: 184(2), 138(100), 123(55), 110(15), 96(64), 81(26), 67(31), 55(19).

Compound (9c): Y%=78%, Z/E=2.4/1, Z isomer: ^1H NMR (200 MHz, CDCl_3) δ 6.63 (d, 1H, J= 9.8 Hz), 4.30 (q, 2H, J=7.0 Hz), 2.37 (m, 1H), 2.31 (s, 3H), 1.60-1.77 (m, 5H), 1.34 (t, 3H, J= 7.0 Hz), 1.21-1.43 (m, 5H); ^{13}C NMR (200 MHz, CDCl_3) δ 197.9, 166.6, 152.5, 135.2, 61.0, 39.1, 31.8, 31.7, 26.7, 25.3, 25.1(2), 14.1; GC-MS: 9.3 min, m/z: 225. E isomer: ^1H NMR (200 MHz, CDCl_3) δ 6.72 (d, 1H, J= 10.6 Hz), 4.26 (q, 2H, J= 7.0 Hz), 2.42 (m, 1H), 2.38 (s, 3H), 1.66-1.77 (m, 5H), 1.27 (t, 3H, J= 7.0 Hz), 1.14-1.26 (m, 5H); ^{13}C NMR (200 MHz, CDCl_3) δ 201.3, 164.7, 152.8, 133.9, 61.0, 38.3, 31.9 (2), 31.3, 25.6, 25.0 (2), 14.1; GC-MS: 10.0 min, m/z: 225.

Compound (9d): Y%=80%, only Z isomer: ^1H NMR (400 MHz, CDCl_3) δ 8.16 (m, 2H), 7.62 (s, 1H), 7.56 (d, 2H, J= 8.4 Hz), 7.50 (d, 2H, J= 8.4 Hz), 4.27 (q, J= 7.2 Hz, 2H), 2.38 (s, 3H), 1.20 (t, J= 7.2 Hz, 3H); ^{13}C NMR (200 MHz, CDCl_3) δ 198.5, 165.2, 147.9, 147.3, 138.9, 132.5 (2C), 130.6, 123.8 (2C), 61.2, 29.8, 14.4.

Compound (9e): Y%=79%, only Z isomer: ^1H NMR (400 MHz, CDCl_3) δ 8.62 (s, 1H), 7.63 (d, 2H, J= 8.3 Hz), 7.27 (d, 2H, J= 8.3 Hz), 4.20 (q, J= 7.1 Hz, 2H), 2.36 (s, 3H), 2.32 (s, 3H), 1.24 (t, J= 7.1 Hz, 3H); ^{13}C NMR (200 MHz, CDCl_3) δ 198.7, 168.9, 165.1, 150.7, 149.1, 130.6, 129.5, 129.4 (2C), 121.7 (2C), 61.3, 28.9, 21.0, 14.2.

Compound (9f): Y%=81%, only Z isomer: ^1H NMR (400 MHz, CDCl_3) δ 8.63 (s, 1H), 7.57 (m, 1H), 7.45 (m, 1H), 7.30 (m, 1H), 7.12 (m, 1H), 4.18 (q, J= 7.3 Hz, 2H), 2.45 (s, 3H), 2.32 (s, 3H), 1.27 (t, J= 7.3 Hz,

3H); ^{13}C NMR (200 MHz, CDCl_3) δ 198.6, 169.0, 165.0, 151.1, 149.0, 148.7, 131.2, 129.8, 125.5, 121.1, 120.9, 62.1, 29.7, 20.4, 14.5.

General procedure for the preparation of (3-oxobutanoyl)-L-amino esters: (10a,h). 2,2,6-trimethyl-4H-1,3-dioxin-4-one (1 eq), triethylamine (1 eq) and amino ester (1 eq) were dissolved in a mixture of toluene/DMF (1mL + 1mL) in the microwave reactor. The mixture was irradiated (250W, 5 minutes) and then allowed to cool to room temperature under stirring. The mixture was diluted with EtOAc and washed with water and brine. The organic layer was dried over Na_2SO_4 and evaporated. The crude product was purified by flash chromatography over silica (cyclohexane/ ethyl acetate 80:20).

Compound (10a): ^1H NMR (400 MHz, CDCl_3) δ 7.21 (bd, 1H), 4.63 (m, 1H), 3.74 (s, 3H), 3.46 (s, 2H), 2.26 (s, 3H), 1.57 (m, 3H), 0.95 (d, 6H, $J=7.2$ Hz); ^{13}C NMR (400 MHz, CDCl_3) δ 203.8, 173.0, 165.6, 52.0, 50.6, 49.6, 40.9, 30.5, 24.6, 22.6, 21.6; LC-ESI-MS: 3.89 min, m/z : $[M + H]^+=230$, $[M + Na]^+=252$, $[2M + Na]^+=481$.

Compound (10b): ^1H NMR (400 MHz, CDCl_3) δ 7.36 (bt, 1H), 4.19 (d, 2H, $J=5.2$ Hz), 4.06 (q, 2H, $J=7.2$ Hz), 3.45 (s, 2H), 2.26 (s, 3H), 1.20 (t, 3H, $J=7.2$ Hz); ^{13}C NMR (400 MHz, CDCl_3) δ 203.4, 175.5, 169.4, 61.0, 49.6, 41.0, 30.0, 13.7. LC-ESI-MS: 3.10 min, m/z : $[M + Na]^+=210$.

Compound (10c): ^1H NMR (400 MHz, CDCl_3) δ 7.35 (bd, 1H, $J=9.6$ Hz), 4.53 (dd, 1H, $J=4.4, 9.6$ Hz), 3.72 (s, 3H), 3.46 (s, 2H), 2.27 (s, 3H), 2.19 (m, 1H), 0.95 (d, 3H, $J=7.2$ Hz), 0.92 (d, 3H, $J=7.2$ Hz); ^{13}C NMR (400 MHz, CDCl_3) δ 203.2, 173.4, 167.7, 57.5, 52.1, 49.4, 30.7, 29.8, 20.0, 19.8; LC-ESI-MS: 2.50 min, m/z : $[M + H]^+=216$, $[M + Na]^+=238$, $[2M + Na]^+=453$.

Compound (10d): ^1H NMR (400 MHz, CDCl_3) δ 7.15-7.41 (m, 6H), 4.82 (m, 1H), 3.76 (s, 3H), 3.39 (s, 2H), 3.00 (m, 2H), 2.18 (s, 3H);

^{13}C NMR (400 MHz, CDCl_3) δ 203.6, 172.4, 166.2, 134.5, 127.8 (2C), 127.2 (2C), 126.8, 58.7, 52.3, 49.2, 37.5, 30.2; LC-ESI-MS: 4.42 min, m/z: $[M + H]^+ = 264$, $[M + Na]^+ = 286$, $[2M + Na]^+ = 549$.

Compound (10e): ^1H NMR (400 MHz, CDCl_3) δ 8.66 (bs, 1H), 7.51 (d, 1H, $J = 7.6$ Hz), 7.34 (d, 1H, $J = 8.0$ Hz), 7.22 (d, 1H, $J = 8.4$ Hz), 6.93-7.15 (m, 3H), 4.88 (dt, 1H, $J = 8.0, 6.4$ Hz), 4.10 (m, 2H), 3.28 (m, 2H), 3.17 (s, 2H), 2.14 (s, 3H), 1.18 (t, 3H, $J = 7.2$ Hz); ^{13}C NMR (400 MHz, CDCl_3) δ 203.9, 172.2, 165.7, 136.1, 127.4, 123.1, 122.1, 119.5, 118.4, 111.3, 109.5, 61.3, 53.0, 49.5, 30.6, 29.6, 14.2; LC-ESI-MS: 4.75 min, m/z: $[M + H]^+ = 317$, $[M + Na]^+ = 339$.

Compound (10f): ^1H NMR (400 MHz, CDCl_3) δ 7.26 (bd, 1H), 4.17 (q, 2H, $J = 7.4$ Hz), 3.53 (dt, 2H, $J = 6.2, 6.8$ Hz), 3.40 (s, 2H), 2.55 (t, 2H, $J = 6.2$ Hz), 2.27 (s, 3H), 1.28 (t, 3H, $J = 7.4$ Hz); ^{13}C NMR (400 MHz, CDCl_3) δ 203.0, 172.6, 166.0, 61.0, 49.7, 36.2, 32.8, 31.0, 14.2; LC-ESI-MS: 1.41 min, m/z: $[M + H]^+ = 188$, $[M + Na]^+ = 210$, $[2M + Na]^+ = 397$.

Compound (10g): ^1H NMR (400 MHz, CDCl_3) δ 7.21 (bd, 1H), 4.62 (m, 1H), 3.65 (s, 3H), 3.64 (s, 3H), 3.41 (s, 2H), 2.28 (s, 3H), 2.01-2.41 (m, 4H); ^{13}C NMR (400 MHz, CDCl_3) δ 203.3, 172.3, 171.7, 162.6, 52.2, 51.5, 50.8, 49.8, 31.2, 27.1, 26.4; LC-ESI-MS: 2.42 min, m/z: $[M + H]^+ = 260$, $[M + Na]^+ = 282$.

Compound (10h): ^1H NMR (400 MHz, CDCl_3) δ 4.52 (m, 1H), 3.78 (s, 3H), 3.20-3.40 (m, 2H), 2.22 (s, 3H), 1.90-2.05 (m, 4H); ^{13}C NMR (400 MHz, CDCl_3) δ 202.9, 172.4, 168.7, 63.8, 52.2, 49.8, 48.6, 29.9, 28.5, 24.6; LC-ESI-MS: 2.38 min, m/z: $[M + H]^+ = 214$.

General procedure for the preparation of alkylidene acetacetamides via one-pot two-step: (11a,g), (12a) and (13a). 2,2,6-trimethyl-4H-1,3-dioxin-4-one (1 eq), amino ester (1 eq) and triethylamine (1 eq) were added to a mixture of toluene/DMF (1:1, 0.5M) and stirred under microwave irradiation for 5 min at 250W. After cooling at room temperature, aldehyde (see Table 2.2) was added and the reaction irradiated again

for 45 min at 250W. The mixture was diluted with EtOAc and washed with water and brine. After drying with sodium sulphate, the organic phase was evaporated and the crude purified by flash chromatography over silica gel (cyclohexane/ ethyl acetate 80:20).

Compound (11a): ^1H NMR (400 MHz, CDCl_3) δ 7.11 (bd, 1H, $J=6.4$), 6.79 (d, 0.1H, $J=10.4$ Hz, E isomer), 6.70 (d, 0.9H, $J=10.0$ Hz, Z isomer), 4.71 (m, 1H), 3.75 (s, 2.7H, Z isomer), 3.74 (s, 0.3H, E isomer), 3.16 (m, 1H), 2.43 (s, 0.3H, E isomer), 2.37 (s, 2.7H, Z isomer), 1.60-1.80 (m, 3H), 1.10 (d, 6H, $J=6.6$ Hz), 0.96 (d, 6H, $J=6.0$ Hz); ^{13}C NMR (400 MHz, CDCl_3) δ 196.5, 172.4, 165.4, 155.0, 135.5, 51.6, 50.2, 40.3, 28.6, 26.4, 24.3, 22.3, 21.5, 21.4, 21.0; LC-ESI-MS: 6.85 min, m/z : $[M + H]^+=283$, $[M + Na]^+=306$.

Compound (11b): ^1H NMR (400 MHz, CDCl_3) δ 7.36 (bt, 1H), 6.80 (d, 0.1H, $J=11.2$ Hz, E isomer), 6.64 (d, 0.9H, $J=10.8$ Hz, Z isomer), 4.17 (q, 2H, $J=6.8$ Hz), 4.06 (d, 2H, $J=5.2$ Hz, Z isomer), 4.01 (d, 0.2H, $J=4.8$ Hz, E isomer), 3.12 (m, 1H), 2.32 (s, 0.3H, E isomer), 2.30 (s, 2.7H, Z isomer), 1.21 (d, 3H, $J=6.6$ Hz), 1.19 (d, 3H, $J=6.6$ Hz), 1.04 (t, 3H, $J=6.8$ Hz); ^{13}C NMR (400 MHz, CDCl_3) δ 197.4, 169.4, 165.9, 156.5, 135.5, 61.2, 41.1, 29.0, 26.6, 21.9 (2C), 14.0; LC-ESI-MS: 5.37 min, m/z : $[M + H]^+=242$, $[M + Na]^+=264$.

Compound (11c): ^1H NMR (400 MHz, CDCl_3) δ 7.18 (bd, 1H, $J=9.6$ Hz), 6.68 (d, 1H, $J=8.8$ Hz), 4.61 (dd, 1H, $J=4.8, 9.6$ Hz), 3.73 (s, 3H), 3.17 (m, 1H), 2.34 (s, 3H), 2.12 (m, 1H), 1.10 (d, 6H, $J=6.6$ Hz), 0.98 (d, 3H, $J=7.2$ Hz), 0.93 (d, 3H, $J=7.2$ Hz); ^{13}C NMR (400 MHz, CDCl_3) δ 198.4, 172.5, 165.1, 153.8, 134.8, 57.1, 52.0, 30.2, 29.8, 24.2, 21.9, 21.7, 20.0, 19.9; LC-ESI-MS: 7.53 min, m/z : $[M + H]^+=270$, $[M + Na]^+=292$.

Compound (11d): ^1H NMR (400 MHz, CDCl_3) δ 7.10-7.34 (m, 5H), 6.98 (bd, 1H, $J=6.8$), 6.61 (d, 1H, $J=10.2$ Hz), 4.98 (m, 1H), 3.77 (s, 3H), 3.21 (dd, 1H, $J=5.6, 14.0$ Hz), 3.11 (dd, 1H, $J=7.2, 14.0$ Hz), 2.91

(m, 1H), 2.35 (s, 3H), 1.02 (d, 3H, J= 6.6 Hz), 0.98 (d, 3H, J=6.6 Hz); ^{13}C NMR (400 MHz, CDCl_3) δ 198.8, 171.9, 157.9, 154.1, 136.7, 134.8, 128.4, 127.7, 125.6, 57.3, 51.6, 37.2, 30.1, 24.6, 22.2, 21.8; LC-ESI-MS: 7.10 min, m/z: $[M + H]^+ = 318$, $[M + Na]^+ = 340$, $[2M + Na]^+ = 657$.

Compound (11e): ^1H NMR (400 MHz, CDCl_3) δ 8.45 (bs, 1H), 7.56 (d, 1H, J= 8.0 Hz), 7.32 (d, 1H, J= 8.4 Hz), 7.06-7.17 (m, 3H), 6.96 (bd, 1H, J= 7.6 Hz), 6.57 (d, 1H, J= 10.6 Hz), 5.01 (m, 1H), 4.11 (m, 2H), 3.37 (dd, 1H, J= 5.6, 12.0 Hz), 3.35 (dd, 1H, J= 6.0, 12.0 Hz), 2.87 (m, 1H), 2.24 (s, 3H), 1.19 (t, 3H, J= 6.8 Hz), 0.97 (d, 3H, J= 6.6 Hz), 0.94 (d, 3H, J= 6.6 Hz); ^{13}C NMR (400 MHz, CDCl_3) δ 197.2, 172.0, 165.9, 155.9, 136.0, 135.7, 127.1, 123.3, 121.6, 119.0, 118.0, 111.2, 108.9, 61.3, 52.7, 31.2, 29.0, 26.4, 21.7, 18.8, 14.1; LC-ESI-MS: 8.81 min, m/z: $[M + H]^+ = 371$, $[M + Na]^+ = 393$, $[2M + Na]^+ = 763$.

Compound (11f): ^1H NMR (400 MHz, CDCl_3) δ 7.08 (bt, 1H), 6.77 (d, 0.2H, J= 11.4 Hz, E isomer), 6.72 (d, 0.8H, J= 11.4 Hz, Z isomer), 4.18 (q, 2H, J= 7.4 Hz), 3.57 (dt, 2H, J= 6.2, 6.8 Hz), 2.82 (m, 1H), 2.57 (t, 2H, J= 6.4 Hz), 2.45 (s, 0.6H, E isomer), 2.42 (s, 2.4H, Z isomer), 1.27 (t, 3H, J= 7.4 Hz), 1.09 (d, 3H, J= 6.8 Hz), 1.07 (d, 3H, J= 6.8 Hz); ^{13}C NMR (400 MHz, CDCl_3) δ 197.1, 172.4, 162.6, 155.2, 136.2, 61.1, 36.3, 31.2, 26.3, 21.7(2C), 14.2; LC-ESI-MS: 5.41 min, m/z: $[M + H]^+ = 256$, $[M + Na]^+ = 278$.

Compound (11g): ^1H NMR (400 MHz, CDCl_3) δ 7.38 (bd, 1H), 6.65 (d, 0.1H, J= 11.2 Hz, E isomer), 6.62 (d, 0.9H, J= 10.8 Hz, Z isomer), 3.76 (s, 3H), 3.75 (s, 3H), 3.03 (m, 1H), 2.38 (s, 3H), 2.01-2.41 (m, 4H), 1.18 (d, 3H, J= 6.6 Hz), 1.06 (d, 3H, J= 6.6 Hz); ^{13}C NMR (400 MHz, CDCl_3) δ 203.4, 172.8, 172.3, 165.9, 149.9, 137.3, 55.3, 51.5, 51.1, 33.4, 26.9, 25.6, 24.5, 19.1, 18.7; LC-ESI-MS: 4.10 min, m/z: $[M + H]^+ = 314$, $[M + Na]^+ = 336$, $[2M + Na]^+ = 649$.

Compound (12a): ^1H NMR (400 MHz, CDCl_3) δ 7.02 (bd, 1H, J= 8.2 Hz), 6.79 (d, 0.1H, J= 10.8 Hz, E isomer), 6.70 (d, 0.9H, J= 10.2 Hz,

Z isomer), 4.72 (m, 1H), 3.72 (s, 2.7H, Z isomer), 3.68 (s, 0.3H, E isomer), 2.84 (m, 1H), 2.41 (s, 0.3H, E isomer), 2.33 (s, 2.7H, Z isomer), 1.56-1.81 (m, 8H), 1.11-1.40 (m, 5H), 0.98 (d, 3H, J= 6.6 Hz), 0.96 (d, 3H, J= 6.6 Hz); ^{13}C NMR (400 MHz, CDCl_3) δ 198.1, 173.2, 164.7, 157.1, 136.2, 52.8, 50.8, 40.5, 33.1 (2C), 31.6, 28.9, 26.4, 25.3 (2C), 24.9, 21.7, 21.0; LC-ESI-MS: 8.82 (Z isomer), 10.08 (E isomer) min, m/z: $[M + H]^+=324$, $[M + Na]^+=346$.

Compound (13a): ^1H NMR (400 MHz, CDCl_3) δ 7.35 (s, 1H), 7.20-7.90 (m, 5H), 6.20 (bd, 1H), 4.69 (m, 1H), 3.78 (s, 3H), 2.41 (s, 3H), 1.45-1.80 (m, 3H), 1.00 (d, 3H, J= 6.6 Hz), 0.98 (d, 3H, J= 6.6 Hz); ^{13}C NMR (400 MHz, CDCl_3) δ 195.0, 172.3, 162.8, 162.3, 139.7, 136.1, 129.3, 128.6, 128.2, 128.1, 51.6, 50.6, 40.3, 31.0, 26.6, 22.4, 21.1; LC-ESI-MS: 7.67 min, m/z: $[M + H]^+=318$, $[M + Na]^+=340$, $[2M + Na]^+=657$.

2.5 Notes and references

The spectroscopic data and the synthetic procedures have been adapted from Ref. [38], [45] and [48], with the proper reuse licenses. See Appendix.

Chapter3

Reactivity of alkylidene or arylidene derivatives for the synthesis of isoxazolidinones, isoxazolines and dehydro- β -prolines

3.1 Introduction

The reactivity of the previously reported alkylidene and arylidene malonates, acetoacetates, malonamides and acetoacetamides is the starting point in the development of more complex structures in order to explore the possibility of their application in different fields of chemistry and biochemistry. One of the most widely employed reactivity of these systems is their versatility in *conjugated addition reactions*. This kind of reactions has a not so long story since the first example was reported in 1883 by Komnenos who studied the reaction between sodium diethyl malonate and diethyl ethylidenemalonate and further developments of this topic were presented in 1887 by Michael in the base-catalyzed reaction between sodium malonates and β -ketoesters to ethylcinnamate. Starting from the first examples in which, as reported above, the main nucleophiles were stabilized carbanions, several improvements were made

in order to expand the spectrum of nucleophiles able to be employed for this purpose. In fact, talking about *conjugated addition* or *1,4-addition*, it is commonly referred to addition of any kind of nucleophile to an unsaturated system usually conjugated with an activating group, in particular an electron-withdrawing group. However, since there is possibility to choose several nucleophiles, carbon- or heteroatom-based, a distinction can be made: with "**Michael addition**" you can refer to addition of stabilized carbanion species on α,β -unsaturated substrates, in the conjugation with an activating group like a carbonyl group; with "**heteroconjugate addition**" you can refer to addition of heteroatom-based nucleophiles to the same unsaturated systems [52]. Considering the existence of more than one electrophilic functionalities on α,β -unsaturated systems conjugated with carbonyl group, it is important to clarify why the 4-position is so reactive towards carbanion and some heteroatom-based nucleophiles: the explanation is based on the theory of frontier molecular orbital (FMO) which shows that the coefficient of LUMO orbital is larger in the β -position, so soft nucleophiles should attack in this position [53]. In particular for heteronucleophiles, the great reactivity in a Michael addition is also due to thermodynamic and kinetic factors related to the gain in terms of energy in the product of the reaction compared to the energies of the two starting materials. In this chapter, we will focus on the addition to unsaturated systems of C-based nucleophile, like indole, for the synthesis of C-C bond and of N-based nucleophile, like hydroxylamines and allyl amines, for the synthesis of C-N bond.

3.1.1 C-C bond formation in MCRs.

As regard the first topic, we studied the conjugated addition of indole to α,β -unsaturated systems in a multicomponent reaction, the **Yonemitsu trimolecular condensation**. Multicomponent reactions (MCRs) are de-

defined as reactions involving three or more components added together in the same vessel leading to a final product that contains the most of atoms of the starting material without the need of purification between different steps of reaction. Starting with the Strecker reaction for the synthesis of α -aminoacids in 1850 and going through the Biginelli reaction in 1981 for the synthesis of dihydropyrimidinones, several examples of these reactions have been reported in literature. Usually, MCRs are considered one-pot reactions since all the reagent are present in the same reactor but it is possible to make a distinction between *domino/cascade* or *tandem* one-pot reaction (in which all the reagents are introduced in the same moment and all the reactions depend on the intermediate produced in previous step) and *multicatalytic* one-pot reaction (in which the reagents are not all present in the same moment)[54]. The particular beauty of MCRs is in the ability to identify simple compounds with high density of reactivity, which means that there could be the possibility to activate different specific functionalities in different moments. In this contest, 1,3-dicarbonyl compounds are very useful since they possess two electrophilic centers and four (or five if they have amides) nucleophilic ones, granting great versatility. The reactivity of 1,3-dicarbonyl compounds in these reactions remained limited until 1990s when they appeared in a Knöevenagel-hetero-Diels-Alder reaction [55]. Among the different family of MCRs 1,3-dicarbonyl-based reactions, those involving one pronucleophilic reactive site will be explored [56]. As consequence of the acidity of the 2-position protons, 1,3-dicarbonyl compounds in cyclic or acyclic form are considered having one pronucleophilic site. One of the first application in MCRs is in the three-components Yonemitsu condensation which uses Meldrum's acid as 1,3-dicarbonyl compound, an aldehyde and indoles in presence of proline as catalyst [57]. Subsequent decarboxylative ethanolysis of the adduct lead to various ethyl 3-substituted indolylpropionate, employed as intermediates for the synthesis of indole-based

alkaloids (Figure 3.1). The reactivity of Meldrum's acid is linked to its

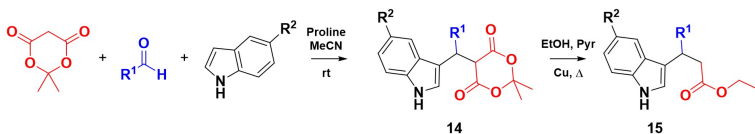


Figure 3.1: Yonemitsu trimolecular condensation.

pKa value lower than that of most commonly used 1,3-dicarbonyl compounds (4.97 for dimethyl malonate vs 13.7). Since it is not so cheap reagent, several examples have been reported in which it is substituted by acyclic methylene active compounds: as consequence of their lower reactivity in Yonemitsu reactions, they have been coupled with Lewis acid catalysts. So in 2008 Renzetti et al. reported a TiCl_4 catalyzed reaction of isobutyraldehyde, indole and dimethyl malonate in dichloromethane in presence of Et_3N as base. In order to expand the scope of the reaction, other aldehydes, substitute-indoles and other dicarbonyl compounds were used in the same conditions [36]. The mechanism of this Ti-catalyzed reaction was explained in 2015 by Renzetti et al.: as partially reported in Chapter 2, they postulate the existence of three steps. Initially (i) TiCl_4 gives a complex together with dicarbonyl compound that evolves through (ii) the formation of O-titanium enolate after addition of the base. This is the substrate for the (iii) Michael addition of indole species. This occurs with two possible mechanisms (path A or B in Figure 3.2). According to path A, there is nucleophilic addition of indole to adduct obtained from Knöevenagel condensation Ti-mediated; the deprotonation of the product of Michael addition by triethylamine restores the aromaticity of indole and produces an anionic intermediate that after protonation of the α -carbon and dissociation of Ti gives the final product. According to path B, the last two steps are inverted. Moreover, the addition of indole starts with the attack of C_3 of indole on C_β of the Knöevenagel adduct,

which can happen from two possible bond plane with several orientation of indole. However, the energetic favoured ones are those in which the N-H of indole is oriented towards the metal (Figure 3.3) [40]. The same reaction was then explored changing Ti-catalyst, using $\text{TiCl}_2(\text{OiPr})_2$ and obtaining comparable results changing the partners of reaction [37].

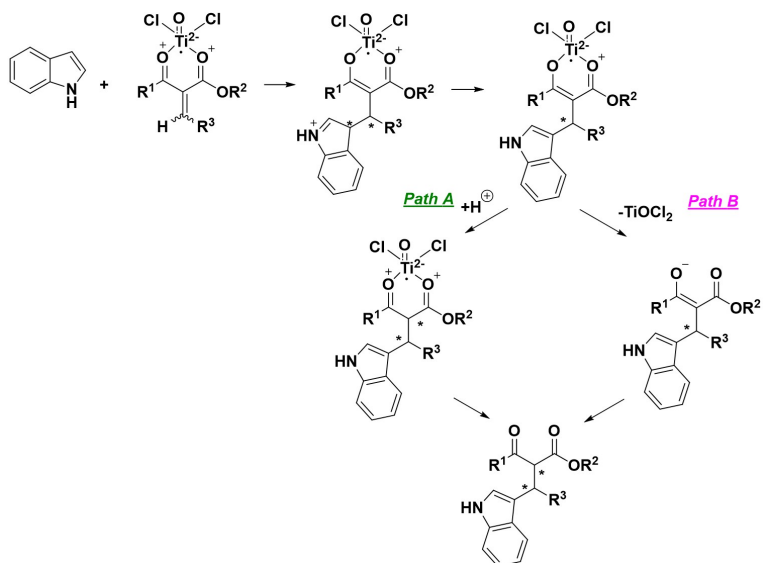


Figure 3.2: Mechanism of Michael addition of indole on α,β -unsaturated-Ti-complex.

Since the reported methods require large amount of catalyst without possibility to recover it, other trials have been reported in which the Ti-catalyst was replaced by earth rare triflate catalysts that allowed to perform reaction even in water and recovering the catalyst. In 2011 Epifano et al. reported an $\text{Yb}(\text{OTf})_3$ -catalyzed Yonemitsu reaction that works under solvent-free conditions with 10mol% of catalyst under sonication for 12h [58]. By changing the earth rare metal, not comparable results have been obtained as consequence of the high oxophilicity of

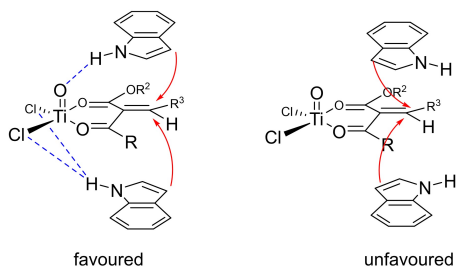


Figure 3.3: Possible facial addition of indole.

Yb^{3+} cation linked to its small ionic radius. Since Indium salts are extensively employed in Friedel-Crafts reaction (and the Michael addition of indole can be considered a sort of it), Acharya et al. reported Yonemitsu-condensation catalyzed by InCl_3 between indole, formaldehyde and secondary amines finding good results in 1,4-dioxane at room temperature even if long reaction times are required (4-24h) [59]. Other examples are those in which the catalyst is a mixture of $\text{Eu}(\text{OTf})_3$ and proline in MeOH, but in this case too the reaction times are too long [60]. Considering that the main drawbacks of this procedures are the long reaction times, we decided to use the microwave-assisted heating to increase the rates, reducing at the same time the formation of side-products. So, we decided to explore the use of microwaves on this reaction to verify the possibility to avoid the use of stoichiometric amount of catalyst and reduce the reaction times [45].

3.1.2 C-N bond formation for the synthesis of isoxazolidinones, isoxazolines and isoxazolidines.

Alkylidene malonate and acetoacetate have been largely employed in the synthesis of **isoxazolidin-5-ones**, **isoxazolidines** and **isoxazolines** since these cyclic structures are easily inserted in biologically active

compounds as consequence of their utility as building blocks for the synthesis of β -aminoacids and γ -lactams. One of the most used synthetic route is based on the heteroconjugated addition of N-hydroxylamine on α,β -unsaturated esters or ketones with consequent cyclization of the N-hydroxyl group on ester for the synthesis of isoxazolidin-5-one and on ketone for the synthesis of isoxazolidine and its derivative isoxazoline. For example, in 1995 Saito et al. reported the addition of N- α -methyl benzylhydroxylamine to homochiral esters for the synthesis of isoxazolidin-5-one (Figure 3.4) [61].

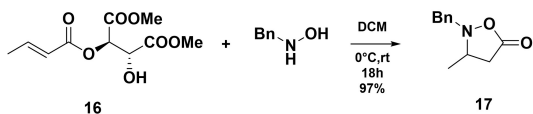


Figure 3.4: Synthesis of isoxazolidin-5-one starting from homochiral esters.

As extension of this work, Bentley et al. reported analogue reaction between unsaturated esters and homochiral lithium N- α -methyl benzylhydroxylamine for the synthesis of isoxazolidin-5-one used for diastereoselectivity tandem alkylation reactions for the synthesis of 3,4,4-trisubstituted derivatives **22** of isoxazolidinone (Figure 3.5). They showed how is possible to generate in situ the lithium derivatives of N-tertbutyl hydroxylamine using n-BuLi solution in THF at -78 °C giving the adduct product **19** with 95:5 diastereomeric ratio. The cyclization was obtained when the hydroxylamine were O-silylated by the use of TBAF with 80% of conversion and 95:5 dr of **20**. With LiTMP in THF at -78 °C was possible to introduce the mono-alkylation at C₄ of **21**, while with LiHMDS was possible the second alkylation that gives with very good yield the desired trisubstitute isoxazolidinone **22** with $> 99 : 1$ dr [62].

The same approach was used by Juarez-Garcia et al. for the synthesis of isoxazolidin-5-one as monomers in the synthesis of β^3 -oligopeptides [63]. They initially used proline as catalyst for the conjugated addition

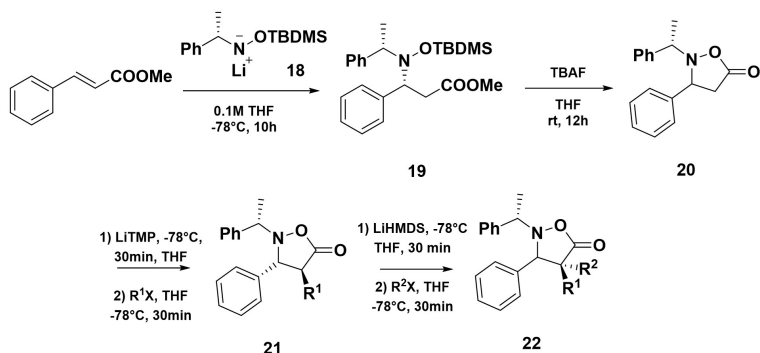


Figure 3.5: Synthesis of isoxazolidin-5-one starting from lithium hydroxylamine.

of N-Cbz-hydroxylamine on α,β -unsaturated aldehydes as reported by Cordoba in 2007: however they found several difficulties in the removal of Cbz group by hydrogenolysis without cleavage of N-O bond of the cycle. So they developed a different strategy by employing substituted acrylonitriles, D-glucose derived hydroxylamine and aldehyde neat at 85-115 °C for 16h affording the cycloadduct that by treatment with triethylamine gives the desired product **27** (Figure 3.6). They applied an analogue procedure on vinylacetate by using carbonate-base instead of triethylamine.

Our group recently reported deeply studied protocols for the conjugated addition of protected-hydroxylamines on alkylidene and arylidene malonates, malonamides and acetoacetates. They represent a great improvement in this field since none example with electron-withdrawing group in the α position of unsaturated ketones or esters was reported before. All these reactions have been performed using N,O-bis(trimethylsilyl)-hydroxylamine and 3-5mol% of Lewis acid as catalyst, with great versatility of alkylidene or arylidene substrates [64] [65] [47]. As regard alkylidene and arylidene malonate, the reaction was performed on isobutyl-

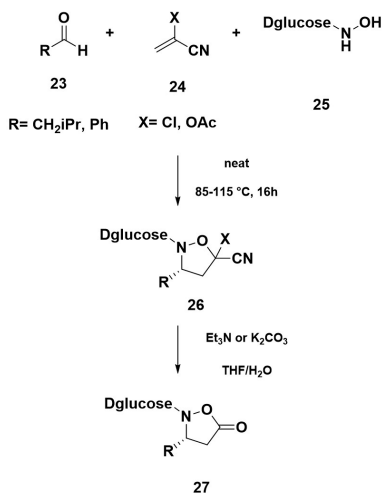


Figure 3.6: Synthesis of N-(D-glucose)-isoxazolidin-5-one.

, *n*-propyl, isopropyl-, heptyl-, phenyl- dimethylmalonates in presence of 3mol% of $\text{Yb}(\text{OTf})_3$ in dichloromethane at -40 °C obtaining the desired product with good yield (Figure 3.7).

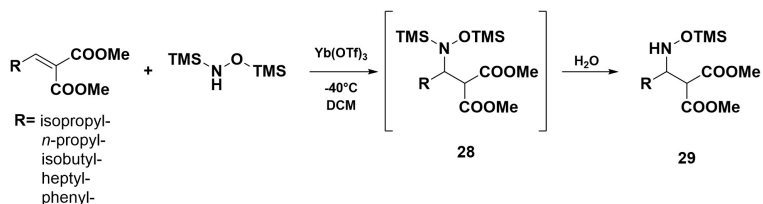


Figure 3.7: Conjugated addition of diprotected hydroxylamine on alkylidene/arylidene malonate.

On N-(benzyl)-methylmalonamide the reaction gave very good yield when catalyzed by 5mol% $\text{Sc}(\text{OTf})_3$ at -40 °C in DCM while on ethyl acetoacetate the reaction was catalyzed by 5mol% of $\text{Yb}(\text{OTf})_3$ (Figure 3.8). In this last case, the cyclization occurs spontaneously at room tem-

perature affording the isoxazolidine **33**, but this process can be accelerated by adding a small amount of silica gel into the crude reaction.

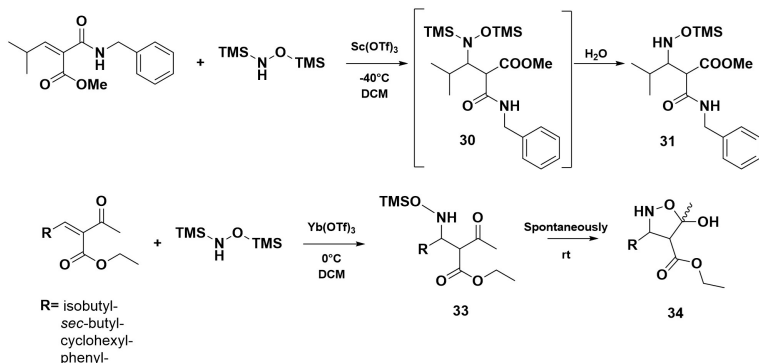


Figure 3.8: Conjugated addition of diprotected hydroxylamine on alkylidene/arylidene malonamides and acetoacetate.

In the first two examples, the cyclization of the adduct was obtained by using TBAF in THF, as reported previously, obtaining the desired products isoxazolidin-5-ones **35** and **36** in high yield (Figure 3.9).

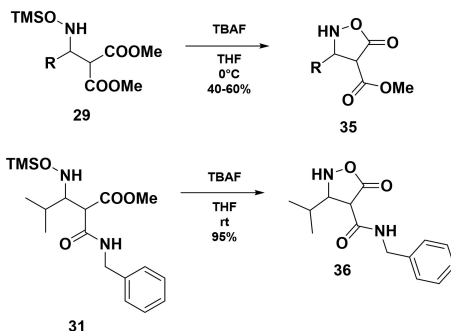


Figure 3.9: Cyclization TBAF induced.

The reaction on alkylidene acetoacetate has been used to explain the

mechanism of the addition (Figure 3.10): after formation of C-N bond, the intermediate has zwitterionic nature with negative charge delocalized on the enolate moiety and positive one on the nitrogen atom; the transfer of TMS group from nitrogen atom to the oxygen gives the intermediate **33'** or the proton transfer to α -carbon gives the intermediate **33**. They slowly and spontaneously converted at room temperature through hemiketalization to a 80:20 mixture of the two C-5 stereoisomers of 3,4-trans-hydroxyisoxazolidines **34** [66].

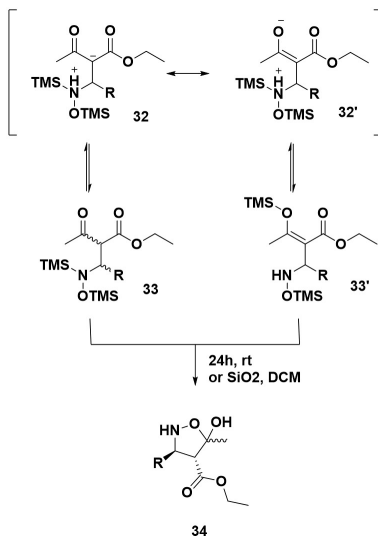


Figure 3.10: Mechanism of addition of hydroxylamine on alkyldiene acetoacetate and cyclization.

3.1.3 C-N bond and subsequent C-C bond formation for the synthesis of 3,4-dehydro- β -pirrole.

With the expression "privileged structures" we commonly refer to all those structures having structural features able to induce easy bind-

ing with a proper receptor as consequence of the spatial disposition of their side chains. Among the natural compounds that can guarantee this behaviour there is proline ring and its derivatives: it can reduce the allowed rotation giving more rigidity to the structure in which it is inserted. For this reason, in peptidomimetic approaches the research of proline analogues represents an interesting matter. In the family of proline analogues β -proline and 3,4-dehydroproline received great attention.[67] The combination of these two structures was part of the focus of this study for the development of a protocol for the synthesis of 3,4-dehydro- β -proline by using the reactivity of alkylidene malonamides and acetoacetates. If the benefits of the β -analogue of proline linked to the possibility to overcome the problem of bioavailability of natural amino acids are well known, it is important to understand why 3,4-dehydro proline is so usefull to explain the fusion of the two mentioned structures (Figure 3.11).

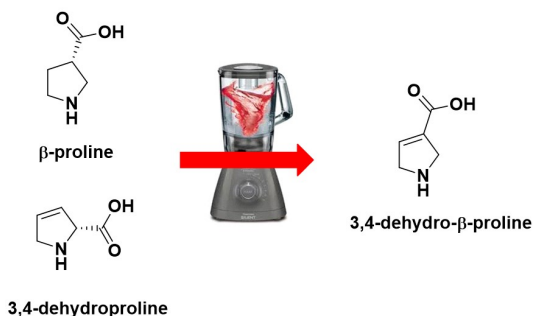


Figure 3.11: β -proline and 3,4.deydroproline.

In fact, it is known that 3,4-dehydroproline can increase the biological activity of the structure containing it (compared to the same structures containing proline) since the double bond between C_{β} and C_{γ} is involved in further binding interactions with the target enhancing the binding affinity; furthermore, it gives bigger restricted conformational

flexibility compared to proline. In the past years, the methods used for the synthesis of this structure and its substituted analogues goes from dehydration of 4-hydroxyproline to enyne metathesis through silver(I)-catalyzed cyclization of amino acids derived allenes [68]. However, ring closing metathesis (RCM) has been largely employed for this purpose, with the Sharpless asymmetric epoxidation, Pd-catalyzed kinetic dynamic asymmetric transformation of vinyl epoxides, Ir-catalyzed allylic amination and regioselective Ru-catalyzed allylic amination. Studies on this last method started in 90's when Grubbs et al. reported several examples of ring closing methathesis of diene mediated by ruthenium carbene **37** for the synthesis of O- and N- unsaturated heterocycles [69]. It was an implementation of a previous work in which they studied the same reactions catalyzed by molybdenum catalyst **38** [70]: they postulated that the ruthenium catalyst **37** was less sensitive to atmospheric oxygen and more tolerant toward a larger spectrum of functionalities compared to the molybdenum one **38** (Figure 3.12). We employed the same chemistry for the synthesis of 3,4-dehydro- β -proline.

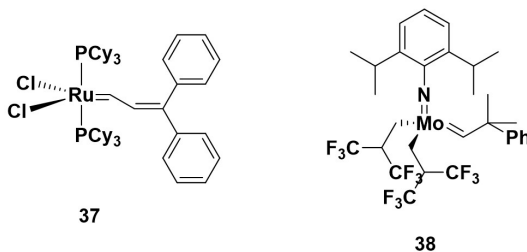


Figure 3.12: Ruthenium and molybdenum catalysts for ring-closing methathesis.

The starting materials for this reaction are N,N'-allylic dienes. Several examples have been reported of allylic amination on allylic carbonate for the synthesis of these syntons: Evans et al. reported allylic amination ruthenium-catalyzed with lithium anion of N-*p*-toluensulphonyl

allylamine on racemic allyl carbonates variously substituted obtaining the desired products in good yields and excellent regiochemistry, with the aim to obtain the product of 1,2-substitution [71]. This approach allowed the synthesis of 2-substituted pyrrole **41** or 2,5-disubstituted pyrrole **43**, if one of the allylic moieties was functionalized (Figure 3.13).

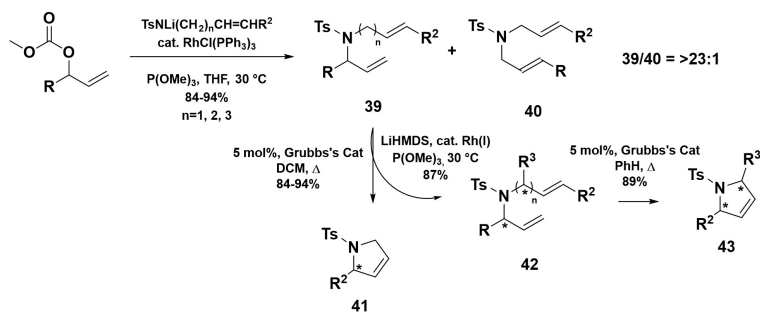


Figure 3.13: Allylic amination of racemic allyl carbonate with Li-N-*p*-toluensulphonyl allylamine.

Regio- and stereoselective P(OPh)₃/Ir-catalyzed allylic amination of allylic ester were reported in 2001 by Takeuchi et al. They found that careful study of the central metal of the catalyst and proper choice of its ligand can influence the results in terms of regio-, stereo- and enantioselectivity. Then, the solvent can influence the same aspects by stabilization of δ -allyl metal intermediate or transition state of the reaction. They postulated that primary amines on allylic carbonates gave monoallylation with S_N2' mechanism (ratio of S_N2' product/S_N2 product >77/23 changing ligand/metal ratio and reaction time), overcoming the problem related to diallylation promoted by palladium-catalyst in the Tsuji-Trost reaction (Figure 3.14) [72]. This work was implemented by Hartwig et al. in 2004 and by Helmchen et al. in 2008 with the introduction of a chiral ligand on Ir-catalyst allowing enantioselective allylic amination [73][74].

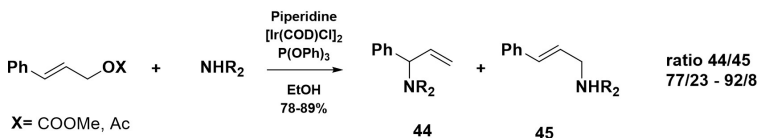


Figure 3.14: Allylic amination of allyl carbonate Ir-catalyzed.

Another approach in this topic is the stereospecific substitution of optically active allyl carbonates by amine nucleophiles [75]. With reaction setup similar to those reported above (chiral ligand/Ir-catalyst), it is possible the enantioselective alcohol displacement with an S_N2' mechanism. Obviously, the enantiomerically pure allyl carbonate can be easily obtained starting from the enantiomeric pure corresponding alcohol. For our purpose, that is to say the introduction in β -position of 3,4-dehydro proline of a carboxylic functionalities, the allyl alcohol derives from alkylidene malonamides or acetoacetates treated with Luche-reduction conditions for the selective reduction of ketones in presence of esters and unsaturation. The resolution of the racemic mixture of substituted alcohols can be treated following a protocol already reported that involves the employment of enzymes [46].

3.2 Results and discussions

3.2.1 Conjugated addition of indole on alkylidene malonate and acetoacetate

In order to develop a library of compounds to verify the versatility of the procedure, we started with the optimization of conjugated addition of indole on compound **8a** (Figure 3.15). As reported above this reaction on alkylidene malonate as been deeply studied, in particular in Lewis acid-catalyzed reactions; but none example of microwave assisted procedure

has been reported. For this reason, the reaction was optimized by changing the irradiation power, the catalyst, the solvent and the reaction times, as reported in Table 3.1.

Table 3.1: Optimization of conjugated addition of indole on alkylidene malonate **8a** and acetoacetate **8b**.

Entry ^a	Reagent	Solvent	Lewis acid	Yield ^b (%)		
				46	47	48
1	8a	Toluene	Yb(OTf) ₃	28	36	—
2	8a	DMF	Yb(OTf) ₃	41	21	15
3	8a	CH ₃ CN	Yb(OTf) ₃	6	29	—
4	8a	DMF	Cu(OTf) ₃	51	21	7
5	8a	DMF	Zn(OTf) ₃	18	—	5
6	8a	DMF	Sc(OTf) ₃	57	—	16
7	8b	DMF	Yb(OTf) ₃	19	9	55
8	8b	DMF	Cu(OTf) ₃	—	12	75
9	8b	DMF	Zn(OTf) ₃	—	9	38
10	8b	DMF	Sc(OTf) ₃	41	7	44
11	8b	DMF	—	—	18	—

[^a] 250 W for 20 min.

[^b] Yield calculated by integration of ¹H NMR and HPLC peaks. The remaining amount is unreacted starting material.

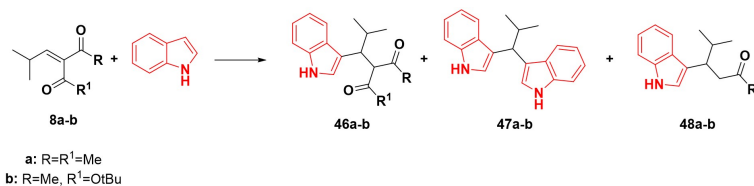


Figure 3.15: Conjugated addition of indole on alkylidene malonate and acetoacetate.

As regard alkylidene malonate **8a**, the first catalyst was Yb(OTf)₃ already used for this purpose: so, we proceeded by changing solvent. When toluene and acetonitrile were used the product **47** is the main product (entry 1 and 3), while in DMF (entry 2) **46a** is obtained with 41%

yield. The product **47** probably derives from **46** and it can be explained with loss of methylene fragment and addition of a second molecule of indole (Figure 3.16). Then, we proceeded by changing the metal salt:

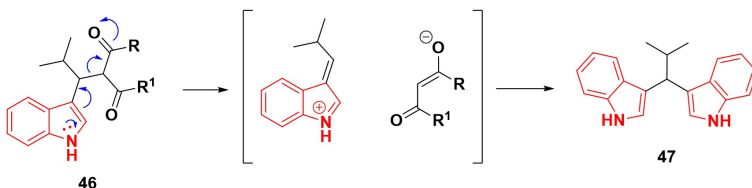


Figure 3.16: Mechanism for the formation of **47**.

with Cu-catalyst compound **46** was isolated in 51% yield (entry 4) together with the product of decarboxylation **48**. When Zn-catalyst was used, very small amount of product was obtained (entry 5), while with Sc-catalyst the product was obtained with good yield (57%) and with small amount of **48** as only co-product (entry 6). The same approach has been used with alkylidene acetoacetate **8b**: this substrate has been less studied since the product of addition has two stereocenters and the keeping of stereodefinition is quite difficult as consequence of the acidity of acetoacetic proton. The irradiation at 250 W for 20 min gave mainly the two co-product **47** and **48** with Yb, Cu and Zn catalyst previously reported (entry 7-9). Only Sc(OTf)₃ gave more or less equal amount of **46** and **48** with traces of **47** (entry 10). Working without catalyst, only **47** can be isolated (entry 11).

With the optimized condition of this step in our hand, and reminding the optimization of the Knöevenagel condensation reported in Chapter 2, we proceeded performing the one-pot two-steps reaction, without purification of intermediates. As usual, the optimization was realized initially for dimethyl malonate. We proceeded in two ways: the first was the adding

Table 3.2: Optimization of one-pot two-steps protocol.

Entry	Reagent	Second step ^a	Solvent	Lewis acid	Yield ^b (%)		
					46	47	48
1	A	250 W 20 min	DMF	Sc(OTf) ₃	33	16	16
2	A	250 W 20 min	DMF	Yb(OTf) ₃	45	25	8
3	A	rt-4h	CH ₃ CN	Yb(OTf) ₃	30	3	9
4 ^c	B	250 W 20 min	DMF	Sc(OTf) ₃	—	5	12
5	B	rt-4h	DMF	Yb(OTf) ₃	—	6	77
6	B	rt-4h	DMF	Sc(OTf) ₃	—	6	85
7	B	rt-4h	CH ₃ CN	Yb(OTf) ₃	67 (51/49)	—	5
8	B	rt-4h	CH ₃ CN	Sc(OTf) ₃	75 (63/37)	7	16
9	B	rt-4h	CH ₃ CN	Cu(OTf) ₃	47 (50/50)	16	12
10	B	rt-4h	CH ₃ CN	Zn(OTf) ₃	23 (51/49)	8	43
11	B	0°C-17h	CH ₃ CN	Sc(OTf) ₃	71 (70/30)	7	16
12	B	0°C-17h	CH ₃ CN	Yb(OTf) ₃	66 (60/40)	8	12
13	B	-20°C-4h	CH ₃ CN	Yb(OTf) ₃	29 (75/25)	2	34

[^a] First step at 250 W for 7 min. [^b] Yield calculated by integration of ¹H NMR and HPLC peaks. The remaining amount is unreacted starting material. [^c] Products of decarboxylation or decomposition were mainly observed.

of indole to the mixture of aldehyde, dimethyl malonate and piperidine, without adding solvent or catalyst irradiating at 250 W for 10 min, but only small amount of **47** was detected; then, we added indole in presence of Yb(OTf)₃ and in the same irradiating conditions only intermediate **8a** was recovered. So, we tried adding all the reagents together: the re-

sults are reported in Table 3.2. After the first step setup at 250 W for 7 min, the second step in DMF was irradiated at 250 W for 20 min giving yields of **46** from 33% to 45% with large amount of **47**, using Sc(OTf)₃ or Yb(OTf)₃ (entry 1-2); changing solvent by using acetonitrile and performing the reaction at room temperature comparable results with those reported for MW-assisted reactions in DMF were recordered (entry 3). Then, we proceeded the study on ethyl acetoacetate. In this case too, the second step was studied first by the assistance of microwaves, but the reaction didn't give any useful result (entry 4). At room temperature with screening of solvents and catalyst, we found that acetonitrile was the best solvent, because in all the trials in which it was employed, it was possible detect satisfactory amount of product **46**. The best results were obtained with Sc(OTf)₃ with yield of 75% (entry 8) and Yb(OTf)₃ with yield of 65% (entry 7). By lowering the temperature, enhancement of diastereomeric ratio was recordered (entry 11-13). The (2S*,3S*) stereochemistry was assigned in comparison with literature [36] [37], but however the acidity of α -proton induces a fast equilibration of the mixture under mild basic condition due to the piperidine. The optimized conditions were applied to the reaction with substituted indoles, whose results are reported in Table 3.3.

The presence of electronwithdrawing or donating group doesn't seem to affect the reactivity. In most of the cases, large amount of bis-indole can be detected; for the reaction with isobutanal, good yields and reduced amount of side products were recordered (entry 5-7). The reaction with 2-OH-benzaldehyde was deeply studied since it is known that the product of the Knöevenagel condensation of this aldehyde with 1,3-dicarbonyl compounds lead to 3-carboxycoumarin derivatives through spontaneous cyclization of intermediates. Considering the relevance that the indole substituent gives from a biochemical point of view, the attempt was to

CHAPTER 3. REACTIVITY OF ALKYLIDENE OR ARYLIDENE DERIVATIVES FOR THE SYNTHESIS OF ISOXAZOLIDINONES, ISOXAZOLINES AND DEYDRO- β -PROLINES

Table 3.3: One-pot two-steps protocol with substituted indoles and aromatic aldehyde.



Entry	R^1	R^2	R^3	Product	Yield 46^a (%)	Yield 47^a (%)
1	Ph	H	H	46c	36	27
2	Ph	F	H	46d	39	30
3	Ph	Me	H	46e	32	29
4	Ph	H	Me	46f	23	33
5	<i>i</i> -Pr	F	H	46g	55	<5
6	<i>i</i> -Pr	Me	H	46h	50	18
7	<i>i</i> -Pr	H	Me	46i	61	18
8	Cyclohexyl	H	H	46j	45	<5
9	4-NO ₂ -Ph	H	H	46k	55	22
10	4-AcO-Ph	H	H	46l	40	26
11	3-AcO-Ph	H	H	46m	53	13

[^a] Yields were calculated by integration of ¹H NMR and HPLC peaks.

The products are 60/40 mixture of diastereoisomers.

The remaining amount is unreacted alkylidene acetoacetate.

realize the Yonemitsu trimolecular condensation between indole, 2-OH-benzaldehyde and ethyl acetoacetate or diethyl malonate (Figure 3.17). The results of the optimization are reported in Table 3.4. The reaction

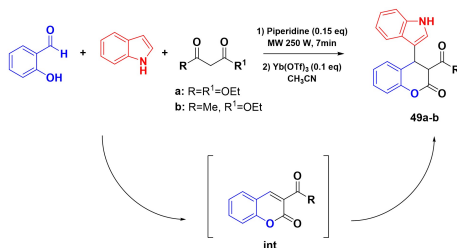


Figure 3.17: Yonemitsu trimolecular condensation for the synthesis of coumarin derivatives.

proceeds slowly at room temperature for them both the 1,3-dicarbonyl compounds, in fact the main product is the intermediate resulting from the cyclization of the Knoevenagel condensation product (entry 1 and 6). By using microwave irradiation the best results for each methylene active substrates have been obtained with 90 min of irradiation at 250 W: as regards diethyl malonate, 45% of product was isolated together with 55% of intermediate (entry 3); for ethyl acetoacetate, a maximum of 27% of product was isolated (entry 8).

3.2.2 1,4-addition of N,O-bis(trimethylsilyl)hydroxyl amine for the synthesis of isoxazolidinones and isoxazolines

The reaction conditions for the addition of N,O-bis(trimethylsilyl)hydroxylamine were optimized on the base of our previous experience and they can be divided depending on the N,O-heterocycle that we want to obtain. As regard the synthesis of isoxazolidine and isoxazoline (Figure 3.18), we proceeded by adding to alkylidene acetoacetate **4** and **7**

Table 3.4: Optimization of Yonemitsu trimolecular condensation between 2-OH-benzaldehyde, indole and 1,3-dicarbonyl compound.

Entry	Reagent	Cat(%)-indole(%)	Conditions	Time (min)	Yield (%)	
					49	int
1	A	10%-1 eq	rt	240	5	95
2	A	10%-1 eq	MW-250 W	50	40	60
3	A	10%-1 eq	MW-250 W	90	45	55
4	A	50%-1 eq	MW-250 W	50	10	90
5 ^[a]	A	10%-2 eq	MW-250 W	50	15	45
6	B	10%-1 eq	rt	240	5	95
7	B	10%-1 eq	MW-250 W	20	25	75
8	B	10%-1 eq	MW-250 W	90	27	73

^[a] Product of decarboxylation was detected.

the above-mentioned hydroxylamine in presence of a catalytic amount of Yb(OTf)₃ as Lewis acid. This procedure allows to avoid the formation of oxime byproduct as a result of the undesired 1,2-addition reaction. The TMS group on N-atom was spontaneously removed during the usual work-up condition inducing the rapid conversion of the intermediate trans-5-hydroxyisoxazolidine-4-carboxylate, as single epimer, through intramolecular hemiketalisation, leading to compounds **50** and **51**. The mechanism of the cyclization and the explanation of the stereodefinition of the reaction can be obtained on the base of previous studies on analogue systems having different substitution on C₃ and different carboxylate group on C₄ (Figure 3.19). Starting from the consideration that from the conjugated addition experimentally is possible to obtain the (3,4)-trans isomer mainly, with two configuration (*R,R*) or (*S,S*), the effect of cyclization on stereodefinition depends on it (the number associated to each atom can be found in Figure 3.18). In this situation, H(13) and H(14) should interact with O(3) and O(5) respectively; rotation of

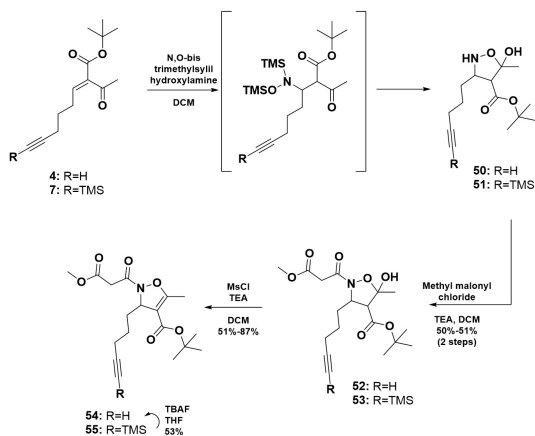


Figure 3.18: Synthesis of isoxazolidines and isoxazolines.

C(9)-N(11) bond allows the cyclization of O(12) on C(2) on *Re* face; the same happens in the *Si* face as consequence of the rotation of C(9)-C(4) bond. Through the cyclization a third stereocenter is defined in C₅ and it can have (*R*) or (*S*) configuration.

This intermediate was used without further purifications in order to stabilize the ring structure since when the N-atom is unprotected is more suitable of ring opening. So, the isoxazolidine ring **50** and **51** were immediately employed for the acylation with methylmalonyl chloride in DCM in presence of triethylamine to obtain the N-acylated isoxazolidine **52** and **53** with yields of 51% and 50% respectively, in two steps. The dehydration of compounds **52** and **53** with MsCl afforded the final N-(methylmalonyl)-isoxazolin-4-carboxylates **54** and **55** with yields of 51% and 87% respectively. In addition, removal of the protective group on terminal alkyne of intermediate **55** gave the same product **54** with 53% yield. The addition of N,O-bis(trimethylsilyl)hydroxylamine on alkyldene malonamides **2a-b** was used for the synthesis of isoxazolidin-5-

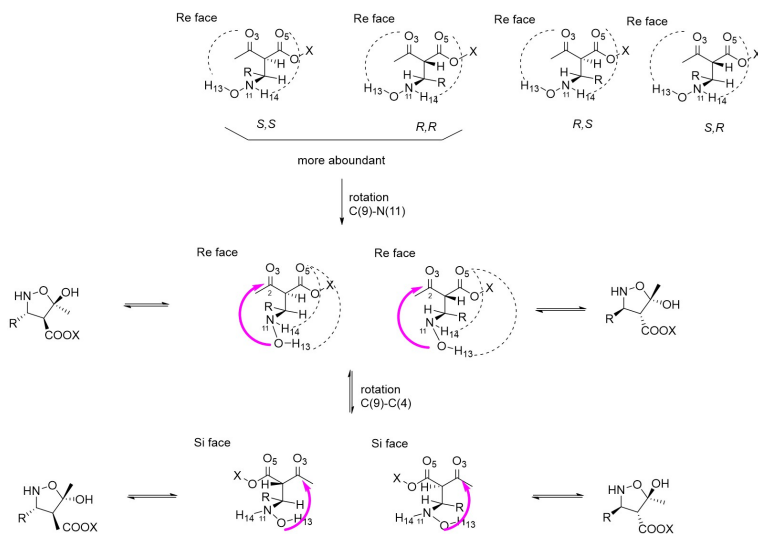


Figure 3.19: Mechanism of intramolecular cyclization for the synthesis of isoxazolidine.

ones **56a,b** (Figure 3.20): as described before, we performed the reaction in DCM in presence of a catalyst that in this case is $\text{Sc}(\text{OTf})_3$ added in catalytic amount after lowering the temperature at -40°C , to avoid the formation of byproducts like the corresponding oxime and to avoid product of retroaldolic reaction. In this condition the diastereomeric ratio is $>95/5$ in favour of the anti-product. The same reaction can be performed without catalyst and at 0° but with longer reaction times and lower diastereomeric ratio. To induce the intramolecular cyclization, we tried to work-up the product of addition but it rapidly degrades on both silica gel and alumina. So, we proceeded by adding TBAF directly in the vessel after disappearance of alkylidene malonamides (after 1.5 h). It gave a tetrabutylammonium hydroxylamino salt that is the real substrate of cyclization, leading in 15 min to isoxazolidinones **56a,b** with yield of 66%

and 63% respectively.

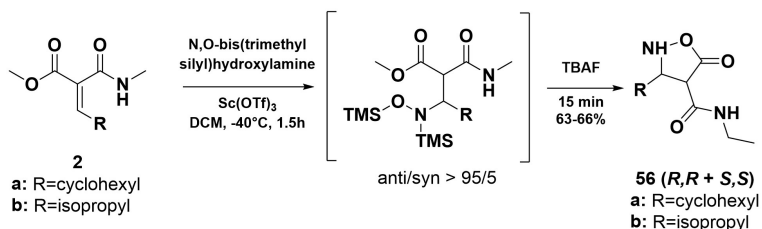


Figure 3.20: Synthesis of isoxazolidin-5-one.

3.2.3 Luche reduction and S_N2' addition for the synthesis of 3,4-dehydro- β -prolines

Alkyldene acetoacetamides and acetoacetates were employed for the synthesis of 3,4-dehydro- β -prolines [76]. For this purpose, compounds **11a** and **8a,b** were subjected to chemoselective Luche reduction using CeCl₃/ NaBH₄ in a mixture of THF/MeOH obtaining the corresponding allyl alcohol **57** and **58a,b** with yields of 80% and 92% respectively. Since the reduction induce the formation of a stereocenter, we proceeded through an enzymatic resolution to resolve the two enantiomers of compound **58a,b**, employed separately for our purposes, while for compound **57** we used the racemic mixture since the purpose of the study on this substrate was focused on its utility as synthon for further transformations: as regard the allyl alcohol **58a,b**, the enzymatic resolution was achieved by using Pseudomonas cepacia lipase on the products of acetylation of **58a,b** with vinyl acetate, affording the acetylated compound (*R*)-**59a,b** and the alcohol (*S*)-**58a,b** in good yield and high enantiomeric excess even if long reaction times are required. The Pseudomonas cepacia lipase (EC 3.1.1.3) is widely used in organic chemistry

for the resolution of racemic secondary alcohols but also for transesterifications and hydrolysis. The acetylation catalyzed by this enzyme was possible by adding vinyl acetate to a solution of **58a,b** in diethyl ether. The enzyme catalyzed the reaction of only one of the two enantiomers, so we were able, after filtering off the enzyme, to recover a 1:1 mixture of acetate and alcohol (detected by ^1H NMR signals), separated by flash chromatography. The acetate (**R**)-**59a,b** was hydrolyzed to the corresponding alcohol (**R**)-**58a,b** by K_2CO_3 in MeOH. The stereoselectivity of the enzyme depends of the relative size of the substituents (small and large) of the alcohol and, according to the Kazlauskas's rule [77], (*S*)-configuration reacts faster than the (*R*) one: we obtained the (*S*)-enantiomer of the allyl alcohol and the (*R*)-enantiomer of the corresponding acetate (Figure 3.21). In both the studies, the compounds **57** and (**R**)-**58a,b**/**(S)**-**58a,b** were converted in the corresponding carbonate **60** and (**R**)-**61a,b**/**(S)**-**61a,b** by using di-*tert*(butyl)-dicarbonate and DMAP in THF (70%) or methyl chloroformate and LiHMDS in THF (75-78%). In the first case, the allylic amination was achieved with allylamine or 4-methoxy-benzylamine in presence of $[\text{Ir}(\text{COD})\text{Cl}]_2$ with $\text{P}(\text{O}^i\text{Pr})_3$ as additional ligand obtaining the product **62a,b** in unsatisfactory yields (23% and 32% respectively) as 70:30 *Z/E* mixture. Probably, the retrodonation in the unsaturated amide is the reason of the low reactivity. For this reason, we introduced an electron-withdrawing *tert*-butyl carbamate on the nitrogen of the amide obtaining **64** in good yield. Repeating the $\text{S}_{\text{N}}2'$ reaction in the same conditions reported above but using 4-amino-benzylamine we were able to isolate the desired product **65** in 52% yield (Figure 3.22). In the second case, the two enantiomers of **61a,b** were subjected to $\text{S}_{\text{N}}2'$ reaction with allylamine in the usual conditions and the crudes were used without further purifications in the next step: (**R**)-**63a,b**/**(S)**-**63a,b** were *N*-protected with (i)Fmoc-group **66b** or functionalized with acylating agents like (ii)methyl mal-

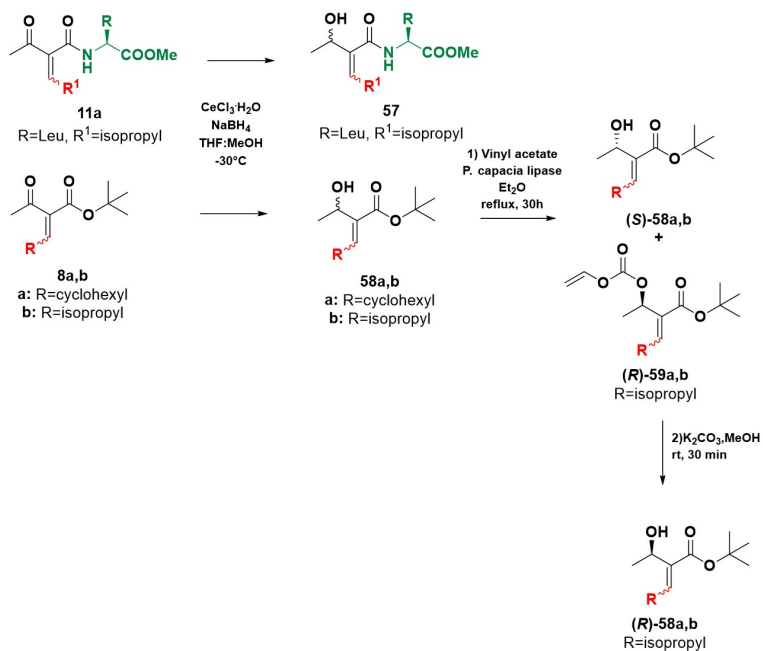


Figure 3.21: Synthesis and resolution of the allyl alcohol.

onyl chloride **67a,b** or (iii)1-isocyanato-2-methylbenzene **68b** in order to perform the ring closing methatesis reaction (Figure 3.23): in fact, experiments on the deprotected analogues gave unsatisfactory results. So, the diallylamines **66b**, **67a,b** and **68b** were the substrates for the ring closing metathesis catalyzed by Grubbs-Hoveyda II generation catalyst in methyl-tertbutyl ether obtaining the products **69b**, **70a,b** and **71b** with yields of (i)79-81%, (ii)80-95% and (iii)60-65%, respectively. Finally, the tert-butyl ester on C₃ was hydrolyze by using TFA for further functionalizations (Figure 3.24).

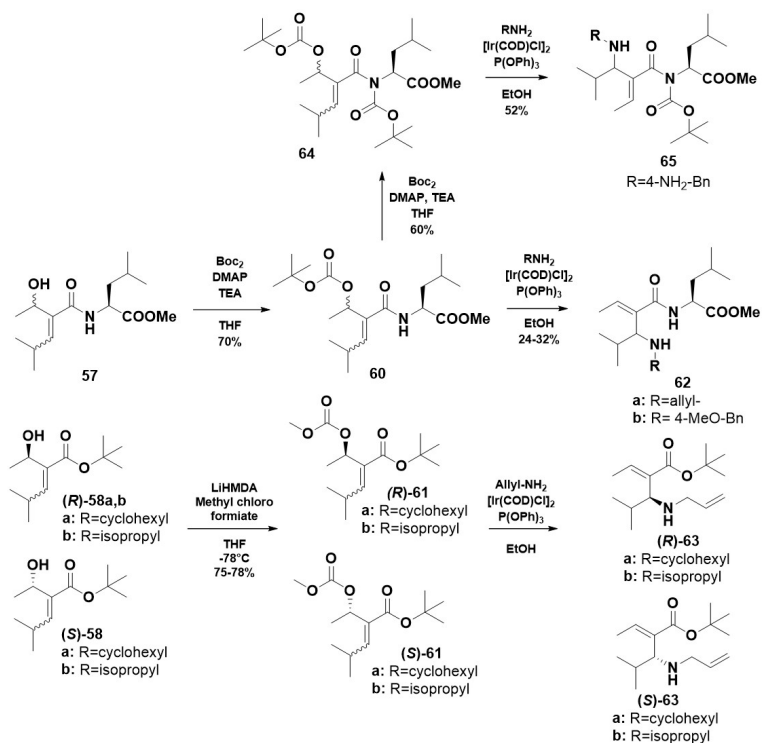


Figure 3.22: Allylic amination.

3.3 Conclusions

Alkylidene and arylidene acetoacetates, malonates, malonamides and acetoacetamides act as versatile building blocks for the synthesis of several heterocycles, that can be incorporated in biologically relevant structures, or for the development of protocols for the conjugated addition of C-based nucleophiles. As consequence of their high reactivity as Michael acceptors and in order to achieve satisfactory results in the con-

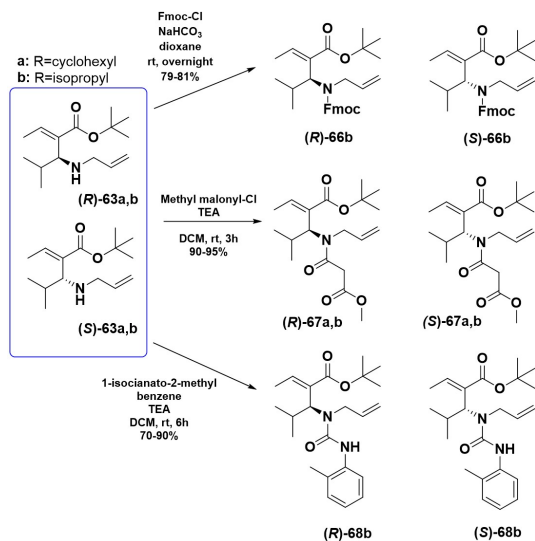


Figure 3.23: Acylation of diallylamines.

denensation of indoles with alkylidene or arylidene malonates or acetoacetates and aldehydes, it was possible to develop a smart protocol in which the reactivity of the Michael acceptors is the key element of Yonemitsu-type trimolecular condensation in presence of Lewis acids as catalysts, by using microwave irradiation. The conditions were optimized for both malonates and acetoacetates and they work very well with substituted aldehydes and indoles. The trick of this procedure is the use of catalytic amount of Lewis acid, together with the significant reduction in reaction times in comparison to the same procedure performed without the assistance of microwaves. The protocol can be applied to the synthesis of coumarin derivatives in order to prepare indole-coumarin compounds with potential biological applications, whose synthesis was not reported with other strategies. The advantages of a one-pot two-steps protocol,

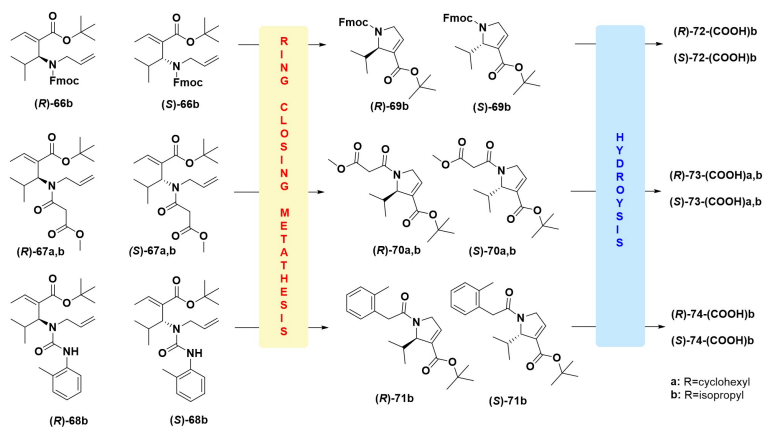


Figure 3.24: Ring closing metathesis.

like the Yonemitsu condensations is, can be maintained also by changing the nucleophiles, choosing N-based ones like hydroxylamines and primary amines. The firsts can be employed for the synthesis of isoxazolidine, isoxazoline and isoxazolidin-5-one largely employed as peptidomimetic structures for the synthesis of bioactive molecules. The addition of hydroxylamine is catalyzed by different Lewis acids, depending on the alkylidene compound, and proceeds with good yield. Through intramolecular cyclization, the adduct gives spontaneously the proper ring which can be functionalized. The primary amines are used as nucleophiles for the allylic amination of allyl alcohol obtained through reduction of alkylidene acetoacetates or malonamides. With this approach, it is possible to generate enantiopure adduct as consequence of the enzymatic resolution performed on the starting allyl alcohol: the amine reacts keeping the initial configuration. The diallyl amine obtained from the conjugated addition is the starting material for the ring closing metathesis that allows the cyclization to obtain 3,4-dehydro- β -proline ring. A

protocol to obtain enantiopure rings was developed, based on the use of Grubbs-Hoveyda II generation catalyst.

3.4 Experimental procedures

3.4.1 General methods

All chemicals were purchased from commercial suppliers and were used without further purification. Microwave-assisted reactions were carried out in Milestone Mycosynth apparatus, with a dual magnetron system with a pyramid-shaped diffuser, 1000 W maximum power output, and temperature monitor and control by optical fiber up to a vessel temperature of 250 °C. Flash chromatography was carried out on silica gel (230-400 mesh). Dowex®50WX2-200(H) ion exchange resin was used for purification of free amino acids or free amines. NMR spectra were recorded with a Varian Mercury Plus 400 or Varian Gemini 200 instruments. Chemical shifts are reported as δ values (ppm), and were calibrated using the residual solvent peaks of: CDCl₃, set at $\delta = 7.27$ ppm (¹H NMR) or $\delta = 77.0$ ppm (¹³C NMR); CD₃OD, set at $\delta = 3.31$ ppm (¹H NMR) and $\delta = 49.0$ ppm (¹³C NMR); D₂O, set at $\delta = 4.79$ ppm (¹H NMR); CD₃CN, set at $\delta = 1.93$ ppm (¹H NMR) and $\delta = 117.7$ ppm (¹³C NMR); (CD₃)₂CO, set at $\delta = 2.04$ ppm (¹H NMR) and $\delta = 29.8$ ppm (¹³C NMR). Coupling constants are given in Hz. LC-MS analysis was carried out with an HP1100 liquid chromatograph coupled to an electrospray ionization mass spectrometer (LC-ESI-MS), using a Phenomenex Gemini C18 - 3 μ - 110 Å column, H₂O/CH₃CN as neutral solvent or H₂O/CH₃CN with 0.2% formic acid as acid solvent at 25 °C (positive-ion mode, $m/z = 100$ -500, fragmentor 70 V). Another set of experiments has been performed on an HP1100 liquid chromatograph coupled with an electrospray ionization-ion trap mass spectrometer MSD1100 using

a Phenomenex Zorbax C18 - 3.5 μ - 80 Å column, H₂O/CH₃CN with 0.08% trifluoroacetic acid as acid solvent (positive scan 100-500 m/z , fragmentor 70 eV).

3.4.2 Synthesis and characterization

General procedure for the one-pot two steps trimolecular condensation with the assistance of MW in the second step. Ethyl acetoacetate or dimethyl malonate (1 eq), aldehyde (1 eq) and piperidine (15 mol%) were added in the microwave reactor and irradiated at 250 W for 7 min. After cooling the mixture at room temperature, DMF (1M), indole (1 eq) and lewis acid (10 mol%) were added and the solution irradiated at 250 W for 20 min. The mixture was allowed to reach room temperature and then it was diluted with water and washed with EtOAc. After drying the organic layer over Na₂SO₄, the solvent was evaporated and the crude purified by flash chromatography on silica gel (cyclohexane/ethyl acetate 90/10).

General procedure for the one-pot two steps trimolecular condensation performing the second step at room temperature. Ethyl acetoacetate or dimethyl malonate (1 eq), aldehyde (1 eq) and piperidine (15 mol%) were added in the microwave reactor and irradiated at 250 W for 7 min. After cooling the mixture at room temperature, the proper solvent (1M), indole (1 eq) and lewis acid (10 mol%) were added and the mixture stirred at rt for 4h. After disappearance of the starting material, the reaction was diluted with water and washed with EtOAc. After drying the organic layer over Na₂SO₄, the solvent was evaporated and the crude purified by flash chromatography on silica gel (cyclohexane/ethyl acetate 90/10).

Compound (46a): ¹H NMR (400 MHz, CDCl₃) δ 8.08 (s, 1H), 7.68 (dd, J= 7.8, 1.5 Hz, 1H), 7.38-7.29 (m, 1H), 7.14-7.07 (m, 2H), 7.04

(d, $J=2.5$ Hz, 1H), 4.00 (d, $J=11.0$ Hz, 1H), 3.83 (dd, $J=11.0$, 4.9 Hz, 1H), 3.75 (s, 3H), 3.36 (s, 3H), 2.17e1.97 (m, 1H), 0.88 (d, $J=6.7$ Hz, 6H); ^{13}C NMR (400 MHz, CDCl_3) δ 169.3, 168.7, 135.6, 128.4, 122.6, 121.8, 119.6, 119.3, 113.0, 110.8, 56.3, 52.6, 52.2, 42.1, 30.6, 21.9, 17.9; LC-ESI-MS: 10.41 min, $[M + H]^+=304$, $[M + Na]^+=326$, $[2M + Na]^+=629$; IR (film) cm $^{-1}$ 3405, 3057, 2957, 2874, 1732, 1619, 1542, 1457, 742; $R_f=0.44$ (7/3 EtOAc/cyclohexane as eluent); Anal. Calcd for $\text{C}_{17}\text{H}_{21}\text{NO}_4$ (303.1): C, 67.31; H, 6.98; N, 4.62. Found: C, 67.50; H, 6.99; N, 4.62.

Compound (46b): ^1H NMR (400 MHz, CDCl_3) 6/4 mixture of isomers δ 8.19 (s, 0.4H, minor), 8.14 (s, 0.6H, major), 7.75-7.56 (m, 1H), 7.33 (dd, $J=8.0$, 3.8 Hz, 1H), 7.21-7.04 (m, 2H), 6.99 (d, $J=2.5$ Hz, 0.6H), 6.89 (d, $J=2.0$ Hz, 0.4H), 4.02 (d, $J=11.5$ Hz, 0.6H), 3.95 (d, $J=12.1$ Hz, 0.4H), 3.86 (dd, $J=11.5$, 4.1 Hz, 0.6H), 3.86 (dd, $J=12.1$, 4.1 Hz, 0.4H), 2.32 (s, 3H), 2.03-2.10 (m, 0.6H), 2.02-1.95 (m, 0.4H), 1.90 (s, 3H), 1.50 (s, 9H), 0.99-0.75 (m, 6H); ^{13}C NMR (400 MHz, CDCl_3) δ 203.9, 203.2, 168.5, 167.5, 135.5, 135.4, 128.9, 128.4, 123.3, 122.9, 121.9, 121.7, 119.9, 119.6, 119.3, 119.2, 113.3, 112.4, 111.0, 110.7, 82.0, 81.3, 66.3, 66.0, 41.9, 41.4, 30.6, 30.4, 29.0, 27.9, 27.4, 27.1, 22.2, 22.1, 17.5, 17.2; LC-ESI-MS: 10.54 min (major), 11.05 min (minor), $[M + Na]^+=352$; IR (film) cm $^{-1}$ 3336, 3186, 2926, 2853, 1728, 1697, 1461, 1376, 733; $R_f=0.56$ (7/3 EtOAc/cyclohexane as eluent). Anal. Calcd for $\text{C}_{18}\text{H}_{23}\text{NO}_3$ (329.2): C, 72.92; H, 8.26; N, 4.25. Found: C, 72.43; H, 8.24; N, 4.24.

Compound (47): ^1H NMR (400 MHz, CDCl_3) δ 7.77 (s, 2H), 7.67 (d, $J=8.2$ Hz, 2H), 7.25 (dd, $J=8.0$, 1.0 Hz, 2H), 7.21-7.03 (m, 4H), 6.99 (d, $J=2.4$ Hz, 2H), 4.27 (d, $J=8.4$ Hz, 1H), 2.76-2.54 (m, 1H), 1.03 (d, $J=6.6$ Hz, 6H); ^{13}C NMR (400 MHz, CDCl_3) δ 137.0, 136.1, 123.6, 121.5, 119.2, 118.7, 110.9, 110.8, 58.9, 41.0, 21.8; LC-ESI-MS: 10.91 min, $[M + H]^+=289$, $[M + Na]^+=311$; IR (Nujol) cm $^{-1}$ 3422, 3020,

1596, 1454, 1376, 744, 704. $R_f = 0.62$ (7/3 EtOAc/cyclohexane as eluent); Anal. Calcd for $C_{20}H_{20}N_2$ (288.2): C, 83.30; H, 6.99; N, 9.71. Found: C, 83.23; H, 6.97; N, 9.73.

Compound (48a): 1H NMR (400 MHz, $CDCl_3$) δ 8.00 (s, 1H), 7.65 (dd, $J = 8.0, 1.3$ Hz, 1H), 7.35 (dd, $J = 8.2, 1.0$ Hz, 1H), 7.14-7.20 (m, 2H), 6.99 (d, $J = 2.4$ Hz, 1H), 3.53 (s, 3H), 3.42-3.29 (m, 1H), 2.83 (dd, $J = 15.0, 5.7$ Hz, 1H), 2.71 (dd, $J = 15.0, 9.6$ Hz, 1H), 2.20-1.97 (m, 1H), 0.94 (d, $J = 6.7$ Hz, 3H), 0.92 (d, $J = 6.7$ Hz, 3H); ^{13}C NMR (400 MHz, $CDCl_3$) δ 170.6, 136.1, 127.5, 121.7, 120.9, 119.2, 119.0, 117.9, 110.9, 49.6, 40.1, 32.6, 30.3, 20.5, 20.1; LC-ESI-MS: 9.36 min, $[M+H]^+ = 246$, $[M+Na]^+ = 268$; IR (film) cm^{-1} 3314, 3078, 2944, 2861, 1698, 1462, 1358, 753; $R_f = 0.62$ (7/3 EtOAc/cyclohexane as eluent); Anal. Calcd for $C_{15}H_{19}NO_2$ (245.1): C, 73.44; H, 7.81; N, 5.71. Found: C, 73.61; H, 7.82; N, 5.70.

Compound (48b): 1H NMR (400 MHz, $CDCl_3$) δ 8.01 (s, 1H), 7.66 (dd, $J = 8.1, 1.3$ Hz, 1H), 7.44-7.29 (d, 2H, $J = 7.2$ Hz), 7.24-7.03 (m, 1H), 6.95 (d, $J = 2.4$ Hz, 1H), 3.35 (dt, $J = 8.0, 6.6$ Hz, 1H), 2.95 (dd, $J = 15.0, 8.0$ Hz, 1H), 2.77 (dd, $J = 15.0, 6.6$ Hz, 1H), 2.18-2.02 (m, 1H), 1.99 (s, 3H), 0.94 (d, $J = 6.7$ Hz, 3H), 0.89 (d, $J = 6.7$ Hz, 3H); ^{13}C NMR (400 MHz, $CDCl_3$) δ 209.4, 136.3, 127.2, 121.9, 121.7, 119.3, 119.0, 117.3, 111.2, 47.0, 39.3, 32.7, 30.1, 20.5, 20.3; LC-ESI-MS: 8.71 min, $[M+H]^+ = 230$, $[M+Na]^+ = 252$, $[M+K]^+ = 268$; IR (film) cm^{-1} 3283, 3055, 2959, 2870, 1694, 1456, 1360, 744. $R_f = 0.66$ (7/3 EtOAc/cyclohexane as eluent). Anal. Calcd for $C_{15}H_{19}NO$ (229.1): C, 78.56; H, 8.35; N, 6.11. Found: C, 78.36; H, 8.34; N, 6.13.

Compound (46c): major isomer: 1H NMR (400 MHz, $CDCl_3$) δ 8.03 (br s, NH), 7.55 (d, 1H, $J = 5.0$ Hz), 7.35-7.02 (m, 9H), 5.06 (d, 1H, $J = 8.0$ Hz), 4.39 (d, 1H, $J = 8.0$ Hz), 3.96 (q, 2H, $J = 7.2$ Hz), 2.16 (s, 3H), 1.01 (t, 3H $J = 7.2$ Hz); ^{13}C NMR (400 MHz, $CDCl_3$) δ 203.1, 168.1, 141.3, 136.2, 128.3, 128.0, 126.7, 126.4, 122.4, 121.4, 119.4, 111.2,

66.6, 61.4, 43.0, 30.3, 13.7; LC-ESI-MS: 9.8 min, $[M + Na]^+ = 358$, $[2M + Na]^+ = 693$. Minor isomer: ^1H NMR (400 MHz, CDCl_3): δ 8.00 (br s, NH), 7.55 (d, 1H, $J = 5.0$ Hz), 7.35e7.02 (m, 9H), 5.09 (d, 1H, $J = 8.0$ Hz), 4.51 (d, 1H, $J = 8.0$ Hz), 3.98 (q, 2H, $J = 7.2$ Hz), 2.03 (s, 3H), 0.99 (t, 3H, $J = 7.2$ Hz); ^{13}C NMR (400 MHz, CDCl_3) δ 202.2, 168.0, 141.3, 136.1, 128.6, 128.1, 126.7, 126.6, 122.2, 120.7, 119.6, 117.2, 111.0, 65.8, 61.6, 42.6, 30.9, 13.6; LC-ESI-MS: 9.6 min, $[M + Na]^+ = 358$, $[2M + Na]^+ = 693$. IR (film) cm^{-1} 3397, 3060, 2931, 2872, 1737, 1715, 1456, 1367, 742. $R_f = 0.37$ (7/3 EtOAc/cyclohexane as eluent). Anal. Calcd for $\text{C}_{21}\text{H}_{21}\text{NO}_3$ (335.1): C, 75.20; H, 6.31; N, 4.18. Found: C, 75.15; H, 6.29; N, 4.20.

Compound (46d): major isomer: ^1H NMR (400 MHz, CDCl_3) δ 8.00 (br s, NH), 7.39-7.11 (m, 7H), 6.99 (d, 1H, $J = 2.0$ Hz), 6.85-6.95 (m, 1H), 6.68 (s, 1H), 4.96 (d, 1H, $J = 12.0$ Hz), 4.37 (d, 1H, $J = 12.0$ Hz), 3.95 (q, 2H, $J = 7.2$ Hz), 2.20 (s, 3H), 0.98 (t, 3H, $J = 7.2$ Hz); ^{13}C NMR (400 MHz, CDCl_3) δ 202.1, 167.9, 157.8 (d, $J_{\text{C-F}} = 214$ Hz), 140.9, 132.7, 128.4 (d, $J_{\text{C-F}} = 10$ Hz), 128.0, 127.3, 126.9, 123.0, 119.3, 111.7, 110.4 (d, $J_{\text{C-F}} = 9$ Hz), 104.6 (d, $J_{\text{C-F}} = 23$ Hz), 66.3, 61.5, 29.6, 28.4, 13.9; LC-ESI-MS: 9.7 min, $[M + Na]^+ = 376$, $[2M + Na]^+ = 729$. Minor isomer: ^1H NMR (400 MHz, CDCl_3) δ 7.97 (br s, NH), 7.39-7.11 (m, 7H), 6.98 (d, 1H, $J = 2.0$ Hz), 6.68 (s, 1H), 6.8-6.95 (m, 1H), 5.00 (d, 1H, $J = 11.6$ Hz), 4.48 (d, 1H, $J = 11.6$ Hz), 3.97 (q, 2H, $J = 7.2$ Hz), 2.20 (s, 3H), 0.98 (t, 3H, $J = 7.2$ Hz); ^{13}C NMR (400 MHz, CDCl_3) δ 202.9, 168.0, 157.5 (d, $J_{\text{C-F}} = 214$ Hz), 143.3, 133.2, 128.5 (d, $J_{\text{C-F}} = 10$ Hz), 127.9, 127.2, 126.4, 122.5, 119.3, 111.6, 110.1 (d, $J_{\text{C-F}} = 8$ Hz), 104.8 (d, $J_{\text{C-F}} = 23$ Hz), 65.6, 61.5, 30.4, 28.4, 13.7; LC-ESI-MS: 9.9 min, $[M + Na]^+ = 376$, $[2M + Na]^+ = 729$. IR (film) cm^{-1} 3389, 2963, 2929, 2866, 1739, 1711, 1459, 1282, 1202, 799. $R_f = 0.34$ (7/3 EtOAc/cyclohexane as eluent). Anal. Calcd for $\text{C}_{21}\text{H}_{20}\text{FNO}_3$ (353.1): C, 71.37; H, 5.70; N, 3.96. Found: C, 71.22; H, 5.71; N, 3.97.

Compound (46e): major isomer: ^1H NMR (400 MHz, CDCl_3) δ 7.95 (br s, NH), 7.37-6.95 (m, 9H), 5.04 (d, 1H, $J=12.0$ Hz), 4.36 (d, 1H, $J=12.0$ Hz), 3.96-4.00 (m, 2H), 2.40 (s, 3H), 2.05 (s, 3H), 0.98 (t, 3H, $J=7.2$ Hz); ^{13}C NMR (400 MHz, CDCl_3) δ 202.3, 168.2, 141.4, 134.5, 128.7, 128.2, 127.9, 127.8, 126.6, 124.0, 121.4, 118.7, 115.7, 110.6, 66.0, 61.4, 30.3, 28.0, 21.6, 13.6; LC-ESI-MS: 10.4 min, $[M + Na]^+=372$, $[2M + Na]^+=721$. Minor isomer: ^1H NMR (400 MHz, CDCl_3) δ 8.00 (br s, NH), 7.37-6.95 (m, 9H), 5.07 (d, 1H, $J=11.8$ Hz), 4.49 (d, 1H, $J=11.8$ Hz), 3.96-4.00 (m, 2H), 2.40 (s, 3H), 2.05 (s, 3H), 1.01 (t, 3H, $J=7.2$ Hz); ^{13}C NMR (400 MHz, CDCl_3) δ 203.1, 168.0, 141.4, 134.5, 128.9, 128.5, 127.9, 127.8, 126.8, 124.1, 121.5, 118.9, 116.7, 110.7, 66.8, 61.2, 30.4, 28.2, 21.4, 13.8; LC-ESI-MS: 10.2 min, $[M + Na]^+=372$, $[2M + Na]^+=721$. IR (film) cm^{-1} 3397, 3089, 2924, 2854, 1740, 1712, 1456, 1366, 701. $R_f \hat{=} \frac{1}{4} 0.41$ (7/3 EtOAc/cyclohexane as eluent). Anal. Calcd for $\text{C}_{22}\text{H}_{23}\text{NO}_3$ (349.4): C, 75.62; H, 6.63; N, 4.01. Found: C, 75.64; H, 6.60; N, 4.02.

Compound (46f): major isomer: ^1H NMR (400 MHz, CDCl_3) δ 7.69-7.11 (m, H), 7.00 (m, 1H), 6.94 (s, 1H), 5.07 (d, 1H, $J=11.0$ Hz), 4.39 (d, 1H, $J=11.0$ Hz), 3.98-4.05 (m, 2H), 3.70 (s, 3H), 2.06 (s, 3H), 0.98 (t, 3H, $J=7.2$ Hz); ^{13}C NMR (400 MHz, CDCl_3) δ 202.0, 167.9, 141.2, 136.9, 130.6, 128.0, 127.7, 126.6, 125.5, 121.7, 119.1, 118.9, 115.6, 109.0, 65.9, 61.3, 42.6, 30.1, 13.8; LC-ESI-MS: 11.2 min, $[M + Na]^+=372$. Minor isomer: ^1H NMR (400 MHz, CDCl_3) δ 7.69-7.11 (m, 8H), 7.00 (m, 1H), 6.94 (s, 1H), 5.10 (d, 1H, $J=11.2$ Hz), 4.50 (d, 1H, $J=11.2$ Hz), 3.98-4.05 (m, 2H), 3.70 (s, 3H), 2.18 (s, 3H), 1.00 (t, 3H, $J=7.2$ Hz); ^{13}C NMR (400 MHz, CDCl_3) δ 202.9, 168.0, 141.6, 136.9, 129.5, 128.2, 127.9, 126.8, 126.0, 121.9, 119.3, 118.9, 114.7, 109.1, 66.6, 61.3, 43.0, 30.8, 13.7; LC-ESI-MS: 10.7 min, $[M + Na]^+=372$. IR (film) cm^{-1} 3058, 2980, 2927, 1714, 1698, 1540, 1471, 741. $R_f=0.53$ (7/3 EtOAc/cyclohexane as eluent). Anal. Calcd for $\text{C}_{22}\text{H}_{23}\text{NO}_3$

(349.2): C, 75.62; H, 6.63; N, 4.01. Found: C, 75.49; H, 6.62; N, 4.03.

Compound (46g): major isomer: ^1H NMR (400 MHz, CDCl_3) δ 8.32 (br s, NH), 7.29 (dd, 1H, $J_{\text{H-H}} = 1$ Hz, $J_{\text{H-F}} = 9.6$ Hz), 7.21 (dd, 1H, $J_{\text{H-H}} = 9.2$ Hz, $J_{\text{H-F}} = 4.4$ Hz), 6.89 (d, 1H, $J = 2.4$ Hz), 6.87 (dd, 1H, $J_{\text{H-H}} = 9.2$ Hz, $J_{\text{H-F}} = 2.4$ Hz), 4.12-4.30 (m, 2H), 4.02 (d, 1H, $J = 12.0$ Hz), 3.77 (m, 1H), 2.03 (m, 1H), 1.94 (s, 3H), 1.31 (t, 3H, $J = 7.2$ Hz), 0.85 (d, 6H, $J = 6.6$ Hz); ^{13}C NMR (400 MHz, CDCl_3) δ 203.3, 169.1, 157.9 (d, $J_{\text{C-F}} = 233$ Hz), 132.1, 129.0 (d, $J_{\text{C-F}} = 10$ Hz), 125.1, 113.4, 111.6, 110.6 (d, $J_{\text{C-F}} = 12$ Hz), 104.5 (d, $J_{\text{C-F}} = 18$ Hz), 64.7, 61.5, 42.0, 30.6, 27.2, 21.9, 17.7, 14.0; LC-ESI-MS: 10.1 min, $[M + Na]^+ = 342$, $[2M + Na]^+ = 661$. Minor isomer: ^1H NMR (400 MHz, CDCl_3) δ 8.20 (1H, br s), 7.29 (dd, 1H, $J_{\text{H-H}} = 1$ Hz, $J_{\text{H-F}} = 9.6$ Hz), 7.21 (dd, 1H, $J_{\text{H-H}} = 9.2$ Hz, $J_{\text{H-F}} = 4.4$ Hz), 7.02 (d, 1H, $J = 2.8$ Hz), 6.87 (dd, 1H, $J_{\text{H-H}} = 9.2$ Hz, $J_{\text{H-F}} = 2.4$ Hz), 4.12-4.30 (m, 2H), 4.10 (d, 1H, $J = 10.8$ Hz), 3.77 (m, 1H); 2.31 (s, 3H), 1.98 (m, 1H), 0.83 (d, 6H, $J = 6.6$ Hz), 0.77 (t, 3H, $J = 7.2$ Hz). ^{13}C NMR (400 MHz, CDCl_3) δ 202.8, 168.5, 158.0 (d, $J_{\text{C-F}} = 233$ Hz), 132.0, 128.7 (d, $J_{\text{C-F}} = 10$ Hz), 124.6, 113.3, 112.4, 110.1 (d, $J_{\text{C-F}} = 12$ Hz), 103.4 (d, $J_{\text{C-F}} = 18$ Hz), 64.8, 61.0, 41.7, 30.9, 29.1, 22.0, 17.2, 13.4. LC-ESI-MS: 9.8 min, $[M + Na]^+ = 342$, $[2M + Na]^+ = 661$. IR (film) cm^{-1} 3376, 2987, 2929, 2857, 1736, 1704, 1454, 1274, 1211, 788. $R_f = 0.48$ (7/3 EtOAc/cyclohexane as eluent). Anal. Calcd for $\text{C}_{18}\text{H}_{22}\text{FNO}_3$ (319.1): C, 67.69; H, 6.94; N, 4.39. Found: C, 67.71; H, 6.90; N, 4.38.

Compound (46h): major isomer: ^1H NMR (400 MHz, CDCl_3) δ 7.97 (br s, NH), 7.45 (s, 1H), 7.23-6.86 (m, 3H), 4.25 (q, 2H, $J = 7.2$ Hz), 4.10 (d, 1H, $J = 11.0$ Hz), 3.83 (dd, 1H, $J = 2.8, 11.0$ Hz), 2.47 (s, 3H), 2.31 (s, 3H), 1.90e2.14 (m, 1H), 1.31 (t, 3H, $J = 7.2$ Hz), 0.88 (d, 6H, $J = 6.6$ Hz); ^{13}C NMR (400 MHz, CDCl_3) δ 203.6, 169.4, 134.6, 128.8, 128.3, 123.6, 121.9, 119.2, 112.5, 110.6, 65.0, 61.0, 41.6, 31.0, 29.2, 21.9, 17.8, 17.3, 13.5. LC-ESI-MS: 10.5 min, $[M + Na]^+ = 338$. Minor isomer: ^1H NMR

(400 MHz, CDCl_3): δ 8.02 (br s, NH), 7.45 (s, 1H), 7.23-6.86 (m, 3H), 4.02 (d, 1H, $J=12.0$ Hz), 3.86 (dd, 1H, $J=4.0, 12.0$ Hz), 3.80 (q, 2H, $J=7.6$ Hz), 2.43 (s, 3H), 1.90-2.14 (m, 1H), 1.92 (s, 3H), 1.02 (d, 3H, $J=6.6$ Hz), 0.88 (d, 6H, $J=6.6$ Hz), 0.81 (t, 3H, $J=7.6$ Hz); ^{13}C NMR (400 MHz, CDCl_3) δ 203.3, 168.6, 134.0, 128.7, 128.1, 123.3, 121.8, 119.0, 111.5, 110.4, 64.9, 61.4, 41.8, 30.8, 29.0, 21.5, 17.6, 17.1, 14.1. LC-ESI-MS: 10.8 min, $[M + Na]^+=338$. IR (film) cm^{-1} 3404, 2960, 2924, 2871, 1735, 1707, 1464, 1367, 795. $R_f=0.53$ (7/3 EtOAc/cyclohexane as eluent). Anal. Calcd for $\text{C}_{19}\text{H}_{25}\text{NO}_3$ (315.2): C, 72.35; H, 7.99; N, 4.44. Found: C, 72.42; H, 7.96; N, 4.45.

Compound (46i): major isomer: ^1H NMR (400 MHz, CDCl_3) δ 7.65 (d, 1H, $J=8.0$ Hz), 7.25-7.08 (m, 3H), 6.74 (s, 1H), 4.23 (q, 2H, $J=7.2$ Hz), 4.09 (d, 1H, $J=10.8$ Hz), 3.81 (dd, 1H, $J=4.4, 10.8$ Hz), 3.70 (s, 3H), 1.96-2.04 (m, 1H), 1.91 (s, 3H), 1.28 (t, 3H, $J=7.2$ Hz), 0.84 (d, 3H, $J=6.6$ Hz), 0.83 (d, 3H, $J=6.6$ Hz); ^{13}C NMR (400 MHz, CDCl_3) δ 203.3, 169.5, 128.7, 127.5, 121.5, 119.7, 119.0, 110.4, 109.1, 64.8, 61.4, 41.7, 32.8, 30.6, 29.0, 22.1, 17.7, 14.1; LC-ESI-MS: 10.8 min, $[M + Na]^+=338$. Minor isomer: ^1H NMR (400 MHz, CDCl_3): δ : 7.65 (d, 1H, $J=8.0$ Hz), 7.25-7.08 (m, 3H), 6.88 (s, 1H), 4.20 (q, 2H, $J=7.2$ Hz), 4.01 (d, 1H, $J=12.0$ Hz), 3.86 (dd, 1H, $J=4.0, 12.0$ Hz), 3.71 (s, 3H), 2.28 (s, 3H), 1.96-2.04 (m, 1H), 0.84 (d, 3H, $J=6.6$ Hz), 0.83 (d, 3H, $J=6.6$ Hz), 0.73 (t, 3H, $J=7.2$ Hz). ^{13}C NMR (400 MHz, CDCl_3) δ 203.2, 168.5, 136.4, 129.0, 121.2, 119.3, 118.8, 111.4, 108.8, 65.0, 60.8, 42.0, 32.7, 30.4, 27.6, 22.0, 17.2, 13.4. LC-ESI-MS: 10.5 min, $[M + Na]^+=338$. IR (film) cm^{-1} 3055, 2961, 2933, 2876, 1710, 1614, 1467, 1356, 739. $R_f\hat{A}\frac{1}{4}0.62$ (7/3 EtOAc/cyclohexane as eluent). Anal. Calcd for $\text{C}_{19}\text{H}_{25}\text{NO}_3$ (315.2): C, 72.35; H, 7.99; N, 4.44. Found: C, 72.60; H, 7.98; N, 4.43.

Compound (46j): mixture of isomers: ^1H NMR (400 MHz, CDCl_3): δ 8.14 (br s, 0.7H, major), 8.09 (br s, 0.3H, minor), 7.72 (d, $J=7.6$ Hz,

0.3H, minor) 7.67 (d, J = 8.0 Hz, 0.7H, major), 7.34 (br d, J = 8.0 Hz, 1H), 7.21-7.09 (m, 2H), 7.03 (d, J = 2.5 Hz, 0.3H, minor), 6.90 (d, J = 2.4 Hz, 0.7H, major), 4.34-4.16 (m, 2H), 4.18 (d, J = 10.8 Hz, 0.3H, minor), 4.11 (d, J = 11.6 Hz, 0.7H, major), 3.86 (dd, J = 11.6, 3.5 Hz, 0.7H), 3.83 (dd, J = 10.8, 5.2 Hz, 0.3H), 2.30 (s, 0.9H, minor), 2.18 (s, 2.1H, major), 1.82-1.50 (m, 7H), 1.39 (t, J = 7.2 Hz, 0.9H, minor) 1.31 (t, J = 7.2 Hz, 2.1H, major), 1.05-1.30 (m, 2H); ^{13}C NMR (400 MHz, CDCl_3) δ 203.8, 203.3, 169.3, 168.6, 135.6, 135.5, 128.1, 128.0, 123.3, 122.9, 121.8, 121.6, 121.4, 121.3, 119.5, 119.4, 119.2, 119.1, 113.6, 112.7, 111.0, 110.8, 64.3, 64.0, 61.4, 41.1, 40.9, 32.4, 32.3, 26.5, 26.4, 26.2, 26.1, 26.0, 25.9, 14.1, 13.3; LC-ESI-MS: 11.32 min (minor), 11.63 (major) $[M + Na]^+ = 364$. IR (film) cm^{-1} 3439, 2972, 2921, 2851, 1731, 1705, 1487, 1367, 754. $R_f = 0.61$ (7/3 EtOAc/cyclohexane as eluent). Anal. Calcd for $\text{C}_{21}\text{H}_{27}\text{NO}_3$ (341.5): C, 73.87; H, 7.97; N, 4.10. Found: C, 73.89; H, 7.94; N, 4.12.

Compound (46k): major isomer ^1H NMR (400 MHz, CDCl_3): δ 8.47 (br s, NH), 8.00-8.10 (m, 2H), 7.45-7.00 (m, 8H), 5.20 (d, 1H, J = 12.0 Hz), 4.45 (d, 1H, J = 12.0 Hz), 3.95-4.08 (m, 2H), 2.18 (s, 3H), 1.07 (t, 3H, J = 7.2 Hz); ^{13}C NMR (400 MHz, CDCl_3) δ 201.7, 167.6, 149.3, 146.5, 136.2, 126.2, 123.7, 122.7, 121.8, 119.9, 118.5, 114.6, 111.3, 65.3, 61.8, 42.2, 30.9, 13.8; LC-ESI-MS: 9.7 min, $[M + \text{water}]^+ = 398$, $[M + Na]^+ = 403$. Minor isomer: ^1H NMR (400 MHz, CDCl_3): δ 8.42 (br s, NH), 8.00-8.10 (m, 2H), 7.45-7.00 (m, 8H), 5.23 (d, 1H, J = 12.0 Hz), 4.55 (d, 1H, J = 12.0 Hz), 3.95-4.08 (m, 2H), 2.16 (s, 3H), 0.99 (t, 3H, J = 7.2 Hz); ^{13}C NMR (400 MHz, CDCl_3) δ 201.0, 167.4, 149.5, 146.6, 136.3, 129.0, 125.9, 123.6, 122.5, 121.2, 119.7, 118.7, 115.4, 111.5, 65.4, 61.7, 41.8, 30.2, 13.6; LC-ESI-MS: 9.6 min, $[M + \text{water}]^+ = 398$, $[M + Na]^+ = 403$. IR (film) cm^{-1} 3405, 3111, 2981, 2856, 1738, 1714, 1519, 1420, 744. $R_f = \frac{1}{4} 0.20$ (7/3 EtOAc/cyclohexane as eluent). Anal. Calcd for $\text{C}_{21}\text{H}_{20}\text{N}_2\text{O}_5$ (380.1): C, 66.31; H, 5.30; N, 7.36. Found: C,

66.10; H, 5.29; N, 7.37.

Compound (46l): major isomer: ^1H NMR (400 MHz, CDCl_3) δ 7.98 (br s, NH), 7.52-6.93 (m, 9H), 5.09 (d, 1H, $J=12.0$ Hz), 4.45 (d, 1H, $J=12.0$ Hz), 3.95-4.05 (m, 2H), 2.22 (s, 3H), 2.05 (s, 3H), 1.04 (t, 3H, $J=7.2$ Hz); ^{13}C NMR (400 MHz, CDCl_3) δ 203.0, 169.3, 168.0, 149.3, 138.9, 136.7, 136.1, 129.0, 127.0, 126.2, 122.5, 121.7, 119.9, 111.2, 65.8, 61.6, 41.8, 30.4, 28.2, 21.0, 13.8. LC-ESI-MS: 9.0 min, $[M + \text{water}]^+=411$, $[M + \text{Na}]^+=416$. Minor isomer: ^1H NMR (400 MHz, CDCl_3) δ 8.04 (br s, NH), 7.52-6.93 (m, 9H), 5.05 (d, 1H, $J=12.0$ Hz), 4.32 (d, 1H, $J=12.0$ Hz), 3.95-4.05 (m, 2H), 2.13 (s, 3H), 2.03 (s, 3H), 0.94 (t, 3H, $J=7.2$ Hz); ^{13}C NMR (400 MHz, CDCl_3) δ 202.1, 169.3, 167.9, 154.0, 138.8, 136.7, 136.2, 129.7, 127.0, 126.4, 123.5, 121.5, 119.7, 111.0, 66.6, 61.5, 42.3, 30.5, 29.6, 21.1, 13.7. LC-ESI-MS: 9.0 min, $[M + \text{water}]^+=411$, $[M + \text{Na}]^+=416$. IR (film) cm^{-1} 3407, 2980, 2927, 2871, 1740, 1738, 1710, 1506, 1368, 1201, 743. $R_f=0.24$ (7/3 EtOAc/cyclohexane as eluent). Anal. Calcd for $\text{C}_{23}\text{H}_{23}\text{NO}_5$ (393.4): C, 70.21; H, 5.89; N, 3.56. Found: C, 70.24; H, 5.91; N, 3.55.

Compound (46m): major isomer: ^1H NMR (400 MHz, CDCl_3) δ 8.10 (br s, NH), 7.55-6.91 (m, 8H), 6.79 (br s, 1H), 5.11 (d, 1H, $J=12.2$ Hz), 4.36 (d, 1H, $J=12.2$ Hz), 4.01-3.97 (m, 2H), 2.26 (s, 3H), 2.06 (s, 3H), 1.03 (t, 3H, $J=7.2$ Hz); ^{13}C NMR (400 MHz, CDCl_3) δ 203.0, 169.4, 167.9, 150.6, 143.1, 136.1, 129.4, 126.2, 125.4, 122.3, 121.6, 121.1, 119.8, 119.6, 118.8, 115.6, 111.1, 66.2, 61.6, 42.5, 30.6, 21.0, 13.6. LC-ESI-MS: 9.0 min, $[M + \text{water}]^+=411$, $[M + \text{Na}]^+=416$. Minor isomer: ^1H NMR (400 MHz, CDCl_3) δ 8.06 (br s, NH), 7.55-6.91 (m, 8H), 6.67 (br s, 1H), 5.08 (d, 1H, $J=12.4$ Hz), 4.49 (d, 1H, $J=12.4$ Hz), 4.01-3.97 (m, 2H), 2.25 (s, 3H), 2.08 (s, 3H), 0.98 (t, 3H, $J=7.2$ Hz); ^{13}C NMR (400 MHz, CDCl_3) δ 202.3, 169.3, 167.8, 150.5, 143.1, 136.1, 129.1, 126.3, 125.7, 122.1, 121.6, 121.0, 119.8, 119.4, 119.1, 111.2, 65.5, 61.5, 42.2, 28.4, 20.9, 14.0. LC-ESI-MS: 8.9 min,

$[M + water]^+ = 411$, $[M + Na]^+ = 416$. IR (film) cm⁻¹ 3400, 2982, 2926, 2854, 1741, 1738, 1725, 1486, 1368, 1206, 744. $R_f = 0.22$ (7/3 EtOAc/cyclohexane as eluent). Anal. Calcd for C₂₃H₂₃NO₅ (393.4): C, 70.21; H, 5.89; N, 3.56. Found: C, 70.23; H, 5.87; N, 3.53.

Compound (49a): ¹H NMR (400 MHz, CDCl₃) δ 8.16 (br s, NH), 7.65-7.02 (m, 8H), 6.81 (d, 1H, J = 3.6 Hz), 5.01 (d, 1H, J = 7.2 Hz), 4.38 (q, 2H, J = 7.2 Hz), 4.18 (d, 1H, J = 7.2 Hz), 1.38 (t, 3H, J = 7.2 Hz); ¹³C NMR (400 MHz, CDCl₃) δ 166.9, 164.6, 150.6, 148.5, 136.6, 134.2, 129.4, 124.7, 124.6, 123.8, 123.4, 121.9, 117.6, 116.4, 116.3, 111.8, 61.6, 52.9, 36.4, 13.9. LC-ESI-MS: 9.7 min, $[M + H]^+ = 336$, $[M + Na]^+ = 358$. IR (film) cm⁻¹ 3357, 3060, 2982, 2931, 2851, 1768, 1715, 1486, 1375, 1244, 1201, 761. $R_f = 0.35$ (7/3 EtOAc/cyclohexane as eluent). Anal. Calcd for C₂₀H₁₇NO₄ (335.1): C, 71.63; H, 5.11; N, 4.18. Found: C, 71.65; H, 5.14; N, 4.20.

Compound (49a): ¹H NMR (400 MHz, CDCl₃) δ 8.18 (br s, NH), 7.44-7.04 (m, 8H), 6.82 (d, 1H, J = 3.6 Hz), 5.02 (d, 1H, J = 7.2 Hz), 4.26 (d, 1H, J = 7.2 Hz), 2.20 (s, 3H); ¹³C NMR (400 MHz, CDCl₃) δ 201.1, 169.5, 165.7, 150.5, 137.0, 136.7, 36.5, 128.8, 128.0, 125.1, 123.4, 122.5, 121.4, 119.9, 118.5, 116.7, 111.8, 59.1, 35.2, 29.7; LC-ESI-MS: 8.8 min, $[M + H]^+ = 306$, $[2M + Na]^+ = 633$. IR (film) cm⁻¹ 3405, 3058, 2924, 2854, 1752, 1718, 1486, 1339, 745. $R_f = 0.34$ (7/3 EtOAc/cyclohexane as eluent). Anal. Calcd for C₁₉H₁₅NO₃ (305.3): C, 74.74; H, 4.95; N, 4.59. Found: C, 74.76; H, 4.97; N, 4.61.

General procedure for the synthesis of isoxazolidine ring: (50) and (51). Under inert atmosphere, **4** or **7** (1 eq) and Yb(OTf)₃ (0.5 eq) were added in DCM (0.5M) and the mixture stirred for 10 min at room temperature. N,O-bis(trimethylsilyl) hydroxylamine (2 eq) was added at 0°C and the reaction stirred for additional 30 min. The solution was diluted with dichloromethane and washed with water. After drying the

organic layer onto Na_2SO_4 , the solvent was evaporated and the crude employed without further purifications in the next step.

General procedure for the acylation of isoxazolidine ring: (52) and (53). Under inert atmosphere, triethylamine (1.5 eq) and methyl malonyl chloride (1.5 eq) were added at 0°C to a solution of (50) or (51) (1 eq) in DCM (0.5M). The mixture was stirred at room temperature for 2.5 h. After this period, the reaction was diluted with dichloromethane and washed with water. After drying the organic layer onto Na_2SO_4 , the solvent was evaporated and the crude was purified by flash chromatography on silica gel (80/20 cyclohexane/EtOAc).

Compound (52): Yield 51% (over two steps); ^1H NMR (400 MHz, CDCl_3) δ 4.65 (dt, $J= 6.8, 7.4$ Hz, 1H), 3.72 (s, 3H), 3.59 (d, $J= 15.5$ Hz, 1H), 3.53 (d, $J= 15.6$ Hz, 1H), 2.86 (d, $J= 7.4$ Hz, 1H), 2.28-2.19 (m, 2H), 1.92 (t, $J= 2.4$ Hz, 1H), 1.83-1.74 (m, 2H), 1.63 (s, 3H), 1.64-1.52 (m, 2H), 1.46 (s, 9H); ^{13}C NMR (400 MHz, CDCl_3) δ 169.3, 168.4, 167.5, 105.3, 83.7, 82.6, 68.7, 61.6, 59.1, 52.3, 40.7, 33.9, 27.8, 24.6, 22.8, 17.8. LC-ESI-MS: 8.3 min, $[M + H]^+=370$, $[M + Na]^+=392$, $[2M + Na]^+=761$.

Compound (53): Yield 50% (over two steps); ^1H NMR (400 MHz, CDCl_3) δ 4.64 (dt, $J= 6.8, 7.2$ Hz, 1H), 3.67 (s, 3H), 3.50 (s, 2H), 2.82 (d, $J= 7.2$ Hz, 1H), 2.21 (dt, $J= 6.8, 6.0$ Hz, 2H), 1.72 (m, 2H), 1.62 (s, 3H), 1.59-1.47 (m, 2H), 1.42 (s, 9H), 0.07 (s, 9H); ^{13}C NMR (400 MHz, CDCl_3) δ 169.2, 168.5, 167.6, 106.7, 105.4, 84.8, 82.6, 61.7, 59.2, 52.4, 40.8, 34.0, 27.9, 24.8, 22.9, 19.4, 0.1. LC-ESI-MS: 11.3 min, $[M + H]^+=442$, $[M + Na]^+=464$, $[2M + Na]^+=905$.

General procedure for the synthesis of isoxazoline: (54) and (55). Under inert atmosphere, triethylamine (2 eq) and methanesulfonyl chloride (2 eq) were added to a solution of (52) and (53) (1 eq) in DCM (0.25M) at 0°C and the mixture stirred at rt for 24h. After this period,

the reaction was diluted with dichloromethane and washed with water. The organic layer dried on Na_2SO_4 and the solvent evaporated. The crude was purified by flash chromatography onto silica gel (80/20 cyclohexane/EtOAc). Yield of (54) 51%; yield of (55) 87%.

Removal of protective group for the synthesis of (54). To a solution of (55) (2 eq) in THF (0.5M), tetrabutylammonium fluoride trihydrate (1.9 eq) was added and the mixture stirred overnight at room temperature. After adding 5 ml of H_2O , THF was removed and the solution diluted with 10 ml of DCM. The organic layer was washed with water, dried over Na_2SO_4 and evaporated. The crude product was purified by flash chromatography on silica gel (80/20 cyclohexane/EtOAc). Yield of (54) 53%.

Compound (54): ^1H NMR (400 MHz, CDCl_3) δ 5.30 (m, 1H), 3.72 (s, 3H), 3.58 (d, $J=15.9$ Hz, 1H), 3.46 (d, $J=15.9$ Hz, 1H), 2.29-2.14 (m, 2H), 2.20 (s, 3H), 1.99 (m, 1H), 1.92 (t, $J=2.4$ Hz, 1H), 1.76 (m, 1H), 1.64-1.53 (m, 2H), 1.48 (s, 9H); ^{13}C NMR (400 MHz, CDCl_3) δ 166.8, 162.0, 161.0, 105.8, 83.8, 80.9, 68.4, 62.8, 52.2, 40.4, 32.4, 28.0, 26.7, 23.6, 17.8, 11.1. LC-ESI-MS: 10.1 min, $[M + H]^+=352$, $[M + Na]^+=374$, $[2M + Na]^+=725$.

Compound (55): ^1H NMR (400 MHz, CDCl_3) δ 5.30 (m, 1H), 3.72 (s, 3H), 3.58 (d, $J=15.9$ Hz, 1H), 3.46 (d, $J=15.9$ Hz, 1H), 2.24 (dt, $J=3.2$, 7.2 Hz, 2H), 2.20 (s, 3H), 1.92 (m, 1H), 1.71 (m, 1H), 1.64-1.53 (m, 2H), 1.48 (s, 9H), 0.12 (s, 9H); ^{13}C NMR (400 MHz, CDCl_3) δ 167.0, 167.9, 162.2, 161.1, 106.9, 106.0, 84.6, 81.1, 63.1, 52.4, 40.6, 32.8, 28.2, 23.9, 19.5, 11.3, 0.1; LC-ESI-MS: 13.2 min, $[M + H]^+=424$, $[M + Na]^+=446$, $[M + K]^+=462$.

Synthesis of isoxazolidin-5-one: (56a,b). Under inert atmosphere, (2a,b) (1 eq) and $\text{Sc}(\text{OTf})_3$ (15 mol%) were stirred in DCM (0.2M) at room temperature for 15 min. N,O-bis(trimethylsilyl) hydroxylamine

(1.5 eq) was added at -40°C and the mixture stirred for 1.5h. After this period, tetrabutylammonium fluoride (2 eq) was added and the mixture stirred at room temperature for 15 min. The solution was diluted with dichloromethane and washed with water. After drying the organic layer onto Na_2SO_4 , the solvent was evaporated and the crude was purified by flash chromatography on silica gel (8:2->7:3 Cy:EtOAc).

Compound (56a): yield 66%; ^1H NMR (400 MHz, CDCl_3) δ 6.27 (bs, 1H), 3.97 (dd, $^3\text{J}=6.4$ Hz, $^3\text{J}=5.6$ Hz, 1H), 3.38-3.27 (m, 2H), 3.31 (d, $^3\text{J}=5.2$ Hz, 1H), 1.84-1.55 (m, 6H), 1.27-1.02 (m, 5H), 1.16 (t, $^3\text{J}=7.2$ Hz, 3H); ^{13}C NMR (400 MHz, CDCl_3) δ 165.5, 163.5, 66.9, 51.9, 40.1, 34.7, 28.9, 26.5, 25.7, 25.4, 25.3, 13.9; LC-ESI-MS: 13.2 min, $[M + H]^+=241$, $[M + Na]^+=263$, $[M + K]^+=279$.

Compound (56b): yield 63%; ^1H NMR (400 MHz, CDCl_3) δ 6.34 (bs, 1H), 3.94(dd, $^3\text{J}=6.4$ Hz, $^3\text{J}=6.4$ Hz, 1H), 1.91 (m, 1H), 1.16 (t, $^3\text{J}=7.2$ Hz, 3H), 0.99 (d, $^3\text{J}=6.8$ Hz, 3H), 0.97 (d, $^3\text{J}=6.8$ Hz, 3H); ^{13}C NMR (400 MHz, CDCl_3) δ 165.9, 163.9, 66.5, 51.4, 35.1, 30.8, 18.9, 18.0, 14.4; LC-ESI-MS: 13.2 min, $[M + H]^+=201$, $[M + Na]^+=223$, $[M + K]^+=239$.

General procedure for Luche reduction of alkylidene malonamide and acetoacetate: (57) and (58a,b). To a solution of compound (11a) or (8a,b) (1 eq) in THF/MeOH 9:1 (0.25M) at room temperature, $\text{CeCl}_3 \cdot 7\text{H}_2\text{O}$ (1.1) and NaBH_4 (1.1 eq) were added and the reaction quenched after disappearance of the starting ketone. After addition of water and removal of THF and MeOH under reduced pressure, the residue was diluted with ethyl acetate and washed with water. The organic layer was dried over Na_2SO_4 and solvent was removed under reduced pressure. Racemic alcohol (57) or (58a,b) was isolated by flash chromatography on silica gel (cyclohexane/ethyl acetate 85/15 as eluant). **Compound (57):** (60:40 mixture of inseparable diastereoisomers): ^1H NMR (400

MHz, CDCl_3) δ 7.06 (d, 0.4H, J = 8.0 Hz), 7.00 (d, 0.6H, J = 8.4 Hz), 5.33 (d, 1H, J = 10.1Hz), 4.43 (m, 1H), 4.17 (q, 1H, J =6.4 Hz), 3.99 (bs, 1H), 3.53 (s, 3H), 2.40-2.80 (m, 1H), 1.18-1.55 (m, 3H), 1.16 (d, 1.2H, J = 6.4 Hz), 1.11 (d, 1.8H, J = 6.4 Hz), 0.69-0.82 (m, 12H); ^{13}C NMR (400 MHz, CDCl_3) δ 172.9, 168.3, 141.2, 136.1, 70.0, 51.6, 50.1, 40.5, 27.5, 24.4, 22.4, 22.3, 21.3, 21.1; LC-ESI-MS: 6.67 min (major), 7.91 (minor), $[M + H]^+$ =286, $[M + Na]^+$ =308.

Enzymatic resolution of allyl alcohol: (58a,b). Racemic (58a,b) was dissolved in diethyl ether and vinyl acetate (5 eq) and Pseudomonas cepacia lipase (35 mg/ml) were added. The mixture was refluxed for 30h and then filtered off to recover the enzyme. After drying the organic layer onto Na_2SO_4 , the solvent was evaporated and the crude purified by flash chromatography on silica gel (95/5 cyclohexane/ethyl acetate) to isolate (*S*)-(58a,b) and the acetate (*R*)-58a,b. It was hydrolyzed by using K_2CO_3 (1 eq) in MeOH, stirring the mixture for 30 min. The reaction was quenched with acid water and extracted with ethyl acetate. The crude (*R*)-58a,b was used without further purifications. **Compound (58b):** yield (*S*)-58b 94%, yield (*R*)-58b 90%. E-isomer: ^1H NMR (400 MHz, CDCl_3) δ 6.37(d, 3J = 10.4 Hz, 1H), 3.03 (m, 1H), 1.51 (s, 9H), 1.32 (d, 3J = 6.6 Hz, 3H), 0.99 (d, 3J = 8 Hz, 6H); ^{13}C NMR (400 MHz, CDCl_3) δ 166.8, 147.3, 131.9, 81.0, 58.6, 29.1, 28.3, 22.6, 22.4. Z-isomer: ^1H NMR (400 MHz, CDCl_3) δ 5.75 (d, 3J = 10 Hz, 1H), 4.36 (q, 3J = 6.4 Hz, 1H), 3.03 (m, 1H), 1.51 (s, 9H), 1.32 (d, 3J = 6.6 Hz, 3H), 0.99 (d, 3J = 8 Hz, 6H); ^{13}C NMR (400 MHz, CDCl_3) δ 167.2, 146.7, 130.1, 81.1, 58.8, 28.2, 27.7, 22.6, 22.4. LC-ESI-MS: 1.6 min, $[M + H]^+$ =215, $[M + Na]^+$ =227, $[2M + Na]^+$ =451. S-enantiomer $[\alpha]^D = -26$, R-enantiomer $[\alpha]^D = +38$ (c 1 in CHCl_3).

Compound (58a): yield (*S*)-58b 45%, yield (*R*)-58b 60%. E-isomer: ^1H NMR (400 MHz, CDCl_3) δ 6.50 (d, 1H, J = 9.8 Hz), 4.70 (q, 1H,

$J = 6.6$ Hz), 2.34 (m, 1H), 1.50 (s, 9H), 1.44-1.73 (m, 5H), 1.39 (d, 3H, $J = 6.6$ Hz), 1.11-1.25 (m, 5H); ^{13}C NMR (400 MHz, CDCl_3) δ 167.7, 147.8, 132.1, 81.0, 60.6, 37.0, 32.1(2), 25.7, 25.4 (2), 23.9, 22.7; GC-MS: 16.81 min, m/z : 226(2), 211(100), 179(18), 165(68), 143(55), 129(38), 119(35), 105(19), 91(32), 81(70), 67(45), 55(43). Z-isomer: ^1H NMR (400 MHz, CDCl_3) δ 5.88 (d, 1H, $J = 10.0$ Hz), 4.41 (q, 1H, $J = 6.6$ Hz), 4.24 (q, 2H, $J = 7.0$ Hz), 2.75 (m, 1H), 2.30 (br s, 1H), 1.60-1.73 (m, 5H), 1.25 (d, 3H, $J = 6.6$ Hz), 1.25 (t, 3H, $J = 7.0$ Hz), 1.01-1.36 (m, 5H); ^{13}C NMR (400 MHz, CDCl_3) δ 167.7, 145.6, 133.4, 81.1, 60.2, 37.9, 32.5, 32.4, 25.9, 25.7, 25.4, 22.5, 22.4; GC-MS: 16.40 min, m/z : 226(2), 208(38), 179(33), 162(100), 147(28), 133(51), 119(37), 107(20), 99(29), 91(36), 81(87), 67(38), 55(34).

Procedure for the synthesis of allylic tertbutylcarbonate: (60).

To a solution of the allylic alcohol 57 (1 eq) in THF, ditertbutyl dicarbonate (2.5 eq), DMAP (0.2 eq) and TEA (1.2 eq) were added and the mixture was stirred for 2h at room temperature. After the addition of water and the removal of THF, ethyl acetate was added and the organic layer extracted and dried over Na_2SO_4 . The crude was purified by flash chromatography on silica gel (cyclohexane/ethyl acetate 85/15 as eluant).

Compound (60): yield 70% (60:40 mixture of inseparable diastereoisomers). ^1H NMR (400 MHz, CDCl_3) δ 6.66 (d, 0.6H, $J = 8.2$ Hz), 6.55 (d, 0.4H, $J = 8.0$ Hz), 5.63 (d, 0.4H, $J = 10.0$ Hz), 5.63 (d, 0.6H, $J = 10.1$ Hz), 5.16 (q, 1H, $J = 7.2$ Hz), 4.65 (m, 1H), 3.99 (bs, 1H), 3.75 (s, 3H), 2.68-2.85 (m, 1H), 1.55-1.75 (m, 3H), 1.49 (s, 9H), 1.43 (d, 3H, $J = 7.2$ Hz), 0.96-1.03 (m, 12H); ^{13}C NMR (400 MHz, CDCl_3) δ 173.0, 167.5, 152.6, 141.9 (142.5), 134.3 (135.0), 82.1, 74.4, 52.0, 50.7, 41.0, 28.1 (3C), 27.6, 24.8, 22.7, 22.5, 21.6, 19.4 (20.1); LC-ESI-MS: 8.2 min, $[M + H]^+ = 386$, $[M + Na]^+ = 408$.

Procedure for the synthesis of allylic methylcarbonate: (61a,b).

Under inert atmosphere, each enantiomer of (58a,b) (1 eq) was dissolved at -78°C in THF and then LiHMDA (1.5 eq) was added. The mixture was stirred for 30 min and then methyl chloroformiate (2 eq) was added dropwise. The mixture was stirred for 1.5h at -78°C . The reaction was diluted with ethyl acetate and washed with water. The crude was purified by flash chromatography on silica gel (95:5=Cy:EtOAc).

Compound (61b): yield of (*S*)-61b: 75%; yield of (*R*)-61b: 78%. E-isomer: ^1H NMR (400 MHz, CDCl_3) δ 5.81 (dd, $^3\text{J}=9.6$ Hz, $^4\text{J}=1.2$ Hz, 1H), 5.44 (q, $^3\text{J}=6.4$ Hz, 1H), 3.77 (s, 3H), 3.15 (m, 1H), 1.51 (s, 9H), 1.40 (d, $^3\text{J}=6.8$ Hz, 3H), 0.99 (d, $^3\text{J}=6.8$ Hz, 6H); ^{13}C NMR (400 MHz, CDCl_3) δ 165.6, 155.0, 146.7, 131.3, 81.2, 74.0, 54.5, 28.1, 26.2, 22.5, 19.8; LC-ESI-MS: 11.8 min, $[M + H]^+=273$, $[M + Na]^+=295$. Z-isomer: ^1H NMR (400 MHz, CDCl_3) δ 5.76 (d, $^3\text{J}=9.6$ Hz, 1H), 4.36 (q, $^3\text{J}=6.4$ Hz, 1H), 3.77 (s, 3H), 3.00 (m, 1H), 1.48 (s, 9H), 1.32 (d, $^3\text{J}=6.4$ Hz, 3H), 0.99 (d, $^3\text{J}=6.8$ Hz, 6H); ^{13}C NMR (400 MHz, CDCl_3) δ 165.6, 155.0, 146.7, 131.3, 81.2, 74.0, 54.5, 28.1, 26.2, 22.5, 19.8; LC-ESI-MS: 8.9 min, $[M + H]^+=273$, $[M + Na]^+=295$. *S*-enantiomer $[\alpha]^D=-30.0$, *R*-enantiomer $[\alpha]^D=+28.9$ (c 1 in CHCl_3).

Compound (61a): E-isomer: ^1H NMR (200 MHz, CDCl_3) δ 5.88 (d, 1H, $\text{J}=10.0$ Hz), 5.60 (q, 1H, $\text{J}=6.6$ Hz), 2.80 (m, 1H), 2.02 (s, 3H), 1.55-1.77 (m, 5H), 1.33 (d, 3H, $\text{J}=6.6$ Hz), 0.89-1.25 (m, 5H); ^{13}C NMR (400 MHz, CDCl_3) δ 170.1, 166.4, 146.7, 130.8, 81.2, 60.2, 37.8, 32.6, 32.4, 26.0, 25.5(2), 22.7, 21.2(2), 19.9; GC-MS 17.40 min, m/z : 268(2), 225(18), 208(55), 179(63), 162(100), 151(10), 143(95), 133(57), 119(35), 105(33), 91(41), 81(84), 67(38), 55(31). $[\alpha]^{D25}=+27.2$ (c 1.0, CHCl_3).

Procedure for the synthesis of N-Boc-derivative: (64). To a solution of the 60 (1 eq) in THF, di-*t*-butyl dicarbonate (2.5 eq), DMAP

(0.2 eq) and TEA (1.2 eq) were added and the solution was refluxed for 1h. After cooling the mixture and quenching it with water, THF was removed and the residue was diluted with ethyl acetate and washed with water. The organic layer was dried over Na_2SO_4 and solvent was removed. Compound (64) was isolated by flash chromatography on silica gel (cyclohexane/ethyl acetate 85/15 as eluant). **Compound (64)**: yield 60% (60:40 mixture of inseparable diastereoisomers): ^1H NMR (400 MHz, CDCl_3) δ 6.60 (bm, 1H), 5.70 (d, 0.4H, $J=10.0$ Hz), 5.68 (d, 0.6H, $J=10.2$ Hz), 5.18 (m, 1H), 4.68 (m, 1H), 3.71 (s, 3H), 2.53 (m, 1H), 1.55-1.75 (m, 3H), 1.49 (s, 9H), 1.42 (s, 9H), 1.45 (d, 3H, $J=7.2$ Hz), 0.98-1.15 (m, 12H); ^{13}C NMR (200 MHz, CDCl_3) δ 171.3, 169.7, 152.9, 150.9, 142.5, 135.3 (135.4), 84.0, 81.9, 72.9, 52.0, 51.9, 38.8, 27.8 (3C), 27.6 (3C), 26.8, 25.2, 22.7, 23.3, 22.0, 21.9, 19.3 (19.5); LC-ESI-MS: 15.1 min, $[M + H]^+=486$, $[M + Na]^+=508$.

General procedure for allylic amination: (62a,b), (63a,b) and (65). Under inert atmosphere, to a solution of $[\text{Ir}(\text{COD})(\text{Cl})_2]$ (5 mol%) and phosphorous ligand (20 mol%) in EtOH, carbonate 60, 61a,b or 64 (1 eq) and amine (5 eq) were added at r.t. The solution was stirred under reflux. After removal of the solvent and the excess of amine, the residue was diluted with ethyl acetate and washed with water, then dried over Na_2SO_4 . The crude was purified by flash chromatography on silica gel (cyclohexane/ethyl acetate 85:15 as eluant).

Compound (62a): (major *Z* isomer) ^1H NMR (400 MHz, CDCl_3) δ 9.52 (bd, 1H), 7.12 (q, 1H, $J=6.8$ Hz), 6.09 (m, 1H), 5.36 (bd, 1H, $J=17.2$ Hz), 5.31 (bd, 1H, $J=10.0$ Hz), 4.79 (m, 1H), 3.89 (s, 3H), 3.61 (d, 1H, $J=8.0$ Hz), 3.24 (dd, 1H, $J=12.4, 6.4$ Hz), 2.89 (dd, 1H, $J=12.4, 8.6$ Hz), 2.17 (d, 3H, $J=6.8$), 1.79 (m, 1H), 1.42-1.46 (m, 3H), 0.99-1.24 (m, 12H); ^{13}C NMR (200 MHz, CDCl_3) δ 173.1, 168.9, 137.4, 136.0, 134.8, 119.4, 58.4, 49.7, 38.1, 33.6, 27.0, 22.5, 22.4, 20.2, 19.3, 17.7;

LC-ESI-MS: 8.98 min (major), 7.17 (minor), $[M + H]^+ = 325$.

Compound (62b): (major Z isomer) ^1H NMR (400 MHz, CDCl_3) δ 9.98 (bd, 1H, $J = 7.6$ Hz), 7.14 (d, 2H, $J = 8.0$ Hz), 6.97 (m, 1H), 6.87 (d, 2H, $J = 8.4$ Hz), 4.47 (m, 1H), 3.81 (s, 3H), 3.81 (s, 3H), 3.79 (s, 3H), 3.71-3.88 (m, 1H), 3.39-3.51 (m, 1H), 3.44 (d, 1H, $J = 6.8$ Hz), 1.75 (d, 3H, $J = 7.2$ Hz), 1.65 (m, 1H), 1.23-1.30 (m, 3H), 0.79-1.03 (m, 12H); ^{13}C NMR (200 MHz, CDCl_3) δ 172.3, 167.7, 159.0, 142.1, 137.0, 131.6, 129.0, 114.1, 60.8, 55.2, 50.7, 41.4, 37.5, 25.0, 22.8, 21.9, 20.4, 20.2, 14.1; LC-ESI-MS: 8.3 min, $[M + H]^+ = 405$.

Compound (63b): ^1H NMR (400 MHz, CDCl_3) δ 6.89 (q, $^3J = 7.2$ Hz, 1H), 5.86 (m, 1H), 5.15 (dd, $^3J = 17.2$ Hz, $^2J = 2$ Hz, 1H), 5.03 (dd, $^3J = 10.4$ Hz, $^2J = 1.6$ Hz, 1H), 3.22 (dd, $^3J = 14$ Hz, $^3J = 5.2$ Hz, 1H), 3.08 (d, $^3J = 9.2$ Hz, 1H), 2.96 (dd, $^2J = 14$ Hz, $^3J = 6.8$ Hz, 1H), 1.92 (m, 1H), 1.75 (d, $^3J = 7.2$ Hz, 3H), 1.46 (s, 9H), 1.07 (d, $^3J = 6.4$ Hz, 3H), 0.74 (d, $^3J = 6.4$ Hz, 3H); ^{13}C NMR (200 MHz, CDCl_3) δ 166.7, 138.4, 136.5, 134.3, 115.0, 80.1, 61.4, 49.7, 32.0, 28.1, 21.0, 20.1, 13.9; LC-ESI-MS: 15.0 min, $[M + H]^+ = 254$; *S*-enantiomer $[\alpha]^D = +19.5$, *R*-enantiomer $[\alpha]^D = -20.6$ (c 1 in CHCl_3).

Compound (65): ^1H NMR (400 MHz, CDCl_3) δ 7.70 (bd, 1H, $J = 8.6$ Hz), 7.14 (d, 2H, $J = 8.0$ Hz), 6.68 (m, 1H), 6.64 (d, 2H, $J = 8.0$), 5.39 (m, 1H), 4.29 (m, 1H), 3.69 (s, 3H), 3.61 (bs, 2H), 2.51 (m, 1H), 1.99 (m, 4H), 1.67-1.88 (m, 2H), 1.46 (s, 9H), 0.92-1.03 (m, 12H); ^{13}C NMR (200 MHz, CDCl_3) δ 171.5, 163.4, 151.3, 145.0, 134.6, 130.5, 130.4, 129.2, 129.1, 114.8, 83.7, 72.9, 62.0, 51.9, 50.0, 38.7, 28.3 (3C), 27.7, 24.9, 23.2, 23.1, 21.9, 21.8, 19.4; LC-ESI-MS: 10.3 min, $[M + H]^+ = 490$, $[M + Na]^+ = 512$.

Procedure for introduction of Fmoc-group on nitrogen: (66). Compound 61 (1 eq), Fmoc-Cl (1 eq) and a NaHCO_3 (4 eq) solution in water (2.5 ml) were added to dioxane (1,4 ml) and the mixture was stirred at

room temperature overnight. The reaction was quenched with water and the crude extracted with EtOAc and purified by flash chromatography (silica gel, 95:5=Cy:EtOAc). Yield of (S)-66: 90%. Yield of (R)-66: 89%. Isomer a: $^1\text{H NMR}$ (400 MHz, CDCl_3) δ 7.73 (d, $^3\text{J}=7.2$ Hz, 2H), 7.57 (dd, $^3\text{J}=7.6$ Hz, $^3\text{J}=7.6$ Hz, 2H), 7.36 (dd, $^3\text{J}=8.4$ Hz, $^3\text{J}=8.4$ Hz, 2H), 7.30-7.24 (m, 2H), 6.83 (q, $^3\text{J}=7.2$ Hz, 1H), 5.57 (m, 1H), 4.82 (m, 2H), 4.52 (m, 3H), 4.20 (m, 1H), 3.90 (m, 2H), 2.62 (m, 1H), 1.87 (d, $^3\text{J}=7.2$ Hz, 3H), 1.45 (s, 9H), 0.82 (d, $^3\text{J}=6.4$ Hz, 3H), 0.76 (d, $^3\text{J}=6.4$ Hz, 3H); $^{13}\text{C NMR}$ (200 MHz, CDCl_3) δ 166.7, 156.8, 143.3, 142.9, 135.1, 134.6, 129.0, 127.5, 126.9, 124.9, 124.4, 118.8, 80.4, 66.8, 59.5, 47.5, 45.5, 28.0, 26.8, 20.0, 19.7, 14.5. Isomer b: $^1\text{H NMR}$ (400 MHz, CDCl_3): δ 7.73 (d, $^3\text{J}=7.2$ Hz, 2H), 7.57 (dd, $^3\text{J}=7.6$ Hz, $^3\text{J}=7.6$ Hz, 2H), 7.36 (dd, $^3\text{J}=8.4$ Hz, $^3\text{J}=8.4$ Hz, 2H), 7.30-7.24 (m, 2H), 6.62 (q, $^3\text{J}=7.2$ Hz, 1H), 5.57 (m, 1H), 4.82 (m, 2H), 4.52 (m, 3H), 4.20 (m, 1H), 3.90 (m, 2H), 2.45 (m, 1H), 1.87 (d, $^3\text{J}=7.2$ Hz, 3H), 1.45 (s, 9H), 0.82 (d, $^3\text{J}=6.4$ Hz, 3H), 0.76 (d, $^3\text{J}=6.4$ Hz, 3H); $^{13}\text{C NMR}$ (200 MHz, CDCl_3) δ 166.7, 156.8, 144.2, 142.7, 135.3, 133.5, 127.3, 126.9, 124.9, 124.4, 119.8, 80.3, 66.8, 66.1, 47.4, 45.8, 28.0, 27.3, 19.8, 19.2, 14.5. LC-ESI-MS: 19.0 min, 21.5 min $[M + H]^+=476$, $[M + Na]^+=498$. *S*-enantiomer $[\alpha]^D = +6.38$, *R*-enantiomer $[\alpha]^D = -2.71$ (c 1 in CHCl_3).

Procedure for the synthesis of N-malonamido derivative: (67a,b).

Methyl malonyl chloride (1.5 eq) and triethylamine (1.5 mmol, 1.5 equiv.) were added at room temperature to a stirred solution of 61a,b (1 eq) in dry DCM (5 mL). After stirring for 3 h, the reaction mixture was diluted with DCM and washed with water. The organic layer was dried over Na_2SO_4 and the solvent was removed. Purification of the crude residue (*Z/E* ratio 4/1) by flash chromatography on silica gel (eluant cyclohexane/EtOAc 9:1) afforded enantiopure compounds (*Z*)-61a,b and (*E*)-61a,b. The desired product was obtained in yields up to 95%.

Compound (67a): Z-isomer: ^1H NMR (400 MHz, CDCl_3) δ 6.85 (q, J= 6.8 Hz, 1H), 5.66 (m, 1H), 5.38 (d, J= 11.2 Hz, 1H), 4.85-5.10 (m, 2H), 4.39 (m, 1H), 3.94 (m, 1H), 3.65 (s, 3H), 3.48 (d, J= 15.2 Hz, 1H), 3.35 (d, J= 15.2 Hz, 1H), 2.38 (m, 1H), 1.92 (d, J = 7.4 Hz, 3H), 1.50-1.65 (m, 5H), 1.45 (s, 9H), 1.02-1.21 (m, 5H); ^{13}C NMR (100 MHz, CDCl_3) δ 168.4, 167.0, 166.7, 144.0, 135.0, 132.6, 15.8, 80.4, 55.7, 52.1, 46.9, 36.9, 30.2, 29.8, 28.0, 26.3, 25.8, 14.7; LC-ESI-MS: 10.3 min, $[M + H]^+ = 394$; HPLC analysis (Chiralpak IA), rt 8.6 min for (R)-Z-67a, 9.2 min for (S)-Z-67a; (S)-Z-67a $[\alpha]^D = +20.4$ (c 1 in CHCl_3), (R)-Z-67a $[\alpha]^D = -16.5$ (c 1 in CHCl_3). E-isomer: ^1H NMR (400 MHz, CDCl_3) δ 6.05 (q, J= 6.8 Hz, 1H), 5.64 (m, 1H), 5.32 (d, J= 11.2 Hz, 1H), 4.85-5.10 (m, 2H), 4.37 (m, 1H), 3.90 (m, 1H), 3.68 (s, 3H), 3.44 (d, J= 15.2 Hz, 1H), 3.33 (d, J= 15.2 Hz, 1H), 2.05 (m, 1H), 1.91 (d, J = 7.2 Hz, 3H), 1.50-1.65 (m, 5H), 1.46 (s, 9H), 1.02-1.21 (m, 5H); ^{13}C NMR (100 MHz, CDCl_3) δ 168.3, 167.1, 166.7, 144.0, 134.1, 132.3, 116.4, 81.1, 53.4, 45.7, 36.9, 30.2, 29.9, 28.1, 26.2, 25.8, 14.1; LC-ESI-MS: 9.7 min, $[M + H]^+ = 394$.

Compound (67b): Z-isomer: ^1H NMR (400 MHz, CDCl_3) δ 6.91 (q, J= 7.2 Hz, 1H), 5.70 (m, 1H), 5.33 (d, J= 11.6 Hz, 1H), 5.13 (d, J= 10.4 Hz, 1H), 5.04 (d, J= 17.2 Hz, 1H), 4.44 (dd, J= 18.2 Hz, 2.4 Hz, 1H), 3.94 (dd, J= 18.2 Hz, 5.2 Hz, 1H), 3.74 (s, 3H), 3.53 (d, J= 15.4 Hz, 1H), 3.38 (d, J = 15.4 Hz, 1H), 2.67 (m, 1H), 1.95 (d, J = 7.4 Hz, 3H), 1.45 (s, 9H), 0.92 (d, J= 6.6 Hz, 3H), 0.81(d, J = 6.6 Hz, 3H); ^{13}C NMR (75 MHz, CDCl_3) δ 168.4, 167.0, 166.6, 143.9, 135.0, 132.9, 115.7, 80.4, 57.0, 52.1, 46.8, 41.2, 28.0, 27.8, 19.7, 14.6; LC-ESI-MS: 10.7 min, $[M + Na]^+ = 376$, $[2M + Na]^+ = 729$; HPLC analysis (Chiralpak IC), rt 33.24 min for (R)-Z-67b, 36.62 min for (S)-Z-67b; (S)-Z-67b $[\alpha]^D = -30.8$ (c 1 in CHCl_3), (R)-Z-67b $[\alpha]^D = +26.7$ (c 1 in CHCl_3); E-isomer: ^1H NMR (400 MHz, CDCl_3) δ 6.18 (q, J= 7.2 Hz, 1H), 5.70 (m, 1H), 5.15 (d, J= 10.0 Hz, 1H), 5.13 (d, J = 10.4 Hz, 1H), 5.04 (d, J= 17.2

Hz, 1H), 4.23 (dd, $J=18.2, 2.0$ Hz, 1H), 4.02 (dd, $J=18.2, 5.0$ Hz, 1H), 3.76 (s, 3H), 3.54 (d, $J=15.4$ Hz, 1H), 3.44 (d, $J=15.4$ Hz, 1H), 2.67 (m, 1H), 1.92 (d, $J=7.4$ Hz, 3H), 1.43 (s, 9H), 0.96 (d, $J=6.6$ Hz, 3H), 0.94 (d, $J=6.6$ Hz, 3H); ^{13}C NMR (100 MHz, CDCl_3) δ 168.4, 167.1, 166.6, 142.7, 135.0, 133.1, 115.0, 80.2, 57.3, 52.1, 46.9, 41.0, 29.2, 27.8, 19.8, 14.3; LC-ESI-MS: 10.1 min, $[M + Na]^+=376$, $[2M + Na]^+=729$; HPLC analysis (Chiralpak IC), rt 48.40 min for (*R*)-E-67b, 59.28 min for (*S*)-E-67b.

Procedure for the synthesis of N-(1-isocyanato-2-methylbenzene)-derivative: (68). To a solution of 61b (1 eq) in dry DCM (0.4M), 1-isocyanato-2-methylbenzene (1 eq) was added at rt and the mixture was stirred for 6h. After removing the solvent, the crude was purified by flash chromatography on silica gel (cyclohexane/ethyl acetate 80:20). *Z* isomer: ^1H NMR (400 MHz, CDCl_3) δ 7.68 (d, $J=7.6$ Hz, 1H), 7.14 (m, 2H), 6.94 (m, 1H), 6.91 (q, $J=7.6$ Hz, 1H, *Z* isomer), 6.60 (bs, 1H), 5.87 (m, 1H), 5.27 (m, 2H), 5.21 (bd, $J=9.2$ Hz, 1H), 4.50 (bd, $J=18.0$ Hz, 1H), 4.00 (dd, $J=18.0, 6.0$ Hz, 1H), 2.68 (m, 1H), 2.18 (s, 3H), 1.98 (d, $J=7.6$ Hz, 3H), 1.49 (s, 9H), 1.00 (d, $J=6.6$ Hz, 3H), 0.85 (d, $J=6.6$ Hz, 3H); ^{13}C NMR (100 MHz, CDCl_3) δ 167.1, 156.4, 142.6, 137.7, 136.3, 133.9, 130.2, 128.1, 126.5, 123.2, 122.3, 116.6, 80.5, 63.0, 58.1, 46.5, 27.9, 20.0, 19.8, 18.4, 14.7; LC-ESI-MS: 14.3 min, $[M + H]^+=387$, $[2M + Na]^+=795$; (*S*)-*Z*-68 $[\alpha]^D=-12.9$ (c 2 in CHCl_3), (*R*)-*Z*-68 $[\alpha]^D=+13.1$ (c 4.8 in CHCl_3). *E* isomer: ^1H NMR (400 MHz, CDCl_3) δ 7.68 (d, $J=7.6$ Hz, 1H), 7.14 (m, 2H), 6.94 (m, 1H), 6.11 (q, $J=7.6$ Hz, 1H, *E* isomer), 6.60 (bs, 1H), 5.87 (m, 1H), 5.27 (m, 2H), 5.21 (bd, $J=9.2$ Hz, 1H), 4.50 (bd, $J=18.0$ Hz, 1H), 4.00 (dd, $J=18.0, 6.0$ Hz, 1H), 2.68 (m, 1H), 2.18 (s, 3H), 1.98 (d, $J=7.6$ Hz, 3H), 1.49 (s, 9H), 1.00 (d, $J=6.6$ Hz, 3H), 0.85 (d, $J=6.6$ Hz, 3H); LC-ESI-MS: 13.8 min, $[M + H]^+=387$, $[2M + Na]^+=795$.

General procedure for ring closing methathesis for the synthesis of 3,4-dehydro- β -pirrole: (69), (70a,b) and (71). To a solution of enantiopure (66) or (67a,b) or (68) (1 eq) in MTBE (0.2M), Hoveyda-Grubbs II generation catalyst (3 mol%) was added and the mixture was stirred at reflux for 3 h. The reaction was then cooled to room temperature and quenched by addition of ethyl vinyl ether. The solvent was removed and the crude residue was purified by flash chromatography on silica gel (cyclohexane/EtOAc 95:5).

Compound (69): yield of (*S*)-69 81%, yield of (*R*)-69 79%. Isomer a: ^1H NMR (400 MHz, CDCl_3) δ 7.75 (d, $^3\text{J}=6.8$ Hz, 2H), 7.62-7.53 (m, 2H), 7.38 (dd, $^3\text{J}=7.6$ Hz, $^3\text{J}=6.8$ Hz, 2H), 7.31 (dd, $^3\text{J}=7.6$ Hz, $^3\text{J}=7.2$ Hz, 2H), 6.64 (m, 1H), 4.87 (m, 1H), 4.56 (d, $^3\text{J}=5.6$ Hz, 2H), 4.55-4.22 (m, 3H), 2.30 (m, 1H), 1.48 (s, 9H), 0.93 (d, $^3\text{J}=6.8$ Hz, 3H), 0.86 (d, $^3\text{J}=6.8$ Hz, 3H); ^{13}C NMR (400 MHz, CDCl_3) δ 162.5, 155.0, 144.0, 143.8, 136.8, 136.0, 127.6, 124.9, 124.7, 119.9, 81.3, 68.8, 67.0, 54.2, 47.3, 32.5, 28.0, 19.0, 18.2. Isomer b: ^1H NMR (400 MHz, CDCl_3) δ 7.75 (d, $^3\text{J}=6.8$ Hz, 2H), 7.62-7.53 (m, 2H), 7.38 (dd, $^3\text{J}=7.6$ Hz, $^3\text{J}=6.8$ Hz, 2H), 7.31 (dd, $^3\text{J}=7.6$ Hz, $^3\text{J}=7.2$ Hz, 2H), 6.64 (m, 1H), 4.87 (m, 1H), 4.56 (d, $^3\text{J}=5.6$ Hz, 2H), 4.55-4.22 (m, 3H), 1.89 (m, 1H), 1.48 (s, 9H), 0.73 (d, $^3\text{J}=6.8$ Hz, 3H), 0.65 (d, $^3\text{J}=6.8$ Hz, 3H); ^{13}C NMR (400 MHz, CDCl_3) δ 162.5, 154.8, 144.0, 143.8, 136.2, 135.6, 127.0, 124.9, 124.6, 119.9, 81.1, 68.4, 66.7, 53.9, 47.3, 32.2, 28.0, 17.8, 17.6. LC-ESI-MS: 15.6 min, $[M+H]^+=434$. (*S*)-Z-69 $[\alpha]^D=-17.7$, (*R*)-Z-69 $[\alpha]^D=+26.5$ (c 1 in CHCl_3)

Compound (70a): 70/30 trans/cis amide ratio. Trans conformer: ^1H NMR (400 MHz, CDCl_3) δ 6.64 (bm, 1H), 4.99 (bm, 1H), 4.28 (dd, J 16.2, 1.8 Hz, 1H), 4.19 (ddd, J= 16.2, 1.6 4.4 Hz, 1H), 3.68 (s, 3H), 3.34 (s, 2H), 1.95 (m, 1H), 1.54-1.71 (m, 5H), 1.41 (s, 9H), 0.88-1.18 (m, 5H); ^{13}C NMR (100 MHz, CDCl_3) δ 167.6, 164.1, 162.3, 137.2,

133.8, 81.2, 67.3, 54.5, 52.2, 42.0, 41.9, 29.2, 28.5, 27.8, 26.2. Cis conformer: ^1H NMR (400 MHz, CDCl_3) δ 6.76 (bm, 1H), 4.64 (bm, 1H), 4.53 (dd, $J = 18.8, 2.8$ Hz, 1H), 4.01 (ddd, $J = 18.8, 1.6, 4.0$ Hz, 1H), 3.69 (s, 3H), 3.44 (d, $J = 15.2$ Hz, 1H), 3.41 (d, $J = 15.2$ Hz, 1H), 1.95 (m, 1H), 1.54-1.71 (m, 5H), 1.41 (s, 9H), 0.88-1.18 (m, 5H); ^{13}C NMR (100 MHz, CDCl_3) δ 167.6, 165.1, 162.3, 136.2, 135.6, 81.4, 67.9, 54.2, 53.7, 44.7, 40.7, 29.0, 28.3, 26.4, 26.1. LC-ESI-MS: 9.74 min, $[M + H]^+ = 352$, $[M + Na]^+ = 374$, $[2M + Na]^+ = 725$. (S)-70a $[\alpha]^D = -39.7$, (R)-70a $[\alpha]^D = +37.6$ (c 1 in CHCl_3)

Compound (70b): 70/30 trans/cis amide ratio. Trans conformer: ^1H NMR (400 MHz, CDCl_3) δ 6.64 (bm, 1H), 5.12 (m, 1H), 4.35 (dd, $J = 16.6, 2.4$ Hz, 1H), 4.27 (ddd, $J = 16.6, 2.0, 4.4$ Hz, 1H), 3.75 (s, 3H), 3.41 (s, 2H), 2.41 (m, 1H), 1.50 (s, 9H), 0.92 (d, $J = 7.0$ Hz, 3H), 0.91 (d, $J = 7.0$ Hz, 3H); ^{13}C NMR (100 MHz, CDCl_3) δ 167.7, 164.3, 162.5, 136.7, 134.1, 81.6, 68.0, 54.6, 52.5, 42.2, 31.8, 28.0, 18.4, 18.3. Cis conformer: ^1H NMR (400 MHz, CDCl_3) δ 6.76 (bm, 1H), 4.77 (m, 1H), 4.60 (dd, $J = 18.8, 2.8$ Hz, 1H), 4.08 (ddd, $J = 18.8, 1.6, 3.0$ Hz, 1H), 3.76 (s, 3H), 3.51 (d, $J = 15.0$ Hz, 1H), 3.45 (d, $J = 15.0$ Hz, 1H), 2.14 (m, 1H), 1.51 (s, 9H), 0.96 (d, $J = 6.6$ Hz, 3H), 0.92 (d, $J = 6.6$ Hz, 3H); ^{13}C NMR (100 MHz, CDCl_3) δ 167.5, 164.8, 162.5, 137.3, 134.9, 81.5, 68.4, 53.8, 52.5, 40.8, 34.5, 28.0, 18.7, 17.5. LC-ESI-MS: 8.25 min, $[M + H]^+ = 312$, $[M + Na]^+ = 334$, $[2M + Na]^+ = 645$. (S)-70b $[\alpha]^D = +34.9$, (R)-70b $[\alpha]^D = -28.7$ (c 1 in CHCl_3).

Compound (71): ^1H NMR (400 MHz, CDCl_3) δ 7.74 (d, $J = 7.2$, 1H), 7.17 (m, 2H), 6.99 (dt, $J = 7.6, 1.2$ Hz, 1H), 6.71 (m, 1H), 5.60 (bs, 1H), 4.95 (bm, 1H), 4.50 (dd, $J = 15.2, 1.6$ Hz, 1H), 4.17 (ddd, $J = 15.2, 5.2, 1.6$ Hz, 1H), 2.33 (m, 1H), 2.25 (s, 3H), 1.49 (s, 9H), 1.00 (d, $J = 7.2$ Hz, 3H), 0.92 (d, $J = 7.2$ Hz, 3H); ^{13}C NMR (50 MHz, CDCl_3) δ 162.5, 154.5, 136.8, 135.7, 130.3, 128.4, 126.7, 123.9, 122.6, 119.8, 81.3, 68.1, 54.2, 32.8, 28.0, 19.2, 17.9, 17.7; LC-ESI-MS: 10.5 min, $[M + H]^+ = 345$,

$[2M + Na]^+ = 711$. (*S*)-71 $[\alpha]^D = -6.0$ (c 0.5 in $CHCl_3$), (*R*)-71 $[\alpha]^D = +6.8$ (c 1 in $CHCl_3$).

General procedure for the hydrolysis of tert-butyl ester: (72), (73a,b) and (74). Ester 69, 70a,b or 71 (1 eq) was dissolved in DCM (0.1M) and TFA (15 eq) was added at 0 \hat{A} $^\circ$ C. The mixture was stirred at room temperature overnight and then evaporated under vacuum. The product was used without further purifications.

Compound (72): yield of (*S*)-72 99%, yield of (*R*)-72 99%. Isomer a: 1H NMR (400 MHz, $CDCl_3$) δ 7.76 (d, $^3J = 7.6$ Hz, 2H), 7.76-7.56 (m, 2H), 7.39 (dd, $^3J = 7.2$ Hz, $^3J = 7.2$ Hz, 2H), 7.32 (dd, $^3J = 6.8$ Hz, $^3J = 6.8$ Hz, 2H), 6.92 (m, 1H), 4.66 (d, $^3J = 5.2$ Hz, 1H), 4.56 (m, 1H), 4.43 (m, 1H), 4.33-4.20 (m, 2H), 4.09 (dd, $^2J = 18.8$ Hz, $^3J = 4.8$ Hz, 1H), 2.30 (m, 1H), 0.94 (d, $^3J = 6.8$ Hz, 3H), 0.84 (d, $^3J = 6.8$ Hz, 3H); ^{13}C NMR (400 MHz, $CDCl_3$) δ 168.7, 156.1, 143.3, 141.4, 140.8, 133.2, 127.8, 127.1, 124.7, 120.0, 68.2, 67.8, 54.5, 47.1, 32.1, 18.9, 17.7. Isomer b: 1H NMR (400 MHz, $CDCl_3$) δ 7.76 (d, $^3J = 7.6$ Hz, 2H), 7.76-7.56 (m, 2H), 7.39 (dd, $^3J = 7.2$ Hz, $^3J = 7.2$ Hz, 2H), 7.32 (dd, $^3J = 6.8$ Hz, $^3J = 6.8$ Hz, 2H), 6.92 (m, 1H), 4.66 (d, $^3J = 5.2$ Hz, 1H), 4.56 (m, 1H), 4.43 (m, 1H), 4.33-4.20 (m, 2H), 4.09 (dd, $^2J = 18.8$ Hz, $^3J = 4.8$ Hz, 1H), 1.87 (m, 1H), 0.70 (d, $^3J = 6.8$ Hz, 3H), 0.62 (d, $^3J = 6.8$ Hz, 3H). ^{13}C NMR (400 MHz, $CDCl_3$) δ 168.7, 156.1, 143.1, 141.3, 140.5, 133.2, 127.8, 127.1, 124.6, 120.0, 68.2, 67.7, 54.2, 47.1, 32.1, 18.9, 17.7. LC(acid)-ESI-MS: 10.0 min, $[M + H]^+ = 378$. (*S*)-72 $[\alpha]^D = -22.22$, (*R*)-72 $[\alpha]^D = +22.46$ (c 1 in $CHCl_3$).

Compound (73a): (70:30 trans/cis amide ratio). Trans conformer: 1H NMR (400 MHz, CD_3OD) δ 6.80 (m, 1H), 5.05 (m, 1H), 4.52 (bdd, $J = 20.0$ Hz, 8.8 Hz, 1H), 4.35 (bdd, $J = 20.0$ Hz, 4.4 Hz, 1H), 3.73 (s, 3H), 3.45 (s, 2H), 1.40-1.55 (m, 6H), 0.80-0.91 (m, 5H); ^{13}C NMR (100 MHz, CD_3OD) δ 167.6, 167.5, 166.5, 137.9, 134.7, 68.0, 55.3, 52.9, 42.2,

41.4, 29.7, 28.7, 26.3. Cis conformer: ^1H NMR (400 MHz, CD_3OD) δ 6.90 (m, 1H), 4.93 (m, 1H), 4.65 (bd, $J= 14.0$ Hz, 1H), 4.10 (bd, $J= 14.0$ Hz, 1H), 3.73 (s, 3H), 3.47 (s, 2H), 1.40-1.55 (m, 6H), 0.80-0.91 (m, 5H); ^{13}C NMR (100 MHz, CD_3OD) δ 167.6, 167.5, 167.3, 140.5, 133.3, 68.4, 54.6, 53.0, 44.6, 40.3, 29.7, 27.5, 26.1. LC-ESI-MS: 8.7 min, $[M + H]^+ = 296$. (*S*)-73a $[\alpha]^D = +33.9$, (*R*)-73a $[\alpha]^D = -30.3$ (c 1 in MeOH).

Compound (73b): (70:30 trans/cis amide ratio). Trans conformer: ^1H NMR (400 MHz, CD_3OD) δ 6.8 (m, 1H), 5.05 (bs, 1H), 4.52 (dd, $J= 18.5$ Hz, 8.8 Hz, 1H), 4.35 (dd, $J= 18.5$ Hz, 4.4 Hz, 1H), 3.73 (s, 3H), 3.42 (s, 2H), 2.35 (m, 1H), 0.92 (d, $J= 7.2$ Hz, 3H), 0.90 (d, $J= 7.2$ Hz, 3H); ^{13}C NMR (100 MHz, CD_3OD) δ 171.2, 164.8, 162.4, 135.9, 134.3, 68.8, 53.2, 52.7, 42.2, 31.4, 18.5, 17.8. Cis conformer: ^1H NMR (400 MHz, CD_3OD) δ 6.90 (m, 1H), 4.93 (bs, 1H), 4.68 (dd, $J= 14.0$, 2.8 Hz, 1H), 4.10 (bd, $J= 14.0$ Hz, 1H), 3.72 (s, 3H), 3.48 (d, $J= 15.0$ Hz, 1H), 3.42 (d, $J= 15.0$ Hz, 1H), 2.22 (m, 1H), 0.98 (d, $J= 7.2$ Hz, 3H), 0.92 (d, $J= 7.2$ Hz, 3H); ^{13}C NMR (100 MHz, CD_3OD) δ 171.3, 164.8, 162.4, 137.2, 134.1, 68.1, 53.9, 52.5, 41.6, 34.1, 18.9, 17.2. LC-ESI-MS: 5.2 min, $[M + H]^+ = 256$, $[M + Na]^+ = 278$. (*S*)-73b $[\alpha]^D = +19.5$, (*R*)-73b $[\alpha]^D = -26.1$ (c 1 in MeOH).

3.5 Notes and references

The spectroscopic data and the synthetic procedures have been adapted from Ref.[38], [45], [48] and [76], with the proper licenses. See Appendix.

Chapter4

Applications of isoxazolidin-5-ones and dehydro- β -prolines in the synthesis of Linezolid-like antibiotics and evaluation of the complex balance with MAO-inhibitory properties.

4.1 Introduction

Among the different tools in the hands of moderne medicine, antibiotics are surely the most useful chemotherapeutic ones. The effectiveness of any kind of chemotherapeutic is due to the complex balance that exists between the biological efficacy and the developement of tolerance or resistance, in the worst case, during the first uses of that drug. This happens for antifungal and antiviral treatments but also for anticancer, antidiabete and antibiotic agents. As regards antimicrobial agents, the diffusion of resistance is the focus of many public health programs since the diffusion of bacterias and the development of their straight is a complex matter difficult to contain. In fact, it is not only a problem for patients already infected and affected by cronic pathologies: they require continuous treatments that can justify the necessity to change the proper drug during the

life in order to maximize the efficacy. It is also a problem that involves all the community as consequence of the high possibility of diffusion of bacterial strains in nosocomial and hospitals, of course in contests of every day life too [78]. The benefits related to the introduction, in the beginning 20th century, of antibiotics were later accompanied to the appearance of several examples of resistance related to more than 400 types of genic modifications on more than 20000 potential resistance genes, even if only limited number of them has been really observed [79]. With the term *antibiotic* you can refer to all those compounds able to inhibit or kill bacteria through specific interaction with a target: for this reason natural and synthetic compounds with this application can be defined antibiotics. Without any doubt, the discovery of antibiotics can be considered an unparagonable relevant health-related event of the last 150 years, not only for their strictly applications. In fact, there are many examples of antibiotics employed for other biological purposes like antiviral and anticancer treatment. Sometimes, the parallel effect is bigger than the antibiotic one, so they are used as drugs for cardiovascular diseases and immunosuppressive agents [80]. On the base of these considerations, the research of new antibiotics selectively active against resistant bacteria is a deeply studied field of medicinal chemistry.

4.1.1 Antibiotic resistance

Bacteria are probably the oldest living species of the earth and for this reason, in all this time, they have been attacked with a lot of substances with the aim to kill them. So they became able to develop resistance mechanisms that explain the behaviour of the most widely employed antibiotics of the last 50 years. Of course, the increasingly resistance of actual antibiotics became a bigger problem if it is considered together with the appearance of multidrug resistance forms. The

multidrug-resistant *ESKAPE* organisms (*Enterococcus* spp., *Staphylococcus aureus*, *Klebsiella* spp., *Acinetobacter baumannii*, *Pseudomonas aeruginosa*, *Enterobacter* spp.), also known as "nosocomial bacteria" or "superbugs", are causes of chronic infections like meningitis, respiratory tract infections, urogenital tract diseases and skin infections. If the role of antibiotic is to block or shut down a particular function of bacterial cells, the resistance mechanism occurs through a proper strategy to prevent the fitting of the drug to a target. Between the most clinically relevant mechanism of resistance three of them received particular attention, since they are related to the use of very common antibiotics: the first regards the inactivation of a drug through destruction of the pharmacophore, as it happens for β -lactamic antibiotics destroyed under the action of β -lactamase; the second concerns target modifications, like for the mutation of 30S ribosomal protein RpsL when streptomycin is used; the third regards changes in penetration or efflux of the drug, like it happens for Linezolid through a specific multidrug pump [81] (Figure 4.1). While in the 70s the major problem came from Gram-negative bacteria, starting from 80s Gram-positive bacteria became the protagonists, with Methicillin-resistant *Staphylococci*, Penicillin-resistant *Pneumococci* and Vancomycin-resistant *Enterococci* [82]; so, several classes of antibiotic agents have been introduced in the last years. As regard bacteria resistant to Vancomycin, Teicoplanin, new antibiotic belonging to the family of glycopeptide like Vancomycin, was introduced for infections due to Gram-positive bacteria. Another approach was the chemical modifications of the two components of Streptogramin (quinupristin and dalfopristin) to generate the new Pristinamycin approved for the infections induced by vancomycin-resistant *Enterococcus faecium*. Daptomycin, antibiotic of the family of lipopeptide, was used since 2003 for skin infections of Gram-positive bacteria resistant to Vancomycin, Methicillin and Linezolid [83]. Among the most recent classes of antibi-

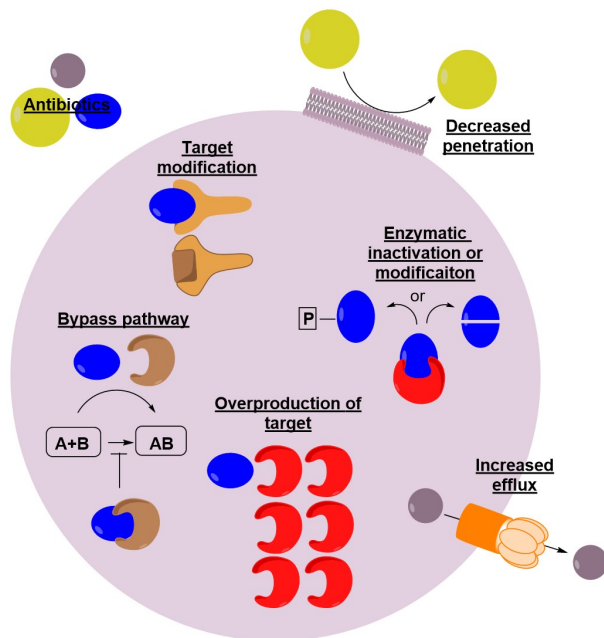


Figure 4.1: Antibiotic resistance mechanisms.

otics, **oxazolidinones** are largely employed against "smartly" modified Gram-positive bacteria.

4.1.2 Oxazolidinones: at the edge of antibiotic activity and anti-depressive role.

Linezolid, commercially available with name Zyvox[®], became the reference compound of the family of oxazolidinones since its approval by FDA in 2000. It is active against Vancomycin-resistant *Enterococci* (VRE), Methicillin-resistant *Staphylococcus aureus* (MRSA) and Penicillin-resistant *Staphylococcus pneumoniae* (PNSSP) [84][85]. Its structure

was introduced together with that of Eperezolid (Figure 4.2) that has almost the same preclinical parameters of Linezolid including solubility, antimicrobial potency and multiple dose toxicity studies. However, Linezolid showed better oral bio-availability. Although these similarities and their similar behavior in clinical phase I, at phase II, Linezolid was selected since it was effective with less doses per day. Like other

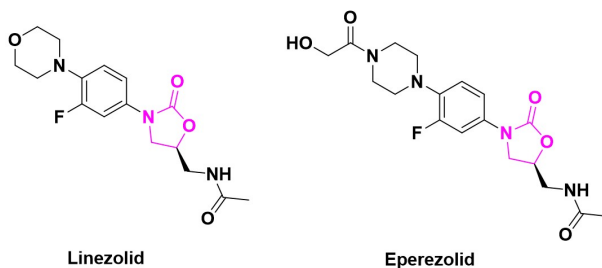


Figure 4.2: Antibiotic resistance mechanisms.

oxazolidinone antibiotics precursors of Linezolid, its mechanism of action regards the binding to peptidyltransferase center (PTC), corresponding to 50S subunit of prokaryotic ribosome, to avoid the formation of a complex between 30S subunit, formylmethionyl-tRNA and mRNA inhibition factors, that is the base for the assembly of an initiation complex for protein synthesis (Figure 4.3). Since it blocks the formation of new virulent factors in a preliminary stage, its mechanism is completely different from those of other inhibitors of protein synthesis [86][87][88]. The structure of Linezolid is made up by four chemical moieties that are the reason for a correct interaction with the binding site (Figure 4.4). *Ring A*, that means the oxazolidinone ring, is the pharmacophore and interacts with specific residues of the PTC pocket through van der Waals interactions. The acetamide NH on the *tail* is involved in an hydrogen bond with the phosphate group on a residue in the upper part of the pocket. *Ring B*, the aromatic one, is in the middle of two π -stacking and gives

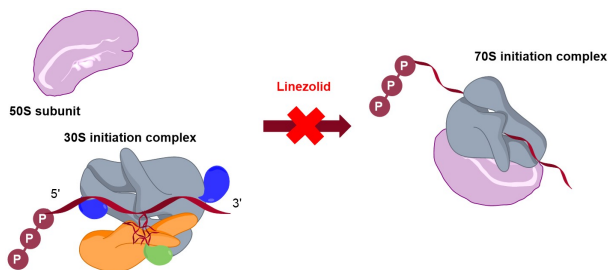


Figure 4.3: Linezolid mechanism of action.

a T-shaped interaction while the C₂ fluorine points out of the pocket, contributing in a coordination with a putative magnesium ion that appears out of the pocket when the binding site is occupied with a ligand in a particular configuration, like that assumed by Linezolid. The morpholine *Ring-C* is not directly involved in particular interactions but it is important for the stabilization of pharmacokinetic aspects [89][90]. Despite all these favorable features, there are several cases of resistance

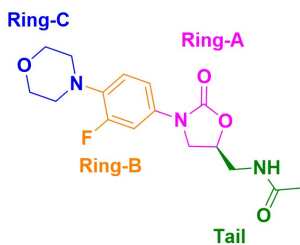


Figure 4.4: Structure of Linezolid divided in relevant moieties.

to Linezolid in patients affected by bacterial infections treated with this drug, but also in people never treated with this therapy, as consequence of horizontal diffusion of strong bacterial strains in nosocomial units [91]. Considering their efficacy and the possibility to introduce modifications to reduce unwanted resistance, oxazolidinones were deeply studied in

structure-activity relationship (SAR) to identify good bioisoster of each part of the molecule. The studies were focused mainly on Ring-A and they showed that bioisosteric modifications should keep an sp^2 center linked to Ring-B, an oxygen atom properly located and stereodefined C_5 linked to acylaminomethyl chain [92]. These requirements are in agreement with the results obtained when oxazolidinone was substituted by dihydrofuran-2-one **a**, tetrahydrofuran-2-one **b**, pyrrolidin-2-one **c**, 3-phenylisoxazoline **d**, 3-phenylisoxazolidinone **e** and 1,2,4-oxadiazole **f**. Microbiological tests, reported as Minimum Inhibitory Concentration (MIC) tests, show that the removal of one or more of the abovementioned requirements gives gradual reduction of antibiotic activity (Figure 4.5) [93][94][95][96]. Changes in Ring-B don't affect significantly the

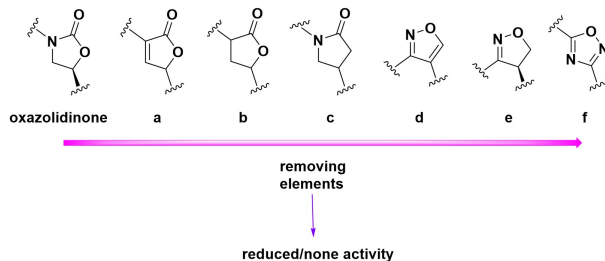


Figure 4.5: Bioisosteres of Ring-A.

activity, but changes in Ring-C have been widely studied and they regard mainly four conceptual framework: the fusion of Ring-B and C, introduction of a spacer between Ring-B and Ring-C, appendage of stabilizing moieties on Ring-C and introduction of new Ring-C [95][96][97]. In particular, reminding that the principal metabolites of Linezolid are produced during the lactone or lactame pathway and they regard the oxidation of morpholine ring [98][99][100], the morpholine has been substituted by piperazine and its derivatives, as reported for Eperzolid and its analogues. Since Linezolid derivatives have C_5 aminomethyl functiona-

lized tail (as amide, urea and thiourea), the resulting structures are similar to another class of chemotherapeutics inhibitors of **monoamino oxidase** (MAOs): Blefoxatone and Toloxatone (Figure 4.6) are active against them both the human isoforms of MAO (indicated as MAO-A and MAO-B). These enzymes are responsible for the metabolism of monoamino neurotransmitters [101], so inhibition of them results in an increased level of neurotransmitters like serotonin, norepinephrine and dopamine and consequent reduction of depressive pathologies and Parkinson diseases associated to low levels of these neurotransmitters. They oxidize amines

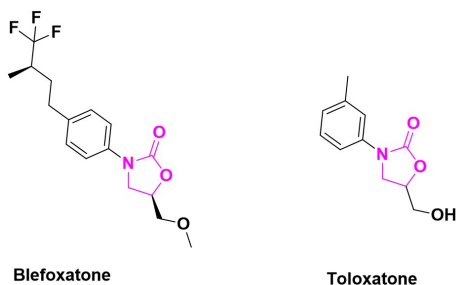


Figure 4.6: Structures of Blefoxatone and Toloxatone.

to imines through reduction of FAD cofactor of MAO, then reoxidized (Figure 4.7). If the ligand present close to FAD is a MAO-inhibitor, the reduction of FAD goes through an anionic semiquinone intermediate to the fully reduced form and no reoxidation of FAD is observed; if the ligand is not an inhibitor, only the fully reduced form can be detected [102]. Linezolid shows reversible MAO-A and MAO-B inhibition [103]. Modifications in the tail carrying "reverse amide" were introduced in Linezolid analogues and reduced MAO activity and myelotoxicity were observed: these side effects normally appear with long treatments with Linezolid [104]. SAR studies revealed that the lipophilicity of oxazolidinones can influence the binding properties since the aromatic ring linked

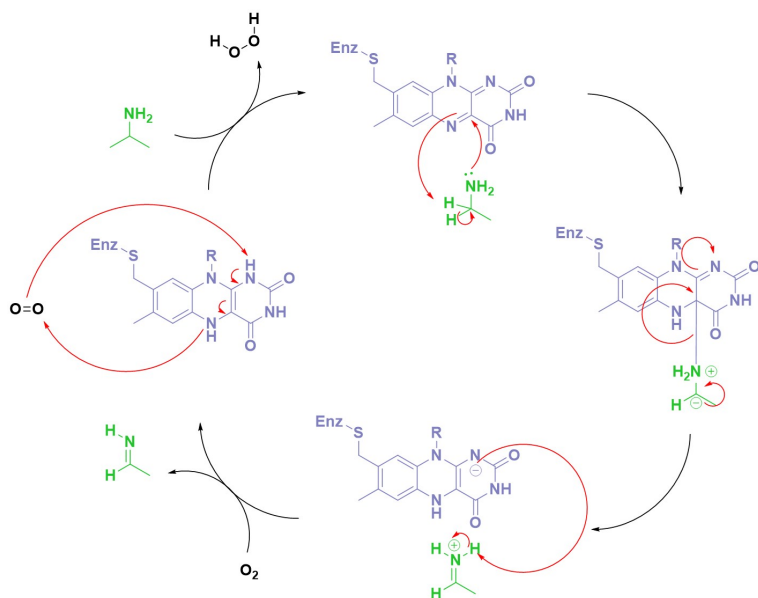


Figure 4.7: General mechanism of action of FAD cofactor.

to nitrogen (or oxygen or sulphur) finds a long and deep hydrophobic cavity in which two tyrosines are aligned with their amine near to N5 of flavin which activate the catalysis [105].

4.2 Results and discussions

With these information in our hand, we designed and synthesized analogues of Linezolid evaluating at the same time the antibiotic properties and the effects as inhibitors of MAOs. So we proceeded step by step, changing initially the Ring-A by introducing a racemic isomer of oxazolidinone, isoxazolidin-5-one, or 3,4-dehydro- β -proline, whose synthesis was partially described in Chapter 3. With the first, we kept

two of the required features previously described, that is to say the sp^2 center linked to aromatic ring and the oxygen atom, while the second ring is a bolder choice since only the sp^2 center is kept. In them both the cases, we introduced (i) substitutions in $C_\alpha N$ to evaluate if they influence the biological data and (ii) reverse N-ethyl amide in $C_\beta N$. The Ring-B was linked to the nitrogen through peptidic bond, keeping the fluorine in the usual position, while Ring-C in some cases was substituted by piperazine or functionalized piperazine. The synthesis, biological evaluation and computational studies on the library will be described in more details as follow.

4.2.1 Molecular design and synthesis

The Ring-A was substituted with isoxazolidin-5-one **56a,b** and 3,4-dehydro- β -proline (**R**)-**72b**/(**S**)-**72b**, whose synthesis was already shown. The desired cyclic synthons were further functionalized to obtain the proper modifications. In particular **72b** enantiomers were coupled with ethyl amine e deprotected from the Fmoc-protecting group to obtain the designed isosteres of Ring-A (**R**)-**76b** and (**S**)-**76b**, in which the original tail of Linezolid has been substituted with an analogue reverse amide (Figure 4.8). To optimize the synthesis we proceeded with a convergent

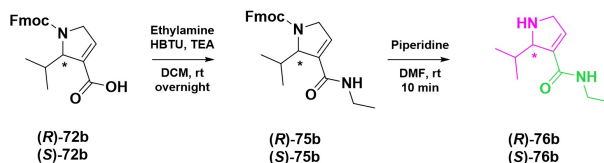


Figure 4.8: Synthesis of functionalized 3,4-dehydro- β -pyrrole ring.

approach, preparing on one hand the couple Ring-A & Tail and on the other the couple Ring-B & Ring-C. While for the first, linear synthesis should have been chosen, for the second we proceeded by divergent syn-

thesis. The starting material was 3,4-difluorobenzoic acid protected as methyl ester by using SOCl_2 and methanol to obtain **77** with 63% yield: the fluorine-aromatic block represents the Ring-B that will be functionalized with Ring-C through the second fluorine atom in position 4. Via

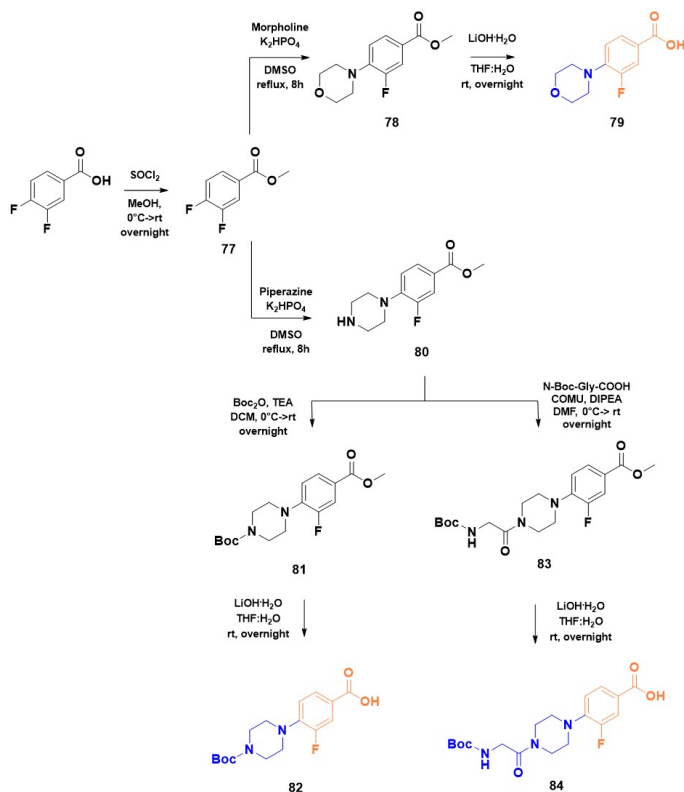


Figure 4.9: Synthesis of Ring-B & Ring-C couple.

nucleophilic substitution we introduced, by K_2HPO_4 in DMSO, morpholine or piperazine obtaining intermediate **78** and **80** with yield of 89-99%. Furthermore, the N-piperazine was functionalized with Boc-group in one

case, obtaining **81** in quantitative yield, and with N-Boc-Gly in the other, by using COMU and DIPEA obtaining **83** in quantitative yield. The three methyl esters **78**, **81** and **83** were hydrolyzed at room temperature with LiOH·H₂O in a 2:1 mixture of THF:H₂O, with yields between 67% and 99% (Figure 4.9). Once the two blocks were synthesized, they were cou-

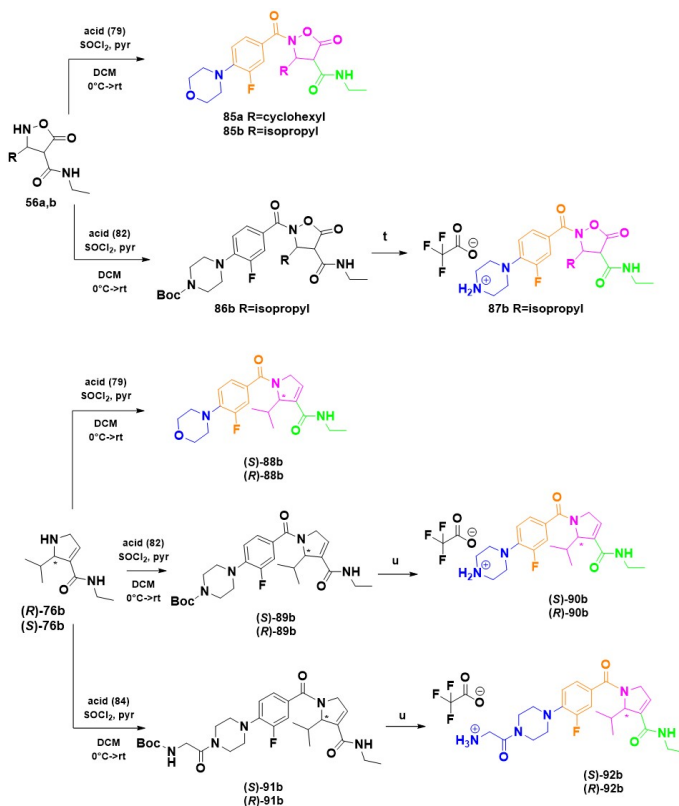


Figure 4.10: Synthesis of isoxazolidin-5-one and 3,4-dehydro- β -pyrrole derivatives.

pled converting in situ the acids **79**, **82** and **84** in the corresponding chloride with thionyl chloride and pyridine: after removing the protective

group with trifluoroacetic acid the final products **85a,b**, **87b**, (**S**)-**88b**, (**R**)-**88b**, (**S**)-**90b**, (**R**)-**90b**, (**S**)-**92b** and (**R**)-**92b** were obtained (Figure 4.10). Their stability in DMSO was studied by 24h monitoring by HPLC but no by-products were observed.

4.2.2 Evaluation of antibiotic activity and MAO inhibition

The antibiotic activity has been evaluated on MRSA and MSSA strains but a preliminary screening on commercial bacterial strains showed unsatisfactory results. Only four selected compounds were further explored and, for this reason, were tested on clinical strains of *S. aureus* from patients affected by cystic fibrosis. The activities have been reported as MIC values (Table 4.1) and showed modest antibiotic activity only for compound **85a** (MIC=32-64 $\mu\text{g/ml}$).

Table 4.1: Antimicrobial activities of tested compounds.

Strains	MIC ($\mu\text{g/ml}$)		MIC-range 12 <i>S. aureus</i> isolates	MIC ₅₀ ($\mu\text{g/ml}$)	MIC ₉₀ ($\mu\text{g/ml}$)
	<i>S. aureus</i> ATCC 29213	<i>E. faecalis</i> ATCC 29212			
Compound					
85a	>128	>128	32->128	64	>128
85b	>128	>128	>128	>128	>128
(R)-88b	>128	>128	>128	>128	>128
(S)-88b	>128	>128	>128	>128	>128
Linezolid	4	2	1-4	2	2

Considering the weak antibiotic activity compared to that of Linezolid (LZD), they were tested in their potential MAO inhibitory activity together to their cytotoxicity. For in vitro tests, HepG2 cells from human hepatocytoma were chosen since this efficient proliferative cell line express the both MAO-A and MAO-B [106][107]. Cell viability tests were

performed to define the dose of compound that should be employed to determine the effects on MAO activity of HepG2: increasing concentration, from 10 to 100 $\mu\text{g/ml}$, of **85a**, **85b**, (**R**)-**88b** and (**S**)-**88b** were administrated to the cells for 24h. If none compound induce mortality at 10 $\mu\text{g/ml}$ concentration, with a ten-times increasing concentration a decrease in cell viability of 10% with **85a**, **85b** and (**R**)-**88b** and 20% with (**S**)-**88b** were observed. Compounds **85a**, **85b** and (**S**)-**88b** showed significant inhibitory effect of 25% at 10 $\mu\text{g/ml}$, so increasing the the drug concentration of ten times 45% of inhibitory effect was reached. On the contrary, the same concentration of Linezolid induces weak enzymatic inhibition (15%), as reported in literature [99].

4.2.3 SAR studies

The substitution with the two isosteres isoxazolidin-5-one and 3,4-dehydro- β -proline led to a loss of antibacterial activity. By prediction of $\log P_{Kow}$ (see section 4.5) is possible to rationalize the biological trend observed. All the compounds containing the isoxazolidinone ring have hydrophilic behaviour in contrast with those containing 3,4-dehydro- β -pyrrole ring that have more lipophilic nature. As regard the first family of compounds, while diisopropyl group does not affect the hydrophilicity of the molecules, the cyclohexyl group gives enhancement of lipophilicity, conferred by higher $\log P_{Kow}$ values. For the second family of compounds, the modulation of the lipophilicity depends on the substitution on Ring-C: going from morpholine to Gly-piperazine through piperazine, the $\log P_{Kow}$ values go toward those associated to a more hydrophilic character. Furthermore, as reported in Table 4.2 compound **85a** has $\log P_{Kow}$ value near to that of Linezolid, confirming that changes in hydrophilicity/lipophilicity detected in the other compounds affect significantly the interaction with the binding site.

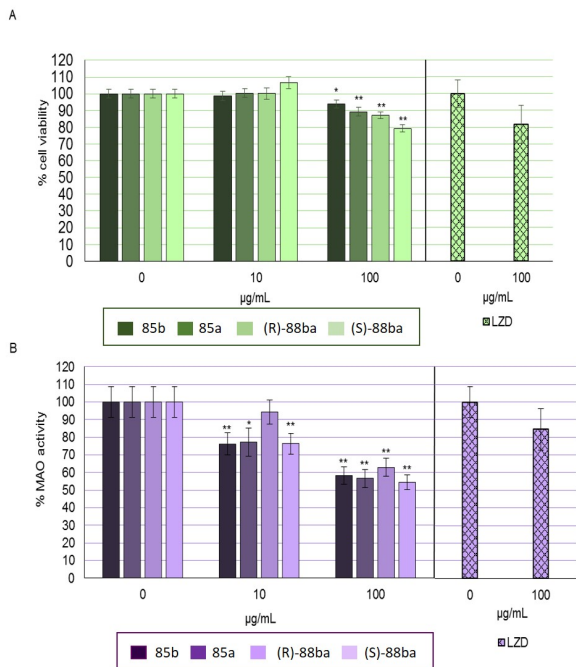


Figure 4.11: A) Cell viability of 85a, 85b, (R)-88b, (S)-88b and Linezolid in HepG2 cells. B) MAO activity of 85a, 85b, (R)-88b, (S)-88b and Linezolid in HepG2 cells.

4.2.4 Docking experiments

To understand the binding poses of the new compounds, docking studies were performed into the active site of human monoamine oxidase isoforms A (MAO-A) and B (MAO-B). Their crystal structures were retrieved from the Protein Data Bank (PDB codes: 2Z5X [108][109] and 2V5Z [110][111], respectively) and processed using Schrödinger Protein Preparation Wizard [112]. A library of compounds was built including the four possible stereoisomers of **85a** and **85b** ((*R,R*)-**85a,b**, (*R,S*)-**85a,b**, (*S,R*)-**85a,b** and (*S,S*)-**85a,b**), the two enantiomers (*R*)-**88b** and

Table 4.2: Prediction of $\log P_{K_{ow}}$.

Compound	$\log P_{K_{ow}}$
85a	1.10
85b	-0.26
87b*	-0.50
(S)-88b	1.72
(S)-90b	1.48
(S)-92b	0.10
Linezolid	1.26

* $\log P_{K_{ow}}$ calculated for the neutral form.

(S)-88b and (S)-Linezolid as reference compound. The optimization of the library was performed with AutoDock Vina [113] by molecular mechanic and docking. The free energy of binding calculated for MAO-A are lower for all the compounds with respect to (S)-Linezolid and only **(R,R)-85a,b**, **(R)-88b** and **(S)-88b** showed negative values (Table 4.3).

Table 4.3: Docking scores on MAO-Aa for (R,R)-85a,b, 88b and Linezolid.

Compound	Free energy binding (kcal/mol)
S-Linezolid	-6.2
S-88b b	-2.0
RR-85a	-1.7
RR-85b	-0.3
R-88b b	-0.2

(S)-88b and (S)-Linezolid direct the morpholine ring toward the MAO-A aromatic cage (made up by FAD, TYR-407 and TYR-444), but only **(S)-88b** penetrates deeply in the binding site to accomodate the bulky isopropyl group in the space occupied by oxazolidinone for (S)-Linezolid

(Figure 4.12). The tail amide gives only one hydrogen bond with VAL-210 as regard (*S*)-Linezolid, as well the central C=O of (*S*)-88b with THR-336.

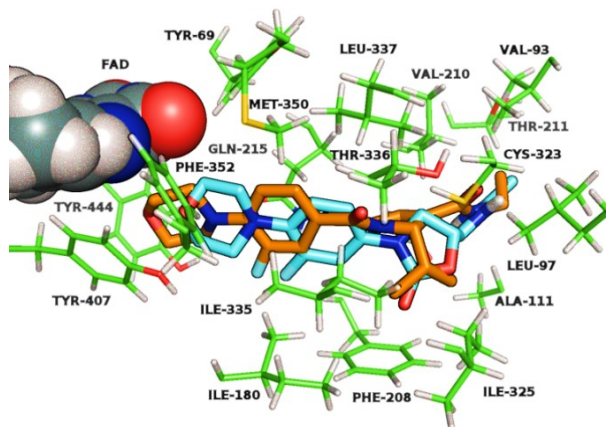


Figure 4.12: Best docking pose of (*S*)-Linezolid (cyan carbon atoms) superimposed to the best docking pose of (*S*)-88b (orange carbon atoms) in the active site of MAO-A. Residues of the binding site are represented with green carbon atoms and FAD as CPK.

Similar binding pose was found for (*R*)-88b, that fits in the deeper part of the cage as consequence of two possible spatial disposition of isopropyl group (Figure 4.13). In the same way, the tail amide gives only an hydrogen bond with PHE-208. The compounds (*R,R*)-85a,b show two superimposable docking poses, completely different to one of (*S*)-Linezolid (Figure 4.14). In fact, the aromatic cage of MAO-A is occupied by N-ethyl amide tail of the two compounds, while the morpholine ring is at the cavity entrance, interacting with VAL-93, LEU-97 and THR-211.

Better result were obtained by docking compounds 85a,b and 88b into MAO-B, as shown by the free energy values reported in Table 4.4. All compounds show a second isoenergetic binding pose that differs only for the relative disposition of Ring-B; with the exception of (*R,R*)-

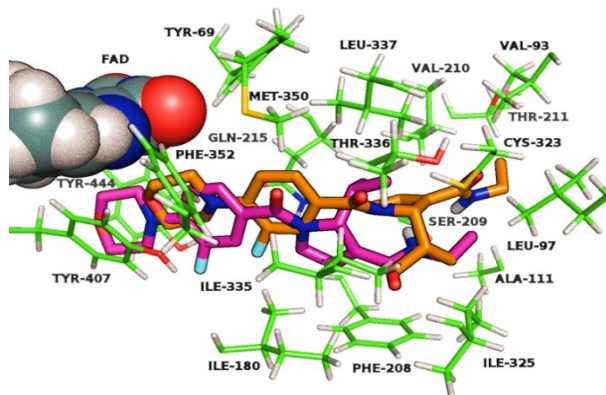


Figure 4.13: Best docking pose of (*S*)-88b (orange carbon atoms) superimposed to the best docking pose of (*R*)-88b (purple carbon atoms) in the active site of MAO-A. Residues of the binding site are represented with green carbon atoms and FAD as CPK.

85a two distinct binding poses with very similar energies were located: the first (A) has the morpholine ring oriented toward the aromatic cage formed by TYR-398 and TYR-435, the second (B) has the tail oriented toward the same space.

Table 4.4: Docking scores on MAO-B for (*R,R*)-85a,b, 88b and Linezolid.

Compound	Free energy binding (kcal/mol)
<i>S</i> -Linezolid	-7.4 (A), -7.6 (B)
<i>S</i> -88b b	-4.1 (A), -3.6 (B)
<i>RR</i> -85b	-7.2 (A), -6.8 (B)
<i>SR</i> -85b	-6.5 (A), -6.7 (B)
<i>RR</i> -85a	-4.5 (A)
<i>R</i> -88b	-8.4 (A), -8.9 (B)

The morpholine ring and the aromatic one of the best poses of (*R*)-88b and Linezolid are almost superimposed and located in the region between

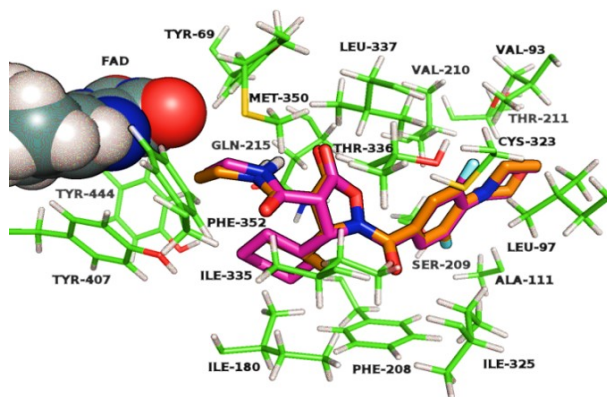


Figure 4.14: Best docking pose of (*R,R*)-85b (orange carbon atoms) superimposed to the best docking pose of (*R,R*)-85a (purple carbon atoms) in the active site of MAO-A. Residues of the binding site are represented with green carbon atoms and FAD as CPK.

the entrance of the cavity and the substrate cavity defined by ILE-199; the aromatic cage contains, instead, the tail amide with residues TYR-398 and TYR-435 (Figure 4.15).

The docking pose is stabilized by four hydrogen bond for (*R*)-88b: (i) between NH of the tail and GLN-206, (ii) between the C=O of the tail and TYR-435 and CYS-172, (iii) between the central C=O and TYR-326. As regard Linezolid, two stabilizing hydrogen bonds were found, between NH of the tail and TYR-398 and between C=O of oxazolidinone and ILE-198. The enantiomer (*S*)-88b has different orientation with respect to its enantiomer R, since it orients the morpholine ring toward the aromatic cage of MAO-B and the amide tail toward the entrance of cavity (Figure 4.16). The central amide C=O is involved in the single hydrogen bond with ILE-199.

As regard the binding poses of (*R,R*)-85b and (*S,R*)-85b, they differ only for the configuration of isopropyl substituted carbon (Figure 4.17 and 4.18). For (*R,R*)-85b, in pose A, three hydrogen bonds involve

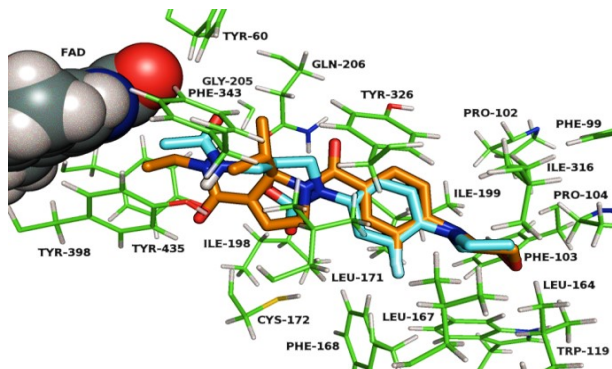


Figure 4.15: Best docking pose of (*S*)-Linezolid (pose B, cyan carbon atoms) superimposed to the best docking pose of (*R*)-88b (pose B, orange carbon atoms) in the active site of MAO-B. Residues of the binding site are represented with green carbon atoms and FAD as CPK.

the isoxazolidinone carbonyl and the tail amide C=O with, respectively, TYR-326 and ILE-199 and with PRO-102. For pose B, the three H-bonds are formed with tail NH, tail amide C=O and central amide C=O with, respectively, GLN-206, LEU-171 and TYR-326. (*S,R*)-**85b** gives two H-bond interaction only in pose A, involving central amide C=O and TYR-326 and the isoxazolidinone carbonyl with PHE-168 (Figure 4.18). Finally, for (*R,R*)-**85a** only one docking pose was found and it was superimposed with that of (*R,R*)-**85b**: they are perfectly superimposed with the cyclohexyl placed between LEU-167, ILE-316 and LEU-164 (Figure 4.19). Furthermore, it gives the same network of hydrogen bonds of (*R,R*)-**85b**.

This results suggest a good selectivity of the new compounds for MAO-B.

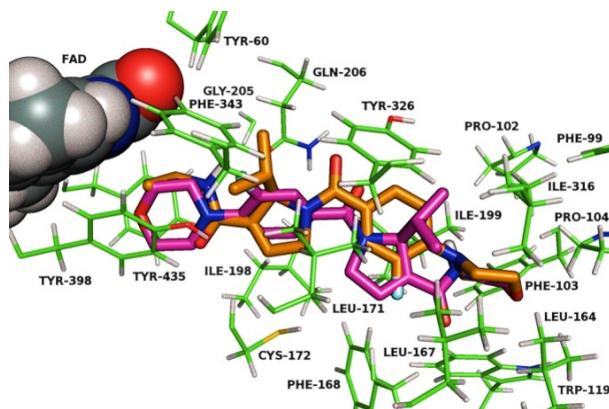


Figure 4.16: Best docking pose of (*R*)-88b (pose B, orange carbon atoms) superimposed to the best docking pose of (*S*)-88b (pose B, purple carbon atoms) in the active site of MAO-B. Residues of the binding site are represented with green carbon atoms and FAD as CPK.

4.3 Conclusions

In the research of new oxazolidinone based compounds is important to keep in mind the balance between antibiotic activity and MAO inhibition. We reported the synthesis of oxazolidinone antibiotic analogues based on isoxazolidin-5-one and 3,4-dehydro- β -proline as bioisosteres of oxazolidinone. The library, that showed weak antibiotic activity against *S. aureus* strains confirming the hypothesis that structural modifications on the molecule backbone of oxazolidinone Linezolid affected the antibiotic activity, was tested to evaluate the effect as inhibitor of monoamino oxidase: we surprisingly found good results, confirmed by docking experiments.

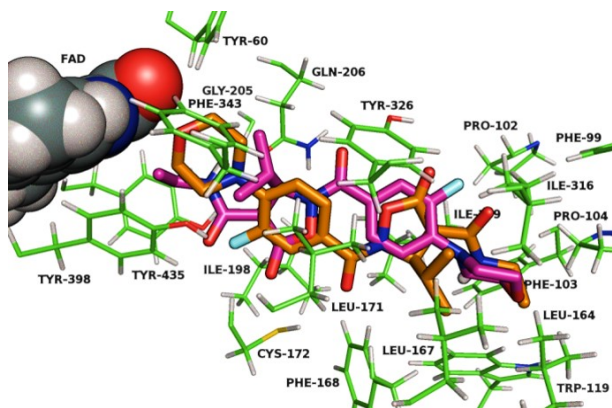


Figure 4.17: Best docking poses of (*R,R*)-85b (pose A, orange carbon atoms; pose B, purple carbon atoms) superimposed in the active site of MAO-B. Residues of the binding site are represented with green carbon atoms and FAD as CPK.

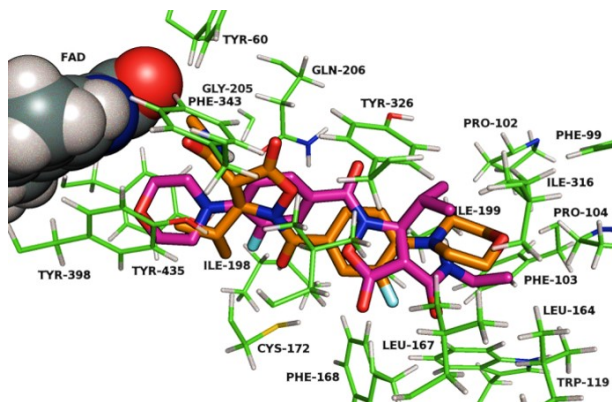


Figure 4.18: Best docking poses of (*S,R*)-85b (pose B, orange carbon atoms; pose A, purple carbon atoms) superimposed in the active site of MAO-B. Residues of the binding site are represented with green carbon atoms and FAD as CPK.

4.4 Experimental procedures

4.4.1 General methods

All chemicals were purchased from commercial suppliers and were used without further purification. Microwave-assisted reactions were car-

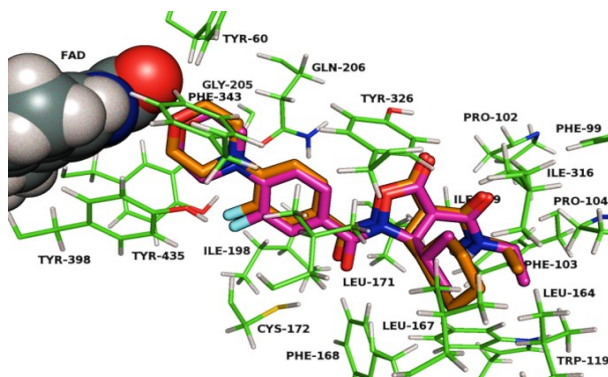


Figure 4.19: Best docking poses of (*R,R*)-85a (orange carbon atoms) superimposed to the best docking pose of (*R,R*)-85b (pose A, purple carbon atoms) in the active site of MAO-B. Residues of the binding site are represented with green carbon atoms and FAD as CPK.

ried out in Milestone Microsynth apparatus, with a dual magnetron system with a pyramid-shaped diffuser, 1000 W maximum power output, and temperature monitor and control by optical fiber up to a vessel temperature of 250 °C. Flash chromatography was carried out on silica gel (230-400 mesh). Dowex®50WX2-200(H) ion exchange resin was used for purification of free amino acids or free amines. NMR spectra were recorded with a Varian Mercury Plus 400 or Varian Gemini 200 instruments. Chemical shifts are reported as δ values (ppm), and were calibrated using the residual solvent peaks of: CDCl_3 , set a $\delta = 7.27$ ppm (^1H NMR) or $\delta = 77.0$ ppm (^{13}C NMR); CD_3OD , set at $\delta = 3.31$ ppm (^1H NMR) and $\delta = 49.0$ ppm (^{13}C NMR); D_2O , set at $\delta = 4.79$ ppm (^1H NMR); CD_3CN , set at $\delta = 1.93$ ppm (^1H NMR) and $\delta = 117.7$ ppm (^{13}C NMR); $(\text{CD}_3)_2\text{CO}$, set at $\delta = 2.04$ ppm (^1H NMR) and $\delta = 29.8$ ppm (^{13}C NMR). Coupling constants are given in Hz. LC-MS analysis was carried out with an HP1100 liquid chromatograph coupled to an electrospray ionization mass spectrometer (LC-ESI-MS), using a Phenomenex Gemini C18 - 3μ - 110 Å column, $\text{H}_2\text{O}/\text{CH}_3\text{CN}$ as neutral solvent or

H₂O/CH₃CN with 0.2% formic acid as acid solvent at 25 °C (positive-ion mode, m/z = 100-500, fragmentor 70 V). Another set of experiments has been performed on an HP1100 liquid chromatograph coupled with an electrospray ionization-ion trap mass spectrometer MSD1100 using a Phenomenex Zorbax C18 - 3.5 μ - 80 Å column, H₂O/CH₃CN with 0.08% trifluoroacetic acid as acid solvent (positive scan 100-500 m/z , fragmentor 70 eV).

4.4.2 Synthesis and characterization

Synthesis of two enantiomers of N-ethyl amide derivative of 3,4-dehydro- β -proline: (75b). Under inert atmosphere, 72b (*R* or *S*) (1 eq), TEA (1.5 eq) and HBTU (1.5 eq) were dissolved in dry DCM (13.5 ml) and ethylamine (2 eq) was added. The mixture was stirred overnight at room temperature. The reaction was diluted with DCM and washed with water. Purification by flash chromatography (silica gel, 6:4 \hat{A} ¹/₄ Cy:EtOAc) allowed to isolate the product. Yield of (*S*)-75b: 98%. Yield of (*R*)-72b: 96%. Isomer a: ¹H NMR (400 MHz, CDCl₃) δ 7.75 (d, ³J= 7.2 Hz, 2H), 7.58 (d, ³J= 7.2 Hz, 2H), 7.47 (bs, 1H), 7.38 (dd, ³J= 7.2 Hz, ³J= 7.2 Hz, 2H), 7.30 (dd, ³J= 7.2 Hz, ³J= 7.2 Hz, 2H), 6.24 (m, 1H), 5.67 (m, 1H), 4.59 (d, ³J= 5.2 Hz, 1H), 4.48-4.21 (m, 3H), 4.05 (m, 1H), 3.34 (q, ³J= 7.2 Hz, 2H), 2.31 (m, 1H), 1.16 (t, ³J= 7.2 Hz, 3H), 0.70 (d, ³J= 6.8 Hz, 3H), 0.60 (d, ³J= 6.8 Hz, 3H); ¹³C NMR (400 MHz, CDCl₃) δ 171.0, 154.8, 143.8, 141.3, 138.7, 138.5, 128.8, 127.6, 124.8, 124.5, 68.8, 66.9, 54.2, 47.3, 34.3, 31.8, 20.9, 14.5; LC-ESI-MS: 11.4 min, $[M + H]^+$ =405. Isomer b: ¹H NMR (400 MHz, CDCl₃) δ 7.75 (d, ³J= 7.2 Hz, 2H), 7.58 (d, ³J= 7.2 Hz, 2H), 7.47 (bs, 1H), 7.38 (dd, ³J= 7.2 Hz, ³J= 7.2 Hz, 2H), 7.30 (dd, ³J= 7.2 Hz, ³J= 7.2 Hz, 2H), 6.24 (m, 1H), 5.67 (m, 1H), 4.59 (d, ³J= 5.2 Hz, 1H), 4.48-4.21 (m, 3H), 4.05 (m, 1H), 3.34 (q, ³J= 7.2 Hz, 2H), 1.85 (m, 1H), 1.16 (t, ³J= 7.2 Hz, 3H),

0.70 (d, $^3J=6.8$ Hz, 3H), 0.60 (d, $^3J=6.8$ Hz, 3H); ^{13}C NMR (400 MHz, CDCl_3) δ 171.0, 154.5, 143.8, 141.2, 138.7, 138.5, 128.3, 126.9, 124.6, 119.8, 68.3, 66.5, 53.9, 47.2, 34.3, 32.1, 20.9, 14.0; LC-ESI-MS: 10.1 min, $[M + H]^+ = 405$. *S*-enantiomer $[\alpha]^D = -22.37$, *R*-enantiomer $[\alpha]^D = +25.81$ (c 1 in CHCl_3).

Deprotection of N-Fmoc group of 3,4-dehydro- β -proline: (76b). 75b (1 eq) was dissolved in a 30% solution of piperidine in DMF and stirred at room temperature for 10 min. The reaction was quenched with water and extracted with EtOAc. The crude was purified by flash chromatography (silica gel, 7:3 $\text{\AA}^{\frac{1}{4}}$ Cy:EtOAc). Yield of (*S*)-76b: 52%. Yield of (*R*)-12: 55%. ^1H NMR (400 MHz, CDCl_3) δ 6.30 (m, 1H), 4.57 (bs, 1H), 4.14-4.03 (m, 2H), 3.34 (q, $^3J=7.2$ Hz, 2H), 2.36 (m, 1H), 1.17 (t, $^3J=7.2$ Hz, 3H), 1.06 (d, $^3J=7.2$ Hz, 3H), 0.90 (d, $^3J=7.2$ Hz, 3H). ^{13}C NMR (400 MHz, CDCl_3) δ 163.3, 143.1, 138.9, 70.3, 52.6, 34.3, 30.1, 19.4, 15.8. LC-ESI-MS: 1.7 min, $[M + H]^+ = 183$. *S*-enantiomer $[\alpha]^D = -23.3$, *R*-enantiomer $[\alpha]^D = +15.8$ (c 1 in CHCl_3).

Esterification of 3,4-difluorobenzoic acid: (77). SOCl_2 (5 eq) was added dropwise in MeOH (0.15M) at 0 $^\circ\text{C}$. After stirring for 15 min, 3,4-difluorobenzoic acid (1 eq) was added and the mixture was stirred at room temperature overnight. The solvent was removed under vacuum and the product was used without further purifications (Y%=63%). ^1H NMR (400 MHz, CDCl_3) δ 7.80 (m, 2H), 7.21 (dd, $^3J=8.4$ Hz, $^3J=18$ Hz, 1H), 3.91 (s, 3H). ^{13}C NMR (400 MHz, CDCl_3) δ 164.5, 153.1 (dd, $^2J_{CF}=13$ Hz, $^1J_{CF}=266$ Hz), 149.6 (dd, $^2J_{CF}=13$ Hz, $^1J_{CF}=247$ Hz), 126.9 (dd, $^4J_{CF}=13$ Hz, $^3J_{CF}=5$ Hz), 126.1 (dd, $^4J_{CF}=3$ Hz, $^3J_{CF}=7$ Hz), 118.3 (d, $^2J_{CF}=18$ Hz), 116.8 (d, $^2J_{CF}=18$ Hz), 51.7. LC-ESI-MS: 8.3 min, $[M + H]^+ = 173$.

General procedure for aromatic nucleophilic substitution: (78) and (80). 77 (1 eq), morpholine or piperazine (2 eq) and K_2HPO_4 (4 eq) were dissolved in DMSO (0.2 ml) and the mixture was refluxed for 8 h. The solution was then poured into water and washed with EtOAc. The crude was purified by flash chromatography (silica gel, 8:2 = Cy:EtOAc). Yield of 78: 89%. Yield of 80: 99%. **Compound (78):** 1H NMR (400 MHz, $CDCl_3$) δ 7.74 (dd, $^3J= 31.6$ Hz, $^4J= 1.6$ Hz, 1H), 7.72 (dd, $^3J= 36.8$ Hz, $^4J= 1.6$ Hz, 1H), 6.94 (dd, $^3J= 8.3$ Hz, $^3J= 8.3$ Hz, 1H), 3.90 (s, 3H), 3.88 (t, $^3J= 4.8$ Hz, 4H), 3.21 (t, $^3J= 4.8$ Hz, 4H); ^{13}C NMR (400 MHz, $CDCl_3$) δ 165.7, 154.0 (d, $^1J_{CF}= 244$ Hz), 143.0 (d, $^2J_{CF}= 8$ Hz), 126.2 (d, $^4J_{CF}= 3$ Hz), 123.2 (d, $^3J_{CF}= 8$ Hz), 117.1 (d, $^3J_{CF}= 3$ Hz), 117.1 (d, $^2J_{CF}= 22$ Hz), 66.4, 51.7, 49.9; LC-ESI-MS: 7.7 min, $[M + H]^+=240$.

Compound (80): 1H NMR (400 MHz, $CDCl_3$) δ 7.69 (dd, $^3J= 31.6$ Hz, $^4J= 1.2$ Hz, 1H), 7.66 (dd, $^3J= 37.2$ Hz, $^4J= 1.2$ Hz, 1H), 6.88 (dd, $^3J= 8.4$ Hz, 1H), 3.86 (s, 3H), 3.15 (t, $^3J= 4.4$ Hz, 2H), 3.02 (t, $J= 4.4$ Hz, 2H), 2.58 (m, 4H); ^{13}C NMR (400 MHz, $CDCl_3$) δ 163.6, 152.2 (d, $^1J_{CF}= 241$ Hz), 142.8 (d, $^2J_{CF}= 7$ Hz), 124.7 (d, $^4J_{CF}= 2$ Hz), 120.8 (d, $^3J_{CF}= 8$ Hz), 116.0 (d, $^3J_{CF}= 4$ Hz), 115.2 (d, $^2J_{CF}= 4$ Hz), 50.0, 44.2, 39.1; LC(acid)-ESI-MS: 1.3 min, $[M + H]^+=239$.

Hydrolysis of methyl esters: (79), (82) and (84). Esters 78 or 81 or 83 (1 eq) was dissolved in a mixture 1:2= H_2O :THF (0.02M), then $LiOH \cdot H_2O$ (2 eq) was added. The mixture was stirred overnight, acidified and the product extracted with EtOAc. Yield of 79: 99%. Yield of 82, 84: 99%.

Compound (79): m.p. 199-201 $^{\circ}C$; 1H NMR (400 MHz, DMSO δ_6) δ 7.62 (dd, $^3J= 46$ Hz, $^4J= 1.6$ Hz, 1H), 7.60 (dd, $^3J= 51.6$ Hz, $^4J= 1.6$ Hz, 1H), 7.06 (dd, $^3J= 8.4$ Hz, $^3J= 8.4$ Hz, 1H), 3.72 (t, $^3J= 4.4$ Hz, 2H), 3.11 (t, $^3J= 4.4$ Hz, 2H), 2.47 (m, 4H); ^{13}C NMR (400 MHz, DMSO δ_6) δ d

166.2, 153.5 (d, $^1J_{CF}$ = 243 Hz), 143.3 (d, $^2J_{CF}$ = 8 Hz), 126.4 (d, $^4J_{CF}$ = 3 Hz), 123.7 (d, $^3J_{CF}$ = 7 Hz), 118.1 (d, $^3J_{CF}$ = 3 Hz), 116.6 (d, $^2J_{CF}$ = 22 Hz), 66.9, 49.7; LC (acid)-ESI-MS: 1.3 min, $[M + H]^+$ =226.

Compound (82): m.p. 218-220 °C; 1H NMR (400 MHz, $CDCl_3$) δ 7.69 (dd, 3J = 29 Hz, 4J = 1.6 Hz, 1H), 7.66 (dd, J = 34.2 Hz, 4J = 1.6 Hz, 1H), 6.88 (dd, 3J)= 6.8 Hz, 3J = 6.8 Hz, 1H), 3.15 (t, J = 4.4 Hz, 4H), 3.02 (t, J = 4.4 Hz, 4H), 1.45 (s, 9H); ^{13}C NMR (400 MHz, $CDCl_3$) δ 170.4, 155.3, 152.9, 144.4, 127.8, 122.8, 117.9, 117.7, 80.2, 49.7, 49.6, 24.4. LC (acid)-ESI-MS: 6.3 min, $[M + H]^+$ =325.

Compound (84): m.p. 223-225 °C; 1H NMR (400 MHz, $CDCl_3$) δ 7.78 (d, 3J = 29.6 Hz, 2H), 7.76 (d, 3J = 34.4 Hz, 1H), 6.91 (dd, 3J = 8.4 Hz, 3J = 8.4 Hz, 1H), 5.56 (bs, 1H), 4.02 (s, 2H), 3.82-3.80 (m, 2H), 3.68 (t, 3J = 4.8 Hz, 2H), 3.24 (t, 3J = 4.8 Hz, 2H), 3.21-3.19 (m, 2H), 1.45 (s, 9H); ^{13}C NMR (400 MHz, $CDCl_3$) δ 169.5, 167.5, 155.6, 153.0, 144.1, 126.9, 123.6, 117.9, 117.8, 79.8, 66.6, 47.2, 38.4, 28.3; LC(acid)-ESI-MS: 7.9 min, $[M + H]^+$ =382.

Synthesis of N-Boc protected compound: (81). Under inert atmosphere, Boc₂O (1 eq) was dissolved in dry DCM (0.2M) and 80 (1.1 eq) was added. TEA (1.5 eq) was added dropwise at 0 °C. The mixture was stirred at room temperature overnight, then poured into HCl 1 M and extracted with DCM. The organic layer was washed with NaHCO₃ sat. sol. and brine. The crude (Y%>99%) was used without further purifications. 1H NMR (400 MHz, $CDCl_3$) δ 7.70 (dd, 3J = 29.6 Hz, 3J = 1.6 Hz, 1H), 7.68 (dd, 3J = 34.8 Hz, 3J = 1.6 Hz, 1H), 6.88 (dd, 3J = 8.4 Hz, 3J = 6.8 Hz, 1H), 3.86 (s, 3H), 3.57 (t, 3J = 4.8 Hz, 4H), 3.12 (t, 3J = 4.8 Hz, 4H), 1.50 (s, 9H); ^{13}C NMR (400 MHz, $CDCl_3$) δ 165.3, 154.0, 153.8 (d, $^1J_{CF}$ = 246 Hz), 143.4 (d, $^2J_{CF}$ = 8 Hz), 126.0 (d, $^4J_{CF}$ = 3 Hz), 123.0 (d, $^3J_{CF}$ = 8 Hz), 117.5 (d, $^3J_{CF}$ = 3 Hz), 116.8 (d, $^2J_{CF}$ = 22 Hz), 79.3, 51.4, 49.3, 27.0; LC-ESI-MS: 11.1 min, $[M + H]^+$ =339.

Synthesis of Gly-derivative: (83). Under inert atmosphere, N-(Boc)-Gly-COOH (1 eq) was dissolved in DMF (0.12M), COMU (1 eq) and DIPEA (3 eq) were added at 0 °C. After stirring for 10 min, 80 (1 eq) was added and mixture stirred at room temperature overnight. The reaction was quenched with HCl 1 M and extracted with EtOAc. The organic layer was washed with NaHCO₃ saturated solution and with brine. The product (Y%>99%) was used without further purifications. ¹H NMR (400 MHz, CDCl₃) δ 7.72 (dd, ³J= 27.2 Hz, ³J= 1.6 Hz, 1H), 7.70 (dd, ³J= 32 Hz, ³J= 1.6 Hz, 1H), 6.88 (dd, ³J= 8.4 Hz, ³J= 8.4 Hz, 1H), 3.99 (s, 2H), 3.87 (s, 3H), 3.79 (t, ³J= 5.2 Hz, 2H), 3.55 (t, ³J= 5.2 Hz, 2H), 3.23-3.12 (m, 4H), 1.44 (s, 9H); ¹³C NMR (400 MHz, CDCl₃) δ 166.7, 165.3, 162.1, 153.7 (d, ¹J_{CF}= 244 Hz), 142.8 (d, ²J_{CF}= 9 Hz), 125.9 (d, ⁴J_{CF}= 3 Hz), 123.4 (d, ³J_{CF}= 7 Hz), 117.5 (d, ³J_{CF}= 3 Hz), 116.8 (d, ²J_{CF}= 22 Hz), 78.9, 66.0, 51.5, 46.7, 43.8, 27.7. LC (acid)-ESI-MS: 8.2 min, [M + H]⁺=396.

General procedure for coupling reaction: (85a,b), (86b), (88b), (89b) and (91b). Under inert atmosphere, acid 79 or 82 or 84 (1.5 eq) was dissolved in dry DCM and thionyl chloride (1.5 eq) was added dropwise at 0 °C. The mixture was stirred at room temperature for 1 h and pyridine (5 eq) was added. The mixture was stirred for 30 min and cyclic amine 56a,b or (S)-76b or (R)-76b (1 eq) was added. The reaction was stirred for 3 h and then quenched with water and extracted with DCM. The crude was purified by flash chromatography (silica gel, 1:1=Cy:EtOAc) to isolate the product. Yield of 85b: 90%. Yield of 85a: 90%. Yield of 86b: 87%. Yield of 88b: 88%. Yield of 89b: 93%. Yield of 91b: 90%.

Compound (85b): ¹H NMR (400 MHz, CDCl₃) δ 7.55 (dd, ³J= 22.4, ⁴J= 1.6 Hz, 1H), 7.52 (dd, ³J= 27.6 Hz, ⁴J= 1.6 Hz, 1H), 6.98 (dd, ³J= 8.4

Hz, $^3J=8.4$ Hz, 1H), 6.13 (bs, 1H), 5.27 (dd, $^3J=28$ Hz, $^3J=6$ Hz, 1H), 3.88 (t, $^3J=4.4$ Hz, 4H), 3.40 (d, $^3J=28$ Hz, 1H), 3.33-3.16 (m, 6H), 2.14 (m, 1H), 1.13 (t, $^3J=7.2$ Hz, 3H), 1.03 (d, $^3J=6.8$ Hz, 6H). 13C NMR (400 MHz, CDCl₃) δ 171.4, 171.1, 162.4, 153.9 (d, $^1J=245$ Hz), 143.3 (d, $^3J=8$ Hz), 126.4 (d, $^3J=4$ Hz), 124.7 (d, $^2J=13$ Hz), 117.5 (d, $^2J=24$ Hz), 117.3 (d, $^3J=4$ Hz), 66.6, 66.0, 50.1, 50.0, 49.6, 35.2, 31.5, 17.9, 17.8, 14.3. LC-ESI-MS: 8.5 min, $[M + H]^+=408$, $[M + Na]^+=430$.

Compound (85a): 1H NMR (400 MHz, CDCl₃) δ 7.54 (dd, $^3J=23.6$ Hz, $^4J=2$ Hz, 1H), 7.51 (dd, $^3J=28.8$ Hz, $^4J=2$ Hz, 1H), 6.90 (dd, $^3J=8.4$ Hz, $^3J=8.4$ Hz, 1H), 6.12 (bs, 1H), 5.25 (dd, $^3J=6$ Hz, $^3J=28$ Hz, 1H), 3.86 (t, $^3J=4.8$ Hz, 4H), 3.44 (d, $^3J=28$ Hz, 1H), 3.36-3.13 (m, 6H), 1.80 (m, 1H), 1.32-1.05 (m, 5H), 1.12 (t, $^3J=7.2$ Hz, 3H), 0.89-0.82 (m, 5H); 13C NMR (400 MHz, CDCl₃) δ 171.6, 171.1, 162.8, 153.6 (d, $^1J=245$ Hz), 143.2 (d, $^2J=8$ Hz), 126.4 (d, $^3J=3$ Hz), 124.9, 117.6 (d, $^2J=23$ Hz), 117.3 (d, $^3J=4$ Hz), 66.7, 65.7, 50.1, 49.9, 41.2, 35.2, 28.5, 28.3, 25.9, 25.6, 14.2; LC-ESI-MS: 10.3 min, $[M + H]^+=448$, $[M + K]^+=486$, $[2M + Na]^+=917$.

Compound (86b): 1H NMR (400 MHz, CDCl₃) δ 7.54 (d, $^3J=20.4$ Hz, 1H), 7.51 (d, $^3J=25.2$ Hz, 1H), 6.90 (dd, $^3J=8.4$ Hz, $^3J=8.4$ Hz, 1H), 6.15 (bs, 1H), 5.26 (dd, $^3J=28$ Hz, $^3J=6$ Hz, 1H), 3.58 (m, 4H), 3.34-3.25 (m, 2H), 3.16-3.09 (m, 4H), 2.12 (m, 1H), 1.46 (s, 9H), 1.12 (t, $^3J=7.2$ Hz, 3H), 1.02 (d, $^3J=6.8$ Hz, 6H); 13C NMR (400 MHz, CDCl₃) δ 171.6, 171.0, 162.1, 154.6, 154.0 (d, $^1J=144$ Hz), 143.4 (d, $^3J=8$ Hz), 126.4 (d, $^3J=3$ Hz), 124.9 (d, $^3J=8$ Hz), 117.8 (d, $^3J=3$ Hz), 117.6 (d, $^2J=24$ Hz), 80.0, 65.9, 49.7 (d, $^3J=4$ Hz), 49.6, 35.3, 31.6, 28.3, 18.0, 17.8, 14.4; LC-ESI-MS: 11.0 min, $[M + H]^+=507$, $[M + Na]^+=529$, $[M + K]^+=545$.

Compound (88b): 1H NMR (400 MHz, CDCl₃) δ 7.46 (bs, 1H), 7.36 (d, $^3J=24.8$ Hz, 1H), 7.34 (d, $^3J=30$ Hz, 1H), 7.05 (dd, $^3J=8.4$ Hz, $^3J=8.4$ Hz, 1H), 6.37 (m, 1H), 5.44 (m, 1H), 4.49 (d, $^3J=15.6$ Hz, 1H), 4.17

(d, $^3J= 16.4$ Hz, 1H), 3.78 (t, $^3J= 4.4$ Hz, 4H), 3.26 (m, 2H), 3.16-3.07 (m, 4H), 2.28 (m, 1H), 1.10 (t, $^3J= 7.2$ Hz, 3H), 0.97 (d, $^3J= 6.8$ Hz, 3H), 0.90 (d, $^3J= 6.8$ Hz, 3H); ^{13}C NMR (400 MHz, CDCl_3) δ 169.8, 163.3, 154.5 (d, $^1J= 247$ Hz), 141.9 (d, $^3J= 8$ Hz), 139.1, 135.1, 129.4, 124.6 (d, $^2J= 60$ Hz), 117.8, 116.0 (d, $^2J= 24$ Hz), 67.6, 66.7, 57.4, 50.3, 34.3, 32.7, 19.3, 17.6, 14.6. LC-ESI-MS: 11.5 min, $[M + H]^+=390$, $[2M + Na]^+=412$; *S*-enantiomer $[\alpha]^D= -58$, *R*-enantiomer $[\alpha]^D= +41$ (c 1 in CHCl_3).

(Compound (89b)): ^1H NMR (400 MHz, CDCl_3) δ 7.28 (dd, $^3J= 13.6$ Hz, $^4J= 1.6$ Hz, 1H), 7.25 (dd, $^3J= 18$ Hz, $^3J= 1.6$ Hz, 1H), 6.90 (dd, $^3J= 8.4$ Hz, $^3J= 8.4$ Hz, 1H), 6.33 (m, 1H), 5.78 (bs, 1H), 5.47 (m, 1H), 4.36 (d, $J= 14.4$ Hz, 1H), 4.16 (d, $^3J= 14.8$ Hz, 1H), 3.58 (t, $^3J= 5.2$ Hz, 4H), 3.38-3.31 (m, 2H), 3.13-3.05 (m, 4H), 2.31 (m, 1H), 1.49 (s, 9H), 1.16 (t, $^3J= 7.2$ Hz, 3H), 1.02 (d, $^3J= 7.2$ Hz, 3H), 0.94 (d, $J= 7.2$ Hz, 3H); ^{13}C NMR (400 MHz, CDCl_3) δ 169.7, 163.3, 155.8, 154.6, 142.0, 139.1, 129.7, 129.4, 124.3, 118.3, 116.0, 79.9, 67.6, 57.4, 50.0, 34.3, 29.2, 28.4, 17.6, 14.6. LC-ESI-MS: 9.3 min, $[M + H]^+=489$, $[M + Na]^+=511$, $[M + K]^+=527$, $[2M + H]^+=976$, $[2M + Na]^+=999$; *S*-enantiomer $[\alpha]^D= -47$, *R*-enantiomer $[\alpha]^D= +40$ (c 1 in CHCl_3).

(Compound (91b)): ^1H NMR (400 MHz, CDCl_3) δ 7.30-7.27 (m, 2H), 6.89 (dd, $^3J= 8.4$ Hz, $^3J= 8.4$ Hz, 1H), 6.33 (m, 1H), 5.73 (bs, 1H), 5.47 (m, 1H), 4.36 (dd, $^3J= 16.4$ Hz, $^3J= 3.6$ Hz, 1H), 4.15 (d, $^3J= 15.6$ Hz, 1H), 3.99 (d, $^3J= 4.4$ Hz, 2H), 3.80-3.78 (m, 2H), 3.57-3.54 (m, 2H), 3.39-3.32 (m, 2H), 3.14-3.07 (m, 4H), 2.33 (m, 1H), 1.44 (s, 9H), 1.16 (t, $^3J= 7.2$ Hz, 3H), 1.02 (d, $^3J= 7.2$ Hz, 3H), 0.94 (d, $^3J= 7.2$ Hz, 3H); ^{13}C NMR (400 MHz, CDCl_3) δ 169.6, 166.9, 163.3, 155.7, 153.4, 141.3, 139.1, 130.3, 129.3, 124.3, 118.4, 116.0 (d, $^3J= 22$ Hz), 79.7, 67.6, 66.6, 57.4, 49.7, 44.3, 34.3, 29.6, 28.3, 19.3, 17.8, 14.6. LC-ESI-MS: 7.27 min, $[M + H]^+=546$, $[2M + Na]^+=569$. *S*-enantiomer $[\alpha]^D= -30$, *R*-enantiomer $[\alpha]^D= +31$ (c 1 in CHCl_3).

General procedure for N-Boc deprotection: (87b), (90b) and (92b).

Carbamate 86b or 89b or 91b (1 eq) was dissolved in DCM (0.1M) and TFA (15 eq) was added at 0 °C. The mixture was stirred at room temperature overnight and then evaporated under vacuum. The product was used without further purifications. Yield of 87b, 90b, 92b: 99%.

(Compound (87b)): $^1\text{H NMR}$ (400 MHz, Acetone δ_6) δ 7.56 (dd, $^3\text{J}= 8.4$ Hz, $^4\text{J}= 1.6$ Hz, 1H), 7.48 (dd, $^3\text{J}= 13.6$ Hz, $^4\text{J}= 2$ Hz, 1H), 7.18 (dd, $^3\text{J}= 8.8$ Hz, $^3\text{J}= 8.8$ Hz, 1H), 5.10 (m, 1H), 3.77 (d, $^3\text{J}= 2$ Hz, 1H), 3.57 (m, 8H), 3.20 (q, $^3\text{J}= 7.2$ Hz, 2H), 2.04 (m, 1H), 1.10 (t, $^3\text{J}= 7.2$ Hz, 3H), 1.03 (d, $^3\text{J}= 6.8$ Hz, 3H), 1.01 (d, $^3\text{J}= 6.8$ Hz, 3H); $^{13}\text{C NMR}$ (400 MHz, Acetone δ_6) δ 171.1, 171.6, 165.9, 154.8 (d, J= 233 Hz), 142.7, 128.0 (d, J= 8 Hz), 127.0 (d, J= 3 Hz), 119.3 (d, J= 3 Hz), 117.9 (d, J= 23 Hz), 68.5, 50.7, 47.7, 44.3, 35.2 (d, J= 13 Hz), 32.5, 18.4, 18.0, 14.6. LC-ESI-MS: 1.5 min, $[M + H]^+=407$, $[2M + H]^+=813$.

(Compound (90b)): $^1\text{H NMR}$ (400 MHz, Acetone δ_6) δ 7.44 (d, $^3\text{J}= 14.4$ Hz, 1H), 7.36 (d, $^3\text{J}= 13.2$ Hz, 1H), 7.16 (dd, $^3\text{J}= 8.8$ Hz, $^3\text{J}= 8.8$ Hz, 1H), 6.37 (m, 1H), 5.43 (m, 1H), 4.52-4.47 (m, 2H), 4.03 (q, $^3\text{J}= 7.2$ Hz, 2H), 3.67-3.53 (m, 6H), 3.30-3.24 (m, 2H), 2.29 (m, 1H), 1.10 (t, $^3\text{J}= 7.2$ Hz, 3H), 0.98 (d, $^3\text{J}= 6.8$ Hz, 3H), 0.91 (d, $^3\text{J}= 6.8$ Hz, 3H); $^{13}\text{C NMR}$ (400 MHz, Acetone δ_6) δ 169.0, 163.4, 159.2, 140.5, 138.6, 131.2, 128.7, 124.6, 117.3, 114.4, 67.8, 57.4, 47.0, 43.8, 38.8, 33.73, 18.8, 17.0, 14.0; LC-ESI-MS: 1.5 min, $[M + H]^+=390$, $[2M + H]^+=777$; *S*-enantiomer $[\alpha]^D = -38$, *R*-enantiomer $[\alpha]^D = +14$ (c 1 in CHCl_3).

(Compound (92b)): $^1\text{H NMR}$ (400 MHz, $\text{CH}^3\text{OH}\delta_4$) δ 7.34 (d, $^3\text{J}= 14$ Hz, 1H), 7.31 (d, $^3\text{J}= 18.4$ Hz, 1H), 7.10 (dd, $^3\text{J}= 8.4$ Hz, $^3\text{J}= 8.4$ Hz, 1H), 6.34 (m, 1H), 5.43 (m, 1H), 5.48 (d, $^3\text{J}= 16.4$ Hz, 1H), 4.16 (d, $^3\text{J}= 16.4$ Hz, 2H), 3.98 (s, 2H), 3.78 (q, $^3\text{J}= 7.2$ Hz, 2H), 3.65-3.58 (m, 2H), 3.27-3.16 (m, 6H), 2.29 (m, 1H), 1.13 (t, $^3\text{J}= 7.2$ Hz, 3H), 1.01 (d, $^3\text{J}= 6.8$ Hz, 3H), 0.94 (d, $^3\text{J}= 6.8$ Hz, 3H); $^{13}\text{C NMR}$ (400 MHz, $\text{CH}^3\text{OH}\delta_4$)

δ 169.7, 166.8, 163.1, 153.4, 141.1, 139.2, 130.5, 129.4, 124.2, 118.3, 117.0 (d, $^3J=22$ Hz), 67.5, 57.7, 49.3, 38.5, 34.1, 29.2, 19.1, 17.5, 14.3; LC-ESI-MS: 1.6 min, $[M + H]^+=446$, $[M + Na]^+=478$; *S*-enantiomer $[\alpha]^D = -17$, *R*-enantiomer $[\alpha]^D = +32$ (c 1 in $CHCl_3$).

4.5 Notes and references

The log $P_{K_{ow}}$ values were calculated by using EPI SuiteTM software. The spectroscopic data and the synthetic procedures have been adapted from Ref.[38], with the proper reuse license. See Appendix. This study has been carried out with the fundamental contribution of "Italian Cystic Fibrosis Research Foundation", "Fondazione del Monte di Bologna e Ravenna", MIUR and University of Bologna. The biological data were produced with the collaboration of E. Lonati, A. Bulbarelli, R. Musumeci and C. Cocuzza in the Department of Medicine and Surgery, University of Milano-Bicocca, Via Cadore 48, 20900, Monza, Italy. The docking experiments have been developed with the collaboration of M. Lombardo, Department of Chemistry, University of Bologna, Vial Selmi 2, 40126, Bologna, Italy.

Chapter5

Applications of dehydro- β -prolines and isoxazolines in the synthesis of integrin ligands as recognition and delivery systems in ligand-receptor interplay

5.1 Introduction

The interactions existing between cells and between cells and extracellular matrix components are determinant to understand the regulation of cellular events behind the mechanisms of cellular growth, differentiation and migration, but also to clarify the phenomena that induce biological and medical processes like inflammation, immune response and tumor cell metastases (Figure 5.1). In the last decades, the strict connection between inflammatory processes and the onset of tumors was found: epidemiological studies revealed, in fact, that chronic inflammations predispose to several forms of cancer since the two phenomena share the same microenvironmental conditions. It seems that the two processes are dependent each other since, through an intrinsic pathway, different classes of oncogenes drives the appearance of inflammatory response, while, through an extrinsic pathway, inflammatory conditions promote cancer

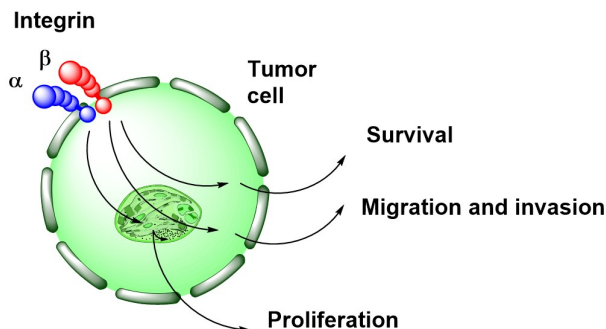


Figure 5.1: Integrin role.

development [114]. In neoplastic processes, the cells act as promoters of tumor growth and proliferation, through genomic instability and promoting angiogenesis. At the same time, inflammatory cells influence all the tumor organs, by differentiation of cell types in the carcinogenic microenvironment. This connection could be due to an attempt of the tumor to subvert immune cell function, favoring the development of cancer [115][116]. Many of the cell-surface interactions regulating these pathological events depend on the activity of cell-surface receptors interacting with adhesion molecules of extracellular matrix. These specific receptors can be employed for the **target-delivery** of molecules on ill tissues since they are normally over-expressed on the surface of affected cells. Antibodies, peptides, protein or small molecules can be employed for this purpose. The main advantage of this approach is that the interaction with normal tissue is significantly reduced, so in the case of targeted delivery of drugs it is possible to reduce the side-effects associated to a particular therapy; therefore, to support this advantage normally cell surface receptors are preferred to intracellular targets, even because there is no need to control the internalization mechanisms that can occur. For this reason, one of the most studied families of receptors for targeted delivery of

chemotherapeutics is the family of **integrins** [117].

5.1.1 Integrins and their ligands: peptidomimetic-chemistry, new frontier of chemotherapy

Integrins are non-covalent heterodimeric transmembrane glycoproteins existing as 24 combinations of 18α and 8β subunits (each of them is made up several domains linked through flexible linkers), able to mediate cell-cell and cell-extracellular matrix (ECM) interactions: they can be divided in five classes in which the same β subunit is combined with different α ones, producing series of proteins with different ligand-binding specificities [118]. The half of them binds extracellular matrix proteins like fibronectin, vitronectin, VCAM-1 and collagen through a specific recognition sequence, and are fundamental for adhesion, migration, signaling and survival of cells. Integrins exist in different conformational states that include (i) the *bent inactive*, in which the inactivators are bound, (ii) the *extended* and (iii) the *fully activated* forms in which integrins are linked to actin and ECM protein together (Figure 5.2). According to the *inside-out activation*, a specific protein of the intracellular space links the integrin in the cytoplasmatic domain: talin links the cytoplasmatic β -domain of integrin in its inactive form, breaking the bridges between the two subunits in the extracellular domain inducing changes in the tilt angle of the protein; kindlins binds the same cytoplasmatic domain enhancing the tail-induced activation. For the *outside-in activation*, the ECM ligand induces the transition between the "closed" to the "open" conformation of the β -subunit domain, without affecting the intracellular domain; when the talin in the intracellular space links the protein, integrin is completely activated [119]. Integrins are widely involved in cancer progression and several sub-types are highly over-expressed on cancer cells. Among them it is possible to mention $\alpha_4\beta_1$,

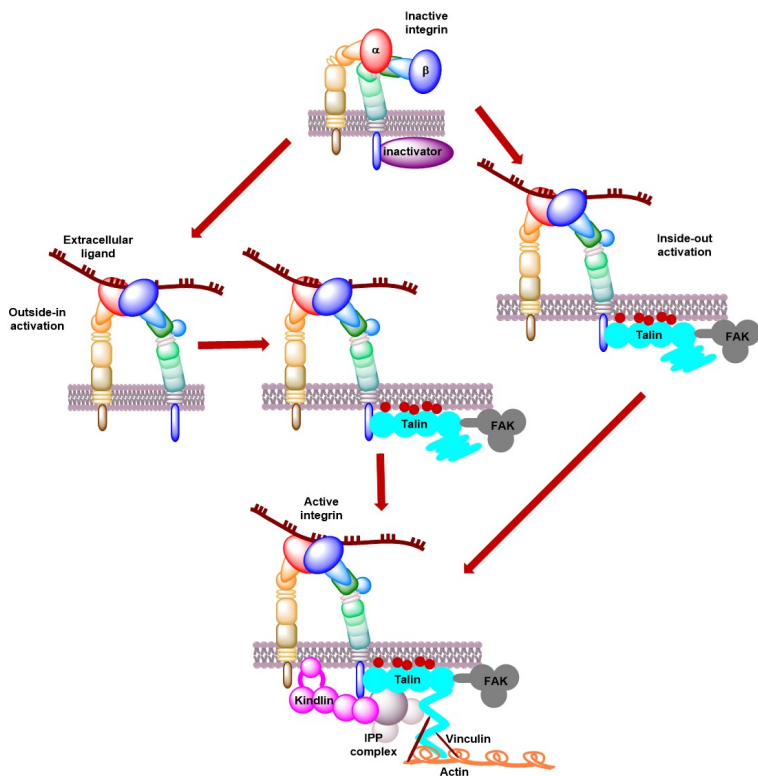


Figure 5.2: Integrin activation.

$\alpha_4\beta_7$, $\alpha_v\beta_3$ and $\alpha_5\beta_1$. Integrin-ligand combinations generate four main classes, based on the nature of the molecular interaction.

$\alpha_4\beta_1$ and $\alpha_4\beta_7$ integrins

$\alpha_4\beta_1$, $\alpha_4\beta_7$, $\alpha_9\beta_1$, the four members of the β_2 subfamily, and $\alpha_E\beta_7$ recognize related sequences in their ligands. In particular, the α_4 -subclasses are expressed on the surface of leukocytes [120] and therefore involved

in inflammatory processes whose dysregulation leads to pathogenesis of chronic inflammations and autoimmune disease like rheumatoid arthritis, multiple sclerosis and Crohn's disease [121]. $\alpha_4\beta_1$, known as "VLA-4", plays a central role in the trafficking of leukocytes and in their activation and migration through the blood-endothelial barrier while inflammatory response is working. It binds its natural ligand, Vascular Cell Adhesion Molecule-1 (VCAM-1, CD106), and a portion of the type III connecting segment of fibronectin (FN) [118]; its pivotal role regards the tumor angiogenesis associated with chronic inflammation, but it is involved also in the recruitment of progenitor cells in the formation of new blood vessels. As consequence of their overexpression in melanoma cells, these integrins are used as markers for prediction of metastatic risk [115][122] [123] [124] [125]. $\alpha_4\beta_7$ is involved in lymphocyte homing to mucosal tissue by adhesion to Mucosal Addressed Cell Adhesion Molecule (MAdCAM), but it links also FN and VCAM-1 [126][127]. It participates to (i) the infiltration of leukocytes in the islets of Langerhans in type I diabetes, (ii) the demyelination in multiple sclerosis, (iii) the migration of T lymphocyte in the gut in inflammatory bowel disease (IBD) subtypes of Crohn's disease [128]. When FN and VCAM-1 are bound, $\alpha_4\beta_1$ forms cluster on the cell surface named focal adhesions: this is the cross point between the ECM, the actine cytoskeleton and the focal adhesion kinase, that activate a signaling cascade that involves extracellular regulated kinase (ERK), promoting proliferation and migration [129]. So, molecules able to interfere with these proteins can be employed for the treatment of inflammations, autoimmune diseases and cancer therapy. Actually, Natalizumab and Vedolizumab, anti- α_4 and anti- $\alpha_4\beta_7$ antibody respectively, are used as chemotherapeutics: Natalizumab, for Crohn's disease and multiple sclerosis even if in same cases it induces progressive multifocal encephalopathy (PML) [130][131][132]; Vedolizumab, for treatment of ulcerative colitis and

Crohn's disease [133][134]. However, the research of small molecules as protein ligands rapidly grew up in the last years, leading to the development of selective or dual ligands of the two types of integrins. They can be cyclic or linear peptides, mimicking the LDV, IDS or LDT recognition sequences: the first is part of fibronectin, the second of VCAM-1 and the third of MADCAM (Figure 5.3). With the aim to develop analogues of

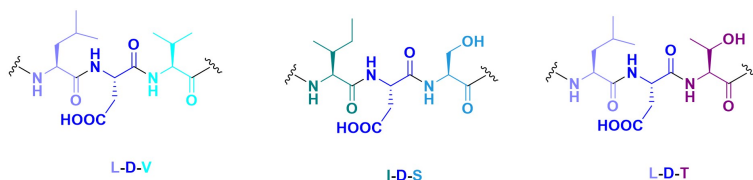


Figure 5.3: LDV, IDS and LDT recognition sequences.

these sequences, several examples of tyrosine and phenylalanine derivatives have been reported, in particular regarding the chemistry of peptidomimetic molecules [135][136]. To understand the allowed changes in the development of new ligands, studies on the binding poses of known compounds have been done by studying the crystal structure of the $\alpha_4\beta_1$ binding fragment of VCAM-1 [137], together to 3D models [138], in silico screening [139] and 3D QSAR studies [140]. The fundamental features for a good binding are the presence of a carboxylate group, a donor of H-bond (amide, for example) in the central part of the molecule and a lipophilic chain mimicking the Leu side chain in LDV [135]. Moreover, PUPA (4[(N-2-methylphenyl)ureido]-phenylacetyl motif) gives enhancement of activity, like observed in BIO1211 (Figure 5.4) [141].

$\alpha_v\beta_3$ and $\alpha_5\beta_1$ integrins

$\alpha_v\beta_3$ and $\alpha_5\beta_1$ support cell adhesion and proliferation of cancer cells, differentiation of mesenchymal stem cells (MSCs) and, in particu-

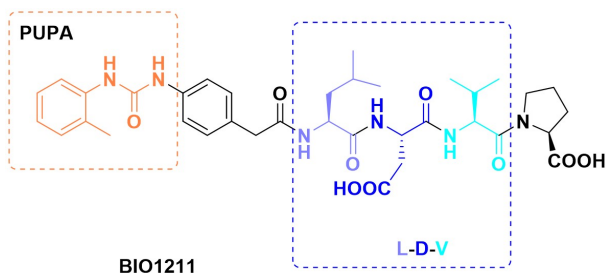


Figure 5.4: Structure of the bioactive $\alpha_4\beta_1$ ligand BIO1211.

lar for $\alpha_v\beta_3$, critical regulation of physiological and pathological angiogenesis, that is a critical step in the progression of a tumor and its metastasis. In tumor at early stages, the hypoxia can induce the "angiogenic switch" in so called dormant cells inducing the production of growth factors and the upregulation of integrins. By interaction with ECM ligands, this integrin participates in the formation of blood vessels, needed for the trafficking of oxygen and nutrients towards cancer cells. While $\alpha_v\beta_3$ can bind several ECM ligands like vitronectin (VN), fibronectin (FN), osteopontin and bone sialoprotein, $\alpha_5\beta_1$ recognize a specific sequence of FN due to the presence on the cell attachment site of the protein of the synergistic amino acid sequence PHSRN. Them both recognized the RGD sequence as minimal adhesive binding motif [142]. Among the drugs active on these integrins reproducing the above-mentioned sequence, surely Cilengitide is the most studied antagonist that reached the clinical phase III in trials for the treatment of glioblastoma and the phase II for other types of cancers [143] (Figure 5.5). By studying the X-ray crystallographic results of the complex $\alpha_v\beta_3$ -cilengitide, it was found that the main interaction is of electrostatic nature in regions of the protein with opposite charges: the Arg interacts with two Asp residues on the α domain, while the carboxylate group of the ligand interacts

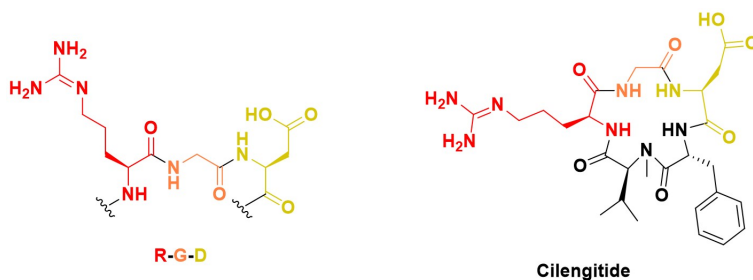


Figure 5.5: Structure of RGD sequence and its synthetic analogue Cilengitide.

with the MIDAS centre, the metal-ion-dependent adhesion site [144]. The research toward peptidomimetic analogues of the RGD sequence is typically voted to the incorporation of rigid heterocyclic scaffolds with acidic and basic moieties properly oriented and distanced or enantiopure non-proteinogenic amino acids. We recently reported a small library of peptidomimetic isoxazoline-containing molecules designed as $\alpha_v\beta_3$ and $\alpha_5\beta_1$ integrin ligands: the isoxazoline core was functionalized in order to mimic the appendages of arginine and aspartate side chains; the resulting structures showed good affinity results, with IC_{50} in the nanomolar range for them both the integrins (Figure 5.6) [145].

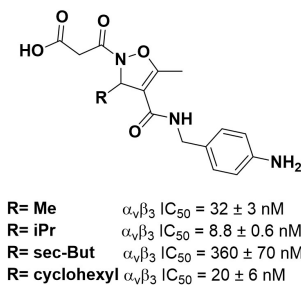


Figure 5.6: Structure of isoxazoline-containing peptidomimetics and biological data.

5.2 Results and discussions

5.2.1 Design and synthesis of ligands

A very common trend in the synthesis of peptidomimetic compounds is the use of five-membered heterocyclic structures as central cores for the preparation of peptidomimetics designed to be integrin ligands. The "privileged structures", possessing the structural elements for a proper binding with the biological target, in this case are the heterocycles described in Chapter 3: the 3,4-dehydro- β proline and the isoxazoline. By adding the proper pharmacophoric groups, these heterocycles have been developed to generate small libraries of integrin ligands, evaluating their affinity/selectivity for $\alpha_4\beta_1/\alpha_4\beta_7$ and $\alpha_v\beta_3/\alpha_5\beta_1$, respectively. As regard the first class of molecules, two different structures have been designed, by changing the substitution pattern on the heterocyclic core and obtaining compounds of family A or B (Figure 5.7). For the compounds

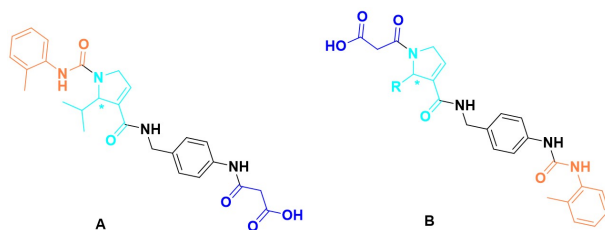


Figure 5.7: Structure of 3,4-dehydro- β -proline peptidomimetics.

belonging to family A, the acilating group on the two enantiomers of 3,4-dehydro- β -proline ring is the PUPA group leading to the intermediates (*R*)-**74b** and (*S*)-**74b**, whose synthesis has been already described. For the compounds of family B, malonic acid has been introduced on the nitrogen atom of the heterocycle generating the intermediates (*R*)-**73a,b** and (*S*)-**73a,b**, with different appendage group in C₂. In both the cases,

the coupling of the free acid in position 3 of the 3,4-dehydro- β -proline ring with HBTU/DIPEA with 4-(aminomethyl)aniline led respectively to intermediates **93b** and **94a,b**, with yield between 75-85% (Figure 5.8).

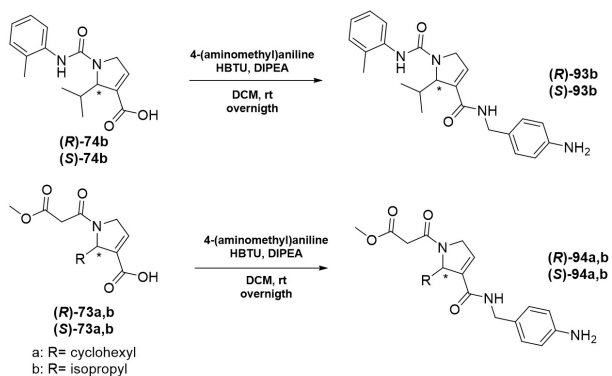


Figure 5.8: Synthesis of amides **93b** and **94a,b**.

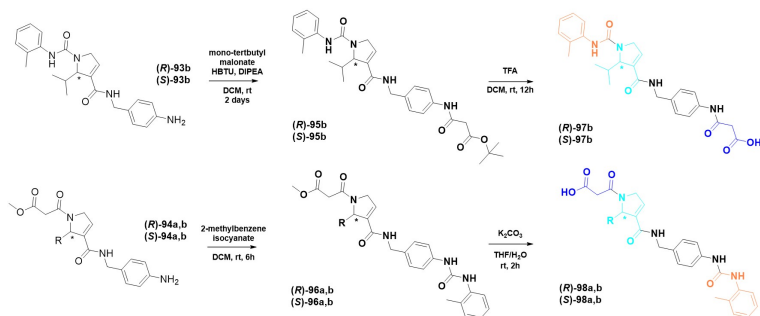


Figure 5.9: Synthesis of the final compounds **97b** and **98a,b**.

The further functionalization of the free aniline was achieved: for the ligand of class A, by using monotert-butyl malonate, with the same coupling conditions, with consequent tertbutyl-ester hydrolysis via TFA

leading to the final ligands **97b**; for the ligand of class B, by using 2-methylbenzene isocyanate and proceeding with the methyl ester hydrolysis in the usual conditions, leading to ligands **98a,b** (Figure 5.9). As regard the ligands of $\alpha_v\beta_3/\alpha_5\beta_1$, starting from the isoxazoline derivatives shown before, we selected the position 3 to introduce an exposed anchorage for covalent ligation of diverse spacers with the aim to not compromise the integrin binding capabilities. For this reason, we introduced the alkyne moiety, like reported in the intermediate **54**, to be exploited in 1,3-dipolar Huisgen cycloaddition with different azide-linkers. To obtain the "clickable" intermediate, we proceeded with the selective removal of tertbutyl ester accomplished with large excess of trifluoroacetic acid in dichloromethane. The arginine mimetic chain was introduced by reaction of the resulting acid **99** with 4-aminobenzylamine, following standard coupling conditions (HBTU/TEA in DCM) to obtain **100** in 76% yield. Hydrolysis of the methyl ester required a particu-

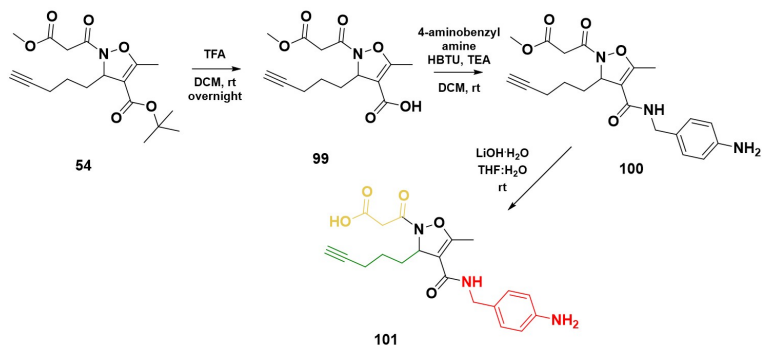


Figure 5.10: Synthesis of the isoxazoline functionalizable ligand 101.

lar effort, since the undesired removal of the malonic side chain, easily occurred, favoured by the following spontaneous aromatization of the heterocycle as confirmed by LC-MS analysis. After several trials under different conditions, excellent results were obtained with a $7 \cdot 10^{-3}$ M

solution of LiOH·H₂O in a 2:1 mixture of THF/water, following the reaction evolution by TLC, and stopping it at the disappearance of the starting ester. The acid **101** was obtained in quantitative yield (Figure 5.10). In the design of the ligand-linker library, NH₂-terminating molecules were first prepared in order to obtain carriers for molecules with carboxylate group, as for example cytotoxic agent like fumagillin and diagnostic tools like DOTA. For this aim, N-Boc-2-azido-ethylamine **102** and N-Boc-3-azido-propylamine **103** were prepared from the corresponding bromide precursors through substitution with NaN₃. They were reacted with methyl ester **100** in presence of Cu⁽⁰⁾ 10 mol% and TEA·HCl salt at room temperature in a 1:1 mixture of tBuOH and water [146]. The click-reaction led to the 1,4-disubstituted [1,2,3]-triazole isomer, exclusively [147], of compounds **104** and **105** in 57% and 67% yield respectively. Removal of the methyl ester with the previous reported conditions led to compounds **106** and **107** with 80% and 87% yields (Figure 5.11). The N-protection was retained in order to avoid unwanted intereaction during the binding assays, mimicking a carbamate linked payload. For the synthesis of molecules with carboxylate terminal group for

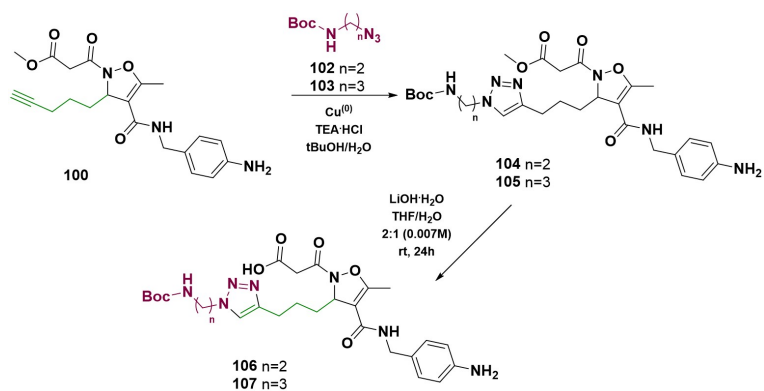


Figure 5.11: Synthesis of the ligand functionalized with amino-terminal moiety with short alkylic chain.

the delivery of compounds with amine or hydroxyl group, we proceeded with the functionalization of compound **100** with t-butyl-2-azido-acetate **108** and t-butyl-3-azido propionate **109** via Huisgen cycloaddition. In this case too, the two azides were prepared from the corresponding bromide. The cycloaddition afforded the products **110** and **111** in low yield (20% and 34%, respectively). Complete regiocontrol was observed in this case too. Selective removal of methyl ester was accomplished as previously described affording the compounds **112** and **113** with 75% yield (Figure 5.12). The retention of t-butyl group was afforded to avoid side interaction with the binding site. In order to understand how the

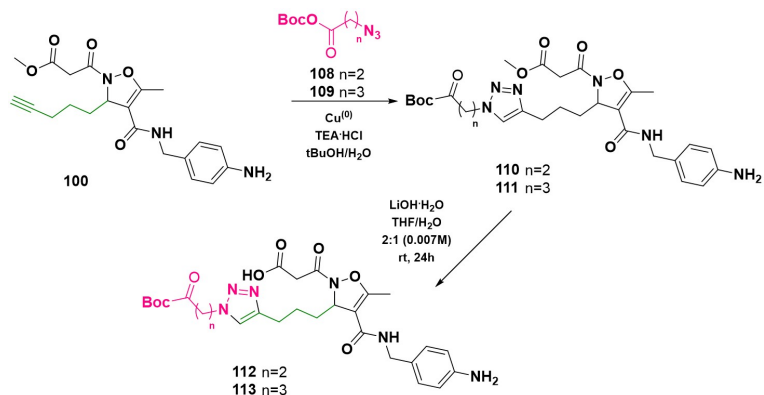


Figure 5.12: Synthesis of the ligand functionalized with carboxylate-terminal moiety with short alkylic chain.

length of the chain can influence the interaction with the binding site, we synthesized more complex systems, whose assembly required different protocols, differing for the order of formation of strategic bonds. The synthetic protocol was optimized for each specific substrate. For the synthesis of **117**, with a succinic moiety as spacer between the carrier and the payload [148], 3-bromo-propylamine was coupled with mono-tert-butyl pentandioic acid and the bromide was substituted with NaN_3 ,

to afford compound **115** in good yield (90%). It was coupled with the methyl ester **100**, with the usual protocol for the cycloaddition, obtaining the compound **116** with 75% yield. Removal of the methyl ester left the compound **117** with 40% yield (Figure 5.13). The synthesis of com-

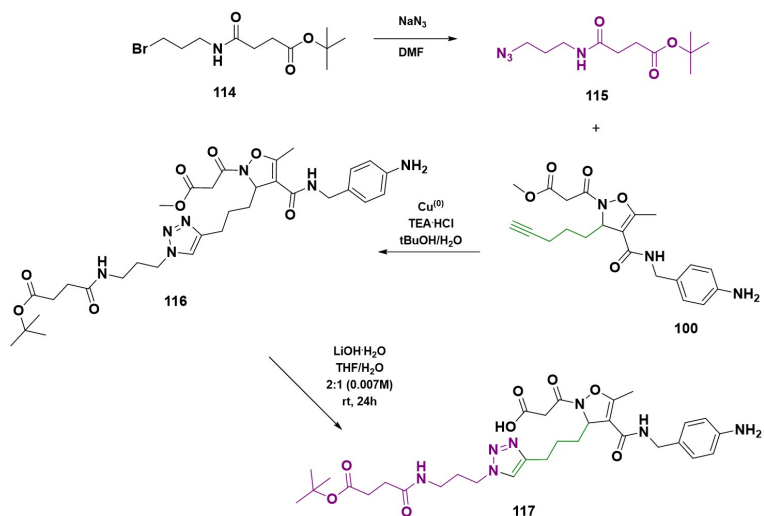


Figure 5.13: Synthesis of the ligand functionalized with carboxylate-terminal moiety by introducing succinic spacer.

pound **119** was realized in one step by cycloaddition of the acid **101** with ethyl-5-azido-pentanoate. Due to the nature of the substrate **101**, the condition of the cycloaddition were modified using $\text{Cu}(\text{OAc})_2$ in presence of sodium ascorbate [148]. The product was obtained with 20% yield, as consequence of the difficulties in the purification from the copper salts (Figure 5.14). There are several examples in literature of PEG-linker employed as drug-ligand connection as consequence of its ability to increase the solubility and to decrease the immunogenicity of the products [149], inducing more stability in vivo and reducing the tendency to enzymatic

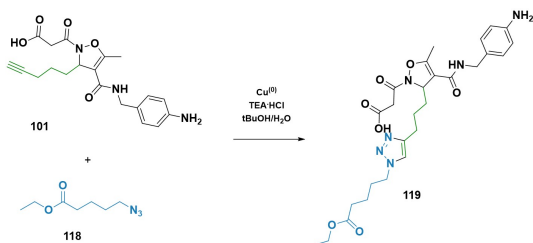


Figure 5.14: Synthesis of the ligand functionalized with carboxylate-terminal moiety with long alkylic chain.

digestion. For this purpose, compound **100** was reacted with commercially available N-Boc-1-amino-3,6-dioxo-8-octaneazide isolating compound **120** in 79% yield; it was then hydrolyzed to the corresponding acid **121** (Figure 5.15). In the same way, the acid **101** was reacted with the azide **122** obtained from the corresponding commercially available acid. Via $\text{Cu}(\text{I})$ -catalysis, compound **123** was isolated in 40% yield as consequence of the difficult purification (Figure 5.16).

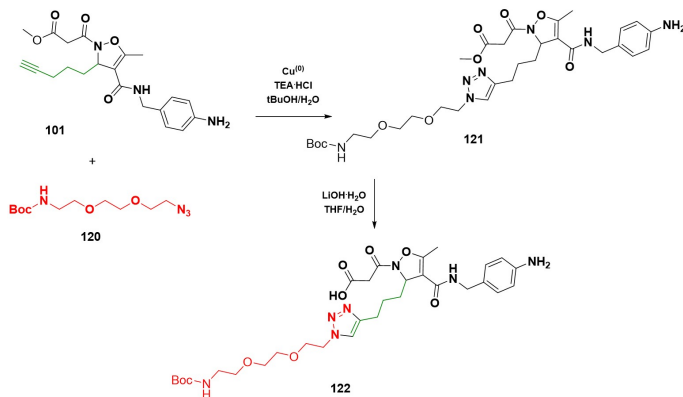


Figure 5.15: Synthesis of the ligand functionalized with PEG-amino-terminal moiety.

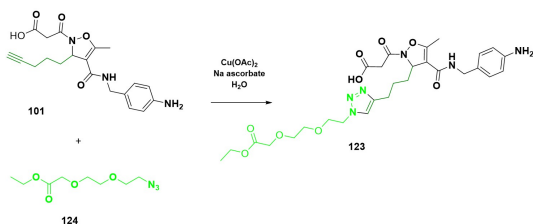


Figure 5.16: Synthesis of the ligand functionalized with PEG-carboxylate-terminal moiety.

5.2.2 Biological evaluation

The enantiopure ligands designed to be active on $\alpha_4\beta_1$ and $\alpha_4\beta_7$ integrins were evaluated in cell adhesion inhibition assays using Jurkat cells in presence of VCAM-1. For compounds belonging to class A, (**R**)-**97b** and (**S**)-**97b**, moderate affinity was detected with IC_{50} values in 10^{-7} M range (entry 1 and 2, Table 5.1), suggesting that the structure designed for these compounds does not guarantee optimal ligand-receptor interaction, independently from the configuration of the stereocenter on the dehydro- β -proline ring.

Table 5.1: Inhibition of Jurkat cell adhesion by dehydro- β -proline-containing peptidomimetics.

Entry	Compound	$\alpha_4\beta_1$ /VCAM-1 IC_{50} (nM) ^a
1	(<i>S</i>)- 97b	110±9
2	(<i>R</i>)- 97b	250±12
3	(<i>S</i>)- 98b	>1000
4	(<i>R</i>)- 98b	10±3
5	(<i>S</i>)- 98a	>1000
6	(<i>R</i>)- 98a	62±11

[^a] Experiments were conducted in quadruplicate and were repeated at least three times. BIO1211 was used as reference compound, inhibiting the adhesion with an IC_{50} of 7.6 nM.

For compounds belonging to class B, the stereodefinition just mentioned seems to influence the bioactivity since the *S*-enantiomers of compounds **98a** and **98b** (entry 3 and 5) are inactive, while the *R*-enantiomers showed excellent activity, especially for compound (*R*)-**98b** (entry 4 and 6). The conformations of compounds **98a,b** have been studied by ROESY experiments that suggested an almost linear disposition of the molecules, as expected on the basis of structural restraints: in fact, we did not observe any significant signals with the exception for trivial ones. This result is in agreement with the preferred conformation of other active $\alpha_4\beta_1$ -integrin ligands [150] [151]. The presence of only one stereocenter in the molecules justified the lack of further computational minimization in solvent box since no useful explanation could have been added on the receptor recognition of the two enantiomers. In the absence of a model for docking, experimental evidence can be explained considering that the disposition of the alkyl group of the dehydro- β -proline ring in the *R*-enantiomer is more favorable than that of the *S*-enantiomer. Comparing these two compounds **98a,b** with the bioactive BIO1211, we hypothesized that the alkyl chain can mimic those of leucine or valine. The bioactive (*R*)-**98a** and (*R*)-**98b** were tested to evaluate their selectivity towards a specific integrin in cell-adhesion assays. As reported in Table 5.2, the two compounds have no activity towards none of the β_1 , β_2 and β_3 families selected. As regards $\alpha_4\beta_7$, the *R*-enantiomers of **98a,b** showed significant activity.

Finally, we investigated (*R*)-**98a** and (*R*)-**98b** on VCAM-1-induced phosphorylation of ERK1/2 in Jurkat cells. The focal adhesion kinase (FAK), activated by integrins $\alpha_4\beta$, activates ERK in two pathways: according to the first, FAK recruits C3G and RAP1, which induces B-Raf activity and ERK activation; according to the second, FAK involves the growth-factor-receptor-bound-2 and son-of-sevenless complex, which activates

Table 5.2: Inhibition of cell adhesion through alternative integrins by most effective $\alpha_4\beta_1$ antagonists, (*R*)-98a and (*R*)-98b.

Compounds	IC ₅₀ (nM) ^a			
	$\alpha_4\beta_7/\text{MAdCAM-1}^b$	$\alpha_5\beta_1/\text{FN}^c$	$\alpha_1\beta_{12}/\text{ICAM-1}^d$	$\alpha_5\beta_1/\text{FN}^e$
(<i>R</i>)-98b	270±33	>1000	>1000	>1000
(<i>R</i>)-98a	343±26	>1000	>1000	>1000

[^a] Experiments were conducted in quadruplicate and were repeated at least three times.^b Performed on RPMI8866 cells. ^c Performed on K-562 cells. ^c Performed on Jurkat cells. ^d Performed on SK-MEL-24 cells.

Ras-ERK [123]. It was reported that VCAM-1 induces ERK phosphorylation in Jurkat cells expressing $\alpha_4\beta_1$ integrin, through the RAF family of serine/threonine kinases, as sorafenib, a selective B-Raf inhibitor prevents this effect [151]. Jurkat cells were serum-starved in RPMI-1640 containing 1% fetal bovin serum (FBS) for 16h; they were incubated with compounds (*R*)-98a and (*R*)-98b for 60min in suspension and plated for 60min on VCAM-1 or poly-L-lisine (used as nonspecific substrate). In cells exposed to VCAM-1, a significant concentration-dependent increase in phosphorylated ERK1/2 was observed 60min after VCAM-1 exposure (Figure 5.17), while poly-L-lysine exposure does not induce any increment in ERK1/2 phosphorylation. (*R*)-98b was more active in the inhibition of phosphorylation of ERK1/2 if compared to (*R*)-98a. The IC₅₀ values, obtained in a separate set of experiments in which different concentration of ligands were employed, are 10 and 131 nM for (*R*)-98b and (*R*)-98a, respectively. These results confirm those obtained from cell adhesion assays, confirming that (*R*)-98b is the most effective selective antagonist of $\alpha_4\beta_1$ integrin.

As regard the compounds designed as ligand for $\alpha_v\beta_3$ and $\alpha_5\beta_1$, on the basis of our previous knowledge, the modification introduced on the alkylic side chain should not affect the interaction with the target. The ability of the synthesized racemic ligands to inhibit the adhesion of

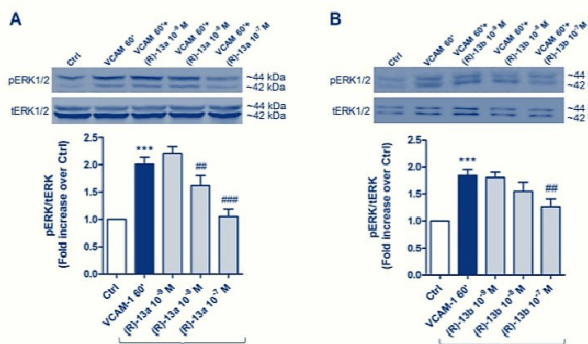


Figure 5.17: Compounds **(R)-98a** and **(R)-98b** prevent VCAM-1-induced phosphorylation of ERK1/2. Jurkat cells were serum-starved in RPMI-1640 containing 1% FBS for 16h; cells were then preincubated with compounds **(R)-98a** (A) and **(R)-98b** (B) for 60 min in suspension. The cells were kept in suspension (Ctrl) or plated on VCAM-1 coated wells. After 60 min, cells were lysed, and lysates were analyzed by Western blot using an antibody directed against phosphorylated ERK1/2 (pERK1/2) or total ERK1/2 (tERK1/2). Representative Western blots show that control cells plated on VCAM-1 had a much stronger signal for pERK1/2 in Jurkat cells (Ctrl). Preincubation with compound **(R)-98a** reduced VCAM-1-induced ERK1/2 phosphorylation significantly only at the concentration 10^{-7} M. Densitometric analysis of the bands (mean \pm SEM; n?6); the amount of pERK1/2 is normalized to the tERK1/2. *** $p < 0.001$ versus Ctrl; * $p < 0.01$ versus VCAM-1 60' (Newman-Keuls test after ANOVA)

K562 cells (human erythroleukemic cells, expressing $\alpha_5\beta_1$ integrin) or SK-MEL-24 cells (human malignant melanoma cells, expressing $\alpha_v\beta_3$ integrin) to immobilized fibronectin was evaluated. These cell models are widely used to investigate potential antagonists of $\alpha_v\beta_3$ or $\alpha_5\beta_1$ integrin-mediated cell adhesion. In these experiments, the cells were seeded onto plates coated with different substrates and allowed to adhere before quantification of the number of adherent cells, in presence of increasing concentrations of the compounds. As a negative control, under these conditions, no significant cell adhesion was observed for BSA-coated plates or nonspecific substrate-coated plates (i.e., collagen I for SK-MEL-24 expressing $\alpha_v\beta_3$ integrin and poly-L-lysine for K562 expressing $\alpha_5\beta_1$ integrin, data not shown). The ability of the new com-

pounds to inhibit the adhesion of SK-MEL-24 and K562 cells to fibronectin was compared with that of the standard compounds, Ac-Asp-Arg-Leu-Asp-Ser-OH (Ac-DRLDS) and H-Gly-Arg-Gly-Asp-Asn-Pro-OH (GRGDNP), known to be potent inhibitors of cell adhesion mediated by $\alpha_v\beta_3$ integrin [152]. The results are summarized in Table 5.3.

Table 5.3: Inhibition of $\alpha_v\beta_3$ and $\alpha_5\beta_1$ integrin-mediated cell adhesion to Fibronectin in presence of isoxazoline ligands, or reference standards.

Entry	Compound	$\alpha_v\beta_3$	$\alpha_5\beta_1$
		IC ₅₀ μM ^[a]	IC ₅₀ μM ^[a]
1	101	0.83 \pm 0.05 (A)	>1000
2	106	0.88 \pm 0.07 (I)	0.28 \pm 0.03 (I)
3	107	>1000	0.0027 \pm 0.0004 (I)
4	112	0.068 \pm 0.11 (A)	>1000
5	113	0.23 \pm 0.08 (A)	>1000
6	117	>1000	6.59 \pm 0.16 (A)
7	119	0.61 \pm 0.08 (A)	>1000
8	122	8.84 \pm 0.14 (I)	>1000
9	123	>1000	>1000
10 ^[b]	Ac-RGDDS	0.025 \pm 0.003	>1000
11 ^[b]	GRGDNP	0.23 \pm 0.03	>1000

^[a] Values are means of three experimnts. (I) adhesion inhibition (A) adhesion activation.^[b] Reference compounds.

According to these results, it can be observed that the affinity towards integrin $\alpha_v\beta_3$ is generally maintained, while few compounds show high affinity towards $\alpha_5\beta_1$. Compounds terminating with a carbamate moiety behave as antagonists to integrin receptors, displaying anyway different selectivities. In particular, **106** displayed similar affinity towards both receptors (entry 2), while the longer **107** is an excellent selective ligand for $\alpha_5\beta_1$ (entry 3). The opposite preference could be observed for compound **122** that showed a good affinity for $\alpha_v\beta_3$ receptor (entry

8). On the other hand, compounds having a terminal ester group in the side chain, behaved generally as agonists, inducing an increase in cell adhesion. All the molecules having a linear chain linked to the triazole ring displayed high affinity for $\alpha_v\beta_3$ integrin (entries 4, 5 and 7) in the submicromolar range. By introducing an amide moiety in the central part of an elongated linker, as in compound **117**, the opposite selectivity was observed, still maintaining an agonist effect (entry 6). The introduction of a short PEG fragment induced complete loss of the activity (compound **123**, entry 9). To complete the study we also performed the cell adhesion assay with the alkyne intermediate **101**, which showed a good affinity and selectivity for $\alpha_v\beta_3$. These data seem to suggest a possible influence of the terminal moiety on the agonist/antagonist role. A structure-activity relationship rationalization is still elusive, moreover because behavior prediction for integrin ligands is known to depend also on the concentration [153]. A recent study on antagonist/agonist behavior of physiological ligand fibronectin [154], suggests that an antagonist is able to "freeze" the receptor in an inactive conformation, while a ligand subjected to binding/unbinding dynamic events may induce the persistence of a receptor activated conformation, thus facilitating adhesion. For fibronectin, this has been ascribed to additional stabilizing interactions of vicinal residues, but for small molecule ligands no rational is still available. Anyway, the good affinity of the members of this class of peptidomimetics confirms their possible use as shuttle for drugs or diagnostic selective delivery to cells overexpressing these two classes of integrins. To gain further information about the agonist/antagonist role of our peptidomimetic integrin ligands and to verify the effect on intracellular signalling, we investigated the effects of the most potent $\alpha_5\beta_1$ antagonist, compound **107**, and the effects of the only identified $\alpha_5\beta_1$ agonist, **117** on integrin-mediated signalling in K562 cells. The mechanism by which components of extracellular matrix generate intracellu-

lar signalling through integrins requires indeed an increased phosphorylation of cytoplasmatic second messengers. Phosphorylation of ERK plays a central role in fibronectin-mediated survival signalling through integrins: in fact, cell adhesion activates ERK by binding of $\alpha_5\beta_1$ integrins at the cell surface to extracellular matrix proteins such as fibronectin. Experiments were performed by serum-starving K562 cells in RPMI-1640 containing 1% FBS for 16 h; thereafter, they were pre-incubated with compound **107** or **117** for 60 minutes and then plated for 60 minutes on fibronectin or poly-l-lysine (used as nonspecific substrate). Cells treated with the agonist **117** were not incubated with fibronectin. When K562 cells were exposed to fibronectin for 60 minutes the western blots showed a much stronger signal for phosphorylated ERK1/2, in comparison to vehicle-treated cells (Figure 5.18 (a)). Pre-incubation with different concentrations of compound **107** (10^{-7} - 10^{-9} M) caused a significant concentration-dependent reduction in the amount of fibronectin-induced ERK1/2 phosphorylation in K562 cells (Figure 5.18 (b)), thus confirming a significant effect of the ligand binding on intracellular signalling cascade. Compound **117**, acting as agonist, significantly increased ERK1/2 phosphorylation in a concentration-dependent manner in K562 cells (Figure 5.18). Integrin trafficking is an important mechanism employed by cells to regulate integrin-extracellular matrix interactions, and thus cellular signaling, during processes such as cell migration and invasion [155]. $\alpha_5\beta_1$ integrin is internalized, trafficked to recycling endosomes and then recycled to the plasma [156]. Membrane trafficking pathways influence the capacity of $\alpha_5\beta_1$ to promote invasion and metastasis [157]. In order to investigate the effects of peptidomimetics on integrin trafficking, $\alpha_5\beta_1$ integrin internalization was observed by confocal microscopy on HEK293 cells transfected with α_5 -enhanced green fluorescent protein (EGFP) plasmid (Figure 5.19). HEK293+ α_5 -EGFP cells were treated with fibronectin (10 $\mu\text{g}/\text{mL}$) alone or in com-

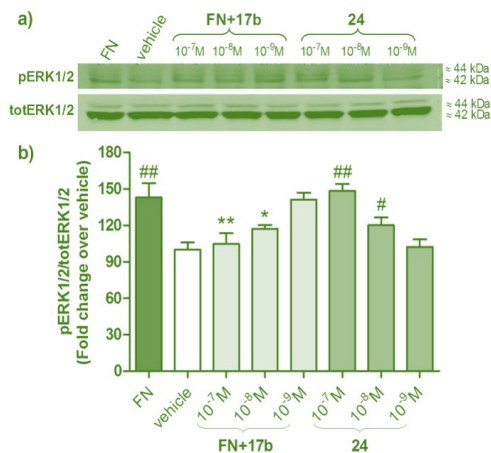


Figure 5.18: Effect of compounds 107 and 117 on ERK1/2 phosphorylation mediated by $\alpha_5\beta_1$ integrin expressed in K562 cells. Cells were serum-starved in RPMI-1640 containing 1% FBS for 16 h; then cells were pre-incubated with different concentrations of the antagonist 107 for 1h and then were allowed to adhere for 1h on fibronectin. Cells treated with the agonist 117 were not incubated with fibronectin. Thereafter, cells were lysed and lysates were analyzed in Western blot using an antibody directed against phosphorylated ERK1/2 (pERK1/2) or total ERK1/2 (tERK1/2). Compound 107 prevented FN-induced phosphorylation of ERK1/2 in a concentration-dependent manner, while agonist 117 significantly increased ERK1/2 phosphorylation. Representative Western blots show that control cells plated on FN had a much stronger signal for pERK1/2 than vehicle-treated cells (vehicle). Densitometric analysis of the bands is shown (mean \pm SEM; n= 4); the amount of pERK1/2 is normalized to that of totERK1/2. * $p < 0.05$, ** $p < 0.01$ versus FN; # $p < 0.05$, ## $p < 0.01$ versus vehicle (Newman-Keuls test after ANOVA).

bination with the antagonist **107** (1 μ M) or with the agonist **117** (1 μ M) alone. As shown in Figure 5.19, after 15 minutes of treatment with the endogenous agonist fibronectin $\alpha_5\beta_1$ integrin was mainly localized in the cytoplasm (Figure 5.19, panels d-f), if compared with vehicle-treated cells in which the integrin is quite completely located on the plasma membrane (Figure 5.19, panels a-c). Moreover, when HEK293+ α_5 -EGFP cells were pre-treated with the antagonist **107** before the addition

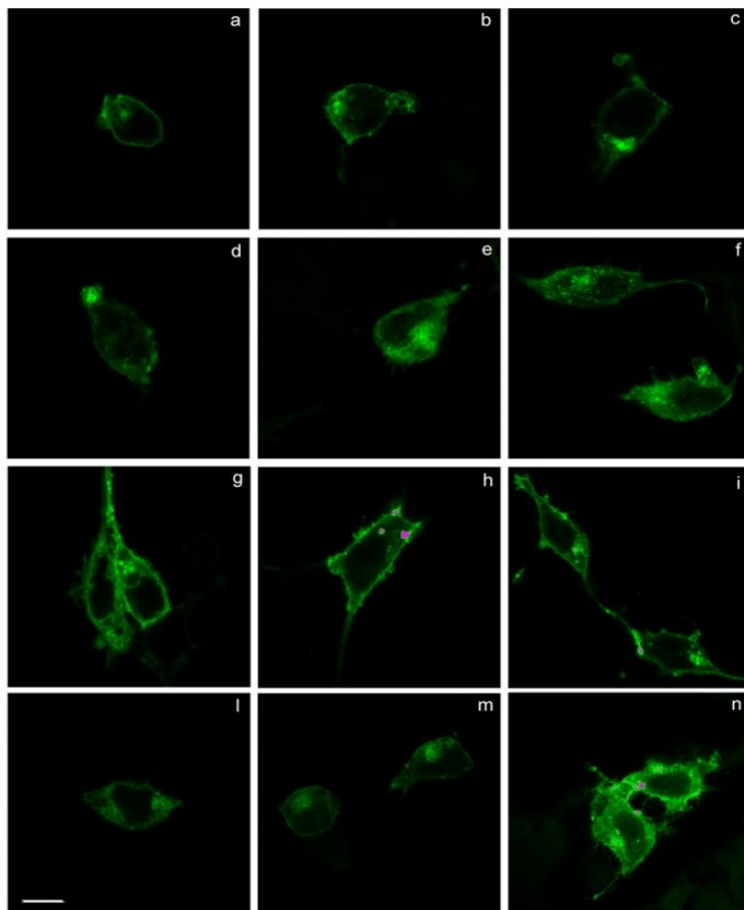


Figure 5.19: Confocal imaging on HEK293+ α_5 -EGFP cells. Cells were pre-treated with compound 107 (1 μ M) for 20 minutes and then fibronectin (FN, 10 μ g/mL) was added for 1 hour incubation at 4 °C. Cells treated with the agonist 117 (1 μ M) were not incubated with fibronectin. Thereafter, cells were moved to 37 °C for 15 minutes to promote integrin internalization and fixed. Panels a-c: vehicle-treated cells; panels d-f: FN-treated cells $\alpha_5\beta_1$ integrin was mainly located in the cytoplasm; panels g-i: FN-treated cells pre-incubated with the antagonist 107 that prevents FN-induced $\alpha_5\beta_1$ internalization; panels j-l: cells treated with the agonist 117 that mimicks FN. ompound 117 induced $\alpha_5\beta_1$ integrin internalization. Scale bar: 10 μ m.

of fibronectin, it prevented integrin internalization, that remained mainly located on the membrane (Figure 5.19, panels g-i). On the contrary, the compound **117**, mimicking the agonist behaviour of fibronectin, induced $\alpha_5\beta_1$ internalization (Figure 5.19, panels l-n): in fact, it was mostly localized in the cytoplasm. The ligands **107** and **117**, which showed the

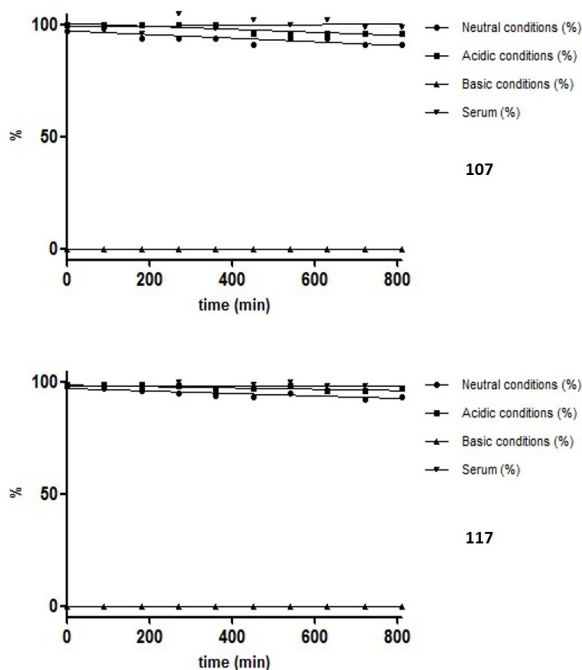


Figure 5.20: Stability assays for 107 (A) and 117 (B) under different pH conditions and in bovine serum.

most interesting results in the biological evaluation, were subjected to stability assays at neutral (pH=7), basic (pH=10) and acidic (pH=3) conditions. LC-MS injections were performed after 30 min from the preparation of the samples and then after each 1,5 hour (Figure 5.20). In the

last synthetic step, the methyl ester deprotection, the amidic bond between the heterocycle and malonyl group showed high sensitivity to the basic environment and, as expected, the hydrolyzed A was detected as the unique degradation product. As a consequence of the spontaneous aromatization of A, also an increasing amounts of B was observed after a short period (Figure 5.21). During the acidic treatment and under neutral conditions, both **107** and **117** resulted quite stable and after several hours only a 5% loss of product was detected, in favor of the formation of A and B. Under basic conditions, the decomposition to A occurred in few minutes. Finally the stability was also checked in bovine serum, confirming that no significant degradation occurs in this physiological medium. The stability in water solution at different values of pH and in bovine serum confirms the potential exploitation of these peptidomimetic molecules for pharmaceutical applications.

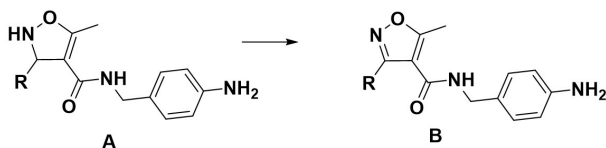


Figure 5.21: Typical degradation products under basic conditions.

5.3 Conclusions

On the basis of the fundamental requirements for the interactions of integrin transmembrane receptors with bioactive ligands, novel classes of dehydro- β -proline- and isoxazoline-containing peptidomimetics, designed to be effective as integrin ligands, has been developed. To this purpose, dehydro- β -proline ring properly functionalized with appendages to the central core have been selected on the basis of previous experience and on the basis of information from the literature. The synthesized pro-

ducts have been tested in cell adhesion inhibition assays and in assays aimed to determine the effect of these α_4 - antagonists: in particular two types of integrins have been chosen, $\alpha_4\beta_1$ and $\alpha_4\beta_7$, in order to evaluate the specificity towards them. A specific compound, **(R)-98b**, resulted to be a good integrin ligand, showing IC₅₀ of 10±3 nM and 270±33 nM on $\alpha_4\beta_1$ and $\alpha_4\beta_7$, respectively. The dependence on the stereochemistry of the heterocyclic central core seems to be related to a preferred disposition of the lipophilic chain for (R)-enantiomers. These ligands could be exploited as lead compounds for therapeutic tools development, considering the great importance of $\alpha_4\beta_1$ integrin (VLA-4) in chronic inflammation, autoimmune diseases, and inflammation related to cancer. In a similar way, the synthesis of a small library of ligands obtained by conjugation of polyfunctionalized linkers to isoxazolidine ring via Huisgen-click reaction, allowed to verify the possibility to use these scaffolds as $\alpha_v\beta_3$ and $\alpha_5\beta_1$ targeting motifs, with the aim to use them as "shuttles" for selective delivery of therapeutics and diagnostics to cancer cells. The different behavior of the members of the library seems to suggest a correlation between the terminal moiety of the linker chain and the cell adhesion inhibition or activation. Anyway a rationale in structure-activity relationship is not predictable and needs further investigation. Compound **107**, that showed affinity towards $\alpha_5\beta_1$ integrin in the nanomolar range as antagonist, reduced integrin-mediated signaling induced by fibronectin. On the contrary, compound **117** induced intracellular signaling activation. Moreover, we observed that it acts as $\alpha_5\beta_1$ agonist of endogenous fibronectin. Present data encourage the study of $\alpha_5\beta_1$ agonists to promote integrin internalization. Further studies are necessary to understand if the ligands are internalized together with the integrin and if they are suitable for specific delivery of therapeutic payload to cancer cells. Anyway, the possibility to choose ligands with different behavior during integrin trafficking, suggests a possible exploitation

of these shuttles to delivery drugs or diagnostics outside or inside the cell, as required by the payload nature.

5.4 Experimental procedures

5.4.1 General methods

All chemicals were purchased from commercial suppliers and were used without further purification. Microwave-assisted reactions were carried out in Milestone Mycosynth apparatus, with a dual magnetron system with a pyramid-shaped diffuser, 1000 W maximum power output, and temperature monitor and control by optical fiber up to a vessel temperature of 250 °C. Flash chromatography was carried out on silica gel (230-400 mesh). Dowex®50WX2-200(H) ion exchange resin was used for purification of free amino acids or free amines. NMR spectra were recorded with a Varian Mercury Plus 400 or Varian Gemini 200 instruments. Chemical shifts are reported as δ values (ppm), and were calibrated using the residual solvent peaks of: CDCl_3 , set at $\delta = 7.27$ ppm (^1H NMR) or $\delta = 77.0$ ppm (^{13}C NMR); CD_3OD , set at $\delta = 3.31$ ppm (^1H NMR) and $\delta = 49.0$ ppm (^{13}C NMR); D_2O , set at $\delta = 4.79$ ppm (^1H NMR); CD_3CN , set at $\delta = 1.93$ ppm (^1H NMR) and $\delta = 117.7$ ppm (^{13}C NMR); $(\text{CD}_3)_2\text{CO}$, set at $\delta = 2.04$ ppm (^1H NMR) and $\delta = 29.8$ ppm (^{13}C NMR). Coupling constants are given in Hz. LC-MS analysis was carried out with an HP1100 liquid chromatograph coupled to an electrospray ionization mass spectrometer (LC-ESI-MS), using a Phenomenex Gemini C18 - 3μ - 110 Å column, $\text{H}_2\text{O}/\text{CH}_3\text{CN}$ as neutral solvent or $\text{H}_2\text{O}/\text{CH}_3\text{CN}$ with 0.2% formic acid as acid solvent at 25 °C (positive-ion mode, $m/z = 100$ -500, fragmentor 70 V). Another set of experiments has been performed on an HP1100 liquid chromatograph coupled with an electrospray ionization-ion trap mass spectrometer MSD1100 using

a Phenomenex Zorbax C18 - 3.5 μ - 80 Å column, H₂O/CH₃CN with 0.08% trifluoroacetic acid as acid solvent (positive scan 100-500 m/z , fragmentor 70 eV).

5.4.2 Synthesis and characterization

General procedure for the coupling of acid 73a,b and 74 and 4-(aminomethyl)aniline: (93b) and (94b). To a stirred solution of each enantiomer of 73a,b and 74b (1 eq) in dry DCM (0.35M) under inert atmosphere, HBTU (1.5 eq) and DIPEA (2 eq) were added at rt. The solution was stirred for 10 min and then 4-(aminomethyl)aniline (2 eq) was added. The reaction mixture was stirred overnight. The organic solution was washed with H₂O, dried over Na₂SO₄ and solvent was removed under reduced pressure. The crude was purified by flash chromatography on silica gel (DCM/cyclohexane/methanol 98:1:1 as eluant).

Compound (93b): ¹H NMR (400 MHz, CDCl₃) δ 7.71 (d, J= 7.6 Hz, 1H), 6.97-7.17 (m, 5H), 6.64 (d, J= 6.4 Hz, 2H), 6.34 (m, 1H), 6.02 (bs, 1H), 5.95 (bs, 1H), 5.05 (bs, 1H), 4.49 (bd, J= 16.4 Hz, 1H), 4.37 (d, J= 5.6 Hz, 2H), 4.14 (ddd, J= 16.4, 5.2, 1.6 Hz, 1H), 2.35 (m, 1H), 2.25 (s, 3H), 0.96 (d, J= 7.2 Hz, 3H), 0.93 (d, J= 7.2 Hz, 3H); ¹³C NMR (100 MHz, CDCl₃) δ 163.6, 154.4, 146.0, 138.7, 136.7, 130.3, 129.3, 128.6, 127.5, 126.7, 124.0, 122.6, 115.2, 68.5, 54.3, 43.2, 32.7, 18.6, 18.0, 17.9; LC-ESI-MS: 5.9 min, [M + H]⁺=393, [2M + H]⁺=785, [2M + Na]⁺=807; S-enantiomer [α]^D= +68.2, R-enantiomer [α]^D= -70.7 (c 1 in CHCl₃).

Compound (94a): (80:20 trans/cis amide ratio) trans conformer: ¹H NMR (400 MHz, CD₃OD) δ 8.55 (bs, 1H), 8.05 (bs, 1H), 7.05 (d, J = 6.8 Hz, 2H), 6.77 (d, J= 6.8 Hz, 2H), 6.33 (m, 1H), 5.06 (m, 1H), 4.20-4.74 (m, 4H), 3.80 (s, 3H), 3.19 (d, J= 7.4 Hz, 1H), 3.15 (d, J= 7.4 Hz, 1H), 2.10 (m, 1H), 1.45-1.80 (m, 5H), 0.80-1.21 (m, 5H). Cis con-

former: ^1H NMR (400 MHz, CD_3OD) δ 8.55 (bs, 1H), 8.05 (bs, 1H), 7.05 (d, J = 6.8 Hz, 2H), 6.67 (d, J = 6.8 Hz, 2H), 6.41 (m, 1H), 5.20 (m, 1H), 4.20-4.74 (m, 4H), 3.78 (s, 3H), 3.67 (d, J = 7.4 Hz, 1H), 3.55 (d, J = 7.4 Hz, 1H), 2.10 (m, 1H), 1.45-1.80 (m, 5H), 0.80-1.21 (m, 5H). ^{13}C NMR (100 MHz, CD_3OD) trans conformer δ 167.5, 164.9, 164.5, 145.5, 137.2, 128.0, 127.7, 114.6, 67.3, 53.7, 50.8, 40.5, 28.1, 27.1, 25.7, 25.4. LC-ESI-MS: 4.9 min, $[M + H]^+ = 400$, $[2M + Na]^+ = 822$; *S*-enantiomer $[\alpha]^D = +27.0$, *R*-enantiomer $[\alpha]^D = -25.2$ (c 1 in CH_3OH).

Compound (94b): (70:30 trans/cis amide ratio) trans conformer: ^1H NMR (400 MHz, CD_3OD) δ 6.95 (d, J = 8.4 Hz, 2H), 6.61 (d, J = 8.4 Hz, 2H), 6.45 (m, 1H), 5.05 (m, 1H), 4.31 (m, 2H), 4.27 (bs, 2H), 3.75 (s, 3H), 3.37 (s, 2H), 2.38 (m, 1H), 0.91 (d, J = 7.2 Hz, 3H), 0.87 (d, J = 7.2 Hz, 3H); ^{13}C NMR (100 MHz, CD_3OD) δ 168.1, 164.7, 163.4, 144.9, 135.9, 134.3, 127.7, 127.4, 115.1, 67.8, 53.6, 51.9, 41.2, 29.4, 18.1, 17.4. Cis conformer: ^1H NMR (400 MHz, CD_3OD) δ 7.05 (d, J = 8.4 Hz, 2H), 6.60 (d, J = 8.4 Hz, 2H), 6.12 (m, 1H), 4.95 (m, 1H), 4.59 (m, 1H), 4.27 (bs, 2H), 3.98 (m, 1H), 3.76 (s, 3H), 3.41 (s, 2H), 2.38 (m, 1H), 0.94 (d, J = 6.8 Hz, 3H), 0.91 (d, J = 6.8 Hz, 3H); ^{13}C NMR (100 MHz, CD_3OD) δ 166.9, 163.2, 162.9, 145.0, 136.2, 134.6, 127.9, 127.2, 114.7, 68.2, 53.3, 52.0, 41.7, 32.1, 18.4, 17.2. LC-ESI-MS: 12.2 min, $[M + H]^+ = 360$; *S*-enantiomer $[\alpha]^D = +27.5$, *R*-enantiomer $[\alpha]^D = -26.5$ (c 1 in CH_3OH).

General procedure for the coupling reaction with tert-butyl malonate: (95b). To a stirred solution of tert-butyl malonate (1 eq) in dry DCM (0.8 ml) under inert atmosphere, HBTU (1.5 eq) and DIPEA (2 eq) were added at rt. The solution was stirred for 10 min and then 93b or 94a,b (1 eq) was added. The reaction mixture was stirred for 2 days. The organic solution was filtered and the solvent evaporated under reduce pressure. The crude product was diluted with DCM and washed with H_2O . The organic phase was dried over Na_2SO_4 and solvent was

removed under reduced pressure. ^1H NMR (400 MHz, DMSO) δ 8.68 (t, J = 6 Hz, 1H), 7.72 (bs, 1H), 7.47 (d, J = 8.4 Hz, 2H), 7.11 (m, 6H), 6.49 (bs, 1H), 5.95 (bs, 1H), 5.04 (bs, 1H), 4.26 (m, 4H), 3.31 (m, 2H), 2.19 (m, 1H), 2.15 (s, 3H), 1.38 (s, 9H), 0.83 (d, J = 6.8 Hz, 3H), 0.75 (d, J = 6.8 Hz, 3H); ^{13}C NMR (100 MHz, CDCl_3) δ 168.1, 164.5, 163.7, 154.7, 141.8, 139.9, 137.8, 134.5, 132.8, 132.7, 130.0, 129.7, 127.6, 125.7, 120.7, 119.0, 81.4, 67.1, 54.6, 43.9, 37.0, 31.9, 27.7, 18.3, 17.7; LC-ESI-MS: 8.6 min, $[M + H]^+$ =535, $[M + Na]^+$ =557. *S*-enantiomer $[\alpha]^D$ = -9.0, *R*-enantiomer $[\alpha]^D$ = +10.2 (c 1 in DMSO).

General procedure for the preparation of urea-derivative: 96a,b.

1-isocyanato-2-methylbenzene (1 eq) was added to a solution of 94a,b (1 eq), in DCM. The reaction was stirred at rt and followed by TLC. After 20h the reaction was complete and the organic layer was washed with water, dried with anhydrous sodium sulfate and concentrated in vacuo. The crude product was purified by flash chromatography on silica gel (cyclohexane/EtOAc 20:80).

Compound (96a): (70:30 trans/cis amide ratio) ^1H NMR (400 MHz, CD_3OD) δ 8.38 (bs, 1H), 7.68 (bs, 2H), 6.94-7.88 (m, 8H), 6.32 (m, 1H, cis isomer), 6.25 (m, 1H, trans isomer), 5.18 (m, 1H, cis isomer), 5.13 (m, 1H, trans isomer), 4.43 (m, 4H), 3.70 (s, 3H), 3.65 (m, 2H), 2.23 (s, 3H), 2.05 (m, 1H), 1.40-1.55 (m, 5H), 0.89-1.32 (m, 5H); ^{13}C NMR (100 MHz, CD_3OD) δ 168.0, 167.6, 167.0, 156.3, 140.3, 139.8, 134.6, 131.9, 13.7, 130.7, 130.0, 129.9, 127.9, 125.9, 124.9, 120.7, 69.9, 56.6, 53.3, 44.0, 43.5, 30.7, 29.8, 28.3, 27.9, 18.5; LC-ESI-MS: 7.7 min, $[M + H]^+$ =533, $[M + Na]^+$ =555. *S*-enantiomer $[\alpha]^D$ = +20.4, *R*-enantiomer $[\alpha]^D$ = -17.5 (c 1 in CH_3OH).

Compound (96b): (65:35 trans/cis amide ratio) ^1H NMR (400 MHz, DMSO) δ 8.95 (bs, 1H), 8.60 (bs, 1H), 7.84 (bs, 1H), 7.38 (m, 2H), 7.06-7.18 (m, 4H), 6.91 (m, 1H), 6.47 (m, 1H), 4.98 (s, 1H), 4.38 (dd,

$J=16$ Hz, $J=4.4$ Hz, 1H), 4.24 (m, 2H), 4.19 (dd, $J=16$ Hz, $J=4.4$ Hz, 1H), 3.62 (s, 3H), 3.51 (d, $J=15.2$, 1H), 3.43 (d, $J=15.2$, 1H), 2.22 (m, 1H), 2.20 (s, 3H), 0.78 (d, $J=6.8$ Hz, 3H), 0.74 (d, $J=6.8$ Hz, 3H); ^{13}C NMR (100 MHz, DMSO) trans conformer δ 169.2, 165.1, 164.6, 154.2, 137.8, 137.5, 136.1, 132.3, 130.0, 127.9, 127.3, 127.2, 126.6, 123.1, 122.9, 114.9, 66.0, 54.4, 51.8, 42.2, 40.6, 30.5, 18.9, 17.6, 16.8; cis conformer δ 167.9, 166.2, 165.1, 153.8, 137.7, 137.6, 136.1, 133.1, 131.0, 127.8, 127.5, 127.4, 126.8, 123.9, 123.8, 115.6, 66.3, 55.1, 51.6, 41.8, 41.2, 32.1, 18.7, 18.3, 17.0; LC-ESI-MS: 6.6 min, $[M+H]^+=493$, $[M+Na]^+=515$, $[2M+H]^+=985$. *S*-enantiomer $[\alpha]^D=+21.0$, *R*-enantiomer $[\alpha]^D=-18.9$ (c 1 in CH_3OH).

Removal of the tert-butyl ester: (97b) and (99). To a solution of 95b (1 eq) in DCM (0.35M), TFA (10-15 eq) was added and the reaction mixture was stirred at rt until complete consumption of the starting material. The solvent and the excess of reagent were removed and the product was used without further purifications.

Compound (97b): ^1H NMR (400 MHz, CD_3OD) δ 7.51 (d, $J=8.4$ Hz, 2H), 7.26 (d, $J=8.4$, 2H), 7.13 (m, 4H), 5.14 (m, 1H), 4.38 (s, 2H), 4.31 (m, 2H), 3.28 (s, 2H), 2.32 (m, 1H), 2.23 (s, 3H), 0.91 (d, $J=6.8$ Hz, 3H), 0.86 (d, $J=6.8$ Hz, 3H); ^{13}C NMR (100 MHz, CDCl_3) δ 168.0, 163.5, 160.4, 154.9, 141.6, 139.2, 137.2, 136.2, 134.8, 133.1, 130.0, 129.0, 127.6, 125.8, 121.6, 119.1, 66.4, 53.9, 42.7, 36.6, 31.4, 19.2, 17.9; LC-ESI-MS: 5.4 min, $[M+H]^+=479$, $[2M+H]^+=957$. *S*-enantiomer $[\alpha]^D=-32.4$, *R*-enantiomer $[\alpha]^D=+32.0$ (c 1 in DMSO).

Compound (99): ^1H NMR (400 MHz, CDCl_3) δ 5.36 (m, 1H), 3.73 (s, 3H), 3.63 (d, $J=15.9$ Hz, 1H), 3.50 (d, $J=16.0$ Hz, 1H), 2.27 (s, 3H), 2.20 (m, 2H), 2.03 (m, 1H), 1.93 (t, $J=2.6$ Hz, 1H), 1.78 (m, 1H), 1.65-1.52 (m, 2H); ^{13}C NMR (400 MHz, CDCl_3) δ 168.3, 167.9, 167.0, 164.4, 104.2, 83.7, 68.7, 62.9, 52.6, 40.4, 32.3, 23.6, 18.0, 11.8; LC-ESI-MS:

5.0 min, $[M + H]^+ = 296$, $[M + Na]^+ = 318$, $[M + K]^+ = 334$, $[2M + Na]^+ = 613$; HRMS (ESI) $[M + H]$ calcd for $C_{14}H_{18}NO_6$ 296.1134 found 296.1131.

Hydrolysis of methyl ester: (98a,b). The ester 96a,b (1 eq) was dissolved in a mixture of THF/H₂O and K₂CO₃ (1 eq) was added. The mixture was stirred at room temperature for 2h. The solvent was removed under reduced pressure and the crude dissolved in ethyl acetate and washed with water. The organic layer was dried on sodium sulphate and the solvent evaporated. The crude was used without further purifications.

Compound (98a): ¹H NMR (400 MHz, acetone-*d*6) δ 8.6 (bs, 1H), 8.38 (bs, 1H), 7.68 (bs, 2H), 6.94-7.88 (m, 8H), 6.35 (s, 1H), 5.13 (s, 1H), 4.31 (dd, $J = 16$ Hz, $J = 4.4$ Hz, 1H), 4.27 (dd, $J = 16$ Hz, $J = 4.4$ Hz, 1H), 4.43 (d, $J = 6$ Hz, 2H), 2.23 (s, 3H), 1.40-1.55 (m, 5H), 0.89-1.32 (m, 6H); ¹³C NMR (100 MHz, CD₃OD) δ 168.7, 165.6, 164.6, 153.8, 137.8, 137.2, 135.8, 132.0, 129.5, 129.2, 128.2, 127.3, 126.3, 125.4, 123.4, 122.7, 122.3, 118.2, 67.4, 54.1, 41.6, 40.9, 28.2, 27.3, 25.8, 25.4, 16.1; LC-ESI-MS: 19.6 min, $[M + H]^+ = 519$, $[M + Na]^+ = 541$, $[2M + Na]^+ = 1059$. *S*-enantiomer $[\alpha]^D = -37.7$, *R*-enantiomer $[\alpha]^D = +39.5$ (c 1 in CH₃OH).

Compound (98b): major and minor isomer on amidic bond; ¹H NMR (400 MHz, acetone-*d*6) δ 8.6 (bs, 1H), 8.38 (bs, 1H), 7.68 (bs, 2H), 6.94-7.88 (m, 8H), 6.47 (s, 1H), 5.13 (s, 1H), 4.31 (dd, $J = 16$ Hz, $J = 4.4$ Hz, 1H), 4.27 (dd, $J = 16$ Hz, $J = 4.4$ Hz, 1H), 4.43 (d, $J = 6$ Hz, 2H), 2.36 (m, 1H), 2.03 (s, 3H), 0.89 (d, $J = 5.6$ Hz, 3H), 0.87 (d, $J = 5.6$ Hz, 3H); ¹³C NMR (100 MHz, CD₃OD) δ 168.9, 165.0, 163.7, 152.6, 137.9, 137.5, 135.7, 131.9, 130.1, 127.8, 127.7, 127.5, 126.0, 122.6, 121.0, 117.9, 66.2, 54.9, 41.6, 40.1, 32.5, 18.3, 17.9, 16.1; LC-ESI-MS: 6.1 min, $[M + H]^+ = 479$, $[2M + H]^+ = 957$. *S*-enantiomer $[\alpha]^D = -25.2$, *R*-enantiomer $[\alpha]^D = +24.5$ (c 1 in DMSO).

Synthesis of isoxazoline- 4-amino benzylamide: (100). Under inert atmosphere, TEA (1.5 eq) and HBTU (1.5 eq) were added to a solution of (99) (1 eq) in DCM (0.12M), and the mixture was stirred at rt for 5 min. 4-aminobenzylamine (2 eq) was then added and the mixture stirred for further 4h. The mixture was diluted with DCM and washed with water. The organic layer was dried over Na_2SO_4 and then evaporated under reduced pressure. The crude product was purified by flash chromatography (silica gel, 80/20 cyclohexane/EtOAc). Yield 76%. ^1H NMR (400 MHz, CDCl_3) δ 7.06 (d, J= 8.0 Hz, 2H), 6.63 (d, J= 8.0 Hz, 2H), 5.62 (bs, 1H), 5.27 (m, 1H), 4.41 (dd, J= 5.6, 14.0 Hz, 1H), 4.29 (dd, J= 5.2, 14.0 Hz, 1H), 3.70 (s, 3H), 3.58 (d, J= 15.9 Hz, 1H), 3.44 (d, J= 16.0 Hz, 1H), 2.38 (m, 1H), 2.21 (m, 1H), 2.02 (s, 3H), 1.97 (m, 1H), 1.65 (m, 1H), 1.58-1.51 (m, 2H); ^{13}C NMR (100 MHz, CDCl_3) δ 168.5, 166.9, 162.0, 159.0, 145.9, 129.1, 127.6, 115.1, 106.5, 83.7, 69.3, 61.6, 52.4, 43.1, 40.5, 38.5, 32.6, 23.0, 17.3, 11.3; LC-ESI-MS: 1.4 min, $[M + H]^+ = 400$, $[M + Na]^+ = 422$, $[M + K]^+ = 438$, $[2M + Na]^+ = 821$; HRMS (ESI) $[M + H]$ calcd for $\text{C}_{21}\text{H}_{26}\text{N}_3\text{O}_5$ 400.1872 found 400.1870.

General procedure for the hydrolysis of malonyl methyl ester: (101), (106), (107), (112), (113), (117) and (122). $\text{LiOH}\cdot\text{H}_2\text{O}$ (1 eq) was added to a solution of ester (1 eq) in a 2/1 mixture of THF/ H_2O (0.007M). The reaction was stopped after disappearance of the starting material, following the evolution by TLC. The solution was neutralized adding dropwise HCl 1M solution and then water was evaporated. The product was purified by flash chromatography (C18 reverse phase silica gel, 8/2 water/ CH_3CN). Yield of (101) 99%; Yield of (106) 80%; Yield of (107) 87%; Yield of (112) 75%; Yield of (113) 75%; Yield of (117) 40%; Yield of (122) 40%.

Compound (101): ^1H NMR (400 MHz, CD_3OD) δ 7.04 (d, J= 8.2 Hz,

2H), 6.66 (d, $J=8.2$ Hz, 2H), 5.43 (m, 1H), 4.84 (m, 2H), 4.36 (d, $J=14.6$ Hz, 1H), 4.17 (d, $J=14.6$ Hz, 1H), 2.22-2.11 (m, 2H), 2, 18 (s, 3H), 1.87 (bs, 1H), 1.86 (m, 1H), 1.66 (m, 1H), 1.57-1.48 (m, 2H); ^{13}C NMR (100 MHz, CD_3OD) δ 172.4, 172.0, 163.6, 158.3, 146.4, 128.3, 128.1, 115.2, 106.6, 83.2, 68.5, 62.3, 42.3, 39.9, 32.8, 23.5, 17.3, 10.0. LC-ESI-MS: 1.6 min, $[M + H]^+=386$, $[M + Na]^+=400$, $[2M + H]^+=771$; HRMS (ESI) $[M + H]$ calcd for $\text{C}_{20}\text{H}_{24}\text{N}_3\text{O}_5$ 386.1716 found 386.1714.

Compound (106): ^1H NMR (400 MHz, CD_3OD) δ 7.64 (s, 1H), 7.61 (bs, 1H), 7.01 (d, $J=8.3$ Hz, 2H), 6.90 (bs, 1H), 6.65 (d, $J=8.3$ Hz, 2H), 5.45 (m, 1H), 4.85 (m, 2H), 4.39 - 4.32 (m, 3H), 4.18 (d, $J=14.4$ Hz, 1H), 3.45 (t, $J=5.6$ Hz, 2H), 2.67 (t, $J=8.0$ Hz, 2H), 2.17 (s, 3H), 1.87-1.53 (m 4H), 1.37 (s, 9H); ^{13}C NMR (100 MHz, CD_3OD) δ 169.7, 163.4, 163.0, 161.9, 158.5, 147.3, 144.9, 129.3, 129.0, 121.9, 115.4, 107.3, 79.8, 61.3, 49.8, 42.7, 40.5, 38.8, 32.4, 28.3, 24.4, 23.2, 11.3; LC-ESI-MS: 1.6 min, $[M + H]^+=572$; HRMS (ESI) $[M + 1]$ calcd for $\text{C}_{27}\text{H}_{38}\text{N}_7\text{O}_7$ 572.2833 found 572.2830.

Compound (107): ^1H NMR (400 MHz, CD_3OD) δ 7.69 (s, 1H), 7.68 (bs, 1H), 7.00 (d, $J=8.0$ Hz, 2H), 6.64 (d, $J=8.0$ Hz, 2H), 5.45 (m, 1H), 4.85 (m, 2H), 4.35-4.31 (m, 3H), 4.17 (d, $J=14.6$ Hz, 1H), 3.01 (t, $J=6.0$ Hz, 2H), 2.67 (t, $J=7.2$ Hz, 2H), 2.17 (s, 3H), 2.01-1.98 (m, 2H), 1.86-1.61 (m, 4H), 1.40 (s, 9H); ^{13}C NMR (100 MHz, CD_3OD) δ 171.9, 169.5, 163.6, 161.7, 158.3, 147.4, 146.4, 135.7, 128.2, 122.0, 115.1, 106.5, 78.7, 62.4, 48.4, 42.2, 37.1, 32.8, 30.1, 29.2, 27.3, 24.3, 24.1, 10.0. LC-ESI-MS: 1.6 min, $[M + H]^+=586$, $[M + Na]^+=608$; HRMS (ESI) $[M + 1]$ calcd for $\text{C}_{28}\text{H}_{40}\text{N}_7\text{O}_7$ 586.2989 found 586.2990.

Compound (112): ^1H NMR (400 MHz, CD_3OD) δ 7.76 (s, 1H), 7.47 (bs, 1H), 7.41 (d, $J=8.0$ Hz, 2H), 7.28 (d, $J=8.0$ Hz, 2H), 5.51 (m, 1H), 5.20 (s, 2H), 4.50 (d, $J=15.2$ Hz, 2H), 4.39 (d, $J=15.2$ Hz, 2H), 2.76-2.69 (m, 2H), 2.20 (s, 3H), 1.85-1.60 (m, 4H), 1.45 (s, 9H); ^{13}C NMR (100 MHz, CD_3OD) δ 173.6, 171.2, 169.9, 169.2, 167.2, 147.0, 146.8,

134.1, 128.2, 122.4, 115.3, 106.6, 82.4, 61.0, 51.4, 43.2, 34.0, 33.3, 27.8, 24.6, 24.0,11.0; LC-ESI-MS(acid eluents): 9.4 min, $[M + H]^+ = 543$, $[M + Na]^+ = 565$; HRMS (ESI) $[M + 1]$ calcd for $C_{26}H_{35}N_6O_7$ 543.2567 found 543.2565.

Compound (113): 1H NMR (400 MHz, $CDCl_3$) δ 7.82 (bs, 1H), 7.80 (s, 1H), 7.44 (d, $J = 8.0$ Hz, 2H), 7.34 (d, $J = 8.0$ Hz, 2H), 5.50 (m, 1H), 4.61-4.56 (m, 3H), 4.46 (d, $J = 12.4$ Hz, 1H), 2.90-2.85 (m, 2H), 2.75-2.71 (m, 2H), 2.20 (s, 3H), 1.86-1.65 (m, 4H), 1.38 (s, 9H); ^{13}C NMR (100 MHz, $CDCl_3$) δ 173.6, 170.8, 170.2, 169.6, 167.5, 147.0, 146.2, 133.8, 128.6, 122.0, 115.1, 106.4, 80.9, 60.7, 48.2, 43.4, 35.4, 33.9, 30.8, 27.6, 24.8, 24.2,11.5; LC-ESI-MS(acid eluents): 10.0 min, $[M + H]^+ = 557$, $[M + Na]^+ = 579$; HRMS (ESI) $[M + 1]$ calcd for $C_{27}H_{37}N_6O_7$ 557.2724 found 557.2726.

Compound (117): 1H NMR (400 MHz, CD_3OD) δ 7.81 (bs, 1H), 7.80 (s, 1H), 7.43 (d, $J = 8.0$ Hz, 2H), 7.35 (d, $J = 8.0$ Hz, 2H), 5.52 (m, 1H), 4.86 (m, 2H), 4.51 (t, $J = 9.6$ Hz, 1H), 4.22-4.35 (m, 3H), 3.18-3.13 (m, 2H),2.78-2.68 (m, 2H), 2.63-2.57 (m, 2H), 2.48-2.44 (m, 2H), 2.21 (s, 3H), 2.08-2.03 (m, 2H), 1.85 (m, 1H), 1.76-1.59 (m, 3H), 1.41 (s, 9H); ^{13}C NMR (100 MHz, CD_3OD) δ 172.5, 172.2, 171.7, 169.1, 165.6, 162.7, 147.0, 146.5, 135.2, 128.6, 122.1, 115.3, 106.2, 80.8, 62.0, 48.4, 42.8, 37.0, 33.1, 31.2, 30.8, 29.4, 28.8, 28.0, 24.4, 24.0,11.0; LC-ESI-MS(acid eluents): 9.4 min, $[M + H]^+ = 642$, $[M + Na]^+ = 664$; HRMS (ESI) $[M + 1]$ calcd for $C_{31}H_{44}N_7O_8$ 642.3251 found 642.3248.

Compound (122): 1H NMR (400 MHz, CD_3OD) δ 7.73 (s, 1H), 7.03 (d, $J = 8.4$ Hz, 2H), 6.67 (d, $J = 8.4$ Hz, 2H), 5.47 (m, 1H), 4.82 (m, 2H), 4.51 (t, $J = 5.2$ Hz, 2H), 4.37 (d, $J = 14.6$ Hz, 1H), 4.20 (d, $J = 14.6$ Hz, 1H), 3.87 (t, $J = 5.2$ Hz, 2H), 3.60-3.57 (m, 4H), 3.46 (t, $J = 5.6$ Hz, 2H), 3.19 (t, $J = 6.0$ Hz, 2H), 2.71 (t, $J = 6.8$ Hz, 2H), 2.20 (s, 3H), 1.85-1.58 (m, 4H), 1.42 (s, 9H); ^{13}C NMR (100 MHz, CD_3OD) δ 175.4, 172.4, 170.3, 168.2, 158.2, 156.9, 147.3, 146.4, 128.4, 128.2, 122.5, 115.1,

107.1, 78.7, 70.0, 69.8, 69.6, 69.0, 49.8, 42.2, 42.1, 39.8, 33.3, 29.3, 27.3, 24.9, 10.3; LC-ESI-MS(acid eluents): 9.9 min, $[M + H]^+ = 660$, $[M + Na]^+ = 682$; HRMS (ESI) $[M + 1]$ calcd for $C_{31}H_{46}N_7O_9$ 660.3357 found 660.3357.

General procedure for the synthesis of azides: (102) and (103).

Under inert atmosphere, to a solution of 2-bromo-ethylamine hydrobromide or 3-bromo-propylamine hydrobromide (1.2 eq) in DCM (0.2M), Boc_2O (1 eq) and TEA (1.5 eq) were added at 0°C and the mixture stirred at room temperature overnight. The mixture was then washed with NH_4Cl saturated solution, $NaHCO_3$ saturated solution, brine and evaporated to afford the N-Boc-bromoamine intermediate that was used without further purifications. The intermediate was dissolved in DMF and NaN_3 (1.4 eq) was added in one portion. The mixture was stirred at 60°C for 4h and then diluted with EtOAc and washed with water. The organic layer was evaporated after anhydrification over Na_2SO_4 to give the azides. Yield of (102) 70%; Yield of (103) 90%.

Compound (102): 1H NMR (400 MHz, $CDCl_3$) δ 4.79 (bs, 1H), 3.40 (t, $J = 5.7$ Hz, 2H), 3.28 (m, 2H), 1.43 (s, 9H); ^{13}C NMR (100 MHz, $CDCl_3$) δ 155.8, 79.9, 50.8, 39.8, 28.2; LC-ESI-MS: 6.5 min, $[M + Na]^+ = 209$, $[2M + H]^+ = 372$, $[2M + K]^+ = 395$; HRMS (ESI) $[M + Na]$ calcd for $C_7H_{14}N_4NaO_2$ 209.1014 found 209.1012.

Compound (103): 1H NMR (400 MHz, $CDCl_3$) δ 4.63 (bs, 1H), 3.33 (t, $J = 8.0$ Hz, 2H), 3.18 (m, 2H), 1.71-1.77 (m, 2H), 1.41 (s, 9H); ^{13}C NMR (100 MHz, $CDCl_3$) δ 162.2, 78.4, 48.7, 36.1, 31.0, 28.0; LC-ESI-MS: 7.4 min, m/z: $[M + Na]^+ = 223$, $[2M + Na]^+ = 423$. HRMS (ESI) $[M + Na]$ calcd for $C_8H_{16}N_4NaO_2$ 223.1171 found 223.1168.

Synthesis of tert-butyl 4-((3-bromopropyl)amino)-succinate: (114).

Under inert atmosphere, to a solution of mono tert-butyl pentandioic acid

(1 eq)) in DCM (1.4M), HBTU (1.5 eq), TEA (1.5 eq) and 3-bromo propylamine hydrobromide (0.9 eq) were added and the mixture stirred at room temperature for 4h. The mixture was diluted with DCM, washed with water and evaporated. The crude product was purified by flash chromatography (silica gel, 9/1 cyclohexane/EtOAc). Yield 50%. $^1\text{H NMR}$ (400 MHz, CDCl_3) δ 5.93 (bs, 1H), 3.43-3.36 (m, 4H), 2.62-2.52 (m, 2H), 2.40 (t, $J=6.8$ Hz, 2H), 2.07 (m, 2H), 1.44 (s, 9H); $^{13}\text{C NMR}$ (100 MHz, CDCl_3) δ 172.3, 172.2, 80.8, 38.0, 32.2, 31.1, 30.8, 30.7, 27.9 ; LC-ESI-MS: 6.7 min, $[2M + Na]^+=611$.

General procedure for the synthesis of azides: (108), (109), (115) and (118). Bromo derivative (1 eq) was dissolved in DMF (0.7M) and NaN_3 (1.1 eq) was added. The mixture was stirred at 60°C for 4h and then diluted with EtOAc and washed with water. Yield of (108): 45% Yield of (109): 45%; Yield of (115): 90%; Yield of (118): 85%.

Compound (108): $^1\text{H NMR}$ (400 MHz, CDCl_3) δ 3.72 (s, 2H); 1.48 (s, 9H); $^{13}\text{C NMR}$ (100 MHz, CDCl_3) δ 167.2, 82.6, 50.6, 27.7.

Compound (109): $^1\text{H NMR}$ (400 MHz, CDCl_3) δ 3.50 (t, $J=6.4$ Hz, 2H); 2.48 (t, $J=6.8$ Hz, 2H); 1.45 (s, 9H); $^{13}\text{C NMR}$ (100 MHz, CDCl_3) δ 169.7, 80.7, 46.6, 35.9, 27.6.

Compound (115): $^1\text{H NMR}$ (400 MHz, CDCl_3) δ 6.00 (bs, 1H), 3.36-3.30 (m, 4H), 2.56 (t, $J=6.8$ Hz, 2H); 2.40 (t, $J=6.8$ Hz, 2H), 1.80-1.72 (m, 2H), 1.43 (s, 9H); $^{13}\text{C NMR}$ (100 MHz, CDCl_3) δ 172.4, 172.0, 80.8, 49.2, 37.0, 31.2, 30.8, 28.8, 28.0; LC-ESI-MS: 6.0 min, $[M + Na]^+=279$, $[2M + Na]^+=535$; HRMS (ESI) $[M + Na]$ calcd for $\text{C}_{11}\text{H}_{20}\text{N}_4\text{NaO}_3$ 279.1433 found 279.1430.

Compound (118): $^1\text{H NMR}$ (400 MHz, CDCl_3) δ 4.10 (q, $J=7.2$ Hz, 2H), 3.27 (t, $J=6.4$ Hz, 2H), 2.31 (t, $J=6.8$ Hz, 2H), 1.73-1.57 (m, 4H), 1.23 (t, $J=7.2$ Hz, 3H); $^{13}\text{C NMR}$ (100 MHz, CDCl_3) δ 172.9, 60.2, 50.9, 33.5, 28.2, 22.0, 14.1; LC-ESI-MS: 8.0 min, $[M + H]^+=172$,

$[M + Na]^+ = 194$; HRMS (ESI) $[M + 1]$ calcd for $C_7H_{14}N_3O_2$ 172.1086 found 172.1089.

Synthesis Ethyl 2-(2-(2-azidoethoxy)ethoxy)acetate: (124). [2-(2-azidoethoxy)ethoxy]acetic acid cyclohexylamine salt (1 eq) was dissolved in Et_2O (1M) and $BF_3 \cdot Et_2O$ (1 eq) was added at $0^\circ C$. The mixture was refluxed for 3h and then evaporated. The crude product was purified by flash chromatography (silica gel, 1/1 EtOAc/cyclohexane). Yield of (124): 40%. 1H NMR (400 MHz, $CDCl_3$) δ 4.20 (q, $J = 7.2$ Hz, 2H), 4.14 (s, 2H); 3.75-3.72 (m, 2H), 3.70-3.66 (m, 4H), 3.38 (q, $J = 5.2$ Hz, 2H), 1.27 (q, $J = 7.2$ Hz, 3H); ^{13}C NMR (100 MHz, $CDCl_3$) δ 170.2, 70.8, 70.7, 70.5, 68.6, 60.6, 50.5, 14.0. LC-ESI-MS: 5.4 min, $[M + H]^+ = 218$, $[M + Na]^+ = 240$. HRMS (ESI) $[M + 1]$ calcd for $C_8H_{16}N_3O_4$ 218.1141 found 218.1145.

General procedure for the Huisgen reaction between methyl ester (100) and azides: (104), (105), (110), (111), (116), (121). In a mixture of $tBuOH:H_2O = 1:1$ (1 ml), TEA (1 eq) and HCl 1M (1 eq) were added and stirred for 2 min. (100) (1 eq), $Cu^{(0)}$ (10 mol%) and azide (1 eq) were added and the mixture stirred at room temperature following the reaction by TLC. The mixture was filtered through celite to remove the copper powder and evaporated. The crude was purified by flash chromatography (silica gel, 9/1 EtOAc/cyclohexane). Yield of (104): 57%; Yield (105): 67%; Yield (110): 20%; Yield (111): 34%; Yield (116): 75%; Yield (121): 79%.

Compound (104): 1H NMR (400 MHz, $CDCl_3$) δ 7.44 (bs, 1H), 7.29 (s, 1H), 7.13 (d, $J = 8.2$ Hz, 2H), 6.66 (d, $J = 8.2$ Hz, 2H), 5.45 (m, 1H), 5.09 (bs, 1H), 4.42-4.35 (m, 4H), 3.69 (s, 3H), 3.56 (d, $J = 16.0$ Hz, 1H), 3.51 (m, 2H), 3.46 (d, $J = 16.0$ Hz, 1H), 2.72-2.67 (m, 2H), 2.24 (s, 3H), 1.85 (m, 1H), 1.75 (m, 1H), 1.61-1.55 (m, 2H), 1.39 (s, 9H); ^{13}C NMR

(100 MHz, CDCl_3) δ 168.9, 167.1, 162.2, 158.9, 155.9, 147.3, 144.9, 129.3, 129.0, 121.9, 115.4, 107.3, 79.8, 61.2, 52.4, 49.8, 42.7, 40.5, 32.3, 29.6, 28.3, 24.4, 23.2, 11.3; LC-ESI-MS: 5.6 min, m/z : $[M + H]^+ = 586$, $[M + Na]^+ = 608$; HRMS (ESI) $[M + 1]$ calcd for $\text{C}_{28}\text{H}_{40}\text{N}_7\text{O}_7$ 586.2989 found 586.2991.

Compound (105): ^1H NMR (400 MHz, CDCl_3) δ 7.35 (bs, 2H), 7.12 (d, $J = 7.9$ Hz, 2H), 6.60 (d, $J = 7.9$ Hz, 2H), 5.52 (m, 1H), 4.88 (bs, 1H), 4.44 (m, 2H), 4.31 (t, $J = 6.9$ Hz, 2H), 3.71 (s, 3H), 3.58 (d, $J = 16.0$ Hz, 1H), 3.48 (d, $J = 15.9$ Hz, 1H), 3.10-3.05 (m, 2H), 2.27 (s, 3H), 2.03-1.99 (m, 2H), 1.87 (m, 1H), 1.77 (m, 1H); 1.63-1.53 (m, 2H), 1.43 (s, 9H); ^{13}C NMR (100 MHz, CDCl_3) δ 168.9, 167.1, 162.2, 158.9, 156.1, 147.2, 145.1, 129.2, 128.9, 121.4, 115.3, 107.3, 79.4, 61.2, 52.4, 47.4, 42.7, 40.5, 37.4, 32.3, 30.5, 28.4, 24.4, 23.0, 11.3; LC-ESI-MS: 6.3 min, $[M + H]^+ = 600$, $[M + Na]^+ = 622$; HRMS (ESI) $[M + 1]$ calcd for $\text{C}_{29}\text{H}_{42}\text{N}_7\text{O}_7$ 600.3146 found 600.3148.

Compound (110): ^1H NMR (400 MHz, CDCl_3) δ 7.54 (s, 1H), 7.02 (d, $J = 8.4$ Hz, 2H), 6.92 (bs, 1H), 6.58 (d, $J = 8.4$ Hz, 2H), 5.39 (m, 1H), 4.26 (d, $J = 6.0$ Hz, 2H), 3.67 (s, 3H), 3.58 (d, $J = 16.4$ Hz, 1H), 3.50 (d, $J = 16.4$ Hz, 1H), 2.81-2.70 (m, 2H), 2.17 (s, 3H), 1.81-1.51 (m, 6H), 1.46 (s, 9H); ^{13}C NMR (100 MHz, CDCl_3) δ 173.9, 171.0, 169.1, 167.3, 163.9, 147.1, 146.4, 134.0, 128.6, 122.2, 115.1, 106.3, 82.2, 60.8, 52.1, 51.6, 43.8, 33.4, 31.5, 27.9, 24.8, 24.3, 11.8; LC-ESI-MS: 6.8 min, $[M + H]^+ = 557$, $[2M + Na]^+ = 1135$; HRMS (ESI) $[M + 1]$ calcd for $\text{C}_{27}\text{H}_{37}\text{N}_6\text{O}_7$ 557.2724 found 557.2721.

Compound (111): ^1H NMR (400 MHz, CDCl_3) δ 7.50 (s, 1H), 7.02 (d, $J = 8.4$ Hz, 2H), 7.29 (bs, 1H), 6.65 (d, $J = 8.4$ Hz, 2H), 5.47 (m, 1H), 4.55 (bs, 1H), 4.38-4.34 (m, 3H), 4.18 (d, $J = 14.4$ Hz, 1H), 3.67 (s, 3H), 3.58 (d, $J = 16.0$ Hz, 1H), 3.47 (d, $J = 16.0$ Hz, 1H), 2.80 (t, $J = 6.4$ Hz, 2H), 2.72 (m, 1H), 2.39 (m, 1H), 2.10 (s, 3H), 1.78-1.54 (m, 4H), 1.38 (s, 9H); ^{13}C NMR (100 MHz, CDCl_3) δ 173.7, 170.9, 169.6,

167.6, 164.2, 147.3, 146.6, 133.7, 128.4, 122.0, 115.3, 106.1, 81.3, 60.6, 52.3, 48.8, 43.6, 35.4, 31.9, 30.4, 27.9, 24.6, 24.2, 11.6. LC-ESI-MS: 6.7 min, $[M + H]^+ = 571$, $[M + Na]^+ = 593$; HRMS (ESI) $[M + 1]$ calcd for $C_{28}H_{39}N_6O_7$ 571.2880 found 571.2877.

Compound (116): 1H NMR (400 MHz, $CDCl_3$) δ 7.67 (s, 1H), 7.07 (m, 1H), 7.00 (d, $J = 8.4$ Hz, 2H), 6.58 (d, $J = 8.4$ Hz, 2H), 5.39 (m, 1H), 4.50 (m, 2H), 4.26 (d, $J = 5.6$ Hz, 2H), 3.67 (s, 3H), 3.29 (m, 2H), 3.16 (m, 2H), 2.70-2.66 (m, 2H), 2.53-2.48 (m, 2H), 2.41-2.38 (m, 2H), 2.17 (s, 3H), 2.07-2.00 (m, 2H), 1.83-1.57 (m, 4H), 1.41 (s, 9H); ^{13}C NMR (100 MHz, $CDCl_3$) δ 172.0, 168.5, 166.8, 161.9, 158.5, 146.9, 145.0, 128.7, 128.5, 121.4, 114.8, 107.0, 80.4, 61.0, 60.0, 52.1, 47.1, 42.3, 40.2, 36.1, 32.0, 30.7, 30.3, 29.6, 27.7, 24.1, 13.8, 10.9; LC-ESI-MS: 6.0 min, $[M + H]^+ = 656$, $[M + Na]^+ = 678$; HRMS (ESI) $[M + 1]$ calcd for $C_{32}H_{46}N_7O_8$ 656.3408 found 656.3406.

Compound (121): 1H NMR (400 MHz, $CDCl_3$) δ 7.53 (bs, 1H), 7.45 (s, 1H), 7.17 (d, $J = 8.4$ Hz, 2H), 6.72 (d, $J = 8.4$ Hz, 2H), 5.59 (m, 1H), 4.95 (bs, 1H), 4.50 (m, 2H), 4.47-4.45 (m, 4H), 3.82 (t, $J = 5.2$ Hz, 2H), 3.71 (s, 3H), 3.61-3.46 (m, 6H), 3.28-3.26 (m, 2H), 3.08 (m, 1H), 2.72 (m, 1H), 2.27 (s, 3H), 1.93-1.76 (m, 2H), 1.63-1.54 (m, 2H), 1.42 (s, 9H); ^{13}C NMR (100 MHz, $CDCl_3$) δ 169.0, 167.0, 162.5, 162.2, 159.0, 155.9, 147.1, 145.2, 129.3, 129.1, 122.2, 115.2, 107.4, 70.5, 70.2, 70.0, 69.5, 61.2, 52.4, 50.1, 42.7, 40.6, 32.3, 36.4, 29.6, 28.4, 24.6, 11.3; LC-ESI-MS: 6.4 min, $[M + H]^+ = 674$, $[M + Na]^+ = 696$; HRMS (ESI) $[M + 1]$ calcd for $C_{32}H_{48}N_7O_9$ 674.3514 found 674.3512.

General procedure for the Huisgen reaction between acid (101) and azides: (119) and (123). In a mixture of $tBuOH:H_2O=6:4$ (0.15M) (101) (1 eq), $Cu(OAc)_2$ (0.2 mol%), Na-ascorbate (0.4 mol%) and azide (1 eq) were added and the mixture was stirred at room temperature following the reaction by TLC. The mixture was filtered through celite and

evaporated. The product was purified by flash chromatography (C18 reverse phase silica gel, 8/2 water/CH₃CN). Yield (119): 20%; Yield (123): 40%.

Compound (119): ¹H NMR (400 MHz, CD₃OD) δ 7.43 (s, 1H), 7.24 (bs, 1H), 7.04 (d, J= 8.0 Hz, 2H), 6.64 (d, J= 8.0 Hz, 2H), 5.46 (m, 1H), 4.85 (m, 2H), 4.35-4.31 (m, 3H), 4.18 (d, J= 15.0 Hz, 1H), 4.08 (q, J= 7.6 Hz, 2H), 3.19-3.14 (m, 2H), 2.72-2.64 (m, 2H), 2.32-2.30 (m, 2H), 2.20-2.15 (m, 2H), 2.13 (s, 3H), 2.01-1.98 (m, 2H), 1.87-1.78 (m, 2H), 1.71-1.52 (m, 2H), 1.28 (t, J= 7.6 Hz, 3H); ¹³C NMR (100 MHz, CD₃OD) δ 173.5, 172.9, 171.8, 169.4, 164.2, 147.2, 146.6, 133.9, 128.3, 122.2, 115.4, 106.1, 61.4, 60.2, 49.2, 43.9, 36.4, 33.5, 30.5, 28.2, 24.5, 24.2, 22.0, 14.1, 10.2; LC-ESI-MS(acid eluent): 9.0 min, m/z: $[M+H]^+$ =557, $[M+Na]^+$ =579; HRMS (ESI) $[M+1]$ calcd for C₂₇H₃₇N₆O₇ 557.2724 found 557.2722.

Compound (123): ¹H NMR (400 MHz, CD₃OD) δ 7.82 (bs, 1H), 7.27 (s, 1H), 7.07 (d, J= 8.4 Hz, 2H), 6.62 (d, J= 8.4 Hz, 2H), 5.48 (m, 1H), 4.86 (m, 2H), 4.56-4.47 (m, 3H), 4.40 (m, 1H), 4.18 (q, J= 7.2 Hz, 2H), 4.11-4.05 (m, 2H), 3.88-3.85 (m, 2H), 3.75-3.56 (m, 4H), 2.70 (m, 1H), 2.34 (m, 1H), 2.20 (s, 3H), 1.87-1.53 (m, 4H), 1.26 (t, J= 7.2 Hz, 2H); ¹³C NMR (100 MHz, CD₃OD) δ 175.5, 172.6, 170.5, 170.0, 168.5, 147.1, 146.4, 128.6, 128.1, 122.4, 115.3, 107.2, 71.8, 70.8, 70.3, 68.6, 61.6, 60.5, 49.8, 42.3, 39.7, 33.2, 29.3, 24.8, 11.3, 14.0. LC-ESI-MS: 1.6 min, $[M+H]^+$ =603. HRMS (ESI) $[M+1]$ calcd for C₂₈H₃₉N₆O₉ 603.2779 found 603.2782.

5.4.3 Cell culture

SK-MEL-24 cells (expressing $\alpha_v\beta_3$ integrin) were routinely grown in MEM supplemented with 10% FBS (Fetal Bovine Serum), nonessential amino acids, and sodium pyruvate. K-562 cells (expressing $\alpha_5\beta_1$ in-

tegrin) and Jurkat cells (expressing $\alpha_4\beta_1$ and $\alpha_L\beta_2$ integrins) were maintained as a stationary suspension culture in RPMI-1640 and L-glutamine with 10% FBS. RPMI8866 cell line (expressing $\alpha_4\beta_7$ integrin; a kind gift of Prof. Santoni Angela (Dept. of Molecular Medicine, "Sapienza" University of Rome) were grown in RPMI 1640 with 10% FBS, enriched with Hepes 5 mM and sodium pyruvate 0,5 mM. Cells were kept at 37°C in a 5% CO₂ humidified atmosphere. Forty hours before the experiment, K-562 cells were treated with 25 ng/mL PMA to induce differentiation with an increased level of expression of cell surface antigens.

5.4.4 Cell Adhesion assay

Assays on $\alpha_4\beta_1$ and $\alpha_4\beta_7$: Plates (96 wells) (Corning, New York, NY) were coated by passive adsorption with integrin ligands: fibronectin (10 $\mu\text{g/mL}$), VCAM-1 (2 $\mu\text{g/mL}$), ICAM-1 (2 $\mu\text{g/mL}$), MadCam-1 (2 $\mu\text{g/mL}$) overnight at 4°C. Jurkat cells were seeded onto 96-well plates coated with different substrata and allowed to adhere before quantitation of the number of adherent cells, in the presence of increasing concentrations of the compounds. In particular, the assays tests were performed on wells precoated with VCAM-1 and preincubating Jurkat cells with the ligand at 37°C for 30 min to reach equilibrium before being plated. Non-specific binding sites were blocked by incubation with a BSA (1%)/HBSS (w/v) solution for 30 minutes at 37°C. The efficacy of putative antagonists (at least seven different concentrations) was determined by the reduction in adherent cells compared to the untreated control. Each experiment was conducted in quadruplicate and the data are presented as the mean \pm S.E.M. of at least three independent assays. Under these conditions, no significant cell adhesion was observed for BSA-coated plates (negative control) or nonspecific substrate-coated plates (poly-l-lysine). BIO1211 was used as reference compound, inhibiting

the adhesion with an IC_{50} of 7.6 nM. Adhesion assay with RPMI8866 cells was performed as with Jurkat cells. For the other cell lines, adhesion assay was performed as previously described. Briefly, cells were counted and exposed to seven different concentrations of each compound for 30 min at room temperature to allow the ligand-receptor equilibrium to be reached. At the end of the incubation, cells were plated and incubated at room temperature for 1 h. Then, all the wells were washed with 1% BSA in PBS to remove nonspecifically adherent cells, and 50 μ L of hexosaminidase [4-nitrophenylN-acetyl- β -D-glucosaminide 7.5 mM in 0.09 M citrate buffer solution (pH 5) and mixed with an equal volume of 0.5% Triton X-100 in water was added in each well. The reaction was blocked by addition of 100 μ L of a stopping solution [50 μ M glycine and 5 μ M EDTA (pH 10.4)], and the plates were read in a Victor2 Multilabel Counter (Perkin-Elmer, Waltham, MA). Experiments were conducted in quadruplicate and were repeated at least three times. Data analysis and IC_{50} values were calculated using Graph-Pad Prism 5.0 (GraphPad Software, San Diego, CA). **Assays on $\alpha_{4v}\beta_3$ and $\alpha_5\beta_1$:** Plates (96 wells) (Corning Costar, Celbio, Milan, Italy) were coated by passive adsorption with fibronectin (10 μ g/mL) or poly-L-lysine (0.002 %) (Sigma-Aldrich SRL) overnight at 4°C. Cells were counted with a hemacytometer and pre-incubated with different concentrations of each compound for 30 min at room temperature to reach a ligand-receptor equilibrium. Stock solutions (10-2 M) of the assayed compounds were prepared in phosphate-buffered saline (PBS)/DMSO. At the end of the incubation time, the cells were plated (50000 cells/well) and incubated at room temperature for 1 h. Then, all the wells were washed with PBS to remove nonadherent cells, and 50 μ L of hexosaminidase [4-nitrophenylN-acetyl- β -D-glucosaminide dissolved at a concentration of 7.5 mM in 0.09 M citrate buffer solution (pH 5) and mixed with an equal volume of 0.5% Triton X-100 in water] was added. This product is a chromogenic substrate for

β -N-acetylglucosaminidase that is transformed in 4-nitrophenol whose absorbance can be measured at 405 nm. There is a linear correlation between absorbance and enzymatic activity. Therefore, it is possible to identify the number of adherent cells among treated wells, interpolating the absorbance values of unknowns in a calibration curve. The reaction was blocked by addition of 100 μ L of a stopping solution [50 μ M glycine and 5 μ M EDTA (pH 10.4)], and the plates were read in a Victor2 Multi-label Counter (Perkin-Elmer, Waltham, MA). Experiments were carried out in quadruplicate and repeated at least three times. Data analysis and IC50 or EC50 values were calculated using Graph-Pad Prism 5.0 (Graph-Pad Software, San Diego, CA).

5.4.5 Western blotting

Analysis on $\alpha_4\beta_1$ and $\alpha_4\beta_7$: Total protein fractions were obtained using the commercial T-PER Tissue Protein Extraction Reagent (Pierce): lysis and resuspension buffer contained a mixture of protease inhibitors composed of 0,5 mg/mL Benzamidine, 2 μ g/mL Aprotinin, 2 μ g/mL Leupeptin, 2 mM phenylmethysulfonyl fluoride, and a cocktail of phosphatase inhibitors 100x (Sigma). Briefly, T-PER Reagent was added to each sample to permit lysis. After 10 minutes of gently agitation at 4 $\hat{\text{A}}^\circ\text{C}$, samples were centrifuged at 10,000 g for 10 minutes to collect supernatants. Sodium dodecyl sulfate-polyacrylamide gel electrophoresis (SDS-PAGE) and Western blotting were performed according to standard procedures: proteins from the total extract (100 μ g) were separated by SDS-PAGE (12%). Proteins were transferred onto a Hybond-ECL nitrocellulose membrane (GE Healthcare); membranes were blocked with 5% non-fat milk in TBS 1X (10mM Tris-HCl, pH 8, containing 150mM NaCl) plus 0,1% Tween-20 for 1 hour at room temperature for phosphorylated ERK1/2 (pERK1/2), and with TBS 1X plus 1% BSA at 37 $^\circ\text{C}$ for

total ERK1/2 (tERK1/2), both for 1 hour incubation in gentle agitation. Then, membranes were incubated overnight at 4°C with specific primary antibodies (pERK1/2: 1:1000 dilution, Cell Signaling; tERK1/2: 1:5000 dilution, Promega). All the membranes were incubated with peroxidase-conjugated secondary antibodies at a dilution of 1:8000 (goat anti-Rabbit HRP conjugated IgG; Santa Cruz), for 1,5 hours at room temperature. Detection of immunoreactive bands was done by the enhanced chemiluminescent method (Immobilon Western Chemiluminescent HRP Substrate - Millipore) and a LAS3000 acquisition camera (Fujifilm, Tokyo, Japan). The bands were quantified with AIDA software. All data are presented as mean \pm SEM from three independent experiments. Statistical significance was determined by Newman-Keuls test after ANOVA using (GraphPad Software Inc., San Diego, CA, USA). P-values <0.05 were considered to be significant.

Analysis on $\alpha_4\beta_1$ and $\alpha_4\beta_7$: K562 cells were incubated in RPMI-1640 with 1% FBS for 16 h. Plates were coated with 10 $\mu\text{g}/\text{ml}$ of fibronectin and blocked with 1% BSA (Sigma-Aldrich SRL). Subsequently, 4×10^6 cells were pre-incubated with different compounds for 30 minutes. Cells were allowed to adhere for 1 hour on fibronectin in RPMI-1640 with 1% FBS. Then, the cells were lysed in M-PER Mammalian Protein Extraction Reagent; (M-PER Pierce, Rockford, IL, USA) supplemented with phosphatase inhibitor (Sigma-Aldrich SRL) for 10 min at 4°C by gently shaking. Cell debris were removed by centrifugation (14,000 \times g for 15 minutes at 4°C) and protein concentrations were estimated by BCA assay (Pierce, Rockford, IL, USA). Protein extracts (100 μg) were denatured at 95°C for 3 min before being loaded and separated in 12% SDS-PAGE gels. The membranes were blocked in 1% BSA and incubated for 2 hours with anti-phospho-ERK 1/2 (extracellular signal-regulated kinase 1/2) (1:2500) or anti-total ERK 1/2 antibodies (1:5000) (Promega, Madison, WI, USA) and, thereafter with

anti-rabbit peroxidase-conjugated secondary antibody. Digital images were acquired and analyzed following previously reported methods.

5.4.6 Compounds (*R*)-98a and (*R*)-98b antagonize VCAM-1-induced ERK1/2 phosphorylation

As regards to compounds (*R*)-98a and (*R*)-98b, a separate set of experiments ($n = 3$) was conducted in Jurkat cells exposed to 5 different concentrations of these antagonists (10^{-6} to 10^{-10} M) in the presence of VCAM-1 ($2 \hat{1}\frac{1}{4}$ μ g/ml), as previously described. Cells extracts were evaluated in western blotting experiments to quantify phosphorylated as well as total ERK1/2 levels (data not shown). After densitometric analysis, the IC_{50} value was generated from concentration-response curve using GraphPad Prism software. The densitometric analysis is reported in Figure 5.22.

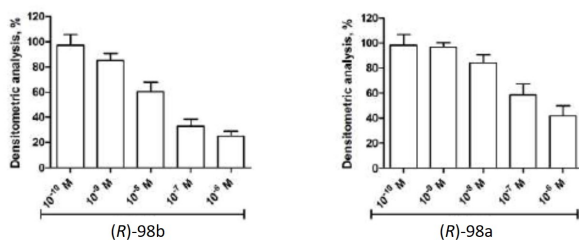


Figure 5.22: Pre-incubation with compounds (*R*)-98a and (*R*)-98b caused a significant, concentration-dependent decrease in the amount of pERK1/2 in Jurkat cells exposed to VCAM-1. Jurkat cells were serum-starved in RPMI-1640 containing 1% FBS for 16 h; cells were then pre-incubated with compound (*R*)-98a or (*R*)-98b for 60 min in suspension and then with VCAM-1 (2μ g/ml) for 60 min. Cells were lysed and analyzed by Western blot to detect phosphorylated ERK1/2 (pERK1/2) or total ERK1/2 (tERK1/2). Densitometric analysis of the bands (mean \pm SEM; $n=3$); the amount of pERK1/2 is normalized to the tERK1/2. IC_{50} values (concentration of ligand causing 50% reduction of pERK1/2 induced by VCAM-1) were (*R*)-98b 10 nM and (*R*)-98a 131 nM.

5.4.7 Confocal laser scanning microscopy

HEK293 cells (not expressing α_5 but endogenously expressing β_1 integrin) were plated in 6 well plates and at 50-60% confluence were transiently transfected with α_5 -enhanced green fluorescent protein (EGFP) plasmid using Lipofectamine2000 transfection reagent (LifeTechnologies). After 48 h from transfection, HEK293+ α_5 -EGFP cells were assessed to verify integrins expression by flow cytometry (data not shown). α_5 -EGFP integrin plasmid was a kind gift from Michael Davidson (Addgene plasmid #56423). HEK293+ α_5 -EGFP cells were treated at 4°C with fibronectin (10 μ g/ml) or the agonist 217 (1 μ M) in MEM for 1 hour. Cells exposed to the antagonist 107 (1 μ M), before the addition of fibronectin, were pre-incubated with the compound for 20 minutes at 4°C. After 1 hour incubation, cells were moved to 37°C for 15 minutes. Then, the cells were washed twice with PBS and fixed with paraformaldehyde (3% in PBS, pH 7.4, 10 min). Thereafter, the cover slips were washed twice with 0.1 M glycine in PBS and twice with 1% BSA (bovine serum albumin) in PBS. Specimens were embedded in Mowiol and analysed and imaged using a Nikon C1s confocal laser-scanning microscope, equipped with a Nikon PlanApo 60X, 1.4-NA oil immersion lens.

5.5 Notes and references

The spectroscopic data and the synthetic procedures have been adapted from Ref.[76], with the proper reuse license. See Appendix. These studies have been carried out with the contribution of MIUR (PRIN project 2010 NRREPL: Synthesis and biomedical applications of tumor-targeting peptidomimetics), "Fondazione del Monte di Bologna e Ravenna" and University of Bologna.

Chapter6

Synthesis of red-shifted fluorescent self-assembled nanoparticles as diagnostic tools

6.1 Introduction

In the last decades, great attention was paid to the development of tools resolving issues related to healthcare, focusing in particular on the research of new material and methods that allow to obtain early diagnosis of diseases by the employment of easy and cheap strategies. The combination of studies on the synthesis, photochemical behaviour and biological applications of these new architectures led to the introduction in the field of medicinal chemistry of nanoparticles based on conjugated polymers as outstanding multifunctional nanostructures with promising applications as imaging agents and biosensors. The main utilities of these conjugated polymer nanoparticles (CPNs), making them desirable focus, are related to (i) the possibility to easily tune their properties in function of the desired application, (ii) the easy synthesis and (iii) the reduced toxicity if compared to the analogue inorganic nanoparticles employed for the same purposes. [158] In particular, fluorescent nanoparticles have been widely studied in the last years for application in bioimaging and

biosensors, since they are small size molecules whose fluorescent properties can be easily modulate by changing the functionalization of the core structures, making them versatile biomaterials. They combine the advantages of inorganic nanoparticles and fluorescent organic ones. Infact, with respect to the first, fluorescent CPNs overcome the problems related to the toxicity of metals and inorganic components. As regard the second, commonly fluorescent organic nanoparticles were constructed starting from vesicles or micelles by incorporation of a fluorescent dye, with the possibility to modulate the affinity toward a specific biological target by chemical modification: with fluorescent CPNs these features are combined in an unique structure. [159] Among the fluorescent organic CPNs developed, the self-assembled ones are the most suitable for therapeutic applications, where the drug delivery is combined to the bioimaging. Infact, supramolecular architectures obtained by self-assembly are interesting since they can host ligands inside the self-assembled structures (like micelles and vesicles do) or they can delivery the payload through covalent linkage to the main backbone; furthermore, they have high extravasation in tumor vasculature and prolonged stability in systemic circulation. [160] [161] [162] The self-assembled nanoparticles can be obtained with, mainly, two methods known as miniemulsion and reprecipitation. In the first case, the polymer is dissolved in an organic solvent immiscible with water and injected in a aqueous solution containing a surfactant. The mixture was sonicated allowing the formation of miniemulsion with droplets of polymer solution. The removal of organic solvent by evaporation gives nanoparticles disperse in water, with size related to the concentration of the initial polymer solution. With reprecipitation method, the polymer is dissolved in a solvent that well dissolves it, like THF, and injected in a poor solvent, like water, miscible with the previous. This allows the formation of nanoparticles, obtained after removal of the organic solvent by evaporation (Figure 6.1).

In this case the driving force is the existence of hydrophobic effects between the polymer and the aqueous media: when it is added to water, the polymer chains try to reduce the interaction with the solvent and for this reason the resulting disposition to minimize the exposure to water is the folding in spherical shapes. In this case, no additives or surfactants are required and it is possible to choose different solvents to obtain the desired result. The size of the nanoparticles depends on the concentration of polymer solution and on the polymer molecular weight. [158] Fluorescent polymer-based π -conjugated nanoparticles (PDots) are par-

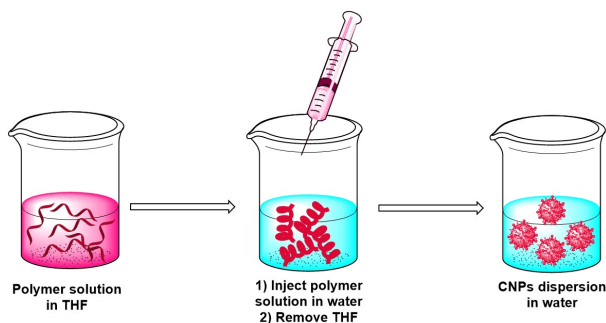


Figure 6.1: Preparation of polymer nanoparticles by reprecipitation method.

ticularly interesting since their photochemical stability, fluorescence and chemical manipulation make them good candidates to develop cellular imaging probes. Several examples are reported in literature of PDots with high photostability and absorption, together with quantum yield up to 40%. But **self-assembled oligomer-based π -conjugated fluorescent nanoparticles** represent a further improvement since they keep the advantage of quantum dots and PDots of incorporation of building blocks in the nanoparticle, allowing at the same time perfect control on the structure and function of the resulting probe. [163] The presence of aromatic moieties enhances the stability in water during the self-assembly due to

π - π interactions and hydrophobic effects. Considering the hydrophobicity of π -conjugated core, hydrophilic side chain can be introduced in order to obtain amphiphilic properties and self-assembly in water. The self-assembled π -conjugated fluorescent nanoparticles employed in bioimaging are mainly based on perylene or fluorene moieties. [164] In this study, the attention was paid on the second one.

6.1.1 Nanoparticles based on fluorene oligomers

The fluorene unit is made up two benzene connected directly by a carbon-carbon bond and a methylene bridge. Its application in fluorescent studies is due to its high quantum yield, photostability and good solubility in the most common organic solvents. [165] By attachment of hydrophilic side chain it is possible to modulate its solubility properties making it more soluble in aqueous media. Examples were reported by Yang [166] and Tagawa [167] who reported oligofluorene moieties functionalized with substituted aniline and alkylic or ethylene glycole chains, respectively (Figure 6.2). In the first case, red-shifted emission

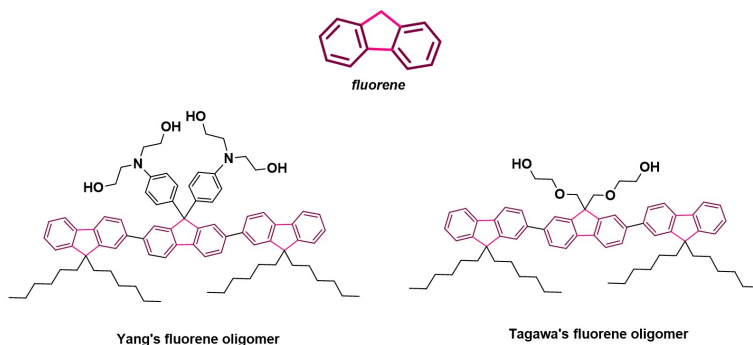


Figure 6.2: Structures of Yang's and Tagawa's fluorene based oligomer.

peak observed in THF moved with ipsocromic-shift when the oligomers

self-assembly in water. In the second, the blue emission in THF left place to a green peak in water. These results prove that the assembly together with the influence of side-chains are responsible for the photochemical properties of the resulting nanostructure. The extension of π -conjugation was reported by Shenning et al. [168] who synthesized fluorene based oligomer in which the two fluorene units were connected by a central aromatic moiety like naphthalene (A, Figure 6.3), quinoxaline (B, Figure 6.3), benzothiadiazole (C, Figure 6.3) and thienopyrazine (D, Figure 6.3) in order to obtain different emission wavelengths. These oligomers were used for the synthesis of bola-amphiphilic nanoparticles, with hydrophilic groups at both ends of the hydrophobic central core: they generate bola-amphiphilic oligomers able to cover all the visible spectra, with also white emission obtained by mixing them. Since the

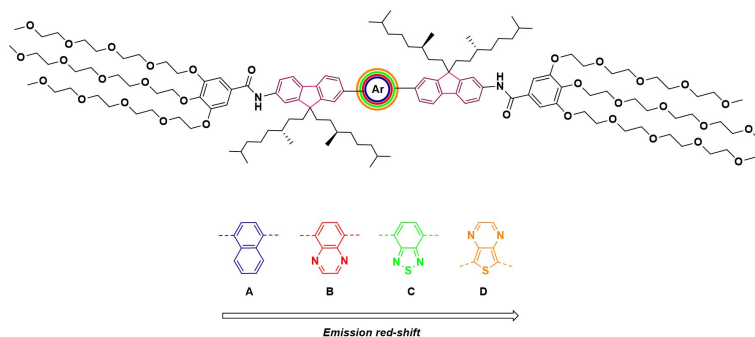


Figure 6.3: Structures of Shenning's bola-amphiphilic fluorene-based oligomers.

resulting nanostructure depends significantly on the structure of the constituent oligomer, several studies are reported in which changes in the side chains were performed in order to correlate them with the size and the shape of the nanoparticles. To this purpose, examples of all polar and all non polar side chains are reported and they revealed that all the fluorene-based oligomers well self-assembly in water, but those with polar side

chains are more dynamic and larger in size if compared with the non-polar ones (Figure 6.4). [169] In order to develop systems for delivery

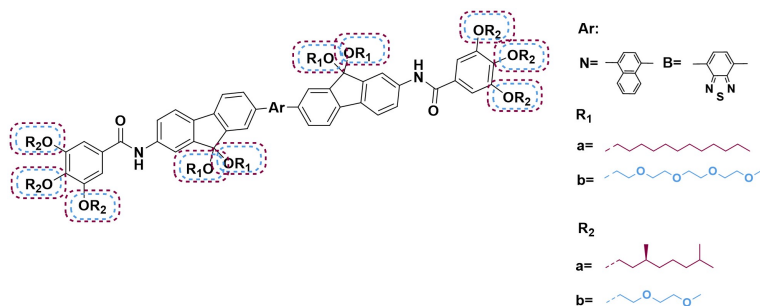


Figure 6.4: Structures of fluorene-based oligomer with polar or apolar side chains.

or probes, the fluorene-based oligomer have been widely functionalized, with azides or mannose attached to the periphery of the oligomer in order to guarantee exposure to aqueous media. The analysis on the shape and size of the resulting nanoparticles showed that these oligomers self-assembly in water giving nanoparticles with same size and optical properties of those without functionalization. So, the introduction of particular functional groups on the periphery of PEG-side chain does not affect the self-assembly that, for this reason, is clearly related to the oligomer central structure. The mannose-oligomer and the azide-oligomer functionalized with a proper ligand (in the second case by means of copper(I)-catalyzed azide-alkyne cycloaddition) not only kept the properties of the not-functionalized ones but, furthermore, expose the ligand at the periphery of the nanostructure (Figure 6.5). To develop nanoparticles red-emitting and able to encapsulate drugs, Tuncel et al. reported fluorene-based nanoparticles that emit in the red region tailing to infrared and can encapsulate drugs like Camptothecin. The oligomer was synthesized coupling divinyl fluorene and di bromobenzothiazole (Figure 6.6). The resulting nanoparticles were stable in water for a long time and can

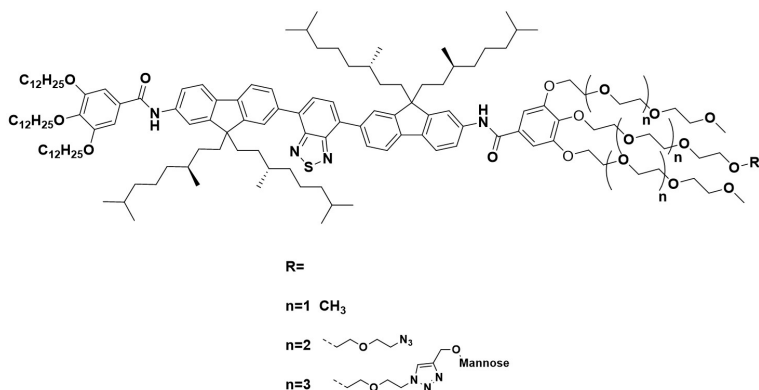


Figure 6.5: Structures of fluorene-based oligomer functionalized with azide or mannose.

carry Camptothecin; with a pH switch toward acidic values disassembly of the nanoparticles and release the drug were observed, as consequence of the repulsive force due to the formation of ammonium ions. [170] On the basis of these results, the aim of the work developed in the

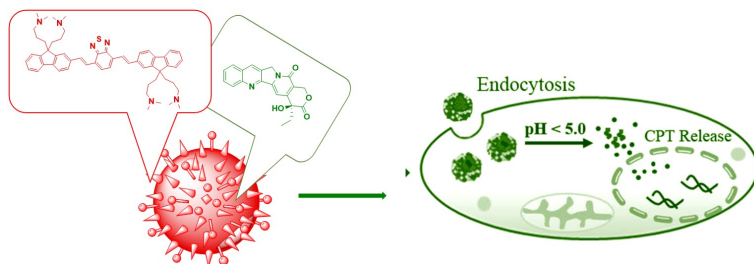


Figure 6.6: Structures of red-emitting fluorene-based oligomer, encapsulating Camptothecin.

prof. L. Brunsveld's research group has been the design, synthesis and optimization of fluorene-based oligomer nanoparticles obtained through Heck-coupling of mono-aminodivinyl fluorene and dibromo benzothio-diazole monomers, followed by functionalization of the amino moieties

with tris(dodeciloxy)benzoic acid (Figure 6.7). The photophysical behavior of these water dispersible nanoparticles was compared to that of molecular disperse solutions in THF and to that of analogue structures to evaluate the entity of the shift in emission and absorption in the region of red tailing to the near-infrared of the spectrum. Furthermore, each intermediate has been studied in order to understand which was the minimum structure that allows the formation of nanoparticles.

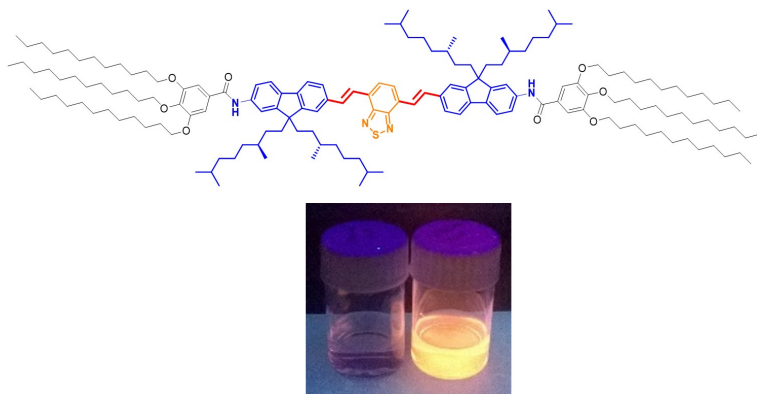


Figure 6.7: Structures of red-emitting fluorene-based oligomer and emission of its nanoparticles in water.

6.2 Results and discussions

6.2.1 Molecular design and synthesis

For the synthesis of the nanoparticles, the first step was the optimization of the synthesis of the oligomer **126** reported in Figure 6.8, the central core of the target structure.

For this purpose, two different pathways were tried according to the available starting materials (Figure 6.9). The first step, the Stille cou-

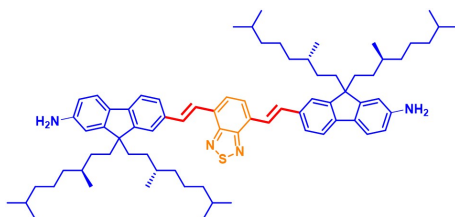
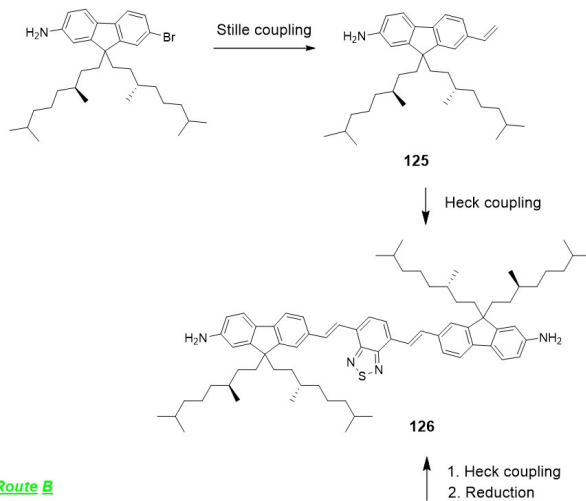


Figure 6.8: Structures of diamminic-fluorene core of the oligomer.

Route A



Route B

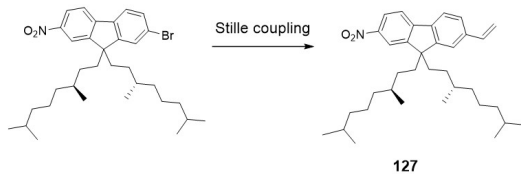


Figure 6.9: Two pathways for the synthesis of intermediate 126.

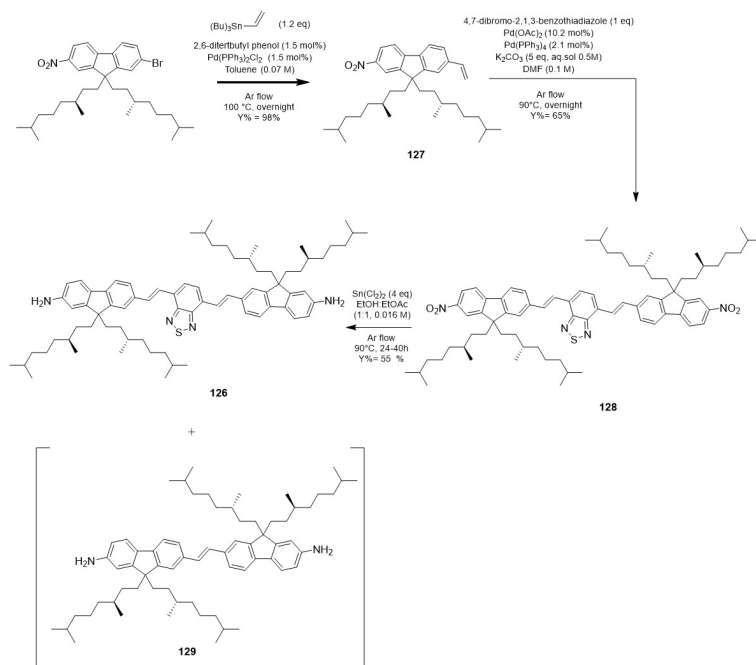


Figure 6.10: Synthesis of 126 starting from the nitro-compound.

pling, has been the most critic one since the conversion was not complete and the separation of the product from the starting material was difficult as consequence of similar polarity of them both the species. Furthermore, the not complete conversion at this stage implicates that in the subsequence step of coupling it is possible to recover the product of omocoupling as byproduct. In a first attempt, tributyl(vinyl)tin, 2,6-di-tert-butylphenol $\text{Pd}(\text{PPh}_3)_2\text{Cl}_2$ 1.5mol% in toluene were added to 7-bromo-9,9-bis((S)-3,7-dimethyloctyl)-9H-fluoren-2-amine but the conversion was around 66-85% as shown by NMR spectra. Increasing the reaction time and changing the Pd catalyst, choosing $\text{Pd}(\text{PPh}_3)_4$ 2mol%, none

considerable improvement was observed and the conversion was confirmed (80%). So, the same procedure with Pd(PPh₃)₂Cl₂, 2,6-di-tert-butylphenol and tributyl(vinyl)tin was used for the second route with 2-bromo-9,9-bis((S)-3,7-dimethyloctyl)-7-nitro-9H-fluorene giving in this case conversion of 98%. The subsequent steps were i) the Heck coupling, performed with 4,7-dibromobenzo[c][1,2,5]thiadiazole, Pd(PPh₃)₄ as catalyst and Pd(OAc)₂ as co-catalyst in toluene, with yield of **128** of 65%, and ii) the reduction of nitro-groups with SnCl₂ in a mixture of EtOH : EtOAc at 90°C for 40h, with yield of **126** of 55% (Figure 6.10). During one of the trials performed, it was possible to isolate a small amount (less than 5%) of byproduct **129** that has been however characterized in its photophysical properties. The intermediate **126** was then mono-acylated with 0.7 eq of tris(dodecyloxy)benzoic chloride, generated in situ starting from the corresponding acid, to obtain with 61% yield the intermediate **130** that was acylated again with excess of chloride giving the final **131** with 50% yield (Figure 6.11).

6.2.2 Formation and characterization of self-assembled nanoparticles

For the preparation of nanoparticles of the final product **131** and of the intermediates **126**, **127**, **128**, **129** and **130**, a mother solution of each compound in THF (1 mmol/mL) was prepared. 15 μL of mother solution were injected into 5 mL of deionized water in one-pot. Then the nanoparticles were characterized by DLS obtaining the data reported in Figures 6.12, 6.13, 6.14. As shown, the smallest nanoparticles have been obtained with intermediate **126** with a radius of 21 nm. The corresponding nitro-compound **128** gives, instead, bigger nanoparticles with radius of 36 nm, maybe due to different interactions of nitro groups with the water compared to amino groups. By adding functionalizations to intermediate **126**, the dimension of the resulting nanoparticles increases to 59

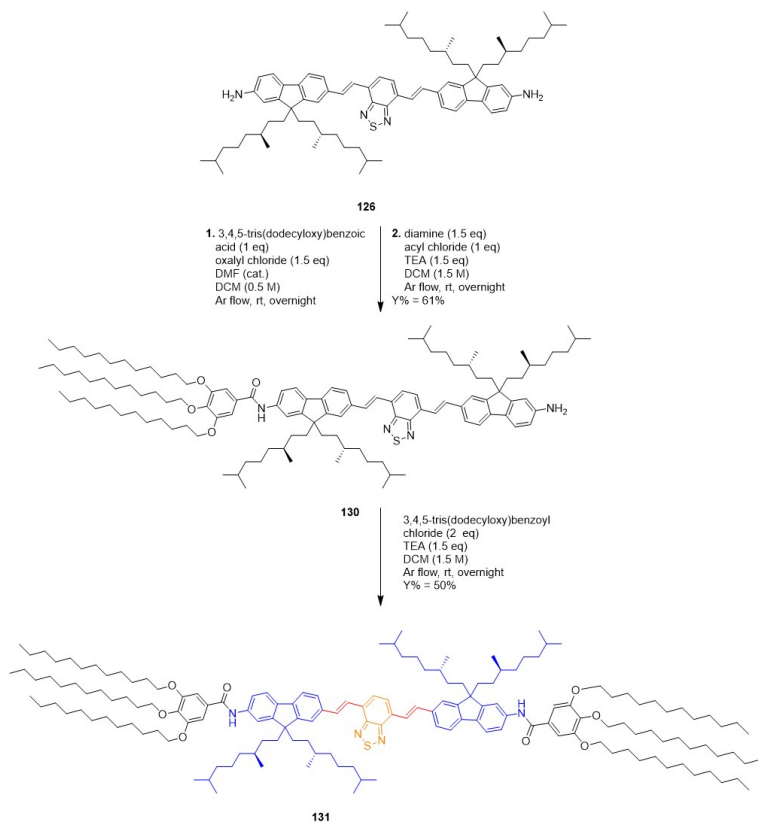


Figure 6.11: Synthesis of 131 starting from 126.

nm, for the mono-acylated **130**, and 71 nm, for final product **131**.

The optical properties of the molecules in THF and the corresponding nanoparticle dispersion in water were studied by UV-visible and fluorescence spectroscopy (Figure 6.15-6.20) and tabulated in Table 6.1.

UV-vis absorption wavelengths of aforementioned intermediates and of the final product in THF exhibit a blue-shift compared to the solu-

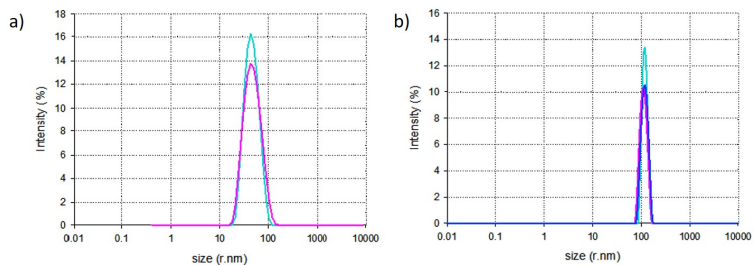


Figure 6.12: DLS measurement of 126 (a) and 127 (b).

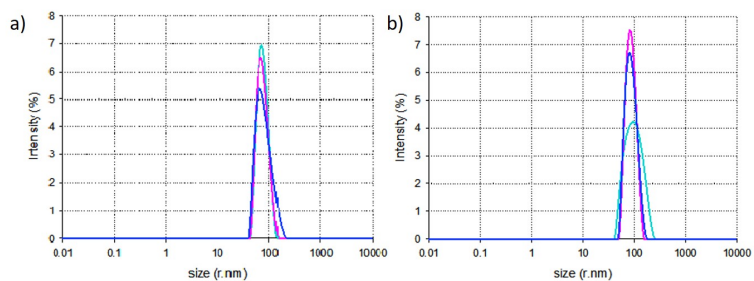


Figure 6.13: DLS measurement of 128 (a) and 129 (b).

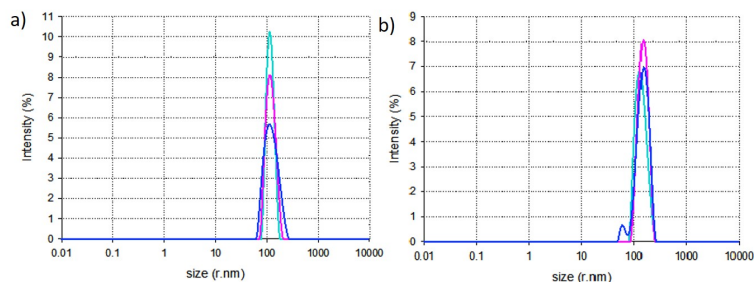


Figure 6.14: DLS measurement of 130 (a) and 131 (b).

Table 6.1: Summary of abs/em values.

Compound	UV-vis absorption		Photoluminescence	
	λ_{max}/nm ($\log(\epsilon)/M_{-1}cm_{-1}$)		λ_{max}/nm	
	water	THF	water	THF
127	342 (4.02)	346 (4.42)	-	-
128	316 (4.37)	316 (4.40)	575	556
	347 (4.42)	399 (4.54)	575	556
126	370 (4.50)	376 (4.85)	(415,) 449, 618	465, 652
	503 (4.34)	517 (4.78)	(415,) 449, 618	465, 652
129	388 (4.51)	393 (4.72)	424	478
130	367 (4.18)	372 (4.40)	635	593
	492 (4.00)	500 (4.31)	635	593
131	365 (4.57)	370 (4.57)	618	594
	490 (4.37)	495 (4.37)	618	594

tions of the same molecules in water. Moreover, excluding intermediate **129** that is not in the serie of the other compounds, it is possible to observe a red-shift increasing the polarity from **127** via **128** to **126**. The mono-acylation and the di-acylation give reduction in polarity and so a blue-shift is observed compared to the previous intermediates: it is less important for the first peak (transition between orbitals of dibenzofulvene), about 2-4 nm, but became a little bit more significative for the second peak (transition between orbitals of double-bond and dibenzofulvene), about 10-17 nm, mostly for the first acylation. The fluorescence spectra show a red-shift of the solution in water increasing the polarity from **128** via **126** to **130**, while the trend is not rationalizable for the same solutions in THF or going from THF to water for each compound. Of great interest is the red-shift of the nanoparticles of intermediate **130** and of the final product in water compared to the results of the same compounds in organic solvent. As regards intermediate **127**, it does not emit

with fluorescence, while intermediate **129**, lacking of benzothiadiazole, emits in the blue region. The changes in the optical properties can be explained by both inter- and intrachain interaction, as well as the solvent polarity.

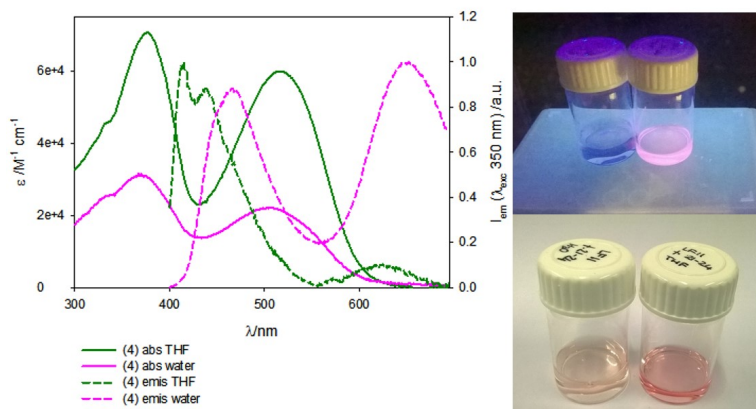


Figure 6.15: Absorption and emission of **126**.

To evaluate if the aim of the project has been reached, the results have been compared with those obtained for analogue structures already reported in literature. Considering the dimensions of nanoparticles, the intermediates **128** and **126** have been compared with the structures **132** and **133**, reported respectively by Pennakalathil et al. [170] and Shenning et al. [171]. The first has been chosen because it has the same building core of the new synthesized ones (dibenzofulvene conjugated through double bond with benzothiadiazole), while the second because it is the smallest nanoparticle synthesized previously in the same research group (Figure 6.21). The intermediate **128** and **126** give nanoparticles smaller than those obtained with the aforereported structures. It is maybe due to the repulsion of the apolar tails for the polar environment. The dimensions of

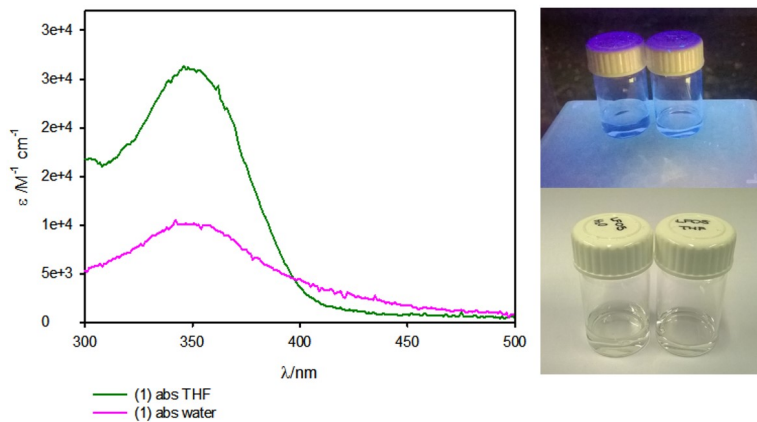


Figure 6.16: Absorption and emission of 127.

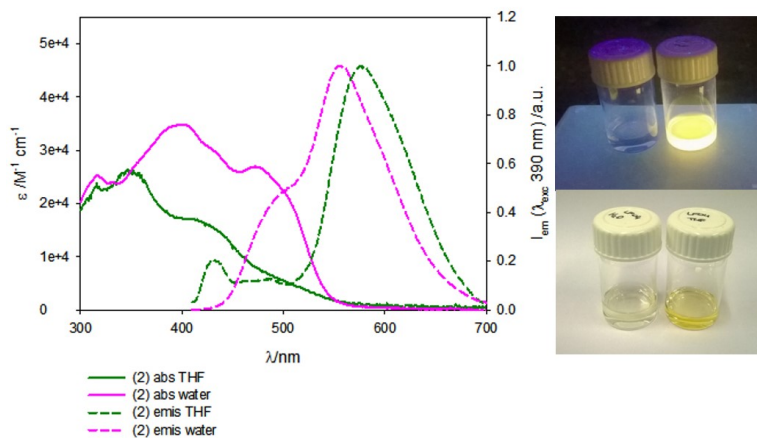


Figure 6.17: Absorption and emission of 128.

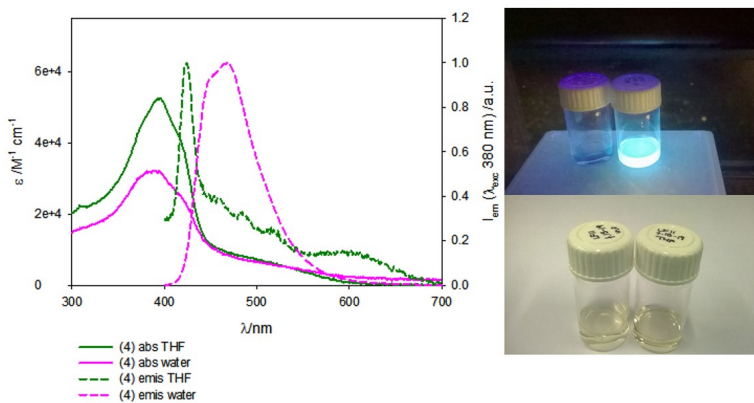


Figure 6.18: Absorption and emission of 129.

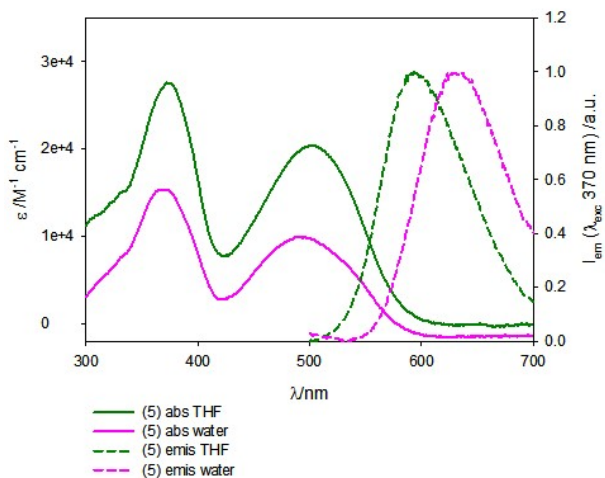


Figure 6.19: Absorption and emission of 130.

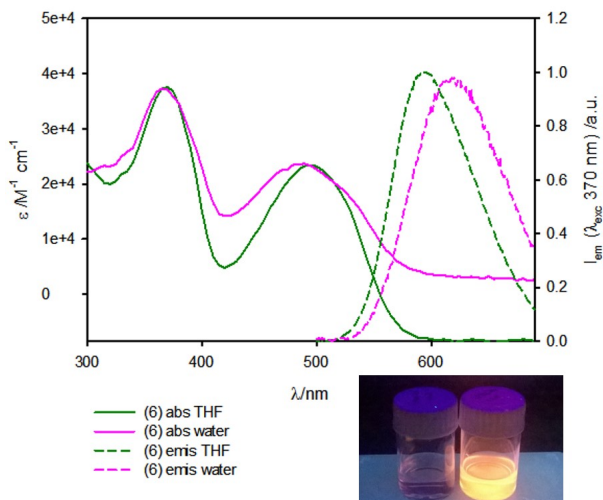


Figure 6.20: Absorption and emission of 131.

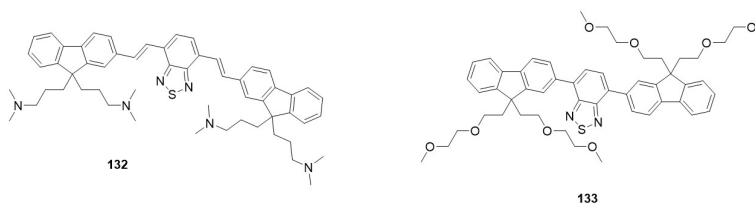


Figure 6.21: Structures of reference compounds 132 and 133.

nanoparticles of intermediate **130** and of the final product **131** have been compared to Apolar-B e Bola1-B (Figure 6.22), reported by Shenning et al. [172]. The comparison shows clearly how the introduction of the double bond between dibenzofulvene e benzothiodiazole does not affect considerably the dimension of the resulting nanoparticles. Considering the UV-vis and fluorescence data obtained for the new compounds, they

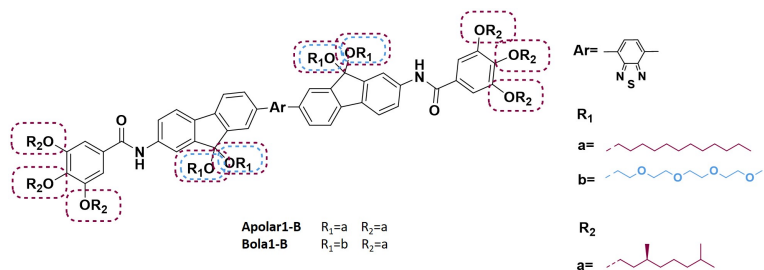


Figure 6.22: Structures of reference compounds Apolar-B and Bola1-B.

have been compared with the same structures aforementioned. So, intermediate **126** ($\lambda_{abs,126}=503_{water}$, $517_{THF}/\lambda_{em,126}=618_{water}$, 652_{THF}) is red-shifted in absorption and emission, in water and THF, if compared to reference **132** ($\lambda_{abs,132}=455_{water}$, $466_{THF}/\lambda_{em,132}=615_{water}$, 605_{THF}) and **133** ($\lambda_{abs,133}=427_{water}$, $415_{THF}/\lambda_{em,133}=522_{water}$, 533_{THF}), while intermediate **128** ($\lambda_{abs,128}=348_{water}$, $399_{THF}/\lambda_{em,128}=575_{water}$, 556_{THF}) is blue-shifted in absorption and in emission, in water and THF, if compared to reference **132**, and it is blue-shifted in absorption but red-shifted in emission if compared to reference **133**. Intermediate **130** and the final product **131** are red-shifted in absorption and in emission, in water, if compared to Apolar-B ($\lambda_{abs,apolar-B}=431_{water}/\lambda_{em,apolar-B}=527_{water}$) and Bola1-B ($\lambda_{abs,bola1-B}=429_{water}/\lambda_{em,bola1-B}=550_{water}$).

6.3 Conclusions

The optimization of a synthetic pathway for the synthesis of red-shifted self-assembled nanoparticles has been developed. The core structure is a fluorene unit properly functionalized for the scope. Each intermediate and the final product have been employed for the preparation of nanoparticles by reprecipitation method. The resulting nanostructures have been characterized in their dimensions and their photochemical pro-

erties. It results in a significant red-shifted emission, if they are compared with the analogue structures reported in literature. In particular, considering the dimension and the optical properties of the nanoparticles obtained from intermediate **126**, the next step will be the conjugation of it with the **RGD-mimetics** reported in Chapter 5. With this approach, it is possible to verify if and how the formation of nanoparticles can be affected by this modification. The resulting structure could be useful to deeply study how the RGD-mimetics interact with integrins in particular, and with cancer cells in general, to understand if it can be internalized by the cells. This is possible because of the optical properties in emission of intermediate **126**, that will act as cargo.

6.4 Experimental procedures

6.4.1 Synthesis and characterization

Synthesis of intermediate 127. In 2-necked round bottom flask, starting material (1 eq, 300 mg) and 2,6-ditertbutyl phenol (1.5 mol%) were added and dried under vacuum for 30 min. Degassed toluene (7.4 ml) and tributyl(vinyl)tin (1.2 eq) were added and the mixture was degassed, then Pd(PPh₃)₂Cl₂ (1.5 mol%) was added. The reaction was stirred at 100 °C overnight and the complete conversion followed by ¹H-NMR of the crude. The solvent was removed under reduced pressure and the crude was purified by flash chromatography (Silica gel 40-60 μm part. size, 95:5 to 8:2=cyclohexane:dichloromethane) to obtain the product(Y%=98%) as a yellow oil. ¹H NMR (400 MHz, CDCl₃) δ 8.25 (dd, J= 16, 4 Hz, 1H), 8.18 (d, J= 4 Hz, 1H), 7.76 (d, J= 16 Hz 1H), 7.73 (d, J= 16 Hz, 1H), 7.46 (dd, J= 16, 4 Hz,1H), 7.39 (s, 1H), 6.81 (dd, J= 2.8, 2 Hz, 1H), 5.85 (d, J= 36 Hz, 1H), 5.34 (d, J= 24 Hz, 1H), 2.03 (m, 4H), 1.39 (m, 4H), 0.95 (m, 12H), 0.78 (d, J= 12 Hz, 12H), 0.67

(d, J= 12 Hz, 6H), 0.61-0.25 (m, 4H). ^{13}C NMR (200 MHz, CDCl_3) δ 152.7, 152.1, 147.4, 147.0, 138.7, 138.5, 136.9, 125.7, 123.3, 121.3, 120.7, 119.7, 118.1, 114.6, 77.7, 77.0, 76.4, 55.4, 39.1, 37.4, 36.4, 32.7, 30.4, 27.9, 24.6, 24.5, 22.6, 22.5, 19.4. MALDI-ToF: 518 $[M + H]^+$

Synthesis of intermediate 128. In 2-necked round bottom flask, intermediate 127 (2.04 eq, 85 mg) and 4,7-dibromobenzo[c]-1,2,5- thiadiazole (1 eq) were added and dried under vacuum for 30 min. Degassed DMF (730 μl) and an aqueous solution of K_2CO_3 (5 eq in 731 μl) were added and the mixture was degassed, then $\text{Pd}(\text{PPh}_3)_4$ (2.1 mol%) and $\text{Pd}(\text{OAc})_2$ (10.2 mol%) were added. The reaction was stirred at 90 $^\circ\text{C}$ overnight. The solvent was removed under reduced pressure and the crude extracted with chloroform and purified by flash chromatography (Silica gel 40-60 μm part. size, 95:5 to 8:2=cyclohexane:ethyl ether) to obtain the product (Y%=98%) as an orange solid. ^1H NMR (400 MHz, CDCl_3) δ 8.28 (d, J= 4 Hz, 2H), 8.22 (s, 2H), 8.17 (d, J= 16 Hz, 2H), 8.11 (d, J= 8 Hz, 2H), 7.81 (m, 4H), 7.77 (s, 2H), 7.73 (d, J= 4 Hz, 2H), 7.64 (s, 2H), 2.11 (m, 8H), 1.41 (m, 4H), 1.17 (m, 4H), 1.05 (m, 20H), 0.90 (m, 4H), 0.77 (d, J= 8 Hz, 24H), 0.71 (d, J= 4 Hz, 12H), 0.54 (m, 8H). ^{13}C NMR (400 MHz, CDCl_3) δ 153.96, 153.01, 152.22, 147.31, 147.14, 139.04, 138.73, 133.60, 130.81, 129.45, 127.49, 126.41, 125.28, 123.45, 121.53, 119.85, 118.19, 55.61, 39.17, 37.51, 37.43, 36.57, 32.82, 30.53, 27.83, 24.60, 24.52, 24.46, 22.63, 22.40, 19.49. MALDI-ToF: 1166 $[M]^+$

Synthesis of intermediate 126. In 2-necked round bottom flask, intermediate 128 (1 eq, 40 mg) was dissolved in a 1:1=EtOAc:EtOH mixture (2.2 ml) and the mixture sparged with Ar for 10 min. SnCl_2 (16 eq) was added and the reaction was stirred at 90 $^\circ\text{C}$ overnight. The solvent was removed under reduced pressure and the crude poured in EtOAc and washed with NaOH 1M. The crude was purified by flash chromatography

(Silica gel 40-60 μm part. size, 95:5 to 8:2=hexane:EtOAc) to obtain the product (Y%=55%) as a red solid. ^1H NMR (400 MHz, CDCl_3) δ 8.08 (d, J= 12 Hz, 2H), 7.72 (s, 2H), 7.67 (d, J= 16 Hz, 2H), 7.58 (m, 4H), 7.53 (s, 2H), 7.49 (d, J= 8 Hz, 2H), 6.67 (s, 4H), 3.80 (bs, 4H), 1.97 (m, 8H), 1.43 (m, 4H), 1.11 (m, 24H), 0.90 (m, 4H), 0.78 (d, J= 8 Hz, 24 H), 0.70 (d, J= 4Hz, 12H), 0.54 (m, 8H). ^{13}C NMR (400 MHz, CDCl_3) δ 154.02, 153.07, 150.28, 146.19, 142.19, 134.81, 133.96, 132.19, 129.29, 126.58, 125.99, 122.76, 120.94, 120.65, 118.55, 114.02, 109.62, 54.62, 39.24, 39.22, 38.02, 37.89, 36.65, 36.60, 32.99, 32.96, 30.51, 30.45, 27.92, 24.68, 24.57, 22.70, 22.69, 22.59, 22.57, 19.55, 19.52. MALDI-ToF: 1106 $[M]^+$

Synthesis of intermediate 130. In 2-necked round bottom flask, tris(dodecyloxy)benzoic acid (1 eq) was dissolved in dry DCM (88 μl) and a catalytic amount of DMF (30 μl) and oxalyl chloride (1.5 eq) were added. The mixture was stirred at room temperature overnight in absence of light. After completion, the solvent was removed under vacuum and the crude added to a solution in dry DCM (200 μl) of intermediate 126 (1.5 eq) and TEA (1.5 eq). The mixture was stirred overnight. The solvent was removed under vacuum and the crude purified by flash chromatography (Silica gel 40-60 μm part. size, 99:1=cyclohexane:EtOAc) to obtain the product (Y%=61%) as a red solid. ^1H NMR (400 MHz, CDCl_3) δ 8.03 (m, 2H), 7.73 (s, 2H), 7.68 (m, 4H), 7.61 (m, 4H), 7.51 (m, 2H), 7.46 (m, 2H) 7.41 (m, 2H), 7.03 (s, 2H), 6.59 (s, 2H), 3.98 (m, 6H), 1.97 (m, 4H), 1.77 (m, 2H), 1.70 (m, 2H), 1.20 (m, 54H), 1.03 (m, 18H), 0.80 (t, J= 4 Hz, 9H), 0.69 (d, J= 4 Hz, 12H), 0.64 (d, J= 4 Hz, 6H), 0.48 (m, 4H). MALDI-ToF: 1106 $[M]^+$

Synthesis of final product 131. In 2-necked round bottom flask, tris(dodecyloxy)benzoic acid (1.5 eq) was dissolved in dry DCM (130

μl) and a catalytic amount of DMF (30 μl) and oxalyl chloride (2.25 eq) were added. The mixture was stirred at room temperature overnight in absence of light. After completion, the solvent was removed under vacuum and the crude added to a solution in dry DCM (400 μl) of intermediate 130 (1 eq) and TEA (1 eq., 3.6 μl). The mixture was stirred overnight. The solvent was removed under vacuum and the crude purified by flash chromatography (Silica gel 40-60 μm part. size, 98:2=cyclohexane:EtOAc) to obtain the product (Y%=50%) as a red solid. ^1H NMR (400 MHz, CDCl_3) δ 8.1 (m, 2H), 7.73-7.54 (m, 18H), 7.1 (s, 2H), 4.06 (m, 12H), 2.04 (m, 4H), 1.84 (m, 2H), 1.76 (m, 2H), 1.27 (m, 114H), 1.06 (m, 18H), 0.88 (t, J= 4 Hz, 18H), 0.76 (d, J= 4 Hz, 12H), 0.70 (d, J= 4 Hz, 6H), 0.54 (m, 4H). MALDI-ToF: 2421 $[M]^+$

6.4.2 Preparation of nanoparticles

The nanoparticles were prepared by injecting 15 μl of 1 mM THF solution in 5 ml of deionized water, which results in 3 μM nanoparticle solution.

6.4.3 Optical Characterization

UV-vis and PL measurements were performed on a Jasco V-650 spectrophotometer and Jasco FP-6500 spectrofluorometer, respectively. The optical density of the samples for fluorescence measurement was below 0.1. Solutions were measured in liquid cells with a 1 cm path length for UV-vis and fluorescence, at room temperature.

6.4.4 Dynamic Light Scattering

DLS experiments were performed on an Zetasizer Nano ZSP. The incident beam was produced by a HeNe laser operating at 633 nm. The intensity signal was sent to a digital correlator. The nanoparticles solutions were prepared via the reprecipitation method described before followed by a filtration via a 0.4 μm pore size cellulose filter to remove dust particles. The calculation of the particle size distribution for all nanoparticles was performed using CONTIN fits.

6.5 Notes and references

This work has been developed during the period abroad in Technische Universiteit of Eindhoven, in the research group of prof. Luc Brusveld who supervised this work together with dr. L.G. Milroy and ir. A.H.A.M. van Onzen.

Appendix

The reuse licenses for those published articles cited in this work, which required it, are reported below.

11/2/2017

Rightslink® by Copyright Clearance Center



RightsLink®

[Home](#)[Account Info](#)[Help](#)ACS Publications
Most Trusted. Most Cited. Most Read.**Title:**Dehydro- β -proline Containing
 α 4 β 1 Integrin Antagonists:
Stereochemical Recognition in
Ligand-Receptor Interplay**Author:**Alessandra Tolomelli, Monica
Baiula, Angelo Viola, et al**Publication:**

ACS Medicinal Chemistry Letters

Publisher:

American Chemical Society

Date:

Jun 1, 2015

Copyright © 2015, American Chemical Society

Logged in as:

Lucia Ferrazzano

[LOGOUT](#)**PERMISSION/LICENSE IS GRANTED FOR YOUR ORDER AT NO CHARGE**

This type of permission/license, instead of the standard Terms & Conditions, is sent to you because no fee is being charged for your order. Please note the following:

- Permission is granted for your request in both print and electronic formats, and translations.
- If figures and/or tables were requested, they may be adapted or used in part.
- Please print this page for your records and send a copy of it to your publisher/graduate school.
- Appropriate credit for the requested material should be given as follows: "Reprinted (adapted) with permission from (COMPLETE REFERENCE CITATION). Copyright (YEAR) American Chemical Society." Insert appropriate information in place of the capitalized words.
- One-time permission is granted only for the use specified in your request. No additional uses are granted (such as derivative works or other editions). For any other uses, please submit a new request.

[BACK](#)[CLOSE WINDOW](#)

Copyright © 2017 [Copyright Clearance Center, Inc.](#) All Rights Reserved. [Privacy statement](#). [Terms and Conditions](#). Comments? We would like to hear from you. E-mail us at customercare@copyright.com

11/2/2017

RightsLink Printable License

**JOHN WILEY AND SONS LICENSE
TERMS AND CONDITIONS**

Feb 11, 2017

This Agreement between Lucia Ferrazzano ("You") and John Wiley and Sons ("John Wiley and Sons") consists of your license details and the terms and conditions provided by John Wiley and Sons and Copyright Clearance Center.

License Number	4045981098339
License date	Feb 11, 2017
Licensed Content Publisher	John Wiley and Sons
Licensed Content Publication	European Journal of Organic Chemistry
Licensed Content Title	One-Pot Two-Step Microwave-Assisted Synthesis of Alkylidene Acetoacetamido Esters, Useful Intermediates for β -Dehydropeptides
Licensed Content Author	Angelo Viola, Lucia Ferrazzano, Roberto Greco, Lucia Cerisoli, Jonathan Caldi, Alessandra Tolomelli
Licensed Content Date	Jun 13, 2016
Licensed Content Pages	6
Type of use	Dissertation/Thesis
Requestor type	Author of this Wiley article
Format	Electronic
Portion	Full article
Will you be translating?	No
Title of your thesis / dissertation	FIVE-MEMBERED NITROGEN HETEROCYCLE DERIVATIVES AS CORE STRUCTURES FOR THE SYNTHESIS OF BIOACTIVE COMPOUNDS CLASSES.
Expected completion date	Apr 2017
Expected size (number of pages)	250
Requestor Location	Lucia Ferrazzano Via Selmi 2 Bologna, 40126 Italy Attn: Lucia Ferrazzano
Publisher Tax ID	EU826007151
Billing Type	Invoice
Billing Address	Lucia Ferrazzano Via Selmi 2 Bologna, Italy 40126 Attn: Lucia Ferrazzano
Total	0.00 EUR
Terms and Conditions	

TERMS AND CONDITIONS

This copyrighted material is owned by or exclusively licensed to John Wiley & Sons, Inc. or one of its group companies (each a "Wiley Company") or handled on behalf of a society with which a Wiley Company has exclusive publishing rights in relation to a particular work (collectively "WILEY"). By clicking "accept" in connection with completing this licensing

<https://s100.copyright.com/AppDispatchServlet>

1/5

Bibliography

- [1] A. D. McNaught and A. Wilkinson. *IUPAC. Compendium of Chemical Terminology*. 1997. [Ref: *Heterocyclic Compounds*. Online at <http://goldbook.iupac.org/H02798.html>. Last access 31-March-2017].
- [2] T. Eicher, S. Hauptmann, and A. Speicher. *In The Chemistry of Heterocycles: Structure, Reactions, Synthesis and Applications*. Wiley-VCH, 2012.
- [3] P. Martins, J. Jesus, S. Santos, L.R. Raposo, C. Roma-Rodrigues, P. Viana Baptista, and A.R. Fernandes. Heterocyclic anticancer compounds: Recent advances and the paradigm shift towards the use of nanomedicine's tool box. *Molecules*, 20:16852–16891, 2015.
- [4] A. Gomtsyan. Heterocycles in drugs and drug discovery. *Chemistry of Heterocyclic Compounds*, 48:7–10, 2012.
- [5] A.D. Abell. Heterocyclic-based peptidomimetics. *Letters in Peptide Science*, 8:267–272, 2002.
- [6] J. Vagner, H. Qu, and V.J. Hruby. Peptidomimetics, a synthetic tool of drug discovery. *Curr. Opin. Chem. Biol.*, 12:292–296, 2008.

- [7] R.B. Silverman. *Drug discovery design and development E7 peptidomimetics - Organic Chemistry of Drug Design and Drug Action*. Elsevier Academic Press, 2004.
- [8] M.A. Estiarte and D.H. Rich. *Peptidomimetics for Drug Design - Burger's Medicinal Chemistry and Drug Discovery*. Donald J. Abraham, 2003.
- [9] M.D. Fletcher and M.M. Campbell. Partially modified retro-inverso peptides: development, synthesis and conformational behavior. *Chem. Rev.*, 98:763–795, 1998.
- [10] G.A. Patani and E.J. LaVoie. Bioisosterism: a rational approach in drug design. *Chem. Rev.*, 96:3147–3176, 1996.
- [11] I. Langmir. Isomorphism, isosterism and covalence. *J. Am. Chem. Soc.*, 41:1543–1559, 1919.
- [12] H.L. Friedman. Influence of isosteric replacements upon biological activity. *NASNRS*, 206:295–358, 1951.
- [13] A. Burger. Isosterism and bioisosterism in drug design. *Prog. Drug Res.*, 37:287–371, 1991.
- [14] A. Burger. *Medicinal Chemistry*. Wiley-Interscience, 1970.
- [15] V.Y. Dudkin. Bioisosteric equivalence of five-membered heterocycles. *Chemistry of heterocyclic compounds*, 48:27–32, 2012.
- [16] A. Gomtsyan. Heterocycles in drugs and drug discovery. *Chemistry of heterocyclic compounds*, 48:7–10, 2012.
- [17] K.E. Andersen, A.S. Jorgensen, and C. Braestrup. Oxadiazoles as bioisosteric transformations of carboxylic functionalities. part i. *Eur. J. Med. Chem.*, 29:393–399, 1994.

- [18] B.H. Kim, Y.J. Chung, G. Keum, J. Kim, and K. Kim. A new peptide bond surrogate: 2-isoxazoline in pseudodipeptide chemistry. *Tetrahedron Lett.*, 33:6811–6814, 1992.
- [19] C.F.R. Jones and G.J. Ward. Amide bond isosteres: imidazolines in pseudopeptide chemistry. *Tetrahedron Lett.*, 29:3853–3856, 1988.
- [20] E. Knoevenagel. *Chem. Ber.*, 27:2346, 1894.
- [21] M.J. Astle and J.A. Zaslowsky. Reactions catalyzed by anion exchange resins. *Ind. Eng. Chem.*, 44:2867, 1952.
- [22] G.A. Strohmeier and C.O. Kappe. Rapid parallel synthesis of polymer-bound enones utilizing microwave-assisted solid-phase chemistry. *J. Comb. Chem.*, 4:154–161, 2002.
- [23] J. S. Yadav, B. V. S. Reddy, A. K. Basak, B. Visali, A. V. Narsaiah, and K. Nagaiah. Phosphane-catalyzed knoevenagel condensation: A facile synthesis of α -cyanoacrylates and α -cyanoacrylonitriles. *Eur. J. Org. Chem.*, 3:546–551, 2004.
- [24] C. Su, Z.-C. Chen, and Q.-G. Zheng. Organic reactions in ionic liquids: Knoevenagel condensation catalyzed by ethylenediammonium diacetate. *Synthesis*, 4:555–559, 2003.
- [25] *Knoevenagel Condensation*, pages 1621–1626. Wiley, 2010.
- [26] G. Jones. *The Knoevenagel Condensation*, pages 204–599. Wiley and Sons Inc., 2004.
- [27] *Green Chemistry - Aspects for the Knoevenagel Reaction. Green Chemistry - Environmentally Benign Approaches*, pages 13–32. Intech, 2012.

- [28] K. Alfonsi, J. Colberg, P.J. Dunn, T. Feving, S. Jennings, T.A. Jhonson, H.P. Kleine, C. Knight, M.A. Nagy, D.A. Perry, and M. Stefaniak. Green chemistry tools to influence a medicinal chemistry and research chemistry based organisation. *Green Chem.*, 10:31–36, 2008.
- [29] G. Cardillo, S. Fabbroni, L. Gentilucci, M. Gianotti, and A. Tolomelli. Green chemistry tools to influence a medicinal chemistry and research chemistry based organisation. *Syn. Commun.*, 33:1587–1594, 2003.
- [30] H.S. Pawar, A.S. Wagh, and A.M. Lali. Triethylamine: a potential n-base surrogate for pyridine in knoevenagel condensation of aromatic aldehydes and malonic acid. *New J. Chem.*, 40:4962–4968, 2016.
- [31] W. Lehnert. Verbesserte variante der knoevenagel-kondensation mit $\text{TiCl}_4/\text{thf}/\text{pyridin}$ (i). alkyli- und arylidenmalonester bei 0 - 25 °C. *Tetrahedron Lett.*, 54:4723–4724, 1970.
- [32] W. Lehnert. Knoevenagel-kondensationen mit $\text{TiCl}_4/\text{base}$ - iii. umsetzungen von ketonen und α -halogenketonen mit malonester. *Tetrahedron*, 29:635–638, 1973.
- [33] W. Lehnert. Knoevenagel-kondensationen mit $\text{TiCl}_4/\text{base}$ -ii. alkyli- und arylidenacet - bzw. -nitroessigester bei 0-22°C. *Tetrahedron*, 28:663–666, 1972.
- [34] H.S. Pawar, A.S. Wagh, and A.M. Lali. Knoevenagel kondensationen mit $\text{TiCl}_4/\text{base}$ -iv. umsetzungen von aldehyden und ketonen mit phosphonoessigester und methyldiphosphonsaureestern. *Tetrahedron*, 30:301–305, 1974.

- [35] M.T. Reetz, R. Peter, and M. von Itzstein. Titanium-mediated stereoselective knoevenagel condensation of ethyl (diethoxyphosphoryl)acetate with aldehydes. *Chem. Ber.*, 120:121–122, 1987.
- [36] A. Renzetti, E. Dardennes, A. Fontana, P. de Maria, J. Sapi, and S. Gerard. $\text{TiCl}_4/\text{Et}_3\text{N}$ -promoted three-component condensation between aromatic heterocycles, aldehydes, and active methylene compounds. *J. Org. Chem.*, 73:6824–6827, 2008.
- [37] S. Gerard, A. Renzetti, B. Lefevre, A. Fontana, P. de Maria, and J. Sapi. Multicomponent reactions studies: Yonemitsu-type trimolecular condensations promoted by Ti(IV) derivatives. *Tetrahedron*, 66:3065–3069, 2010.
- [38] L. Ferrazzano, A. Viola, E. Lonati, E. Bulbarelli, R. Musumeci, C. Cocuzza, M. Lombardo, and A. Tolomelli. New isoxazolidinone and 3,4-dehydro- β -proline derivatives as antibacterial agents and mao-inhibitors: a complex balance between two activities. *Eur. J. Med. Chem.*, 124:906–919, 2016.
- [39] P. Cruciani, R. Stammer, C. Aubert, and M. Malacria. New cobalt-catalyzed cycloisomerization of ϵ -ketoesters. application to a powerful cyclization reactions cascade. *J. Org. Chem.*, 61:2699–2708, 1996.
- [40] A. Renzetti, A. Marrone, S. G  rard, J. Sapi, H. Nakazawa, N. Re, and A. Fontana. TiCl_4 -promoted condensation of methyl acetoacetate, isobutyraldehyde, and indole: a theoretical and experimental study. *Phys. Chem. Chem. Phys.*, 17:8964–8972, 2015.
- [41] N. Elander, R. Jones, S.Y. Lu, and S. Stone. Microwave-enhanced radiochemistry. *Chem. Soc. Rev.*, 29:239–249, 2000.

- [42] N.F.K. Kaiser, U. Bremberg, M. Larhed, C. Moberg, and A. Hallberg. Fast, convenient, and efficient molybdenum-catalyzed asymmetric allylic alkylation under noninert conditions: An example of microwave-promoted fast chemistry. *Angew. Chem. Int. Ed.*, 39:3595–3598, 2000.
- [43] A. de la Hoz, A. Diaz-Ortiz, and A. Moreno. Microwaves in organic synthesis. thermal and non-thermal microwave effects. *Chem. Soc. Rev.*, 34:164–178, 2005.
- [44] C.O. Kappe. Controlled microwave heating in modern organic synthesis. *Angew. Chem. Int. Ed.*, 43:6250–6284, 2004.
- [45] A. Viola, L. Ferrazzano, G. Martelli, S. Ancona, L. Gentilucci, and A. Tolomelli. An improved microwave assisted protocol for yonemitsu-type trimolecular condensation. *Tetrahedron*, 70:6781–6788, 2014.
- [46] F. Benfatti, G. Cardillo, L. Gentilucci, E. Mosconi, and A. Tolomelli. Enzymatic resolution of ethyl-3-hydroxy-2(1'-substituted-methylidene)-butyrate by pseudomonas cepacia lipase catalyzed acetylation. *Tetrahedron Asymmetry*, 18:2227–2232, 2007.
- [47] A. Tolomelli, G. Cardillo, L. Gentilucci, R. Juris, A. Viola, and E. Juaristi. Exploring the reactivity of alkylidene malonamides: synthesis of polyfunctionalized isoxazolidinones, aziridines and oxazolines. *Arkivoc*, 5:196–209, 2012.
- [48] A. Viola, L. Ferrazzano, R. Greco, L. Cerisoli, J. Caldi, and A. Tolomelli. One-pot two-step microwave-assisted synthesis of alkylidene acetoacetamido esters, useful intermediates for β -dehydropeptides. *Eur. J. Org. Chem.*, pages 3217–3222, 2016.

- [49] J.A. Hyatt, P.L. Feldman, and R.J. Clemens. Ketenes. 20. thermal decomposition of 2,2,6-trimethyl-4h-1,3-dioxin-4-one and 1-ethoxybutyn-3-one. acetylketene. *J. Org. Chem.*, 49:5105–5108, 1984.
- [50] R.J. Clemens and J.S. Witzeman. Kinetic and spectroscopic studies on the thermal decomposition of 2,2,6-trimethyl-4h-1,3-dioxin-4-one. generation of acetylketene. *J. Am. Chem. Soc.*, 111:2186–2193, 1989.
- [51] S.V. Ryabukhin, A.S. Plaskon, D.M. Volochnyuk, S.E. Pipko, A.N. Sivanyuk, and A.A. Tolmachev. Combinatorial knoevenagel reactions. *J. Comb. Chem.*, 9:1073–1078, 2007.
- [52] P. Perlmutter. *Conjugate Addition Reactions in Organic Synthesis*. 1992.
- [53] I. Fleming. *Frontier orbitals and organic chemical reactions*. 1976.
- [54] R.P. Herrera and E. Marques-Lopez. *Multicomponent reactions: concepts and applications for design and synthesis*. 2015.
- [55] L.F. Tietze and N. Rackelmann. *Multicomponent reactions*. 2005.
- [56] J. Zhu, Q. Wang, and M. Wang. *Multicomponent reactions in organic synthesis*. 2015.
- [57] Y. Oikawa, H. Hirasawa, and O. Yonemitsu. Meldrum's acid in organic synthesis. 1. a convenient one-pot synthesis of ethyl indolepropionates. *Tetrahedron Lett.*, 19:1759–1762, 1978.
- [58] F. Epifano, S. Genovese, O. Rosati, S. Tagliapietra, C. Pelucchini, and M. Curini. Ytterbium triflate catalyzed synthesis of β -functionalized indole derivatives. *Tetrahedron Lett.*, 52:568–571, 2011.

- [59] C. Acharya, S. Dey, and P. Jaisankar. Indium trichloride catalyzed three component one-pot route to 1-hydroxymethyl-3-aminomethyl indoles. *Tetrahedron Lett.*, 53:5548–5551, 2012.
- [60] A. Renzetti, E. Boffa, M. Colazzo, S. Gerard, J. Sapi, T. Chan, H. Nakazawa, C. Villani, and A. Fontana. Yonemitsu-type condensations catalysed by proline and *eu(otf)*₃. *RSC Adv.*, 4:47992–47999, 2014.
- [61] T. Ishikawa, K. Nagai, T. Kudoh, and S. Saito. Asymmetric synthesis of substituted isoxazolidinone from α,β -unsaturated esters and hydroxylamines by means of double stereodifferentiation. *Synlett*, pages 1171–1173, 1995.
- [62] S.A. Bentley, S.G. Davies, J.A. Lee, P.M. Roberts, and A.J. Russell. Conjugate addition of lithium n-tert-butyldimethylsilyloxy-n-(α -methylbenzyl)-amide: asymmetric synthesis of $\beta^{2,2,3}$ -trisubstituted amino acids. *Tetrahedron*, 66:4604–4620, 2010.
- [63] M.E. Juarez-Garcia, S. Yu, and J.W. Bode. Asymmetric synthesis of enantiopure isoxazolidinone monomers for the synthesis of β^3 -oligopeptides by chemoselective amide ligation. *Tetrahedron*, 66:4841–4853, 2010.
- [64] F. Benfatti, G. Cardillo, L. Gentilucci, E. Mosconi, and A. Tolomelli. Lewis acid induced highly regioselective synthesis of a new class of substituted isoxazolidines. *Synlett*, 17:2605–2608, 2008.
- [65] G. Cardillo, L. Gentilucci, M. Gianotti, R. Perciaccante, and A. Tolomelli. Synthesis of aziridine-2,2-dicarboxylates via 1,4-addition of n,o-(bistrimethylsilyl)hydroxylamine to $\alpha\beta$ -unsaturated malonates. *J. Org. Chem.*, 66:8657–8660, 2001.

- [66] F Benfatti, A. Bottoni, G. Cardillo, L. Gentilucci, M. Monari, E. Mosconi, M. Stenta, and A. Tolomelli. Synthesis of ethyl 5-hydroxyisoxazolidine-4-carboxylates via michael addition/intramolecular hemiketalisation. *Eur. J. Org. Chem.*, pages 6119–6127, 2008.
- [67] A. Tolomelli, L. Gentilucci, E. Mosconi, A. Viola, and E. Paradisi. A straightforward route to enantiopure 2-substituted-3,4-dehydro- β -proline via ring closing metathesis. *Amino Acids*, 41:575–586, 2011.
- [68] S. Werner, D. Kasi, and K.M. Brummond. Design and synthesis of a 3,4-dehydroproline amide discovery library. *J. Comb. Chem.*, 9:677–683, 2007.
- [69] G.C. Fu, S.T. Nguyen, and R.H. Grubbs. Catalytic ring-closing metathesis of functionalized dienes by a ruthenium carbene complex. *J. Am. Chem. Soc.*, 115:9856–9857, 1993.
- [70] G.C. Fu and R.H. Grubbs. Synthesis of nitrogen heterocycles by catalytic ring-closing metathesis of dienes. *J. Am. Chem. Soc.*, 114:7324–7325, 1992.
- [71] P.A. Evans and J.E. Robinson. Regioselective rh-catalyzed allylic amination/ring-closing metathesis approach to monocyclic azacycles: diastereospecific construction of 2,3-disubstituted pyrroline. *Org. Lett.*, 1:1929–1931, 1999.
- [72] R. Takeuchi, N. Ue, K. Tanabe, K. Yamashita, and N. Shiga. Iridium complex-catalyzed allylic amination of allylic esters. *J. Am. Chem. Soc.*, 123:9525–9534, 2001.
- [73] A. Leitner, C. Shu, and F. Hartwig. Editing the stereochemical elements in an iridium catalyst for enantioselective allylic amination. *PNAS*, 101:5830–5833, 2004.

- [74] C. Gnamm, G. Franck, N. Miller, T. Stork, K. Brodner, and G. Helmchen. Enantioselective iridium-catalyzed allylic aminations of allylic carbonates with functionalized side chains. asymmetric total synthesis of (s)-vigabatrin. *Synthesis*, 20:3331–3350, 2008.
- [75] M. Roggen and E.M. Carreira. Stereospecific substitution of allylic alcohols to give optically active primary allylic amines: unique reactivity of a (p,alkene)ir complex modulated by iodide. *J. Am. Chem. Soc.*, 132:11917–11919, 2010.
- [76] A. Tolomelli, M. Baiula, A. Viola, L. Ferrazzano, L. Gentilucci, S.D. Dattoli, S. Spampinato, E. Jaristi, and M. Escudero. Dehydro- β -proline containing α integrin antagonists: stereochemical recognition in ligand-receptor interplay. *ACS Med. Chem. Lett.*, 6:701–706, 2015.
- [77] R.J. Kazlauskas, A.N. Weissfloch, A.T. Rappaport, and L.A. Cucchia. A rule to predict which enantiomer of a secondary alcohol reacts faster in reactions catalyzed by cholesterol esterase, lipase from pseudomonas cepacia, and lipase from candida rugosa. *J. Org. Chem.*, 56:2656–12665, 1991.
- [78] *Food and Drug Consumer Health Informations*, November 2013.
- [79] J. Davies and D. Davies. Origins and evolution of antibiotic resistance. *Microbiology and molecular biology reviews.*, 74:417–433, 2010.
- [80] A.L. Demain and S. Sanchez. Microbial drug discovery: 80 years of progress. *J. Antibio.*, 62:5–16, 2009.
- [81] K. Lewis. Platforms in antibiotic discovery. *Nat. Rev. Drug Discovery*, 12:371–387, 2013.

- [82] R. C. Jr Moellering. Problems with antimicrobial resistance in gram-positive cocci. *Clin. Infect Dis.*, 26:1177–1178, 1998.
- [83] K.L. LaPlante and M.J. Rybak. Daptomycin - a novel antibiotic against gram-positive pathogens. *Expert Opin. Pharmacother.*, 5:2321–2331, 2004.
- [84] K.J. Shaw and M.R. Barbachyn. The oxazolidinone: past, present and future. *Ann. N. Y. Acad. Sci.*, 1241:48–70, 2011.
- [85] P.W. Ament, N. Jamshed, and J.P. Horne. Linezolid: its role in the treatment of gram-positive , drug resistant bacterial infections. *Am. Fam. Physician*, 65:663–670, 2002.
- [86] A.H. Lin, R.W. Murray, T.J. Vidmar, and K.R. Marotti. The oxazolidinone eperzolid binds to the 50s ribosomal subunit and competes with binding of chloramphenicol and lincomycin. *Antimicrob. Agents Chemother.*, 41:2127–2131, 1997.
- [87] D.C. Eustice, P.A. Feldman, I. Zajac, and A.M. Slee. Mechanism of action of dup721: inhibition of an early event during initiation of protein synthesis. *Antimicro. Agents Chemother.*, 31:1218–1222, 1988.
- [88] D.N. Shinabarger, K.R. Marotti, R.W. Murray, A.H. Lin, E.P. Melchior, S.M. Swaney, D.S. Duniak, W.F. Demyan, and J.M. Buysse. Mechanism of action of oxazolidinones: effects of linezolid and eperzolid on translation reactions. *Antimicrob. Agents Chemother.*, 41:2133–2136, 1997.
- [89] D.N. Wilson, F. Schluenzen, J.M. Harms, A.L. Starosta, S.R. Connell, and P. Fucini. The oxazolidinone antibiotics perturb the ribosomal peptidyl-transferase center and effect trna positioning. *PNAS*, 105:13339–13344, 2008.

- [90] S.J. Brickner, M.R. Barbachyn, D.K. Hutchinson, and P.R. Manninen. Linezolid (zyvox), the first member of a completely new class of antibacterial agents for treatment of serious gram-positive infections. *J. Med. Chem.*, 51:3353–3356, 2008.
- [91] A.C. Gales, H.S. Sader, S.S. Andrade, L. Lutz, A. Machadoc, and A.L. Barth. Emergence of linezolid-resistant staphylococcus aureus during treatment of pulmonary infection in a patient with cystic fibrosis. *Int. J. Antimicrob. Agents*, 27:300–302, 2006.
- [92] M.R. Barbachyn, G.J. Cleek, L.A. Dolak, S.A. Garmon, J. Morris, E.P. Seest, R.C. Thomas, D.S. Toops, W. Watt, D.G. Wishka, C.W. Ford, G.E. Zurenko, J.C. Hamel, R.D. Schaadt, D. Stapert, B.H. Yagi, W.J. Adams, J.M. Friis, J.G. Slatter, J.P. Sams, N.L. Oien, M.J. Zaya, L.C. Wienkers, and M.A. Wynalda. Identification of phenylisoxazolines as novel and viable antibacterial agents active against gram-positive pathogens. *J. Med. Chem.*, 46:284–302, 2003.
- [93] A. Denis and T. Villette. 5-aryl- β,γ butenolide, a new class of antibacterial derived from the n-aryl oxazolidinone dup 721. *Bioorg. Med. Chem. Lett.*, 4:1925–1930, 1994.
- [94] A.D. Borthwick, K. Biggadike, V. Rocherolle, D.M. Cox, and G.A. Chung. 5-(acetamidomethyl)-3-aryldihydrofuran-2-ones and 5-(acetamidomethyl)-3-aryltetrahydrofuran-2-ones, two new classes of antibacterial agents. *Med. Chem. Res.*, 6:22–27, 1996.
- [95] A. Renslo, G.W. Luehr, and M.F. Gordeev. Recent developments in the identification of novel oxazolidinone antibacterial agents. *Bioorg. Med. Chem.*, 14:4227–4240, 2006.
- [96] A. Palumbo Piccionello, R. Musumeci, C. Cocuzza, C.G. Fortuna, A. Guarcello, P. Pierro, and A. Pace. Synthesis and preliminary an-

- tibacterial evaluation of linezolid-like 1,2,4-oxadiazole derivatives. *Eur. J. Med. Chem.*, 50:441–448, 2012.
- [97] O.A. Phillips, R. D’Silva, T.O. Bahta, L.H. Sharaf, E.E. Udo, L. Benov, and D.E. Walters. Synthesis and biological evaluation of novel 5-(hydroxamic acid) methyl oxazolidinone derivatives. *Eur. J. Med. Chem.*, 106:120–131, 2015.
- [98] J.G. Slatter, D.J. Stalker, K.L. Feenstra, I.R. Welshman, J.B. Bruss, J.P. Sams, M.G. Johnson, P.E. Sanders, M.J. Hauer, P.E. Fagemess, R.P. Styd, G.W. Peng, and E.M. Shobe. Pharmacokinetics, metabolism and excretion of linezolid following an oral dose of [¹⁴C] linezolid to healthy human subjects. *Drug Metab. Dispos.*, 29:1136–1145, 2001.
- [99] M.A. Wynalda, M.J. Hauer, and L.C. Wienkers. Oxidation of novel oxazolidinone antibiotic linezolid in human liver microsomes. *Drug Metab. Dispos.*, 20:1014–1017, 2000.
- [100] M.E. Brier, D.J. Stalker, D.H. Aronoff, D.H. Batts, K.K. Ryan, M. O’Grady, N.K. Hopkins, and G.L. Junglubuth. Pharmacokinetics of linezolid in subjects with renal dysfunctions. *Antimicrob. Agents Chemother.*, 47:2775–2780, 2003.
- [101] J. Wouters, F. Moureau, G. Evrard, J. Koenig, S. Jegham, P. George, and F. Durant. A reversible monoamino oxidase a inhibitor, blefoxatone: structural approach of its mechanism of action. *Bioorg. Med. Chem.*, 7:1683–1693, 1999.
- [102] T.Z. Jones, P. Fleming, C.J. Eyermann, M.B. Gravestock, and R.R. Ramsay. Orientation of oxazolidinones in the active site of monoamine oxidase. *Biochem. Pharm.*, 70:407–416, 2005.

- [103] K.R. Lawrence, M. Adra, and P.K. Gillman. Serotonin toxicity associated with the use of linezolid: a review of postmarketing data. *Clin. Infect. Dis.*, 42:1578–1583, 2006.
- [104] C. Binda, M. Li, F. Huba'lek, N. Restelli, D.E. Edmondson, and A. Mattevi. Insight into the mode of inhibition of human mitochondrial monoamine oxidase b from high-resolution crystal structures. *Proc. Natl. Acad. Sci. USA*, 100:9750–9755, 2003.
- [105] T. Poel, R.C. Thomas, W.J. Adams, P.A. Aristoff, M.R. Barbachyn, F.E. Boyer, J. Brieland, R. Brideau, J. Brodfuehrer, A.P. Brown, A.L. Choy, M. Dermeyer, M. Dority, C.W. Ford, R.C. Gadwood, D. Hanna, C. Hongliang, M.D. Huband, C. Huber, R. Kelly, J. Kim, J.P. Jr Martin, P.J. Pagano, D. Ross, L. Skerlos, M.C. Sulavik, T. Zhu, G.E. Zurenko, and J.V.N.V. Prasad. Antibacterial oxazolidinones possessing a novel c-5 side chain. (5r)-trans-3-[3-fluoro-4-(1-oxotetrahydrothiopyran-4-yl)phenyl]-2-oxoxazolidine-5-carboxylic acid amide (pf-00422602), a new lead compound. *J. Med. Chem.*, 50:5886–5889, 2007.
- [106] J. Grimbsy, N.C. Lan, R. Neve, K. Chen, and J.C. Shih. Tissue distribution of human monoamine oxidase a and b mrna. *J. Neurochem.*, 55:1166–1169, 1990.
- [107] S.D. Sivasubramaniam, C.C. Finch, M.J. Rodriguez, N. Mahy, and E.E. Billett. A comparative study of the expression of monoamine oxidase-a and -b mrna and protein in non-cns human tissue. *Cell Tissue Res.*, 313:291–300, 2003.
- [108] S.Y. Son, J. Ma, Y. Kondou, M. Yoshimura, E. Yamashita, and T. Tsukihara. Structure of human monoamine oxidase a at 2.2 aa resolution: the control of opening the entry for substrates/inhibitors. *PNAS*, 105:5739–5744, 2008.

- [109] 2Z5X. Crystal structure of human monoamine oxidase a with harmine (2.2 aa resolution). www.rcsb.org/pdb/explore.do?structureId=2z5x.
- [110] C. Binda, P. Newton-Vinson, F. Hub á lek, D.E. Edmondson, and A. Mattevi. Structure of human monoamine oxidase b, a drug target for the treatment of neurological disorders. *Nat. Struct. Biol.*, 9:22–26, 2002.
- [111] 2V5Z. Structure of human mao b in complex with the selective inhibitor safinamide (1.6 aa resolution). www.rcsb.org/pdb/explore.do?structureId=2v5z.
- [112] G.M. Sastry, M. Adzhigirey, T. Day, R. Annabhimoju, and W. Sherman. Protein and ligand preparation: parameters, protocols and influence on virtual screening enrichment. *J. Comput. Aided Mol. Des.*, 27:221–234, 2013.
- [113] O. Trott and A.J. Olson. Autodock vina: improving the speed and accuracy of docking with a new scoring function, efficient optimization and multithreading. *J. Comput. Chem.*, 31:455–461, 2010.
- [114] F. Colotta, P. Allavena, A. Sica, C. Garlanda, and A. Mantovani. Cancer-related inflammation, the seventh hallmark of cancer: links to genetic instability. *Carcinogenesis*, 30:1073–1081, 2009.
- [115] L.M. Coussens and Z. Werb. Inflammation and cancer. *Nature*, 420:860–867, 2002.
- [116] S.R. Nahoum. Why cancer and inflammation? *Yale J. Biol. Med.*, 79:123–130, 2006.
- [117] U.K. Marelli, F. Rechenmacher, T.R.A. Sobahi, C. Mas-Moruno, and H. Kessler. Tumor targeting via integrin ligands. *Front. Oncol.*, 3:1–12, 2013.

- [118] A.P. Mound, A. Komoriya, K.M. Yamada, and M.J. Humphries. The cs5 peptide is a second site in the iiics region of fibronectin recognized by integrin $\alpha_4\beta_1$. *J. Biol. Chem.*, 266:3579–3585, 1991.
- [119] D. Bouvard, J. Pouwels, N. De Franceschi, and J. Ivaska. Integrin inactivators: balancing cellular functions in vitro and in vivo. *Nature Rev. Mol. Cell. Biol.*, 14:430–442, 2013.
- [120] A.A. Postigo, J. Teixidó, and F. Sanchez-Madrid. The $\alpha_4\beta_1$ /vcam-1 adhesion pathway in physiology and disease. *Res. Immunol.*, 144:723–735, 1993.
- [121] Y.M. Hyun, C.T. Lefort, and M. Kim. Leukocyte integrins and their ligand interactions. *Immunol. Res.*, 45:195–208, 2009.
- [122] B. Garmy-Susini, H. Jin, Y. Zhu, R.Y. Sung, R. Hwang, and J. Varner. Integrin $\alpha_4\beta_1$ -vcam-1-mediated adhesion between endothelial and mural cells is required for blood vessel maturation. *J. Clin. Invest.*, 115:1542–1551, 2005.
- [123] S. Shishido, H. Bönig, and Y.M. Kim. Role of integrin alpha4 in drug resistance of leukemia. *Front Oncol.*, 4:1–10, 2014.
- [124] H. Jin, A. Aiyer, J. Su, P. Borgstrom, D. Stupack, M. Friedlander, and J. Varner. A homing mechanism for bone marrow-derived progenitor cell recruitment to the neovasculature. *J. Clin. Invest.*, 116:652–662, 2006.
- [125] M. Valcarcel, T. Carrascal, O. Crende, and F. Vidal-Vanaclocha. Il-18 regulates melanoma v α -4 integrin activation through a hierarchical sequence of inflammatory factors. *J. Inv. Dermatol.*, 134:470–480, 2014.

- [126] A.A. Postigo, P. Sanchez-Mateos, A. Lazarovits, F. Sanchez-Madrid, and M.O. de Landazuri. $\alpha_4\beta_7$ integrin mediates b cell binding to fibronectin and vascular cell adhesion molecule-1. expression and function of α_4 integrins on human b lymphocytes. *J. Immunol.*, 151:2471–2483, 1993.
- [127] C. Berlin, E.L. Berg, M.J. Briskin, D.P. Andrew, P.J. Kilshaw, B. Holzmann, I.L. Weissman, A. Hamann, and E.C. Butcher. $\alpha_4\beta_7$ integrin mediates lymphocyte binding to the mucosal vascular addressin in madcam-1. *Cell*, 74:185–195, 1993.
- [128] J. Meenan, J. Spaans, T.A. Gools, S.T. Pals, G.N. Tytgat, and S.J. van Deventer. Altered expression of $\alpha_4\beta_7$, a gut homing integrin, by circulating and mucosal t cells in colonic mucosal inflammation. *Gut*, pages 241–246, 1997.
- [129] J.D. Hood and D.A. Cheresh. Role of integrins in cell invasion and migration. *Nat. Rev. Cancer*, pages 91–100, 2002.
- [130] P.L. McCormack. Natalizumab: a review of its use in the management of relapsing-remitting multiple sclerosis. *Drugs*, pages 1463–1481, 2013.
- [131] A. Sakuraba, K. Keyashian, C. Correia, J. Melek, R.D. Cohen, S.B. Hanauer, and D.T. Rubin. Natalizumab in crohn’s disease: results from a us tertiary inflammatory bowel disease center. *Inflamm. Bowel. Dis.*, pages 621–626, 2013.
- [132] B.K. Kleinschmidt-DeMasters and K.L. Tyler. Progressive multifocal leukoencephalopathy complicating treatment with natalizumab and interferon beta-1a for multiple sclerosis. *New Engl. J. Med.*, pages 369–374, 2005.

- [133] I. Mitroulis, V.I. Alexaki, I. Kourtzelis, A. Ziogas, G. Hajishen-gallis, and T. Chavakis. Leukocyte integrins: role in leukocyte re-cruitment and as therapeutic targets in inflammatory disease. *Phar-macol Ther.*, pages 123–135, 2015.
- [134] K.P. Garnock-Jones. Vedolizumab: a review of its use in adult pa-tients with moderately to severely active ulcerative colitis or crohn’s disease. *Biodrugs*, pages 57–67, 2015.
- [135] E. Gerard, A. Meulle, O. Feron, and J. Marchand-Brynaert. Di-aryl urea ldv peptidomimetics as $\alpha_4\beta_1$ integrin antagonists: synthe-sis, adhesion inhibition and toxicity evaluation on ccrf-cem cell line. *Med. Chem. Com.*, pages 199–212, 2012.
- [136] E. Locardi, J. Boer, A. Modlinger, A. Schuster, B. Holzmann, and H. Kessler. Synthesis and structure-activity relationship of mannose-based peptidomimetics selectively blocking integrin $\alpha_4\beta_7$ binding to mucosal address in cell adhesion molecule-1. *J. Med. Chem.*, pages 5752–5762, 2003.
- [137] E.Y. Jones, K. Harlos, M.J. Bottomley, R.C. Robinson, P.C. Driscoll, R.M. Edwards, J.M. Clements, T.J. Dudgeon, and D.I. Stu-art. Crystal structure of an integrin-binding fragment of vascular cell adhesion molecule-1 at 1.8 Å resolution. *Nature*, pages 539–544, 1995.
- [138] T.J. You, D.S. Maxwell, T.P. Kogan, Q. Chen, J. Li, J. Kassir, G.W. Holland, and R.A.F. Dixon. Small molecule agonist of very late antigen-4 (vla-4) integrin induces progenitor cell adhesion. *Biophys.*, pages 447–457, 2002.
- [139] S. Thagapandian, J. Shalini, S. Sakkiah, and K.W. Lee. Discovery of potential integrin vla-4 antagonists using pharmacophore model-

- ing, virtual screening and molecular docking studies. *Chem. Biol. Drug Des.*, pages 289–300, 2011.
- [140] O.E. Hutt, S. Saubern, and D.A. Winkler. Modeling the molecular basis for $\alpha_4\beta_1$ integrin antagonism. *Bioorg. Med. Chem.*, pages 5903–5911, 2011.
- [141] K.C. Lin, H.S. Ateeq, S.H. Hsiung, L.T. Chong, C.N. Zimmermann, A. Castro, W.C. Lee, C.E. Hammond, S. Kalkunte, L.L. Chen, R.B. Pepinsky, D.R. Leone, A.G. Sprague, W.M. Abraham, A. Gill, R.R. Lobb, and S.P. Adams. Selective, tight-binding inhibitors of integrin $\alpha_4\beta_1$ that inhibit allergic airway responses. *J. Med. Chem.*, pages 920–934, 1999.
- [142] C. Mas-Moruno, R. Fraioli, F. Rechenmacher, S. Neubauer, T.G. Kapp, and H. Kessler. $\alpha_v\beta_3$ - or $\alpha_5\beta_1$ -integrin-selective peptidomimetics for surface coating. *Angew. Chem. Int. Ed.*, pages 7048–7067, 2016.
- [143] M.A. Dechantsreiter, E. Planker, B. Matha, E. Lohof, G. Hölzemann, A. Jonczyk, S.L. Goodman, and H. Kessler. N-methylated cyclic rgd peptides as highly active and selective $\alpha_v\beta_3$ integrin antagonists. *J. Med. Chem.*, 16:3033–3040, 1999.
- [144] J.P. Xiong, T. Stehle, R. Zhang, A. Joachimiak, M. French, S.L. Goodman, and M.A. Arnaout. Crystal structure of the extracellular segment of integrin $\alpha_v\beta_3$ in complex with an arg-gly-asp ligand. *Science*, pages 151–155, 2002.
- [145] A. Tolomelli, L. Gentilucci, E. Mosconi, A. Viola, S.D. Dattoli, M. Baiula, S. Spampinato, L. Belvisi, and M. Civera. Development of isoxazoline-containing peptidomimetics as dual $\alpha_v\beta_3$ and $\alpha_5\beta_1$ integrin ligands. *ChemMedChem*, pages 2264–2272, 2011.

- [146] C. Ornelas, J. Broichagen, and M. Weck. Strain-promoted alkyne azide cycloaddition for the functionalization of poly(amide)-based dendrons and dendrimers. *J. Am. Chem. Soc.*, pages 3923–3931, 2010.
- [147] X. Creary, A. Anderson, C. Brophy, F. Crowell, and Z. Funk. Method for assigning structure of 1,2,3-triazoles. *J. Org. Chem.*, pages 8756–8761, 2012.
- [148] J. Yuqin, R. Baoqi, L. Xiaomeng, Z. Weiwei, L. Wei, and X. Guiqing. *J. Chem. Res.*, pages 243–246, 2015.
- [149] Y. Tu and L. Zhu. *J. Contr. Release*, pages 94–102, 2015.
- [150] C.M. Carlevaro, J.H. Martins da Silva, W. Savino, and E.R. Caffarena. Plausible binding mode of the active antagonist, mk-0617, determined by docking and free energy calculations. *J. Theor. Comp. Chem.*, pages 1250108–1/16, 2013.
- [151] W.S. Brown, J.S. Khalili, T.G. Rodriguez-Cruz, G. Lizee, and B.W. McIntyre. B-raf regulation of integrin $\alpha_4\beta_1$ -mediated resistance to shear stress through changes in cell spreading and cytoskeletal association in t cells. *J. Biol. Chem.*, pages 23141–23153, 2014.
- [152] H. Fujii, H. Komazawa, H. Mori, M. Kojima, I. Itoh, J. Murata, I. Azuma, and I. Saiki. Antimetastatic activities of synthetic arg-gly-asp-ser (rgds) and arg-leu-asp-ser (rlds) peptide analogues and their inhibitory mechanisms. *Biol. Pharm. Bull.*, pages 1681–1688, 1995.
- [153] S.M. Weis, D.G. Stupack, and D.A. Cheresh. Agonizing integrin antagonists? *Cancer Cell*, pages 359–361, 2009.
- [154] J.F. Van Agthoven, J.P. Xiong, J.L. Alonso, X. Rui, B.D. Adair, S.L. Goodman, and M.A. Arnaout. Structural basis for pure antago-

- nism of integrin $\alpha_v\beta_3$ by a high-affinity form of fibronectin. *Nature Struct. Mol. Biol.*, pages 383–388, 2014.
- [155] N. De Franceschi, H. Hamidi, J. Alanko, P. Sahgal P, and J. Ivaska. Integrin traffic - the update. *J Cell Sci.*, pages 839–852, 2015.
- [156] P.T. Caswell and J.C. Norman. Integrin trafficking and the control of cell migration. *Traffic*, pages 14–21, 2006.
- [157] M.A. Dozynkiewicz, N.B. Jamieson, I. Macpherson, J. Grindlay, P.V. van den Berghe, A. von Thun, J.P. Morton, C. Gourley, P. Timpson, and C. Nixon. Rab25 and clic3 collaborate to promote integrin recycling from late endosomes/lysosomes and drive cancer progression. *Dev. Cell.*, pages 131–145, 2012.
- [158] D Tuncel and H.V. Demir. Conjugated polymer nanoparticles. *Nanoscale*, pages 484–494, 2010.
- [159] A. Kaeser and A.P.H.J. Shenning. Fluorescent nanoparticles based on self-assembled π -conjugated systems. *Adv. Mater.*, pages 2985–2997, 2010.
- [160] O.C. Farokhzard and R Langer. Impact of nanotechnology on drug delivery. *ACS Nano*, 3:16–20, 2009.
- [161] J.B.H. Parag Aggarwal, J.B. Hall, C.B. McLeland, M.A. Drobovolskaia, and S.E. McNeil. Nanoparticle interaction with plasma proteins as it relates to particle biodistribution, biocompatibility and therapeutic efficacy. *Adv. Drug Deliv. Rev.*, 61:428–437, 2009.
- [162] Q. Gao, H. ana He. *Expert Opin. Drug Deliv.*, page 409, 2014.
- [163] I. Fischer, K. Petkau-Milroy, Y.L. Dorland, A.P.H.J. Schenning, and L. Brunsveld. Self-assembled fluorescent organic nanoparticles for live-cell imaging. *Chem. Eur. J.*, pages 16646–16650, 2013.

- [164] J. Schill, A.P.H.J. Shenning, and L. Brunsveld. Self-assembled fluorescent nanoparticles from π -conjugated small molecules: en route for biological applications. *Macromol. Rapid. Commun.*, pages 1306–1321, 2015.
- [165] R. Abbel, A.P.H.J. Shenning, and E.W. Meijer. Fluorene-based materials and their supramolecular properties. *J. Polym. Sci. Part A: Polym. Chem.*, 47:4215–4233, 2009.
- [166] L. Zhu, C. Yang, and J. Qin. An aggregation-induced blue shift of emission and the self-assembly of nanoparticles from a novel amphiphilic oligofluorene. *Chem. Commun.*, pages 6303–6305, 2008.
- [167] Y. Koizumi, S. Seki, S. Tsukada, S. Sakamoto, and S. Tagawa. *J. Am. Chem. Soc.*, 128:9036–, 2006.
- [168] R. Abbel, R. van der Weegen, E.W. Meijer, and A.P.H.J. Shenning. Multicolour self-assembled particles of fluorene-based bolaamphiphiles. *Chem. Commun.*, pages 1697–1699, 2009.
- [169] A. Kaeser, I. Fischer, R. Abbel, P. Besenius, D. Dasgupta, M.A.J. Gillisen, G. Portale, A.L. Stevens, L.M. Herz, and A.P.H.J. Shenning. Side chains control dynamics and self-sorting in fluorescent organic nanoparticles. *ACS Nano*, 7:408–416, 2013.
- [170] J. Pennakalathil, E. Jahja, E.S. zdemir, O. Konu, and D. Tuncel. Red emitting, cucurbituril-capped, ph-responsive conjugated oligomer-based nanoparticles for drug delivery and cellular imaging. *Biomacromolecules*, 15:3366–3374, 2014.
- [171] R. Abbel, C. Grenier, M.J. Pouderoijen, J.W. Stouwdam, P.E.L.G. Leclère, R.P. Sijbesma, E.W. Meijer, and A.P.H.J. Schenning. White-light emitting hydrogen-bonded supramolecular copolymers

based on π -conjugated oligomers. *J. Am. Chem. Soc.*, 131:833–843, 2009.

- [172] K. Petkau, A. Kaeser, I. Fischer, L. Brunsveld, and A.P.H.J. Schenning. Pre- and postfunctionalized self-assembled π -conjugated fluorescent organic nanoparticles for dual targeting. *J. Am. Chem. Soc.*, 133:17063–17071, 2011.

Acknowledgement

Come solitamente accade, il primo ringraziamento va al proprio tutor. Ma in questo caso particolare, il primo ringraziamento a lei é una necessitá della mia coscienza prima che un dovere morale. Grazie ad Alessandra per essere stata innanzitutto un modello: é una donna di una forza incredibile prima che una grande scenziata, che ha saputo insegnarmi tante cose dal punto professionale e personale. E' sempre stata un importante punto di riferimento in questi anni, ed é per questo piú di tutto che le sono grata. Ha saputo spronarmi quando era necessario, bacchettarmi davanti ai normali cedimenti di questo lavoro, ascoltarmi quando avevo bisogno di parlare con qualcuno, ignorarmi quando non avevo voglia di farlo. Prima di augurarmi il meglio per la mia carriera, non posso non sperare che anche gli altri riconoscano le sue capacitá, che l'etichetta "professore" non si raggiunge solo con i titoli, ma soprattutto con i meriti concreti. Spero di aver imparato il meglio da lei, in prima fila la sua intraprendenza e il suo non demordere anche quando non ne hai piú. Si puó concludere con il mantra del gruppo Tolomelli: il capo piú figo ce l'abbiamo noi.

Il secondo ringraziamento va alla meravigliosa famiglia che é stata dietro ogni singolo giorno di questa e altre fatiche. Le piante migliori

crescono solo dove il terreno é buono e loro sono stati senza dubbio il migliore possibile. Mamma e papá, grazie per avermi insegnato che la positività viene sempre prima di tutto, che le difficoltà si superano sempre dove c'è l'amore e il supporto reciproco; grazie per avermi permesso di studiare, e di regalarmi così il dono piú prezioso che dei genitori possano fare, l'indipendenza; grazie per essere sempre un porto in cui tornare, perché in fin dei conti nessun posto é come casa tua. Michele, grazie per essere stato sempre quel gradino in piú della scala sul quale arrivare: ogni volta che io ne ho fatto uno, tu ne avevi sempre uno in piú e questo é stato importante per riuscire a trovare la voglia di impegnarsi; grazie perché, anche se con modi discutibili, mi accogli sempre nel momento del bisogno; le "molestie" affettive che mi regalavi quando eravamo piccoli si sono trasformate in attenzioni diverse e so che su queste potrò sempre contare. Grazie a Irene, che é stata un importante acquisto: spesso non siamo in sintonia ma é fondamentale che lei conosca la stima che nutro nei suoi confronti, perché devi essere matta o santa per sopportare suo marito; grazie per essere spesso il "cuscinetto di non belligeranza".

L'elemento della famiglia che merita un ringraziamento a parte é senza dubbio la piccola peste, Sofia. Non é necessario spendere tante parole in questo caso: é semplicemente la gioia piú bella che io abbia provato. Ti auguro di realizzare i tuoi sogni, di crescere serena e diventare una grande donna. Spero di saper essere la tua spalla forte e quella da cui correre ogni volta che lo vorrai.

Grazie a Dario, con il quale ho potuto completare il triplete di gioie della mia vita. Grazie per esserti preso sempre cura di me con la grande attenzione che sai dedicare alle cose a cui piú tieni. Sei l'altro piatto della bilancia con il quale raggiungere l'equilibrio perfetto: ogni tanto abbiamo perso qualche colpo, ma abbiamo saputo rimetterci in piedi con la certezza di avere accanto qualcuno su cui contare. Spero tu possa

riuscire a raggiungere tutti i tuoi obiettivi, io "ti prenderó mano nella mano per non perdersi o resteró dietro ad osservarti di nascosto".

Nel ringraziamento ammucciata vanno ovviamente tutti i ragazzi che sono passati nel laboratorio in questi anni: forse a voi vanno in effetti i ringraziamenti principali perché avete contribuito a completare questo lavoro. Grazie a Nicola C., Angelo, Roberto, Lucia e Nicola Z. che sono stati i fratelli maggiori del laboratorio, quelli a cui affidarsi davanti ad un dubbio o con cui confrontarsi quando ti viene un'idea geniale (questi momenti sono stati decisamente meno frequenti). Grazie a tutti i laureandi, che invece sono stati i fratelli minori, da guidare, di cui prendersi cura e a cui insegnare a camminare con le proprie gambe. A voi vanno anche le scuse per le sclerate inopportune, per le bacinelle di vetreria da lavare e per l'incapacità di risolvere anche i vostri dubbi piú assurdi. Ho pensato se si potesse fare una classifica dei laureandi a cui hai voluto piú bene perché alla fine per un po' viviamo in simbiosi; direi di sí, per questo grazie in particolare a Giulia, Margherita, Roberto, Eleonora, Paolo e Dario: é stato come partorirvi chimicamente perciò sono molto orgogliosa di voi e vi auguro di diventare dei chimici migliori di me.

Grazie a tutto lo staff Ciamician. Al Garelli, unico-irreprensibile-insostituibile, perché in fondo é un po' la sede distaccata di mio padre...e anche di mia madre, e ti voglio tanto bene anche se mi piacerebbe che tu riuscissi, finché saró ancora al Ciamician, a salvare un file all'HPLC con il nome giusto. A Stefano, il chimico incazzato, che se solo venisse impiegato maggiormente per le sue qualità di chimico, quel posto sarebbe un posto migliore. Al prof. Lombardo perché, se Alessandra é la "lei" della mia formazione, é senza dubbio il "lui". Se da studentessa mi sono appassionata alla chimica organica é stato merito suo, per cui finché le cose andranno per il verso giusto lo ringrazieró. Al Gualla, il custode dello scibile dei nostri lab. La stima nei suoi confronti é enorme: spero che gli studenti sappiano apprezzarlo. A tutti i ragazzi del bunker: As-

sunta, Mengo, Giulia, BettaSeiBuonissima. É stato bello condividere le paranoie e i pasticcini con voi.

Grazie a tutti i miei colleghi del dottorato, anche a quelli che non hanno fatto il questionario! Siamo stati un bel gruppo unito nello smadonnamendo e nella condivisione delle gioie.

Grazie a Ceciona e Marianna. A voi non serve dire molto: state fuori completamente ma io vi voglio bene e sono felice che quando un giorno saremo tutte disoccupate apriremo la nostra libreria con sala té, dove Marianna venderá i libri e Ceci preparerá i dolcetti mentre io all'ingresso faró la selezione, per cui non avremo mai nessun cliente e i manicaretti di Ceci ce li potremo mangiare noi. Grazie a Marianna per tutte le uscite che non abbiamo fatto, sei una certezza. Grazie a Ceci, per gli esami rimandati e le torte preparate, sei una certezza anche tu!

Grazie a Simon. L'Inghilterra é sicuramente un posto migliore adesso che ci sei tu. Potrai raccontare ai tuoi figli che per un periodo della tua vita sei stata la piú gnocca della nazione.